UDK 66:54(05) CODEN HMIDA 8 ISSN 0367–598 X

4 Hemijska industrija

Vol. 69

Časopis Saveza hemijskih inženjera

Chemical Industry

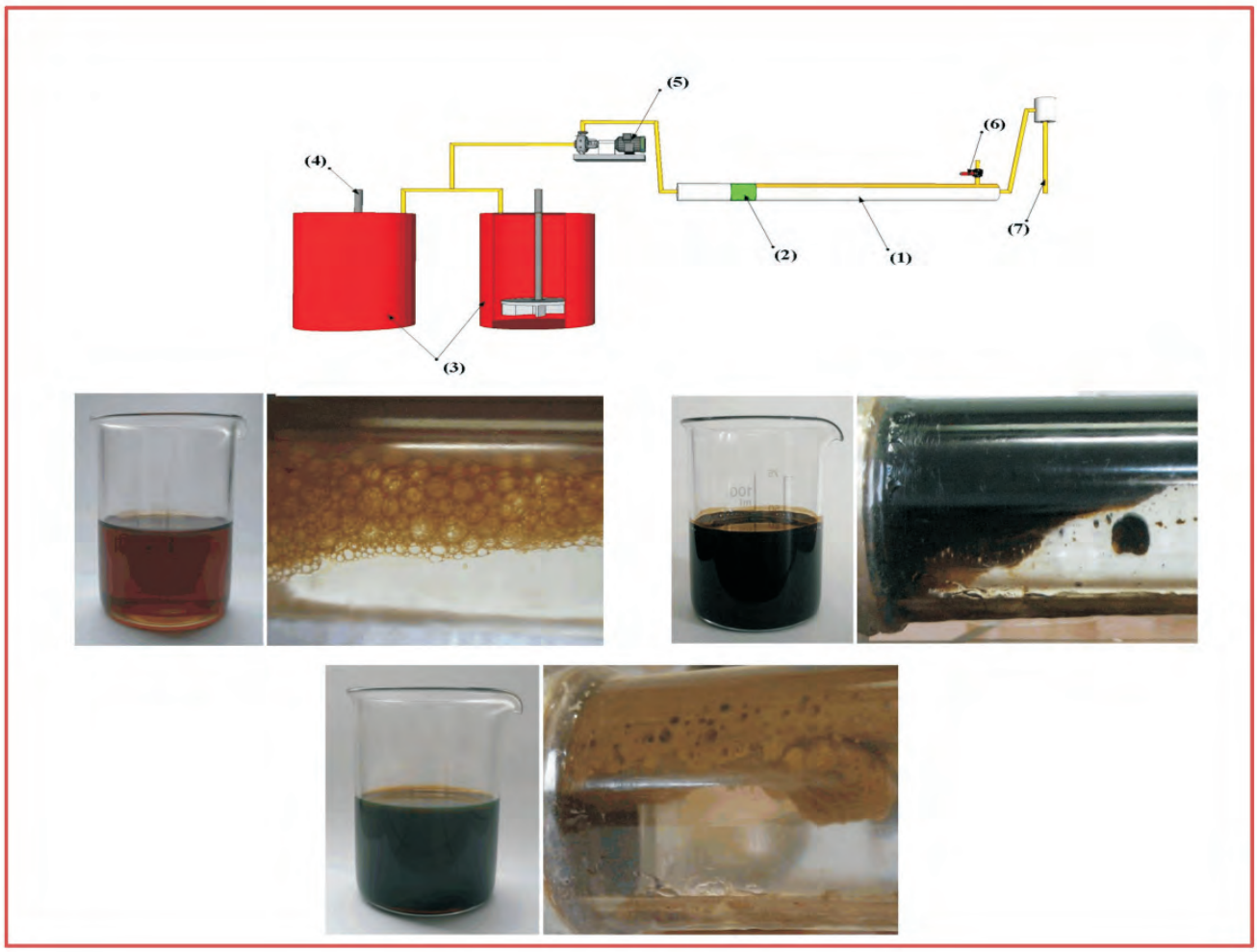

BEOGRAD, JUL-AVGUST 2015. HMIDA 8, 69 (4) 331-441 (2015)

GENERALNI POKROVITELJ

HEMOFARM KONCERN

VRŠAC, Beogradski put bb, tel. 013/821-345, 821-027, 821-129
BEOGRAD, Prote Mateje 70, tel. 011/344-26-63, faks: 344-17-87
E-pošta: info@hemofarm.com

IZDAVANJE ČASOPISA POMOGLA JE:

INŽENJERSKA KOMORA SRBIJE
Bulevar vojvode Mišića 37
11000 Beograd

SUIZDAVAČI

Tehnološko-metalurški fakultet
Univerziteta u Beogradu, Beograd

Prirodno-matematički fakultet Univerziteta
u Novom Sadu, Novi Sad

Hemijski fakutet
Univerziteta u Beogradu
Beograd

Institut za tehnologiju nuklearnih i drugih
mineralnih sirovina, Beograd

HIP Petrohemija a.d. Pančevo

Tehnološki fakultet Univerziteta
u Novom Sadu, Novi Sad

NU Institut za hemiju,
tehnologiju i metalurgiju
Univerziteta u Beogradu,
Beograd

„Nevena Color“ d.o.o.
Leskovac

Tehnološki fakultet Univerziteta
u Nišu, Leskovac

DCP Hemigal, Leskovac

Chemical Industry
Химическая промышленность

Hemijska industrija

Časopis Saveza hemijskih inženjera Srbije
Journal of the Association of Chemical Engineers of Serbia
Журнал Союза химических инженеров Сербии

VOL. 69 **Beograd, jul–avgust 2015** **Broj 4**

Redakcija
11000 Beograd, Kneza Miloša 9/I
Tel/fax: 011/3240-018
E-pošta: shi@yubc.net
www.ache.org.rs

Izlazi dvomesečno, rukopisi se ne vraćaju

Za izdavača
Tatijana Duduković

Sekretar redakcije
Slavica Desnica

Izdavanje časopisa pomaže
Republika Srbija, Ministarstvo prosvete, nauke i tehnološkog razvoja

Uplata pretplate i oglasnog prostora vrši se na tekući račun Saveza hemijskih inženjera Srbije, Beograd, broj 205-2172-71, Komercijalna banka a.d., Beograd

Kompjuterska priprema
Vladimir Panić

Štampa
Razvojno-istraživački centar grafičkog inženjerstva, Tehnološko-metalurški fakultet, Univerzitet u Beogradu, Karnegijeva 4, 11000 Beograd

Indeksiranje
Radovi koji se publikuju u časopisu *Hemijska Industrija* ideksiraju se preko *Thompson Reuters Scietific®* servisa *Science Citation Index - Expanded™* i *Journal Citation Report (JCR)*, kao i domaćeg *SCIndeks* servisa Centra za evaluaciju u obrazovanju i nauci

SADRŽAJ/CONTENTS

SADRŽAJ Nastavak
CONTENTS Continued

Phenol composition, DPPH radical scavenging and antimicrobial activity of Cornelian cherry (*Cornus mas*) fruit and leaf extracts

Ana S. Milenković-Andjelković[1], Marko Z. Andjelković[1], Aleksandra N. Radovanović[2], Blaga C. Radovanović[1], Vesna Nikolić[3]

[1]*University of Niš, Faculty of Natural Sciences and Mathematics, Niš, Serbia*
[2]*University of Belgrade, Faculty of Chemistry, Belgrade, Serbia*
[3]*University of Niš, Faculty of Technology, Leskovac, Serbia*

Abstract

Fruit is rich in different phenolic compounds which are recognized as potential natural medicaments and have been used in folk medicine for centuries. In order to evaluate phenol composition, the Cornelian cherry (*Cornus mas*) fruit and leaf extracts were subjected to the spectrophotometric and HPLC analysis. The radical scavenging activity was estimated using DPPH test and antimicrobial activity by disc diffusion and microwell dilution tests. All extracts showed high phenol content from 89.89±0.45 to 117.34±1.40 mg of gallic acid equivalents GAE/g extract dry matter (DM), but different composition of phenol compounds. Flavonols, anthocyanins, flavan-3-ols and phenolic acids were the main phenol classes found in the investigated fruit and leaf extracts. All extracts showed significant radical scavenging activity and a correlation with total phenol content (R^2 = 0.9832). Significant antimicrobial activity was found against Gram-positive, followed by Gram-negative strains, and yeast in all tested extracts. Cornelian cherry fruit and leaf extracts, rich in phenolic content, with significant antiradical and antimicrobial activity, can be used as additives in food and medicaments.

Keywords: Cornelian cherry, phenols, anthocyanins, radical scavenging activity, antimicrobial activity.

Available online at the Journal website: http://www.ache.org.rs/HI/

SCIENTIFIC PAPER

UDC 582.788.1:54:66:615.282

Hem. Ind. **69** (4) 331–337 (2015)

doi: 10.2298/HEMIND140216046M

Phenolic compounds are produced by plants, both edible and inedible, as a response to the environmental stress and pathogens. They are present in all plant parts in different quantities, depending on the stage of plant development and the environment influence. Phenolic compounds are mainly represented by anthocyanins, phenolic acids, flavan-3-ols and flavonols. These compounds are recognized as potential antioxidant agents with possible applications as food and medical ingredients. Fruit is recognized as plants which are rich in different phenolic compounds and have been used in folk medicine for centuries [1–3].

Cornelian cherry was recognized as a medical plant from ancient times, mainly due to its astringent properties. Traditionally, the Cornelian cherry was applied for treatment of fevers (bark, shoots and root), diarrhea (fruit) and its leaves against diarrhea and diabetes [3]. Today, it can be used for various ailments: stomach aches and cramps, diarrhea, different skin infections, intestinal parasites and hemorrhoids.

Correspondence: A.S. Milenković-Andjelković, University of Niš, Faculty of Natural Sciences and Mathematics, Višegradska 33, Niš, Serbia.
E-mail: ana.andjelk@gmail.com
Paper received: 16 February, 2014
Paper accepted: 27 May, 2014

There have been many studies on antioxidant [4–17], anti-cancer, anti-inflammatory [18], antimicrobial activities [1,4,5,9] of berry fruit extracts which are rich in phenol content [1–13]. However, there is less research on antioxidant activity and phenol content of Cornelian cherry fruit [6,9,14,15] and leaf extracts [16,17] . Antimicrobial activity of Cornelian cherry fruit was partially described [9,18,19] and there are no research papers on Cornelian cherry leaf extracts.

The objectives of this study were first to identify phenolic compounds of Cornelian cherry (*Cornus mas*) berry fruit and leaf extracts from Southeast Serbia for two consecutive seasons and then to determine their radical scavenging and antimicrobial potentials.

MATERIALS AND METHODS

Samples

Cornelian cherry (*Cornus mas*) fruit and leaf samples were collected at the maturity stage of fruit from Southeast Serbia for two consecutive seasons (2012 and 2013). Fruit and leaf samples were washed and dried at 60 °C. Dried samples were crushed in a grinder for 2 min and then used for extractions.

Reagents and chemicals

Methanol, acetonitrile and formic acid of HPLC--grade were obtained from Merck (Darmstadt, Germany). The standard phenolic compounds and 2,2'--diphenyl-1-picrylhydrazyl (DPPH) free radical were supplied from Sigma Chemical Co. (St. Louis, MO). Nutrient agar and nutrient broth were purchased from Merck and all other chemicals from Sigma. The reagents used were of analytical quality.

Bacterial strains and yeast

The antimicrobial activity of the test samples was evaluated using the following laboratory control strains: *Clostridium perfringens* ATCC 19404, *Bacillus cereus* ATCC 8739, *Listeria monocytogenes* ATCC 7644, *Staphylococcus aureus* ATCC 8538, *Sarcina lutea* ATCC 9341 and *Micrococcus flavus* ATCC 40240 (Gram (+) bacteria), *Escherichia coli* ATCC 25922, *Pseudomonas aeruginosa* ATCC 9027, *Salmonella enteritidis* ATCC 13076, *Shigella sonnei* ATCC 25931, *Klebsiella pneumoniae* ATCC 10031 and *Proteus vulgaris* ATCC 8427 (Gram (–) bacteria) and *Candida albicans* ATCC 10231 (Yeast) obtained from the American Type Culture Collection. The inocula of the bacterial strains and yeast were prepared from overnight broth cultures, and the suspensions were adjusted to 0.5 McFarland standard turbidity (corresponding to 10^7–10^8 CFU/ml).

Extraction procedures

The samples of dry berries and leaves (0.5 g DW) were extracted with 40 ml solvent system of methanol/acetone/water/formic acid (30/42/27.5/0.5) by stirring continuously at room temperature in the dark for 30 min, and then centrifuged for 10 min at 2500×*g*. The supernatants were collected and the precipitates were extracted again with the same solvent (40 ml). The extracts were centrifuged (10 min at 2500×*g*) and the supernatants were removed and combined with the previously collected supernatants and made up a final volume of the extracts. These extracts were evaporated under vacuum rotary evaporator and diluted in 10 ml methanol. Extracts were filtered through a 0.45 µm syringe filter before analysis.

Determination of phenols

Total phenols, hydroxycinnamoyl acids and flavonols in tested extracts were determined according to previously described spectrophotometric method [9]. Results were expressed as milligrams (mg) of gallic acid equivalents (GAE) for total phenols, mg of caffeic acid equivalents (CAE) for total hydroxycinnamoyl acids and mg of quercetin equivalents (QE) for total flavonols per g of extract dry matter (DM).

Total anthocyanins were determined also spectrophotometrically [11]. Malvidin-3-glucoside was employed as a calibration standard and results were expressed as mg malvidin-3-glucoside equivalents (ME) per g of extract DM.

Phenol composition of selected extracts was analyzed by high performance liquid chromatography (HPLC). The apparatus used for separation and determination of individual phenols from leaf extracts was an Agilent Technologies 1200 chromatographic system, equipped with an Agilent photodiode array detector (DAD) 1200 with RFID tracking technology for flow cells and UV lamp, an automatic injector, and ChemStation software. The column was thermostated at 30 °C. The separation was performed on an Agilent-Eclipse XDB C-18 4.6 mm×150 mm column. The HPLC method used was according to previously described [10] with some modifications. Briefly, the HPLC grade solvents used were formic acid/water (5:95, *V*/*V*) as solvent A and acetonitrile/formic acid/water (80:5:15, *V*/*V*) as solvent B. The elution gradient was linear as follows: from 0 to 10 min, 100% A + 0% B, from 10 to 20 min, 90% A + 10% B, from 20 to 30 min, 75% A + 25% B, from 25 to 35 min, 60% A + 40% B, from 35 to 40 min, 50% A + 50% B, from 40 to 45 min, 20% A + 80% B, and for last 10 min again 100% A + 0% B. The injection volume was 5 µl and the flow rate was 0.8 ml/min. The detection wavelengths were 280, 320, 360 and 520 nm for UV, and 275/322 nm ($\lambda_{Ex}/\lambda_{Em}$) for fluorescence-detection. The different phenolic compounds were identified by comparing their retention times and spectral characteristics with data of original reference standard compounds and with data given in the literature [9–11]. The calibration curves (five data points, n = 2) were linear with R^2 = 0.99. Results were expressed as mg/g extract DM.

DPPH test

The antioxidant activity of all investigated extracts was estimated determining the free radical scavenging activity of extracts by previously described DPPH test [11]. The radical scavenging activities of investigated extracts were expressed as median efficient concentrations (EC_{50}). This is the concentration of extract (mg/ml) necessary for a decrease in absorbance of DPPH solution to 50%.

Determination of antimicrobial activity

Preliminary antimicrobial tests were carried out by disc diffusion method [9] using 100 µl of bacterial suspension spread on Mueller–Hinton agar (MHA, Torlak, Serbia) in sterilized Petri dishes (90 mm in diameter). The discs (9 mm in diameter, HiMedia Laboratories Pvt. Limited) were impregnated with 50 µl of the testing samples, and placed on the inoculated agar (20 ml). The inoculated plates were incubated for 24 h at 37 °C. Reference antibiotic, tetracycline (30 µg/disc) served as a positive control, while the solvent (methanol, 50

µl/disc) was used as a negative control. Antibacterial activity was evaluated by measuring the zone of inhibition (in mm) against the test bacterial strains. A broth microdilution method [9] was used to determine the minimum inhibitory concentration (*MIC*) and minimum bactericidal concentration (*MBC*). Serial doubling dilutions of the testing samples were prepared in a 96/well microtiter plate over the range of 1500–0.25 µg/ml in inoculated nutrient broth (the final volume 100 µl and the final bacterial concentration was 10^6 CFU/ml in each well). Two growth controls consisting of medium with methanol (negative control) and medium with tetracycline (positive control) were also included. The microbial growth was determined by absorbance at 620 nm using the universal microplate reader (ThermoLabsystems, Multiskan EX, Software for Multiscan, ver. 2.6.). MIC was defined as the lowest concentration of test samples at which microorganisms showed no visible growth. The *MBC* is defined as the lowest concentration of the test samples at which 99.9% of inoculated microorganisms were killed.

Statistical analysis

All the experiments were performed in triplicate. Values are presented as means ± standard deviation. Significant differences were determined by analysis of variance (ANOVA), followed by the Tukey's test.

RESULTS AND DISCUSSION

Phenol content of fruit and leaf extracts

The results of the spectrophotometric analysis of Cornelian cherry fruit and leaf extracts are shown in Table 1.

Leaf extracts showed significant higher total phenol, hydroxycinnamoyl acid and flavonol content than fruit extracts. On the other hand fruit extracts were rich in anthocyanin content. Also, there were no significant differences in phenolic content during two consecutive seasons. Others also found significant phenol and anthocyanin content in Cornelian cherry fruits [14,15]. Some authors found higher total phenolic content [18] and others lower in Cornelian cherry leaf extracts [19]. This can be explained by different genotypes, environmental conditions and extraction procedures.

In order to determine more accurately phenolic content and composition in investigated extracts, the HPLC method was used. The selected method allows analysis of extracts without changing the chromatographic conditions by recording at 280, 320, 360 and 520 nm on DAD detector and at 275/322 nm (*Ex*/*Em*) on a fluorescent detector. Results (Table 2) are in good agreement with those obtained by spectrophotometric determination (Table 1). The results showed quite various phenolic compositions, which belong mainly to the following phenol classes: phenolic acids, flavonols, flavan-3-ols and anthocyanins (Table 2).

Few data exist about phenol acid, flavonol and anthocyanin composition [6,14,15] and there are no studies about flavan-3-ol composition in Cornelian cherry fruits except in previously described study for the acidified methanol extracts [9]. The (+)-catechin was predominant falavan-3-ol in fruit extracts, followed by (–)-epicatechin and procyanidin B2, while in leaf extracts (–)-epicatechin was predominant and procyanidin B2 was not found. The presence of these compounds was reported by Vagiri *et al*. in blackcurrant leaf extracts [20] and Buricova *et al*. in blackberry and raspberry leaf extracts [8].

Fruit extract showed slightly higher amount of phenol acids than leaf extracts. Ellagic acid was predominant phenol acid in all extracts, followed by chlorogenic and gallic acids. Others also reported the presence of gallic and ellagic acids in cornelian cherry fruit [6].

Leaf extracts showed significant higher amount of flavonol than fruit extracts. Flavonol compounds found in tested extracts were quercetin-3-glucoside, rutin, quercetin-3-galactoside, luteolin-3-glucoside and kaempferol-3-glucoside. Some authors reported the presence of quercetin and kaempferol derivates in Cornelian cherry fruit extracts [6,14]. The kaempferol-3--glucoside and rutin were predominant flavonols in fruit extracts while quercetin-3-glucoside was less abundant and luteolin-3-glucoside was not detected. On the other hand quercetin-3-glucoside was predominant flavonol in leaf extracts followed by rutin, kaempferol-3-glucoside and luteolin-3-glucoside. The high concentration of quercetin and kaempferol in leaves of *Rosa* L. species was reported [7] and also for *Rubus* L. [8,21].

Table 1. Total phenol, hydroxycinnamoyl acid and flavonol contents (mg/g DM) and radical scavenging activity, EC_{50}, of Cornelian cherry fruit and leaf extracts determined by spectrophotometric analysis; Data are expressed as mean ± SD (n = 3); nd – not detected; means in the same column bearing different superscripts are significantly different (p < 0.05), as analyzed by the Tukey's test

Extract	Year	Total phenols	Hydroxy-cinnamoyl acids	Flavonols	Anthocyanins	EC_{50} / mg ml^{-1}
Fruit	2012	89.89±0.45^b	4.45±0.06^a	4.17±0.08^b	15.5±0.18^b	1.09±0.50^b
	2013	91.12±0.59^b	4.33±0.06^a	4.29±0.08^b	16.1±0.27^b	0.94±0.34^b
Leaf	2012	112.91±1.40^a	4.17±0.08^a	32.77±0.19^a	nd	0.58±0.13^a
	2013	117.34±1.40^a	4.23±0.16^a	35.19±0.32^a	nd	0.47±0.09^a

Table 2. Phenol composition (mg/g DM) of Cornelian cherry fruit and leaf extracts determined by HPLC analysis; data are expressed as mean ± SD (n = 3); nd – not detected; means in the same row bearing different superscripts are significantly different (p < 0.05), as analyzed by the Tukey's test

Phenolic compound	Fruit		Leaf	
	2012	2013	2012	2013
Gallic acid	0.57±0.08[a]	0.62±0.10[a]	0.41± 0.02[b]	0.37± 0.04[b]
Ellagic acid	2.08±0.15[b]	2.11±0.13[b]	2.55±0.04[a]	2.62±0.11[a]
Chlorogenic acid	0.87±0.14[a]	0.85±0.11[a]	0.28±0.03[b]	0.33±0.07[b]
Σ Phenolic acids	3.52±0.12[a]	3.58±0.11[a]	3.24±0.05[a]	3.32±0.08[a]
Quercetin-3-glucoside	0.22±0.06[b]	0.20±0.04[b]	9.28±0.21[a]	9.37±0.33[a]
Quercetin-3-galactoside	0.54±0.07[a]	0.57±0.09[a]	nd	nd
Rutin	0.76±0.11[b]	0.81±0.12[b]	6.11±0.11[a]	6.09±0.23[a]
Luteolin-3-glucoside	nd	nd	0.11±0.01a	0.15±0.04a
Kaempferol-3-glucoside	1.06±0.24[b]	1.11±0.20[b]	4.27±0.10[a]	4.37±0.19[a]
Σ Flavonols	2.58±0.16[b]	2.69±0.15[b]	19.77±0.11[a]	19.98±0.22[a]
(+)-Catechin	3.95±0.77[a]	3.91±0.68[a]	2.22±0.07[b]	2.28±0.11[b]
(–)-Epi-catechin	2.02±0.64[b]	2.11±0.71[b]	4.07±0.15[a]	4.15±0.14[a]
Procyanidin B2	1.61±0.34[a]	1.55±0.28[a]	nd	nd
Σ Flavan-3-ols	7.58±0.51[a]	7.57±0.42[a]	6.29±0.11[b]	6.43±0.13[b]
Cyanidin 3-galactoside	3.21±0.14[a]	3.27±0.12[a]	nd	nd
Pelargonidin 3-glucoside	10.16±0.94[a]	10.23±1.03[a]	nd	nd
Delphinidin-3-galactoside	0.49± 0.12[a]	0.53± 0.16[a]	nd	nd
Σ Anthocyanins	13.86±0.46[a]	14.03±0.67[a]	nd	nd

Cyanidin-3-galactoside, pelargonidin-3-glucoside and delphinidin-3-galactoside were anthocyanins which were found only in fruit extracts (Table 2). Our results of the anthocyanin qualitative composition were similar with those previously described [6,14]. Pelargonidin-3-glucoside was the predominant anthocyanin, followed by cyanidin-3-galactoside. Delphinidin-3-galactoside was the least abundant one and present only in 3%. The seasonal differences in the anthocyanin composition of fruit extracts can be explained by environmental conditions during the fruit development [11].

Radical scavenging activity of fruit and leaf extracts

Radical scavenging activity of investigated extracts was estimated by the DPPH test. The results are shown in Table 1, expressed as EC_{50} values (mg/ml). Lower EC_{50} values correspond to higher radical scavenging activity of extracts. All extracts showed strong radical scavenging activity, ranged from 0.47±0.09 for leaf to 1.09±0.50 mg/ml for fruit extracts. Leaf extracts showed higher radical scavenging activity than fruit extracts. Strong radical scavenging activity of leaf extracts, corresponding to their high phenol content, suggests that the phenolic compounds at least partially are responsible for the strong radical scavenging activity of these extracts. The significant correlation was found between radical scavenging activity and total phenol content (R^2 = 0.9832). The literature data also confirm the presence of correlation between radical scavenging activity and total phenol content of Cornelian cherry extracts [6,15–17]. We also found correlation between radical scavenging activities and the individual classes of phenols, but lower than with total phenol content (flavonols) and negative correlation for flavan-3-ols and phenolic acids. The HPLC analysis showed that extracts of fruit and leaf are a wide mixture of phenolic, and other compounds such as ascorbic acid and carotenoids not identified in this study. It is possible that these constituents may interact to produce synergistic or antagonistic antioxidant effects with each other and with other compounds [7,22].

Antimicrobial activity of fruit and leaf extracts

The antimicrobial activity data for all investigated extracts and tetracyclin – antibiotic (positive control) against 13 microbial species are given in Tables 3 and 4 (inhibition zones and *MIC*/*MBC* values). Methanol (negative control) did not show any inhibitory effects on the 13 microbial species. All extracts tested by disc diffusion method showed significant antimicrobial activity against Gram-positive, Gram-negative strains and yeast (Table 3). The leaf extracts showed higher antimicrobial activity than fruit extracts. Antimicrobial activity of these extracts can be connected with their high total phenol content. The existing correlation between total phenol content and antimicrobial activity of plant extracts also was reported by others [3–5]. There are some reports about quite different antimicrobial acti-

Table 3. Antimicrobial activities (inhibition zone diameters, mm) of fruit leaf extracts (50 µl/disc) and reference antibiotics (30 µg/disc) against Gram-positive strains, Gram-negative strains and yeast; data are expressed as mean ± SD (n = 3); Te. – tetracyclin; nd – not detected

Strain	Fruit		Leaf		Te.
	2012	2013	2012	2013	
Gram-positive strains					
Clostridium perfringens	14.4±2.0	14.7±1.3	19.2±1.3	19.5±1.2	29.0±2.0
Bacillus cereus	15.3±1.2	15.9±1.0	18.8±1.3	18.7±1.1	23.9±1.0
Staphylococcus aureus	16.5±2.0	16.7±1.4	18.2±1.2	18.6±1.1	18.5±1.3
Listeria monocytogenes	15.1±1.8	15.5±1.1	16.1±1.3	16.7±1.4	18.7±1.2
Sarcina lutea	16.7±1.8	16.9±1.7	17.0±1.4	17.5±1.2	20.0±1.2
Micrococcus flavus	14.3±1.8	14.1±1.5	15.2±1.1	15.9±1.3	23.6±0.7
Gram-negative strains					
Escherichia coli	13.8±0.9	14.2±0.5	14.1±1.2	14.5±0.9	23.2±1.2
Pseudomonas aeruginosa	12.6±2.4	12.7±1.4	15.6±1.3	15.9±1.2	20.8±1.5
Salmonella enteritidis	14.3±3.1	14.6±2.3	15.2±1.1	15.2±1.5	23.3±1.3
Shigella sonnei	15.4±2.5	15.8±2.0	17.6±1.3	17.8±1.1	31.1±0.8
Klebsiella pneumoniae	12.49±1.1	13.01±1.3	16.6±1.1	16.9±1.2	23.6±0.6
Proteus vulgaris	14.4±1.9	14.6±1.5	16.0±1.2	16.3±1.1	16.0±1.2
Yeast					
Candida albicans	14.7±2.2	14.7±2.2	15.1±1.0	15.3±1.1	19.2±0.5

vity of Cornelian cherry fruit extracts in different solvent [18,19]. This can be explained by using different extraction conditions and also with the fact that the disc diffusion test can give us approximate results of antimicrobial activity of these extracts. In order to know *MIC*/*MBC* values of (Table 4) we used a more precise broth microdilution method. Investigated extracts were meanly more sesitive on Gram-positive strains compared to Gram-negative strains and yeast, which is in agreement with literature data [9,18,19]. *Sarcina lutea, Listeria Monocytogenes* and *Staphylococcus aureus* were the most sensitive Gram-positive strains, and *Shigella sonnei* and *Salmonella enteritidis* Gram-negative strains for the most investigated Cornelian cherry fruit and leaf extracts.

CONCLUSION

Both methods, spectrophotometric and HPLC confirmed high phenol content in all examined Cornelian cherry fruit and leaf extracts. There were no significant differences in phenolic content during two consecutive seasons. These compounds are responsible for significant antioxidant and antimicrobial activities of fruit and leaf extracts. In this paper, flavan-3-ols were reported for the first time in both, fruit and leaf extracts of Cornelian cherries as well as antimicrobial activity of leaf extracts against 13 species of bacteria strains and yeast. Extracts of the leaves contain considerably more flavonols than fruit extracts. Leaf extract showed higher phenolic content, antiradical and antimicrobial activity than fruit extracts. This allows further work on the combination of different extracts, *i.e.*, phenol compounds in order to obtain the extract with a stronger antimicrobial and antioxidant potential. Simple extraction procedure of these compounds from fruit and leaves opens the possibility for application in the food and pharmaceutical industry.

Table 4. Antibacterial (MIC)/bactericidal (MBC) activities (µg/ml) of fruit berry leaf extracts and reference antibiotic against Gram-positive strains, Gram-negative strains and yeast; Te. – tetracyclin

Strain	Fruit		Leaf		Te.
	2012	2013	2012	2013	
Gram-positive strains					
Clostridium perfringens	63/125	63/63	31/31	16/31	0.9/0.9
Bacillus cereus	31/63	31/63	31/63	31/31	0.9/0.9
Staphylococcus aureus	63/63	31/63	16/31	16/31	0.12/0.9
Listeria monocytogenes	63/63	63/63	16/16	16/16	0.46/0.9

Table 4. Continued

Strain	Fruit		Leaf		Te.
	2012	2013	2012	2013	
Gram-positive strains					
Sarcina lutea	31/31	31/31	16/31	16/31	0.06/0.06
Micrococcus flavus	125/125	63/125	63/63	63/63	0.4/0.9
Gram-negative strains					
Escherichia coli	125/250	125/250	125/250	125/250	3.8/7.5
Pseudomonas aeruginosa	250/250	250/250	63/125	63/125	7.5/7.5
Salmonella enteritidis	63/125	63/63	63/125	63/125	0.9/1.9
Shigella sonnei	125/125	125/125	31/125	31/63	0.06/0.12
Klebsiella pneumoniae	125/125	63/125	63/125	63/125	0.9/1.9
Proteus vulgaris	125/250	125/250	63/125	63/63	0.9/1.9
Yeast					
Candida albicans	250/500	250/500	125/250	125/250	16/16

Acknowledgements

The present research was supported by the EU, FP7 - Regpot 2007-3-01, the project "Chromlab-Antioxidant", No. 204756, and by the Ministry of Education, Science and Technological Development of the Republic of Serbia, projects Nos. 34012, 31020 and 176006.

REFERENCES

[1] T. Ryan, J. Wilkinson, H.M.A. Cavanagh, Antibacterial activity of raspberry cordial *in vitro*, Res. Vet. Sci. **71** (2001) 155–159.

[2] P.R. Venskutonis, A. Dvaranauskaite J. Labokas, Radical scavenging activity and composition of raspberry (*Rubus idaeus*) leaves from different locations in Lithuania, Fitoterapia **78** (2007)162–165.

[3] E. Yeşilada, E. Sezik, G. Honda, Y. Takaishi, Y. Takeda, T. Tanaka, Traditional medicine in Turkey IX: Folk medicine in north-west Anatolia, J. Ethnopharmacol. **64** (1999) 195–210.

[4] R. Puupponen-Pimia, L. Nohynek, H.L. Alakomi, K.M. Oksman-Caldentey, The action of berry phenolics against human intestinal pathogens, BioFactors **23** (2005) 243–251.

[5] L. Ördögh, L. Galgóczy, J. Krisch, T. Papp, C. Vágvölgyi, Antioxidant and antimicrobial activities of fruit juices and pomace extracts against acne-inducing bacteria, Acta Biol. Szegediensis **54** (2010) 45-49.

[6] K. Pyrkosz-Biardzka, A.Z. Kucharska, A. Sokół-Łętowska, P. Strugała, J. Gabrielska. A Comprehensive Study on Antioxidant Properties of Crude Extracts from Fruits of *Berberis vulgaris* L., *Cornus mas* L. and *Mahonia aquifolium*, Nutt. Pol. J. Food Nutr. Sci. **64** (2014), DOI: 10.2478/v10222-012-0097-x, in press.

[7] R. Nowaka, U. Gawlik-Dzikib, Polyphenols of *Rosa* L. Leaves Extracts and their Radical Scavenging Activity, Z. Naturforsch **62c** (2007) 32–38.

[8] L. Buricova, M. Andjelkovic, A. Cermakova, Z. Reblova, O. Jurcek, E. Kolehmainen, R. Verhe, F. Kvasnicka, Antioxidant capacities and antioxidants of strawberry, blackberry and raspberry leaves, Czech. J. Food Sci. **29** (2011) 181–189.

[9] B.C. Radovanović, A.S. Milenković-Anđelković, A.B. Radovanović, M.Z. Anđelković, Antioxidant and Antimicrobial Activity of Polyphenol Extracts from Wild Berry Fruits grown in Southeast Serbia, Trop. J. Pharm. Res. **12** (2013) 813–819.

[10] B. Radovanovic, A. Radovanovic, J.M. Souquet, Phenolic profile and free radical-scavenging activity of Cabernet Sauvignon wines of different geographical origins from the Balkan region, J. Sci. Food Agric. **90** (2010) 2455––2461.

[11] M. Andjelkovic, B. Radovanovic, A. Radovanovic, A.M. Andjelkovic, Changes in Polyphenolic Content and Antioxidant Activity of Grapes cv Vranac During Ripening, S. Afr. J. Enol. Vitic. **34** (2013) 147–155.

[12] N. Deighton, R. Brennan, C. Finn, H. Davies, Antioxidant properties of domestic and wild Rubus species, J. Sci. Food Agric. **80** (2000) 1307–1313.

[13] M.M. Radojković, Z.P. Zeković, S.S. Vidović, D.D. Kočar, P.Z. Mašković, Free radical scavenging activity and total phenolic and flavonoid contents of mulberry (*Morus* spp. L., *Moraceae*) extracts, Hem. Ind. **66** (2012) 547––552.

[14] A.M. Pawlowska, F. Camangi, A. Braca, Quali-quantitative analysis of flavonoids of Cornus mas L. (Cornaceae) fruits, Food Chem. **119** (2010) 1257–1261.

[15] G.E. Pantelidis, M. Vasilakakis, G.A. Manganaris, Gr. Diamantidis, Antioxidant capacity, phenol, anthocyanin and ascorbic acid contents in raspberries, blackberries, red currants, gooseberries and Cornelian cherries, Food Chem. **102** (2007) 777–783.

[16] E. Celep, A. Aydın, H. Kırmızıbekmez, E. Yesilada, Appraisal of *in vitro* and *in vivo* antioxidant activity potential of cornelian cherry leaves, Food Chem. Toxicol. **62** (2013) 448–455.

[17] K. Savikin, G. Zdunic, T. Jankovic, T. Stanojkovic, Z. Juranic, N. Menkovic, *In vitro* cytotoxic and antioxidative activity of Cornus mas and Cotinus coggygria, Nat. Prod. Res. **23** (2009) 1731–1739.

[18] A.U. Turker, A.B. Yildirim, F.P. Karakas, Antibacterial and antitumor activities of some wild fruits grown in Turkey, Biotechnol. Biotechnol. Eq. **26** (2012) 2765–2772.

[19] J. Krisch, L. Galgoczy, M. Tolgyesi, T. Papp, C. Vagvolgyi, Effect of fruit juices and pomace extracts on the growth of Gram-positive and Gram-negative bacteria, Acta Biol. Szegediensis. **52** (2008) 267–270.

[20] M. Vagiri, A. Ekholm, S.C. Andersson, E. Johansson, K. Rumpunen, An Optimized Method for Analysis of Phenolic Compounds in Buds, Leaves, and Fruits of Black Currant (Ribes nigrum L.), J. Agric. Food Chem. **60** (2012) 10501–10510.

[21] J. Gudej, M. Tomczyk, Determination of Flavonoids, Tannins and Ellagic Acid in Leaves from *Rubus* L. Species, Arch. Pharm. Res. **27** (2004) 1114–1119.

[22] P. Iacopini, M. Baldi, P. Storchi, L. Sebastiani, Catechin, epicatechin, quercetin, rutin and resveratrol in red grape: Content, *in vitro* antioxidant activity and interactions, J. Food Comp. Anal. **21** (2008) 589–598.

IZVOD

FENOLNI SASTAV, AKTIVNOST HVATANJA DPPH RADIKALA I ANTIMIKROBNA AKTIVNOST EKSTRAKATA VOĆA I LIŠĆA DRENA (*Cornus mas*)

Ana S Milenković-Andjelković[1], Marko Z Andjelković[1], Aleksandra N Radovanović[2], Blaga C Radovanović[1] i Vesna Nikolić[3]

[1]*Univerzitet u Nišu, Prirodno-matematički fakultet, Niš, Srbija*
[2]*Univerzitet u Beogradu, Hemijski fakultet, Beograd, Srbija*
[3]*Univerzitet u Nišu, Tehnološki fakultet, Leskovac, Srbija*

(Naučni rad)

Voće je bogato različitim fenolnim jedinjenjima, koja su prepoznata kao potencijalni prirodni lekovi i koriste se u narodnoj medicini vekovima. U cilju procene fenolnog sastava, ekstrakti voća i lišća drena (*Cornus mas*) podvrgnuti su spektrofotometrijskoj i HPLC analizi. Aktivnost hvatanja (neutralizacije) DPPH radikala procenjena je pomoću DPPH testa, a antimikrobna aktivnost korišćenjem disk difuzionog testa i testa mikro-razblaženja. Svi ekstrakti su pokazali visok sadržaj fenola od 89,89±0,45 do 117,34±1,40 mg/GAE g SM ekstrakta, ali različiti sastav fenonih jedinjenja. Flavonoli, antocijani, flavan-3-oli i fenolne kiseline su bile najzastupljenije klase fenola nađene u ispitivanim ekstraktima voća i lišća. Svi ekstrakti su pokazali značajnu aktivnost hvatanja radikala i značajnu korelaciju sa ukupnim fenolnim sadržajem (R^2 = 0,9832). U svim ispitivanim ekstraktima nađena je značajna antimikrobna aktivnost u inhibiciji gram-pozitivnih, gram-negativneih sojeva i kvasca. Ekstrakti voća i lišća drena bogati fenolima, sa značajnom antiradikalnom i antimikrobnom aktivnošću, mogu se koristiti kao aditivi u hrani i lekovima.

Ključne reči: Dren • Fenoli • Antocijani Aktivnost hvatanja radikala • Antimikrobna aktivnost

Separation of mineral oil droplets using polypropylene fibre bed coalescence

Dragan D. Govedarica[1], Radmila M. Šećerov Sokolović[1], Arpad I. Kiralj[1], Olga M. Govedarica[1], Dunja S. Sokolović[2], Milica S. Hadnadjev-Kostic[1]

[1]*University of Novi Sad, Faculty of Technology, Novi Sad, Serbia*
[2]*University of Novi Sad, Faculty of Technical Sciences, Novi Sad, Serbia*

Abstract
This paper investigates the separation possibilities of model emulsion oil-in-water using polypropylene fibre bed coalescence. Experiments were carried out over a wide range of physicochemical characteristics of mineral oils, bed permeability and operating fluid velocities. The aim of this study was to analyze the influence of the dispersed oil phase nature and of the bed geometry on the separation efficiency. From the obtained results, it can be concluded that polypropylene fibers in the broadest studied range of bed permeabilities and fluid velocities, effectively separate oil that is highly polar. On the contrary, for the other two investigated oils at low values of bed permeability a region was detected in which the coalescer is incapable to operate. It has to be emphasized that the polypropylene fibres efficiently separate all three investigated oils at the highest studied bed permeability.

Keywords: oily water separation, bed coalescence, fiber material, polypropylene.

Available online at the Journal website: http://www.ache.org.rs/HI/

SCIENTIFIC PAPER

UDC 544.7:66:678.742.3

Hem. Ind. **69** (4) 339–345 (2015)

doi: 10.2298/HEMIND140322047G

Fibre bed coalescence is a separation technique that is used in the industry for the phase separation of the emulsion. When the emulsion passes through the filter media, the droplets of the dispersed phase form larger droplets that leave the bed enabling easy separation by gravity settling in the effluent stream. This separation technique has proved to be effective for the separation of oil-in-water emulsions, as well as for water-in-oil emulsion, if the droplets of the dispersed phase have diameters smaller than 100 µm.

For the bed formation of filter media in coalescers, the fibres with high and low surface energy can be used [1-–10]. Glass fibres, stainless steel fibres and ceramic fibres are used as high surface energy materials, whereas polypropylene, polyurethane, polyethylene terephthalate, polybutylene terephthalate, nylon and teflon are most commonly used as materials with low surface energy. For the separation of the dispersed oil, the polymer fibres are most frequently applied. Polypropylene is extensively employed in the industry due to low cost and wide production of fibres with various diameters, which are broadly available as waste. Additional reasons for the application of this material are the highly desired properties, such as: high strength and elasticity, fatigue resistance, as well as chemical stability [11–16].

Correspondence: D. Govedarica, Faculty of Technology, University of Novi Sad, Bulevar cara Lazara 1, 21000 Novi Sad, Serbia.
E-mail: dragang@uns.ac.rs
Paper received: 22 March, 2014
Paper accepted: 27 May, 2014

Wei *et al*. [17] analyzed the wettability of polypropylene by injecting low-viscosity oil with a micro-injector onto the surface of fibres. They concluded that polypropylene fibres had a hydrophobic surface, while the wetting angle of the investigated oil was less than 20°, indicating the affinity of this surface to oil.

Li and Gu [18] have studied the phenomenon of bed coalescence of the emulsion oil-in-water using polypropylene and nylon. They concluded that the smaller diameter of polypropylene fibres are, the greater the efficiency of the separation is. However, the authors ignored the influence of other properties of fibres, of the bed and the physical-chemical characteristics of the dispersed oil phase.

Clayfield *et al*. [19] have investigated the mechanisms of fibre bed coalescence for polypropylene and other polymeric materials. The experiments were carried out using the vertically upward orientation of the emulsion flow. They concluded that the coalescence efficiency strongly depends on the mechanisms of droplet coalescence on the surface of the fibres. Hughes [20] analyzed the emulsion separation of crude oil and kerosene in the water using the bed formed of pure polypropylene and polypropylene fibres coated with a layer of silane. He concluded that the efficiency of separation dominantly depends on the interaction between drops and fibres.

Kulkarni *et al.* [16] have added polypropylene nanofibres to the bed of glass fibres. They investigated the separation efficiency of water from oil and concluded that the polypropylene fibres due to different values of the wetting angle in relation to the glass fibres consi-

derably influence the separation efficiency of the water droplets. The same authors [3] examined the possibility for separation using the filter media composed of glass, polypropylene and polyester fibres. They concluded that this combination of filter media can provide high coalescence efficiency.

In this study the separation possibilities of oil droplets in water with different dispersed oil phase nature, using polypropylene fibre bed was investigated. In addition to changing the nature of the oil phase, the bed geometry of polypropylene fibres was also varied by increasing its compression. In this way, the flexibility of the polypropylene fibres application in the coalescer was also examined.

EXPERIMENTAL

Experimental device and working conditions

Experiments were carried out using the model oil-in-water emulsion and bed coalescer of polypropylene fibres. Three mineral oils of different physicochemical characteristics were investigated as the dispersed phase. The apparatus which was used for the experimental program is shown in Figure 1. The experimental device consists of a Plexiglas tube 5 cm in diameter (1) a total length of 1.2 m. The length of the polypropylene bed (2) was 5 cm. The emulsion of oil-in-water at the temperature of 20 °C was prepared in two tanks with volume of 80 litres each (3). The oil was dispersed in water by continuous stirring with stainless steel impeller (4) at a rate of 650 rpm for a period of 45 min prior to the experiment, and continuously throughout the whole duration of the experiment. In this way the average droplet diameter of 10 µm was maintained. Transport of fluid through the apparatus was initiated by the membrane dosage pump (5). After leaving the porous bed, merging of smaller droplet to larger ones was established enabling easy separation by gravity settling and collecting in the upper part of the tube, after which oil was discharged discontinuously by a valve (6). Fluid velocity, *v*, was maintained constant for 60 min. In order to measure the effluent oil concentration, a composite sample, consisting of three individual samples, was taken after 45 min at 5-min interval at the exit of the apparatus (7). Each composite sample was stabilized by the addition of concentrated hydrochloric acid. The efficiency of coalescence was monitored *via* the effluent concentration of the dispersed phase, C_i, measured by ThermoNicolet 5700 FTIR spectrophotometer. The sample preparation for FTIR analysis was performed by extraction of the oil phase from the emulsion with carbon tetrachloride. In our previous investigations [8,21,22], if the effluent oil concentration was lower than 15 mg/l, the experiments were resumed at higher fluid velocity.

All experiments were photographed attaining valuable data that simplified the analysis of the obtained results.

Properties of the oil phase

Three mineral oils of different physicochemical characteristics, containing no additives, were investigated as the dispersed phase: naphthenic crude oil (A), naphthenic-base vacuum fraction (A4), and blended petroleum product with a high paraffinic content (P1). For the analysis of physicochemical properties of the dispersed phase numerous methods and techniques were employed in order to determine: density, viscosity, relative molecular mass, interfacial tension, surface tension, pour point, neutralization number, dielectric constant and emulsivity, Table 1. The oil density was determined by SRPS ISO 12185:2004 method, oil viscosity by SRPS ISO 3104:2003 method, relative molecular mass of oil using ASTM D 2502-67, interfacial tension by ASTM D 971 method, the surface tension was determined by stalagmometric method, pour point using SRPS ISO:3016 1997 method, neutralization num-

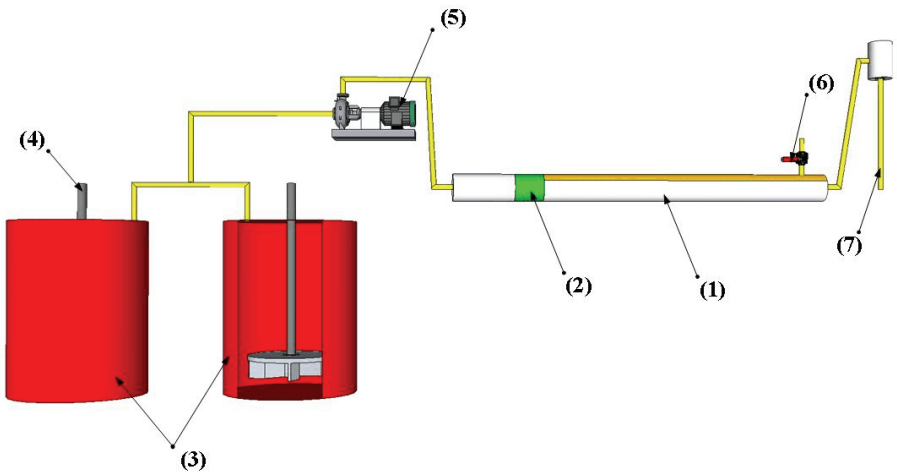

Figure 1. Scheme of experimental apparatus.

ber by SRPS ISO 6619:1994 method, the dielectric constant by EN 60247:2008 method, while emulsivity was determined by the method developed at the Central Laboratory NIS [23].

Table 1. Physicochemical properties of dispersed oil

Property	Sample		
	A	A4	P1
Density at 15 °C, kg/m^3	916.7	923.3	883.3
Density at 20 °C, kg/m^3	915.5	918.9	879.0
Viscosity at 40 °C, mPa s	43.350	168.904	10.316
Neutralization number mg KOH/l	1.42	1.71	0.13
Pour point, °C	–42	–3	+3
Interfacial tension, mN/m	18.8	30.5	32.4
Surface tension, mN/m	26.56	27.72	30.16
Emulsivity, vol.%	99.92	70.00	54.17
Dielectric constant	0.1612	0.1905	0.0645
Relative molecular mass kg/kmol	410	520	300
Distillation range, °C	150–550	315–550	320–415

Properties of the filter material

Density and the melting point were measured for the filter media, Table 2, using the pycnometer method for the density and the DSC method for the melting point.

Bed permeability, K_0, was experimentally determined using the Darcy test and presented in Table 3 [24].

Table 2. Properties of filter media

Material	Density, kg/m^3	Melting point, °C
Polypropylene	900	168.60

Table 3. Polypropylene fibre bed permeability (10^{-9} m^2)

Material	Bed permeability				
Polypropylene	K_{01}	K_{02}	K_{03}	K_{04}	K_{05}
	5.389	2.426	1.128	0.380	0.180

RESULTS AND DISCUSSION

Analysis of the results from the coalescence filtration was performed based on the 3D plots representing the interdependence of the effluent oil concentration, bed permeability and the fluid velocity.

The dependence of the effluent concentration and fluid velocity was investigated at five different permeabilities for all three oils. Since the experiments were performed in a wide range of fluid velocity, the effluent oil concentration dependence on velocity was exponential for all operating conditions.

For the investigation of oil coalescence using the polypropylene fibre bed, mineral oils with a wide range of physicochemical characteristics were selected. The experiments were carried out also in a broad range of the following parameters: viscosity (10.316–168.904 mPa s), density (879–918.9 kg/m^3), neutralization number (0.13–1.71 mg KOH/l), interfacial tension (18.8–32.4 mN/m), surface tension (26.56–30.16 mN/m), emulsivity (54.17–99.92 vol.%) and relative molecular mass (300–520 kg/kmol).

During the separation of oil A, low values of the effluent concentration were observed at fluid velocities below 50 m/h and in the whole range of bed permeability, Figure 2. The region where the effluent concentration is lower than 15 mg/l is wide. Figures 3 and 4 present the dependence of the effluent concentration on the fluid velocity and bed permeability for oils A and P1. The plots illustrate the region of fluid velocity and bed permeability corresponding to the effluent concentration above 15 mg/l. It should be noticed that this region corresponds to the lowest bed permeability and low fluid velocity, contributing thus to a drastic increase in the effluent concentration. In our previously published papers [8,21,22,25] this region is defined as the critical bed permeability and is the region unsuitable for the coalescer. The absence of the critical permeability region was only observed for oil A. Therefore, it is necessary to give an explanation of why the effluent concentration does not change during the separation of oil A at low bed permeability values.

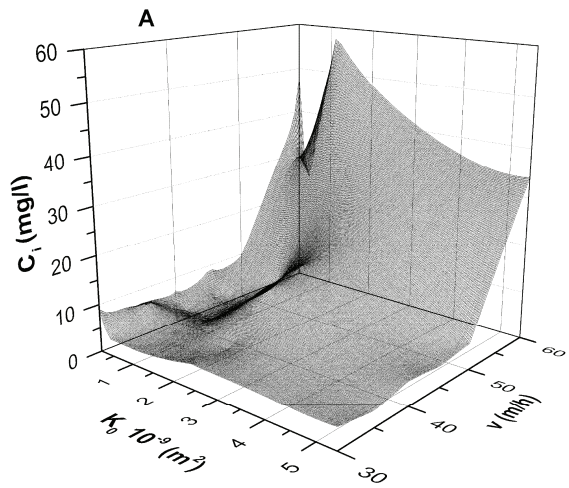

Figure 2. 3D dependence of effluent oil concentration on velocity and fibre bed permeability for oil A.

The region favourable for efficient separation for oil A4 is narrower (K_0 = (0.380–5.389)×10^{-9} m^2 and v = 30–50 m/h) compared to the region of the oil A (K_0 = (0.180–5.389)×10^{-9} m^2 and v = 30–50 m/h). However, this region is significantly wider compared to the region of oil P1 (K_0 = (2.426.180–5.389)×10^{-9} m^2 and v = 19–40

m/h). Remarkably, polypropylene fibres have the lowest separation efficiency for oil P1, since the operating range is extremely narrow. Therefore, it is also necessary to explain why this phenomenon occurs just with oil P1. From the results, it can be concluded that polypropylene fibres show significant sensitivity to changes in the nature of the dispersed oil phase. This is a disadvantage for the coalescer bed material.

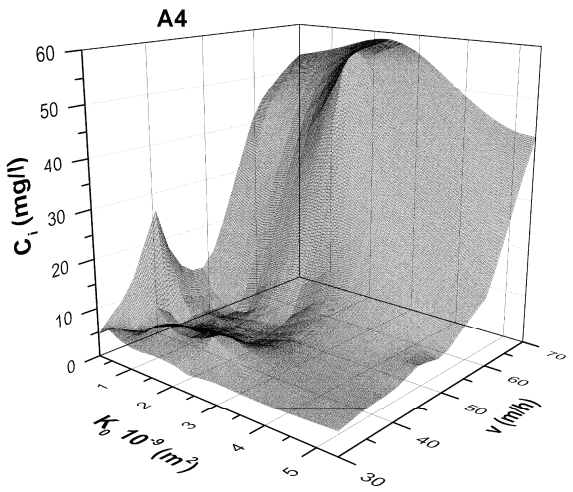

Figure 3. 3D dependence of effluent oil concentration on velocity and fibre bed permeability for oil A4.

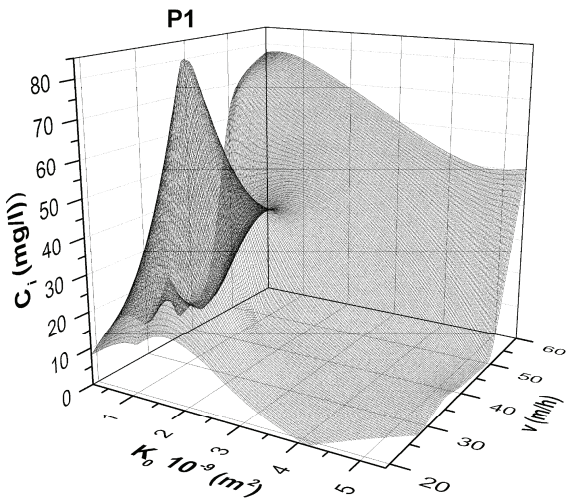

Figure 4. 3D dependence of effluent oil concentration on velocity and fibre bed permeability for oil P1.

During the passing of the emulsion through the fibre bed several coalescence mechanisms simultaneously take place: coalescence between the droplets in the bed pores, droplets coalescence on the surface of the fibres and droplets coalescence into the surface of the capillary-conducted oil phase. In addition coalescence of the droplets takes place after leaving the bed forming the oil continuous phase [26]. It is safe to assume that all the mentioned mechanisms always occur during the separation of any oil, but their rate varies. Which of these coalescence mechanisms will predominate depends significantly on the properties of the oil phase, on the nature of the fibres, as well as on their mutual influence and bed permeability.

Based on presented 3D plots for all three oils it can be observed that at the highest bed permeability the maximum fluid velocity not exceeding the effluent concentration of 15 mg/l is achieved. At the highest bed permeability the pore diameters, as well as the total bed porosity, is the highest, and therefore consequently the interstitial velocity in such pores is the lowest. Also, due to the high porosity, a significant amount of capillary-conducted phase is formed. In such cases the oil droplets coalescence on the surface of the capillary-conducted phase is favoured becoming the dominant mechanism of coalescence. Spielman and Goren concluded that the oil amount in the form of the capillary-conducted phase and the presence of high porosity bed in a steady state ranges from 30 to 40% of the total pore volume [27]. Flowing of the emulsion through the bed and the distribution of the capillary-conducted phase at the cross-section of the device in the horizontal fluid flow orientation is predominantly influenced by the density and viscosity of the dispersed phase, the bed geometry and the intensity of the hydrodynamic forces [9]. When the bed permeability is low, the intensity of the hydrodynamic forces is the highest because the pore diameter is the lowest and the bed is highly compressed. In these conditions there is a minimum amount of the capillary-conducted phase in the bed leading to the increase of effluent concentration for the oils A4 and P1. As already mentioned, the region of the critical bed permeability for the oil A does not exist. This could be explained by the domination of the following coalescence mechanisms: coalescence of the droplets on the fibres surface, and/or the coalescence of the adjacent droplets in the pore space. The release of enlarged droplets from the downstream side of the fibre bed was photographed in all experiments. Furthermore, the efficiency of fibre bed coalescence was evaluated using image analysis. The appearance, the shape, the amount and the colour of the oil formed after leaving the fibre bed differs for all three oils. For the oil P1 after leaving the polypropylene bed, the phase inversion occurs and water droplets wrapped with a thin layer of oil were detected leading to the formation of the double emulsion, Figure 5. From the downstream side of the polypropylene fibre bed, these droplets of different diameters were retarded at the continuous oil/water interface. It is important to note that the formation of the dual emulsion was not observed for the other two oils. The agglomeration of water droplets wrapped with oil P1 was detected. Also, stratification of droplets that leave the bed occurs leading to the formation of the hexagonal structure of

agglomerated drops. The largest agglomerates are retained at the interface, while smaller droplets leaving the bed are located the farthest from the phase interface. It can be assumed that the coalescence of released droplets from the downstream side of the bed is not efficient. Furthermore, it may be the main reason for the limited success of oil P1 coalescence. The cause may be due to the poor separation efficiency of droplets for oil P1 with polypropylene fibres. It is interesting to note that when membrane pump was turned off, quick destruction of agglomerated droplets occurred and separation of oil in the continuous oil phase was observed. This phenomenon can be explained by the cracking of the oil film around the water droplets when the effect of hydrodynamic forces is eliminated.

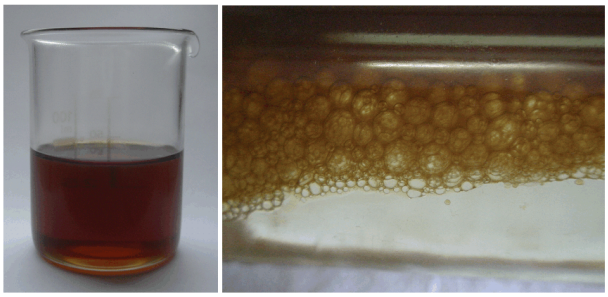

Figure 5. Mineral oil P1 before experiment and after separation of emulsion using polypropylene fibre bed.

In order to form a continuous oil phase from the downstream side of the bed, phase inversion is needed. It is considered that the conditions for the occurrence of the inversion phase are reached when the concentration of dispersed droplets is around 75%. This would imply that the phase inversion during the separation process occurs for all three oils, but is observed only for the oil P1. It is clear that the coalescence of the oil P1 is considerably slower than A and A1. Figure 6 shows the layer of oil at the outlet of the bed. This layer is formed of the capillary-conducted phase dislocated from the fibre bed. From this layer of oil, larger droplets were detached and formed a continuous oil phase in the settling zone. This coalescence mechanism was also observed by other authors [27]. The polypropylene fibres most efficiently separate oil A over a wide range of bed permeabilities. Therefore, it can be assumed that the mentioned mechanism contributes to higher coalescence efficiency.

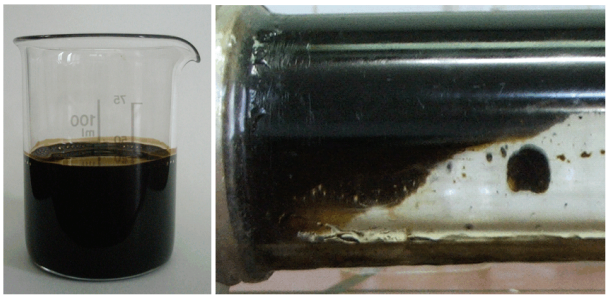

Figure 6. Mineral oil A before experiment and after separation of emulsion using polypropylene fibre bed.

In the case of oil A4 (Figure 7) the change in colour of oil phase, as well as changes in the oil structure leaving the bed were observed. The observations suggest that oil A4 emulsifies when passing through the bed of polypropylene fibres and that a small amount of water is retained in this oil.

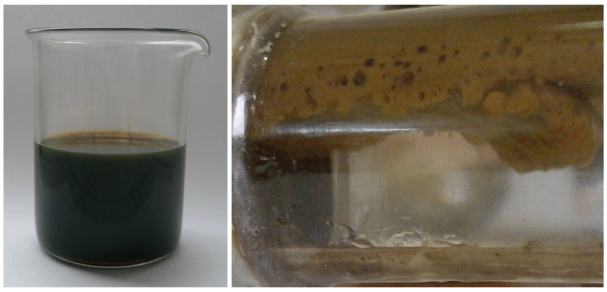

Figure 7. Mineral oil A4 before experiment and after separation of emulsion using polypropylene fibre bed.

Analysing the properties of the investigated oils the following can be pointed out: oil A has an average value of the density, viscosity and relative molecular mass. But oil A has the highest value of emulsivity and neutralization number. According to the mentioned properties oil A has the highest polarity suggesting that such a feature of oil is favoured when working with polypropylene fibres. Since the mineral oils are a complex mixture of many compounds, droplets are chemically heterogeneous in nature. Furthermore, in the composition of the mineral oils, there are also natural surfactants that are measurable through the emulsivity and neutralization number.

CONCLUSION

During the separation of oil A using the polypropylene fibre bed, low values of the effluent concentration were observed at fluid velocities below 50 m/h and at the whole range of studied bed permeabilities. For oils A4 and P1 a region in which the effluent concentration rises steeply at lower values of bed permeability was detected. This region is defined as the critical bed permeability and is the region in which the coalescer is incapable to operate. It was determined that the polypropylene fibres have the lowest separation efficiency for oil P1, since the operating range is extremely narrow. It can be concluded that polypropylene fibres show significant sensitivity to changes in the nature of the dispersed oil phase. This phenolmenon is a disadvantageous for the material used for coalescence.

Acknowledgement

The research in this paper was carried out in the framework of the project number 172022, funded by the Ministry of Education, Science and Technological Development of Republic of Serbia.

REFERENCES

[1] S. Bansal, V. von Arnim, T. Stegmaier, H. Planck, Effect of fibrous filter properties on the oil-in-water-emulsion separation and filtration performance, J. Hazard. Mater. **190** (2011) 45–50.

[2] S. Agarwal, V. von Arnim, T. Stegmaier, H. Planck, A. Agarwal, Role of suface wettability and roughness in emulsion separation, Sep. Purif. Technol. **107** (2013) 19––25.

[3] P.S. Kulkarni, S.U. Patel, G.G. Chase, Layered hydrophilic/hydrophobic fiber media for water-in-oil coalescence, Sep. Purif. Technol. **85** (2012) 157–164.

[4] G. Viswanadam, G.G. Chase, Water–diesel secondary dispersion separation using superhydrophobic tubes of nanofibers, Sep. Purif. Technol. **104** (2013) 81–88.

[5] S. Agarwal, V. von Arnim, T. Stegmaier, H. Planck, A. Agarwal, Effect of fibrous coalescer geometry and operating conditions on emulsion separation, Ind. Eng. Chem. Res. **52** (2013) 13164−13170.

[6] D.D. Govedarica, R.M. Šećerov Sokolović, D.S. Sokolović, S.M. Sokolović, A novel approach for the estimation of the efficiency of steady-state fiber bed coalescence, Sep. Purif. Technol. **104** (2013) 268–275.

[7] D.D. Govedarica, R.M. Šećerov Sokolović, D.S. Sokolović, S.M. Sokolović, Evaluation of the separation of liquid−liquid dispersions by flow through fiber beds, Ind. Eng. Chem. Res. **51** (2012) 16085−16091.

[8] R. Šećerov Sokolović, T.J. Vulić, S.M. Sokolović, R.P. Marinković Nedučin, Effect of fibrous bed permeability on steady-state coalescence, Ind. Eng. Chem. Res. **42** (2003) 3098–3102.

[9] R.M. Šećerov Sokolović, D.D. Govedarica, D.S. Sokolović, Separation of oil-in water emulsion using two coalescers of different geometry, J. Hazard. Mater. **175** (2010) 1001–1006.

[10] R. Šećerov Sokolović, S. Sokolović, S. Šević, Oily water treatment using a new steady-state fiber-bed coalescer, J. Hazard. Mater. **162** (2009) 410–415.

[11] S.S. Sareen, P.M. Rose, R.C. Gudesen, R.C. Kintner, Coalescence in fibrous beds, AIChE J. **12** (1966) 1045––1050.

[12] J.N. Chieu, E.F. Gloyna, R.S. Schechter, Device for evaluating coalescence of oil emulsions, J. Environ. Eng. Div. (Am. Soc. Civ. Eng.) **103** (1977) 163–175.

[13] H. Sharifi, J.M. Shaw, Secondary drop production in packed-bed coalescers, Chem. Eng. Sci. **51** (1996) 4817––4826.

[14] E.J. Clayfield, A.G. Dixon, A.W. Foulds, R.J.L. Miller, The coalescence of secondary dispersions. I. The effect of wettability and surface energy, J. Colloid Interface Sci. **104** (1985) 500–511.

[15] S.U. Patel, P.S. Kulkarni, S.U. Patel, G.G. Chase, The effect of surface energy of woven drainage channels in coalescing filters, Sep. Purif. Technol. **87** (2012) 54–61.

[16] P.S. Kulkarni, S.U. Patel, S.U. Patel, G.G. Chase, Coalescence filtration performance of blended microglass and electrospun polypropylene fiber filter media, Sep. Purif. Technol. **124** (2014) 1–8.

[17] Q. Wei, Y. Liu, X. Wang, F. Huang, Dynamic studies of polypropylene nonwovens in environmental scanning electron microscope, Polym. Test. **26** (2007) 2–8.

[18] J. Li, Y. Gu, Coalescence of oil-in-water emulsions in fibrous and granular beds, Sep. Purif. Technol. **42** (2005) 1–13.

[19] E.J. Clayfield, A.G. Dixon, A.W. Foulds, R. J. Lionel Miler, The coalescence of secondary dispersions: I. The effect of wettability and surface energy, J. Colloid Interface Sci. **104** (1985) 500–511.

[20] V.B. Hughes, A.W. Foulds, Coalescence of oil-in-water emulsions: development of a novel fibrous bed coalescer using surface treated polypropylene fibres, in Proc. of 4th World Filtration Congress, Revised Edition – Proceedings, Ostende, Belgium, 1989, pp. 11.13–11.25.

[21] R. Šećerov Sokolović, T.J. Vulić, S.M. Sokolović, Effect of bed length on steady-state coalescence of oil-in-water emulsion, Sep. Purif. Technol. **56** (2007) 79−84.

[22] R. Šećerov Sokolović, T.J. Vulić, S.M. Sokolović, Effect of fluid flow orientation on the coalescence of oil droplets in steady- state bed coalescers, Ind. Eng. Chem. Res. **45** (2006) 3891−3895.

[23] S. Šević, Influence of Formation Water on Production and Transport of Petroleum and Natural Gas (Uticaj ležišne vode na proizvodnju i transport nafte i gasa); DIT NIS-Naftagas: Novi Sad, 2000, pp. 207−235.

[24] O. Stanimirović, Fluiddynamics and Coalescence in Porous Beds Contactors (Fluidodinamika i koalescencija u kontaktoru sa poroznim slojem) M. S. Thesis, University of Novi Sad, Faculty of Technology, Novi Sad, 2003.

[25] T. Vulić, The effect of bed permeability and fluid flow orientation on emulsion coalescence in porous bed (Uticaj permeabilnosti sloja i orijentacije toka fluida na koalescenciju emulzije u poroznom sloju) M. S. Thesis, University of Novi Sad, Faculty of Technology, Novi Sad, 2000.

[26] D.D. Govedarica, Fiber Bed Coalescence of Mineral Oil (Koalescencija mineralnih ulja u vlaknastom sloju), Ph.D. Dissertation, University of Novi Sad, Faculty of Technology, Novi Sad, 2011.

[27] L.A. Spielman, S.L. Goren, Progress in induced coalescence, and a new theoretical framework for coalescence by porous media, Ind. Eng. Chem. **62** (1970) 10−24.

IZVOD

SEPARACIJA KAPI ULJA RAZLIČITE PRIRODE PRIMENOM SLOJA VLAKANA POLIPROPILENA

Dragan D. Govedarica[1], Radmila M. Šećerov Sokolović[1], Arpad I. Kiralj[1], Olga M. Govedarica[1], Dunja S. Sokolović[2], Milica S. Hadnađev-Kostić[1]

[1]*Univerzitet u Novom Sadu, Tehnološki fakultet, Novi Sad, Srbija*
[2]*Univerzitet u Novom Sadu, Fakultet tehničkih nauka, Novi Sad, Srbija*

(Naučni rad)

U ovom radu su ispitane mogućnosti separacije model emulzije ulja u vodi primenom koalescencije u sloju vlakana polipropilena. Eksperimenti su realizovani u širokom opsegu fizičko-hemijskih karakteristika mineralnog ulja, permeabilnosti sloja i radne brzine. Cilj rada bio je da se analizira uticaj promene prirode uljne faze i geometrije sloja na efikasnost separacije kroz sloj vlakana polipropilena. Promena geometrije sloja vlakana polipropilena postignuta je povećanjem njegove kompresije tj. variranjem permeabilnosti sloja. Na taj način ispitivana je fleksibilnost primene vlakana polipropilena u koalesceru. Analiza fenomena koalescencije izvršena je na osnovu 3D dijagrama zavisnosti izlazne koncentracije ulja od permeabilnosti sloja i radne brzine. Na osnovu toga su ispitani i definisani radni parametri koalescera sa horizontalnom orijentacijom proticanja koji omogućavaju efikasno izdvajanje dispergovanog ulja i postizanje izlazne koncentracije niže od 15 mg/l. Može se konstatovati da polipropilenska vlakna u najširem opsegu permabilnosti i radne brzine efikasno separišu ulje koje je izrazito polarno, ulje A. Prilikom separacija druga dva ulja, ulje A4 i P1, pojavljuje se pri niskim vrednostima permeabilnosti nepovoljna oblast za rad, to je oblast kritične permeabilnosti. U oblasti kritične permeabilnosti izlazna koncentracija naglo raste. Takođe, oblast kritične permeabilnosti je nepovoljna za rad koalescera. Fenomen kritične permeabilnosti su autori već razmatrali u svojim ranijim radovima. Polipropilenska vlakna efikasno separišu sva tri ispitivana ulja pri najvišoj permeabilnosti sloja. Kako su svi ogledi fotografisani, analiza fotografija omogućila je da se dođe nekih objašnjenja fenomena koji su uočeni. Izgled, oblik, količina i boja ulja formiranog posle sloja različita je pri radu sa ova tri ulja. Zaključeno je da mehanizmi koalescencije značajno zavise od osobina uljne faze, permeabilnosti sloja, prirode vlakana, kao i od njihovog međusobnog uticaja.

Ključne reči: Separacija zauljenih voda • Koalescencija u poroznom sloju • Vlaknasti materijal • Polipropilen

The influence of membrane composition on the release of polyphenols from liposomes

Radoslava N. Pravilović[1], Vesna S. Radunović[2], Nevenka M. Bošković-Vragolović[1], Branko M. Bugarski[1], Rada V. Pjanović[1]

[1]*Faculty of Technology and Metallurgy, University of Belgrade, Belgrade, Serbia*
[2]*Research and Development Center, Beohemija Business Group, Belgrade, Serbia*

Abstract
Polyphenols are compounds which are widely studied due to their antioxidative and potential therapeutic properties. Systems for the controlled release of drugs offer a number of benefits comparing with traditional forms of medicines and because of that these systems are widely researched. The objective of this paper is to investigate the possibility of using liposomes as carriers of polyphenols and influence of the membrane composition on the release rate of encapsulated polyphenols. Experiments show how the membrane modification affects the mass transfer comparing to a conventional liposomes. Liposomes were modified with surfactants Tween 20 and Tween 60, and thyme tea extract was used as a source of polyphenols. The diffusion of polyphenols from thyme extract, dispersion of conventional liposomes and liposomes modified with Tween 20 and Tween 60 were studied using Franz diffusion cell. From the experimental data diffusion coefficients were determined for each of the systems, as well as the corresponding diffusion resistances. From the obtained results it can be concluded that the encapsulation of polyphenols in liposomes significantly slows diffusion, and with membrane modification can be achieved further slowing. The diffusion resistance of the liposome membrane modified with Tween 20 and Tween 60 is about 5 times higher compared to the diffusion of unencapsulated polyphenols from the thyme extract.

Keywords: diffusion coefficient, diffusion resistance, liposomes, membrane modification, polysorbate, tea polyphenols.

Available online at the Journal website: http://www.ache.org.rs/HI/

SCIENTIFIC PAPER

UDC 547.565:576:66:615

Hem. Ind. **69** (4) 347–353 (2015)

doi: 10.2298/HEMIND140220060P

In recent years researchers have paid particular attention to the biologically active ingredients, especially polyphenols, due to their positive effects on human health [1]. Polyphenols are secondary plant metabolites that are involved in a wide range of specialized physiological functions [2,3] and they are found to exhibit highly potent anti-oxidant activity [4]. Bioactive compounds of herbal plants such as antioxidants have shown to exibit multifunctional and remedial properties that include anti-radical, anti-carcinogenic, anti-inflammatory effects, as well as the reduction of oxidative stress and cardio-protection [5–7]. Therefore, there is a considerable interest in new natural antioxidants, such as polyphenols, to replace the synthetic ones and thyme (*Thymus vulgaris* L.) leaves appeared to be a promising source [8]. Thyme is a medicinal herb belonging to the Lamiaceae family, cultivated worldwide for culinary, cosmetic and medical purposes. This species is known for its beneficial functions such as antispasmodic, expectorant, antiseptic, antimicrobial and as mentioned, antioxidant [9,10]. The main phenolic compounds in thyme are: glycuronids of apigenin, luteolin, eriodyctiol, luteolin glycosides, rosmarinic acid and quercitine [11–13].

Polyphenols are mainly isolated from plants using water extraction procedure [14,15] and since being natural antioxidants, they should be protected from the surrounding medium [16]. This can be done by encapsulation into the adequate system which would promote better product stability due to the isolation of active compounds from the detrimental effects of oxygen, moisture or incompatible compounds [5]. Ecapsulation is used not only to protect active components, but also to trap and release them under controlled conditions [16]. Additionally, controlled delivery could enhance bioavailability of an active compound by customizing the release mechanism [5]. As an overall result, the encapsulation could be useful tool for the commercial sector when value added products are developed or in cases when product differentiation from competitors is achieved [5].

Encapsulation of therapeutics into liposomes represents a novel approach to sustained drug delivery [17]. Liposomes as drug carriers were first introduced around 1980 [18] and have been comprehensively

Correspondence: R.N. Pravilović, Department of Chemical Engineering, Faculty of Technology and Metallurgy, University of Belgrade, Karnegijeva 4, Belgrade, Serbia.
E-mail: radap17@yahoo.com
Paper received: 20 February, 2014
Paper accepted: 3 July, 2014

investigated as carriers for the improved delivery of a broad spectrum of agents for more than 20 years [19]. They are lipid based microscopic vesicles that consist of an aqueous core entrapped by one or more bilayers composed of natural or synthetic lipids [17, 18]. Because of the ability to carry a broad range of substances, their structural diversity and their composition that makes them biocompatible and biodegradable, liposomes have been studied for many different therapeutic situations [18,19] and they represent one of the best colloidal drug carriers described by Bangham [17,20].

Possibility to adjust the drug release rate and the affinity for the target site by modifying the vesicular composition or surface properties, has made the development of liposomes as carriers to an ever-growing research area [21,18]. Due to the limited stability of liposomes during storage and administration [22], the research on liposome technology has progressed from conventional vesicles to "second-generation liposomes" in which liposomes with modified surfaces have also been developed using several molecules, such as surfactants [18]. Conventional liposomes are defined as vesicles which are commonly composed of solely phospholipids (neutral and/or negatively charged) and/or cholesterol [19]. Surfactants are indispensable as solubilizing agents in the isolation, purification and reconstruction of membranes. The interaction of surfactants with phospholipid membranes of liposome vesicles leads to different aggregated structures and ultimately to the formation of mixed micelles [23–26]. Phospholipid-detergent systems have been widely investigated, but it still remains undetermined how can the release of loaded therapeutics be affected by their encapsulation into the liposomes modified by surfactants [26]. For modification purposes, nonionic polysorbates (*i.e.*, Tween surfactants) are most frequently used [22,26,17].

The aim of this paper is to study diffusion coefficient and diffusion resistance.

Model of actives release from the carrier systems

As discussed, encapsulation of active substances is used to control their release [16] which is possible due to a fact that encapsulation will primly lead to actives' sustained release caused by the decrease of the mass transfer coefficient and thus slower diffusion [27–31]. In order to characterize systems with sustained release, diffusion coefficient and diffusion resistance should be determined. The release of actives from various carriers could be treated as an unsteady diffusion process and their diffusion from a solution to another across a membrane in the standard Franz cell, could be approximated using Fick's second law and the following equation [27]:

$$\frac{c_{\mathrm{A,D}} - c_{\mathrm{A,R}}}{c^0_{\mathrm{A,D}} - c^0_{\mathrm{A,R}}} = e^{-\beta D t} \tag{1}$$

where $c_{\mathrm{A,D}}$ and $c_{\mathrm{A,R}}$ are concentrations of active in donor and receptor compartments at time t, and $c^0_{\mathrm{A,D}}$ and $c^0_{\mathrm{A,R}}$ are concentrations at time t = 0. D is the diffusion coefficient, t is time and β is the geometrical constant and represents characteristic of the particular geometry of the diffusion cell.

Mass transfer resistance (R) could be calculated as:

$$R = \frac{\delta}{D} \tag{2}$$

where δ is the sample thickness measured in the direction of mass transfer.

A serial diffusion resistance model could describe systems that include more than one diffusion resistance where the overall diffusion resistance represents the sum of individual resistances [27]:

$$R = \sum \frac{\delta_i}{D_i} \tag{3}$$

MATERIALS AND METHODS

Preparation of thyme extract

Thyme extract was prepared in compliance with the traditional aqueous extraction [14,15]. 10 g of dried thyme (Institute of Medicinal Plants Research Dr Josif Pancic, Serbia) was poured with 0.2 L of distilled water heated to 100 °C. The slurry was left to cool in a sealed glass beaker at room temperature, for 30 min. Supernatant solution was filtered.

Preparation of liposomes

Conventional liposomes, as well as liposomes with modified membrane, were prepared by the proliposome method [32]. The method is based on the initial formation of a proliposome mixture containing lipid, ethanol and water, which is converted to liposomes by a simple dilution step [32]. Phospholipon 90G (Phospholipid GmbH, Germany) was used as a membrane lipid. It comprises of phosphatidylcholine (min. 94 mass%) which is an unsaturated phospholipid and ensures liposomes to be highly bioavailable [33]. Ethanol was used as a lipid solvent and thyme extract as excess water.

Phospholipon 90G was measured at a glass beaker which was followed by the addition of the proper amounts of ethanol and water. The mixture was heated in a sealed beaker up to 60 °C with continuous stirring provided by the magnetic stirrer at 700 rpm. Stirring was applied at 60 °C until a homogenous dispersion was obtained. The composition was then cooled down to 25 °C. Afterwards, the liposomes were prepared by a

one-step addition of thyme extract into the lipid dispersion. Thyme extract was instilled whilst stirring at 700 rpm. The same stirring conditions were applied for additional 15 min. As a result, liposomal dispersion was obtained.

Preparation of modified liposomes was conducted following the same procedure, with the addition of corresponding Tween surfactant along with Phospholipon 90G. Compositions of liposomal dispersions for conventional liposomes, liposomes modified by Tween 20 and liposomes modified by Tween 60 are shown in Table 1.

Diffusion experiments

Diffusion of polyphenoles through cellulose acetate membrane (pore size 0.20 µm) from thyme extract, liposomal dispersions of conventional liposomes, liposomes modified by Tween 20 and liposomes modified by Tween 60 was investigated. Experiments were conducted using the standard static Franz diffusion cell (PermeGear, Inc., USA) characterized by a 20 mL volume and diffusion area of 4.91 cm^2 [27].

Continuous stirring of the receptor fluid by a magnetic bar at 700 rpm was applied. The Franz diffusion cell was thermostated at 25 °C for 30 min, whilst donor and receptor chambers were charged with distilled water. Subsequently, the receptor chamber was filled with the receptor fluid – distilled water (25 °C). These were the initial steps for all of the diffusion experiments. The thyme extract was placed in the donor chamber which was then sealed with parafilm. Samples (0.5 mL) were taken from the receptor chamber and then compensated with the injection of the fresh receptor fluid (0.5 mL, 25 °C). Sampling was performed after designated time intervals: 15 min intervals for 2 h and then 30 min intervals until the experiment completion. Diffusion of polyphenoles from thyme extract was observed for 3 h.

The same procedure was applied in all experiments and the liposomal dispersions of conventional liposomes, liposomes modified by Tween 20 and liposomes modified by Tween 60 were placed in the donor chamber. Diffusion of polyphenoles from all liposomal dispersions was observed during 6 h. All experiments were replicated twice.

Determination of total polyphenol content (TP)

Total polyphenol content (TP) in thyme extract and samples collected during the diffusion experiments was spectrophotometrically determined using Folin–Ciocalteu's reagent, according to a modified method [34].

The procedure was as follows: 0.5 mL of the sample was pipetted into a 50 mL volumetric flask containing 30 mL of distilled water. Thereafter, 2.5 mL of Folin–Ciocalteu's reagent (Sigma-Aldrich, Germany) and 7.5 mL of 20% Na_2CO_3 were added. Content was mixed and the volume was made up with distilled water. After two hours the absorbance was measured by the UV spectrophotometer (UV/Vis Scanning Models/UV-3100 (PC), China) at 765 nm against a blank sample – distilled water. Gallic acid was used as the standard and the calibration curve was constructed with the results expressed as mg/L of gallic acid equivalents (GAE) [2].

RESULTS AND DISCUSSION

Concentration of polyphenoles in the receptor chamber as a function of time, for all systems, was determined based on experimental data obtained from diffusion experiments. The results were then transformed into the dimensionless number, mass fraction $m_{R,t}/m_{D,0}$ and plotted against time as shown in Fig. 1a and b, where $m_{R,t}$ is the mass of polyphenols that was detected in the receptor chamber at a particular time and $m_{D,0}$ is the mass of polyphenoles that was introduced into the donor chamber within the carrier system.

Figure 1a and b show that the vast accumulation of polyphenols in the receptor chamber was noted during the first 1.5, 2.5, 3.5 and 4 h for thyme extract, liposomal dispersions of conventional liposomes, liposomes modified by Tween 20 and liposomes modified by Tween 60, respectively. After these periods of time the diffusion of polyphenols gradually slows because the driving force is decreased. Therefore, the mass transfer is being reduced as the system approaches the steady state.

Plotted curves indicate that encapsulation of polyphenols in coventional and modified liposomes decreases the diffusion rates significantly. Comparation of the curves shows that the membrane modification of

Table 1. Compositions (g) of liposomal dispersions

Component	Conventional liposomes	Liposomes modified by Tween 20	Liposomes modified by Tween 60
Phospholipon 90G	0.50	0.89	0.89
Ethanol	0.50	2.00	1.00
Distilled water	1.00	1.00	2.00
Thyme extract	10.00	20.00	20.00
Tween 20	–	0.17	–
Tween 60	–	–	0.17

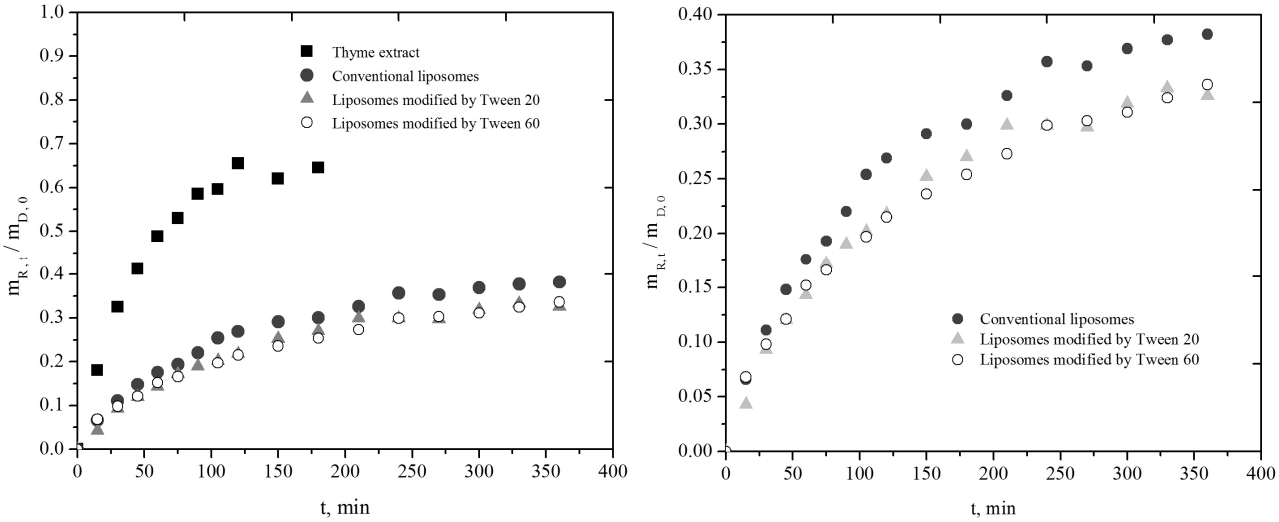

Figure 1. Released polyphenoles from thyme extract, conventional liposomes, liposomes modified by Tween 20 and liposomes modified by Tween 60 as a function of time.

liposomes with Tween 20 and Tween 60 additionally contributes to the decrease of the diffusion rate. In order to determine precisely the extent to which diffusion rate of polyphenols from modified liposomes is decreased, all experimental systems must be quantified. This is achieved by calculation and comparison of diffusion coefficients.

Diffusion coefficients of polyphenols from thyme extract and liposomal dispersions, across the membrane were calculated according to Eq. (1) from the slope of the linear part of curves:

$$\ln\left(\frac{c_D{}^0 - c_R{}^0}{c_D - c_R}\right)$$

versus time (Fig. 2a and b). β is the geometrical constant and represents characteristic of the particular geometry of the diffusion cell and membrane used in the experiments ($\beta = 2.49\times10^4$ m^{-2}) [27]. Diffusion coefficient (*D*) of polyphenols from thyme extract is 8.77×10^{-9} m^2/s, from liposomal dispersions are 2.31×10^{-9}, 1.78×10^{-9} and 1.69×10^{-9} m^2/s for conventional liposomes, liposomes modified by Tween 20 and liposomes modified by Tween 60, respectively.

Based on the values of diffusion resistances, it can be concluded to what extent encapsulation of polyphenols in liposomes contributes to the mass transfer decrease and how effective is the membrane modification. Known values of diffusion coefficients and sample thicknesses enable calculation of the diffusion resistances using Eq. (2). Since investigated systems

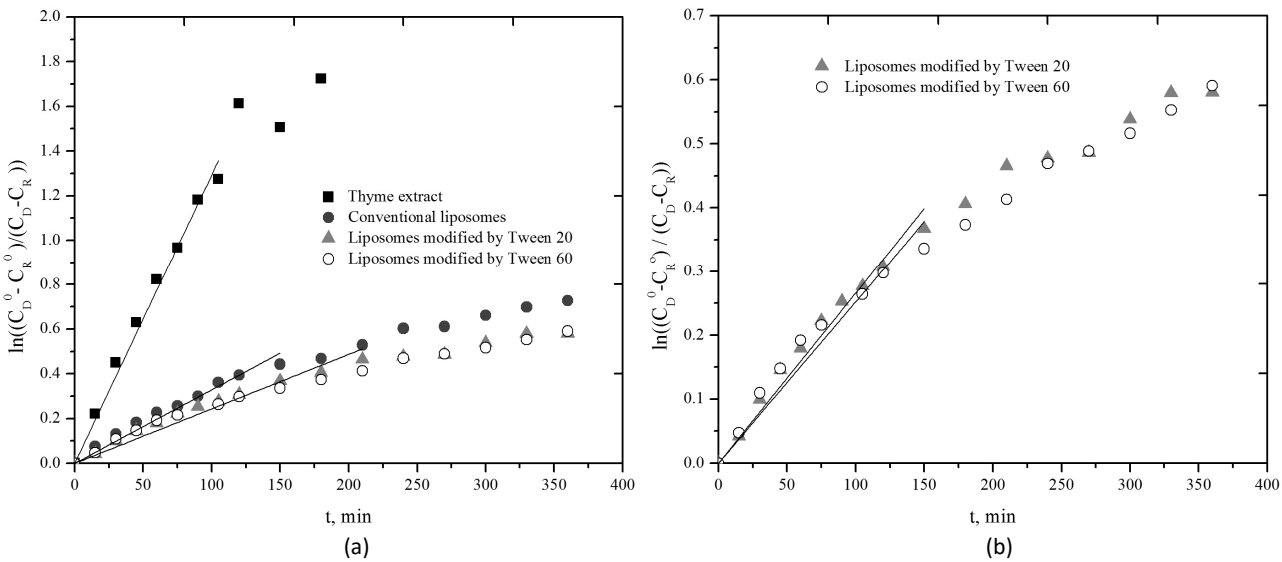

Figure 2. Dimensionless plot of polyphenoles concentration versus time for diffusion from investigated systems (a) and dispersions of modified liposomes (b).

include two different diffusion resistances (the cellulose acetate membrane and the liposome particles), the serial diffusion resistance model can be applied as shown by Eq. (3). The diffusion resistance from thyme extract is the resistance that the cellulose acetate membrane provides diffusion of polyphenols. Overall diffusion resistances (R) are given in Table 2.

The diffusion resistance of liposomal membrane (R_{lip}) can be calculated as a difference between R values for specific liposomal dispersion and thyme extract. The results are shown in Table 3.

The results show that liposomes contribute to a higher overall diffusion resistance and that diffusion resistance of liposomal membrane is significantly higher when compared to the values obtained for system with unencapsulated polyphenols (thyme extract). Encapsulation of polyphenols into the conventional liposomes decreases the diffusion rate 3.80 times due to the liposomal membrane, which provides the additional diffusion resistance.

following the polyoxyethylene part refers to the total number of oxyethylene –(CH_2CH_2O)– groups found in the molecule. The number following the polysorbate part is related to the type of fatty acid associated with the polyoxyethylene sorbitan part of the molecule. Monolaurate is indicated by 20, monostearate is indicated by 60. It could be concluded from the experimental data that the diffusion of polyphenols from liposomes is not affected by the length of the fatty acid ester moiety, and mainly depends on the polyoxyethylene chain, and because of that, liposomes modified by both surfactants have similar diffusion resistance.

Table 3. Diffusion resistances of liposomes

Type of liposomes	R_{lip}·/ 10^6 s m^{-1}
Conventional liposomes	1.38
Liposomes modified by Tween 20	1.89
Liposomes modified by Tween 60	1.91

Table 2. Diffusion coefficients and overall diffusion resistances

System	D·/ 10^{-9}m² s^{-1}	R·/ 10^6 s m^{-1}
Thyme extract	8.77	0.48
Liposomal dispersion – conventional liposomes	2.31	1.86
Liposomal dispersion – liposomes modified by Tween 20	1.78	2.37
Liposomal dispersion – liposomes modified by Tween 60	1.69	2.39

Liposomal membrane, which is modified by Tween 20, demonstrates further increase of diffusion resistance, thus slower diffusion rate which is 4.93 times slower, when compared with unencapsulated polyphenols. This type of modified liposomes also manifests different properties from the conventional liposomes. The permeability of the membrane with incorporated molecules of Tween 20 is lower than the one that is composed of phospholipids only, which is reflected by a fact that liposomes modified by Tween 20 show additional diffusion resistance in comparison with conventional liposomes.

Liposomes modified by Tween 60 exhibit similar features (Figure 2b). These particles show no significant difference in diffusion rates of polyphenoles compared to liposomes modified by Tween 20. The results show that the diffusion rate is 4.98 times slower than in a system with unencapsulated polyphenols. The values of TP concentrations in the receptor chamber are very close to the ones obtained for system with liposomes modified by Tween 20. The explanation for this behavior could be found in a fact that both molecules Tween 20 and Tween 60 are polyoxyethylene (20) derivative of polysorbate, sorbitan monolaurate and sorbitan monostearate, respectively. The number 20

CONCLUSIONS

Liposome presence leads to a higher overall diffusion resistance compared to polyphenoles diffusion resistance seen in thyme extract alone, and thereby promotes their prolonged release. Values of the diffusion resistance in liposome dispersions are about 4 times higher of those associated with unencapsulated polyphenols. This implies that liposomes are promising vehicles for protection and sustained release of polyphenols.

The liposome membrane modification can affect the rate of diffusion of the encapsulated polyphenols. Experimental results showed that the molecules of Tween 20 and Tween 60 further slow diffusion compared to conventional liposomes.

Acknowledgements

This work was supported by the Ministry of Education, Science and Technological Development, Republic of Serbia (Project No. III46010).

Phospholipon 90G, a generous gift from Phospholipid GmbH (Germany) and Standard Franz diffusion cell, a kind gift from PermeGear, Inc., Hellertown, PA, USA.

REFERENCES

[1] D. Horžić, D. Komes, A. Belscak, K. Kovacevic Ganin, D. Ivekovic, D. Karlovic, The composition of polyphenols and methylxanthines in teas and herbal infusions, Food Chem. **115** (2008) 441–448.

[2] G. Rusak, D. Komes, S. Likic, D. Horzic, M. Kovac, Phenolic content and antioxidative capacity of green and white tea extracts depending on extraction conditions and the solvent, Food Chem. **110** (2008) 852–858.

[3] C.A. Ewané, P. Lepoivre, L. Bellaire, L. Lassois, Involvement of phenolic compounds in the susceptibility of bananas to crown rot. A review, Biotechnol. Agron. Soc. Environ. **16** (2012) 393–404.

[4] S.L. Kosaraju, L. Dath, A. Lawrence, Preparation and characterisation of chitosan microspheres for antioxidant delivery, Carbohyd. Polym. **64** (2006) 163–167.

[5] E-S. Chan, Z-H. Yim, S-H. Phan, R.F. Mansa, P. Ravindra, Encapsulation of herbal aqueous extract through absorption with Ca-alginate hydrogel beads, Food Bioprod. Process. **88** (2009) 195–201.

[6] R.W. Owen, A. Giacosa, W.E. Hull, R. Haubner, B. Spiegelhalder, H. Bartsch, The antioxidant/anticancer potential of phenolic compounds isolated from olive oil, Eur. J. Cancer **36** (2000) 1235–1247.

[7] P.M. Kris-Etherton, M. Lefevre, G.R. Beecher, M.D. Gross, C.L Keen, T.D. Etherton, Bioactive compounds in nutrition and health-research methodologies for establishing biological function: the antioxidant and anti-inflammatory effects of flavonoids on atherosclerosis, Annu. Rev. Nutr. **24** (2004) 511–538.

[8] A. Dapkevicius, T.A. van Beek, G.P. Lelyveld, A. van Veldhuizen, A. de Groot, J.P.H. Linssen, Isolation and structure elucidation of radical scavengers from *Thymus vulgaris* leaves, J. Nat. Prod. **65** (2002) 892–896.

[9] A. Mirzaei-Aghsaghali, S. Alireza Syadati, H. Fathi, Some of thyme (*Thymus vulgaris*) properties in ruminant's nutrition, Ann. Biol. Res. **3** (2012) 1191–1195.

[10] R. Abdulkarimi, A. Mirza Aghazadeh, M. Daneshyar, Growth performance and some carcass charactristics in broiler chickens supplemented with Thymus extract (*Thymus vulgaris*) in drinking water, J. American. Sci. **7** (2011) 400–405.

[11] A.M. Hassan, I.A.H. Barakat, Assessment of Oxidative Stress Induced by Nickel Chloride and Antioxidant Effects of Basil (*Ocimum Basilicum* L.) and Thyme (*Thymus vulgaris* L.), J. Genet. Eng. Biotechnol. **6** (2008) 29––38.

[12] M.D. Guillen, M.J. Manzanos, Study of the composition of the different parts of a Spanish *Thymus vulgaris* L. plant, Food Chem. **63** (1998) 373–383.

[13] U. Justesen, Negative atmospheric pressure chemical ionisation low-energy collision activation mass spectrometry for the characterisation of flavonoids in extracts of fresh herbs, J. Chromatogr.. A **902** (2000) 369–379.

[14] D. Komes, A. Belscak-Cvitanovic, D. Hodzic, G. Rusak, S. Lekic, M. Beredinka, Phenolic Composition and Antioxidant Properties of Some Traditionally Used Medicinal Plants Affected by the Extraction Time and Hydrolysis, Phytochem. Analysis **22** (2010) 172–180.

[15] M. Kratchanova, P. Denev, M. Ciz, A. Lojek, A. Mihailov, Evaluation of antioxidant activity of medicinal plants containing polyphenol compounds. Comparison of two extraction systems, Acta Biochim. Pol. **57** (2010) 229––234.

[16] L. Deladino, P.S. Anbinder, A.S. Navarro, M.N. Martino, Encapsulation of natural antioxidants extracted from *Ilex paraguariensis*, Carbohyd. Polym. **71** (2008) 126––134.

[17] M. Pichandy, M. Mishra, S. Kanaiyan, S. Rao, J. Anbu, Formulation and psychopharmacological evaluation of surfactant modified liposome for parkinsonism disease, Asian J. Pharm. Clin. Res. **3** (2010) 46–54.

[18] M.L. Immordino, F. Dosio, L. Cattel, Stealth liposomes: review of the basic science, rationale, and clinical applications, existing and potential, Int. J. Nanomed. **1** (2006) 297–315.

[19] G. Storm, D.J.A. Cromelin, Liposomes: *quo vadis*?, Pharm. Sci. Technol. Today **1** (1998) 19–31.

[20] A.D. Bangham, M.M. Standish, J.C. Watkins, Diffusion of univalent ions across the lamellae of swollen phospholipids, J. Mol. Biol. **13** (1965) 238–252.

[21] L.D. Marzio, C. Marianeccib, M. Petronea, F. Rinaldib, M. Carafab, Novel pH-sensitive non-ionic surfactant vesicles: comparison between Tween 21 and Tween 20, Colloids Surfaces, B **82** (2011) 18–24.

[22] L-M. Tasi, D-Z. Liu, W-Y. Chen, Microcalorimetric investigation of the interaction of polysorbate surfactants with unilamellar phosphatidylcholines liposomes, Colloids Surfaces, A **213** (2003) 7–14.

[23] N. Deo, P. Somasundaran, Disintegration of Liposomes by Surfactants: Mechanism of Protein and Cholesterol Effects, Langmuir **19** (2003) 2007–2012.

[24] A. Helenius, D.R. McCaslin, E. Fries, C. Tanford, Properties of detergents, Method. Enzymol. **56** (1979) 734––749.

[25] M.R. Wenk, J. Seelig, Interaction of octyl-beta-thioglucopyranoside with lipid membranes, Biophys. J. **73** (1997) 2565–2574.

[26] A. M. Fadda, B. M. Baroli, A. M. Maccioni, C. Sinico, D. Valenti, F. Alhaique, Phospholipid-detergent systems: effects of polysorbates on the release of liposomal caffeine, Farmaco **53** (1998) 650–654.

[27] R. Pjanovic, N. Boskovic-Vragolovic, J. Veljkovic-Giga, R. Garic-Grulovic, S. Pejanovic, B. Bugarski, Diffusion of drugs from hydrogels and liposomes as drug carriers, J. Chem. Technol. Biotechnol. **85** (2010) 693–698.

[28] S. Mourtas, S. Fotopoulou, S. Duraj, V. Sfika, C. Tsakiroglou, S.G. Antimisiaris, Liposomal drugs dispersed in hydrogels. Effect of liposome, drug and gel properties on drug release kinetics, Colloids Surfaces, B **55** (2007) 212–221.

[29] F.P. Bonina, L. Montenegro, N. Scrofani, E. Esposito, R. Cortesi, E. Menegatti, Effects of phospholipid based formulations on *in vitro* and *in vivo* percutaneous absorption of methyl nicotinate, J. Controll. Release **34** (1995) 53–63.

[30] Z. Pavelic, N. Skalko-Basnet, R. Schubert, Liposomal gels for vaginal drug delivery, Int. J. Pharm. **219** (2001) 139–149.

[31] R. Singh, S.P. Vyas, Topical liposomal system for localized and controlled drug delivery, J. Dermatol. Sci. **13** (1996) 107–111.

[32] S. Perrett, M. Golding, W.P. Williams, A simple method for the preparation of liposomes for pharmaceutical applications: Characterization of the liposomes, J. Pharm. Pharmacol. **43** (1991) 154–161.

[33] G. Cevc, G. Blume, Hydrocortisone and dexamethasone in very deformable drug carriers have increased biological potency, prolonged effect, and reduced therapeutic dosage, Biochim. Biophys. Acta **1663** (2004) 61–73.

[34] J. Lachman, V. Hosnedl, V. Pivec, M. Orsak, Polyphenols in cereals and their positive and negative role in human and animal nutrition, in Proceedings of the Conference Cereals for Human Health and Preventive Nutrition, Brno, Czech Republic, 1998, pp. 118–125.

IZVOD

UTICAJ SASTAVA MEMBRANE NA BRZINU OTPUŠTANJA POLIFENOLA IZ LIPIDNIH MIKROČESTICA

Radoslava N. Pravilović[1], Vesna S. Radunović[2], Nevenka M. Bošković-Vragolović[1], Branko M. Bugarski[1], Rada V. Pjanović[1]

[1]*Tehnološko–metalurški fakultet, Univerzitet u Beogradu, Beograd, Srbija*
[2]*Istraživačko–razvojni centar, Beohemija poslovni sistem, Beograd, Srbija*

(Naučni rad)

Sistemi za kontrolisano otpuštanje lekova predstavljaju istraživačku oblast koja se intenzivno proučava zbog niza prednosti koje ovi sistemi pružaju i mogućeg unapređenja dosadašnjih, tradicionalnih formi lekova. Fosfolipidne mikročestice (lipozomi) su se pokazale potencijalno pogodnim nosačima aktivnih supstanci u sistemima ovog tipa. Predmet ovog rada je ispitivanje uticaja sastava membrane lipozoma na brzinu oslobađanja inkapsuliranih polifenola. Eksperimentalna ispitivanja su pokazala kako modifikacija membrane lipozoma utiče na prenos mase, u odnosu na konvencionalne lipozome. Lipozomi su modifikovani površinski aktivnim materijama Tween 20 i Tween 60, dok je kao izvor polifenola korišćen čajni ekstrakt biljke majčine dušice. Eksperimenti su izvedeni korišćenjem Franz–ove difuzione ćelije, u kojima je praćena difuzija polifenola iz: čajnog ekstrakta, disperzije konvencionalnih lipozoma, disperzije lipozoma modifikovanih pomoću Tween 20 i disperzije lipozoma modifikovanih pomoću Tween 60. Obradom eksperimentalnih rezultata određeni su koeficijenti difuzije za svaki od sistema, kao i odgovarajući difuzioni otpori. Na osnovu dobijenih rezultata može se zaključiti da se inkapsulacijom polifenola u fosfolipidne mikročestice–lipozome, značajno usporava njihova difuzija, a da se modifikacijom membrane može postići dodatno usporavanje prenosa mase, što zavisi od strukture molekula kojim se modifikacija vrši. Molekuli Tween 20 kao i Tween 60 su se pokazali uspešnim modifikatorima membrane lipozoma. Otpori koje membrane modifikovane navedenim polisorbatima pružaju difuziji polifenola su veći i dovode do 4,9 puta sporije difuzije u odnosu na sistem sa neinkapsuliranim polifenolima.

Ključne reči: Koeficijent difuzije • Difuzioni otpor • Lipozomi • Modifikacija membrane • Polisorbati • Polifenoli

Enzymatic spectrophotometric reaction rate determination of aspartame

Kata T. Trifković[1], Lucyna Łękawska-Andrinopoulou[2], Branko M. Bugarski[1], Constantinos A. Georgiou[2]

[1]*Faculty of Technology and Metallurgy, University of Belgrade, Belgrade, Serbia*
[2]*Chemistry Laboratory, Agricultural University of Athens, Athens, Greece*

Abstract
Aspartame is an artificial sweetener of low caloric value (approximately 200 times sweeter than sucrose). Aspartame is currently permitted for use in food and beverage production in more than 90 countries. The application of aspartame in food products requires development of rapid, inexpensive and accurate method for its determination. The new assay for determination of aspartame was based on set of reactions that are catalyzed by three different enzymes: *α*-chymotrypsin, alcohol oxidase and horseradish peroxidase. Optimization of the proposed method was carried out for: *i*) *α*-chymotrypsin activity; *ii*) time allowed for *α*-chymotrypsin action, *iii*) temperature. Evaluation of the developed method was done by determining aspartame content in "diet" drinks, as well as in artificial sweetener pills.

Keywords: aspartame determination, enzymatic method, *α*-chymotrypsin.

Available online at the Journal website: http://www.ache.org.rs/HI/

SCIENTIFIC PAPER

UDC 664.162:543.42.577

Hem. Ind. **69** (4) 355–359 (2015)

doi: 10.2298/HEMIND140526049T

Aspartame (*N*-L-*α*-aspartyl-L-phenylalanine, 1--methyl ester) is a low-calorie artificial sweetener that is about 200 times sweeter than table sugar. It is composed of two amino acids (aspartic acid and phenylalanine) and methanol [1,2]. Aspartame is used in variety of beverages and foods, as well as in tabletop sweeteners, pharmaceuticals and supplements [3]. There is a concern regarding safety of use of aspartame in human diet. However, numerous studies have shown that aspartame is non-toxic and safe [4]. Also, there are lists of artificial high-intensity sweeteners approved for utilization in European Union, as well as in USA, and both lists contain aspartame [5,6].

The increased utilization of aspartame resulted in need for development of fast and efficient methods for its determination [2,7–11]. There are a number of methods described in literature, but most of them are time-consuming and expensive. This particularly refers to HPLC methods where prior to the determination of aspartame, samples need to be subjected to an extensive pre-treatment [7]. Furthermore, numerous spectroscopic methods have also been examined, such as those based on ninhydrin [12] and *N*-bromsuccinilimide-metol-sulfanilamide [13]. However, these methods are often not suitable for aspartame determination due to the large and variable blank values [7]. The modern analytical methodologies employ enzymes in the determination techniques as a result of their selectivity and the tendency to replace the hazardous chemical substances, leading to the cleaner processes and sustainable chemistry [14].

After all being said, there is a real exigency for development of rapid, inexpensive and accurate method for aspartame determination, which will overcome the listed deficiency of existing methods. This paper describes a new assay for determination of aspartame, based on following reaction cascade:

$$\text{Aspartame} + H_2O \xrightarrow{\alpha\text{–Chymotrypsin}} \text{L-Asp-L-Phe} + H^+ + CH_3OH \quad (1)$$

$$CH_3OH + O_2 \xrightarrow{\text{Alcohol oxidase}} HCHO + H_2O_2 \quad (2)$$

$$2H_2O_2 + \text{Phenol} + \text{4-aminoantipyrine} \xrightarrow{\text{Horseradish peroxidase}} \text{4-}N\text{-(}p\text{-benzoquinoneimine)-antipyrine} + 4H_2O \quad (3)$$

In the reaction (1) methanol is released by *α*-chymotrypsin (*α*-CHY). Methanol is subsequently oxidized by alcohol oxidase (AO) creating hydrogen peroxide, Eq. (2), that reacts further in a reaction catalyzed by horseradish peroxidase (HRP), Eq. (3). During that reaction 4-*N*-(*p*-benzoquinoneimine)-antipyrine, coloured product is formed, and the formation is followed spectrophotometrically at 505 nm.

MATERIALS AND METHODS

Aspartame stock solution, 33.3 mM. An amount of 9.79 g of aspartame was placed in 1000 mL volumetric flask, and volume was brought up using phosphate buffer (pH 7.4).

Correspondence: K.T. Trifković, Faculty of Technology and Metallurgy, University of Belgrade, Karnegijeva 4, 11000 Belgrade, Serbia; E-mail: ktrifkovic@tmf.bg.ac.rs
L. Łękawska-Andrinopoulou, Chemistry Laboratory, Agricultural University of Athens, 75 Iera Odos, 11855 Athens, Greece; E-mail: lekawska@aua.gr
Paper received: 26 May, 2014
Paper accepted: 17 June, 2014

Enzyme working solution. Phenol, 7.5 mM; 4-amino -antipyrine, 2.50 mM; KH_2PO_4, 0.1 M; AO 1 U/mL, HRP 40 U/mL. The amounts of 0.706 g of phenol, 0.508 g of 4-aminoantipyrine and 13.608 g of KH_2PO_4 were placed in 800 mL of deionized water and pH was adjusted to 7.5, using 1 M NaOH. After adjustment of pH, 1000 U of AO and 40,000 U of HRP were added and prepared solution was transferred to a 1000 mL volumetic flask and brought up to the volume [15].

α-Chymotrypsin solution. 80 U/mL, an amount of 8000 U of *α*-CHY was placed in a 100 mL volumetric flask and brought up to the volume using deionized water.

Calibration standard aspartame solutions. 5.00, 10.00, 20.00, 30.00 and aspartame solutions used as samples: 1.00, 2.00, 7.00, 15.00, 25.00, 35.00 mM aspartame. All samples were prepared placing the appropriate volume of stock aspartame solution in 100 mL of phosphate buffer.

Phosphate buffer. 0.1 M, an amount of 13.61 g of KH_2PO_4 was dissolved in 900 mL of deionized water, and pH was adjusted to 7.4 using 1 M NaOH; the solution was placed in 1000 mL volumetric flask and brought up to the volume using deionized water.

Spectrophotometer: Jasco V-550.

Experimental procedure

An aliquot of 0.5 mL of standard or sample was placed in a 3 mL quartz cuvette in the spectrophotometer. Solution containing 12 U of *α*-chymotrypsin was pipetted into cuvette, with repeated flushing of the pipette tip to evenly disperse the enzyme added, and pre-incubated for 2 min for reaction (1) to proceed. Then, an aliquot of 2.5 mL of enzyme working solution was added in the cuvette and the software for kinetic measurement was started at 505 nm wavelength. Blank samples were prepared as described above, using the same amount of phosphate buffer instead of aspartame solution. Reaction rates were calculated in units of mA s^{-1}. Further on, the calibration curve was constructed.

To check the precision, the reaction rate from the 15 mM aspartame solution was measured ten times using *α*-CHY solution of 12 U.

RESULTS AND DISCUSSION

Optimization of the assay

Optimization of α-CHY activity

In order to check the influence of the activity of *α*-CHY used, the optimization test was conducted. The *α*-CHY activity was varied in range from 8 to 32 U. As can be seen from Table 1, analytical signal increased along *α*-CHY activity. The increase from 12 to 32 U was 7.2%. This small analytical signal increase did not justify the increase of the enzyme cost, therefore 12 U was selected for further experiments.

Optimization of pre-incubation time

In reaction (1), aspartame is cleaved by *α*-chymotrypsin to L-Asp-L-Phe and methanol. The goal was to determine the optimum time for this reaction. Results in Table 2 showed that analytical signal increased along pre-incubation time. While increasing pre-incubation time by 12 min, analytical signal increase was just 7.4%. In this respect, 2 min pre-incubation time was selected.

Interesting result shown in both Tables 1 and 2 is that blank signal was almost zero in most of the cases.

Table 1. Effect of α-CHY activity; 33.3 mM aspartame, 2 min pre-incubation time, 20.2 ℃

α-Chymotrypsin activity, U	Aspartame slope value ± *SE* mA s^{-1}	Correlation coefficient R^2	Blank (water) slope value ± *SE* mA s^{-1}
8	4.07±0.02	0.995	–0.014±0.002
12	4.40±0.02	0.996	–0.003±0.002
16	4.58±0.02	0.996	0.002±0.002
20	4.65±0.02	0.997	–0.004±0.002
24	4.67±0.02	0.997	0.009±0.002
28	4.74±0.02	0.997	0.001±0.002
32	4.75±0.02	0.997	0.000±0.002

Table 2. Effect of pre-incubation time; 33.3 mM aspartame, 12 U α-CHY, 20.2 ℃

Pre-incubation time, min	Aspartame slope value ± *SE* mA s^{-1}	Correlation coefficient R^2	Blank (water) slope value ± *SE* mA s^{-1}
2	4.72±0.02	0.997	0.015±0.002
6	4.85±0.02	0.997	0.006±0.002
10	4.97±0.02	0.997	0.008±0.002
14	5.07±0.02	0.997	0.011±0.002

Temperature effect

Temperature effect was investigated by adjusting temperature of reaction (1) in a water bath. Results shown in Figure 1 were as expected – reaction rate increased along temperature.

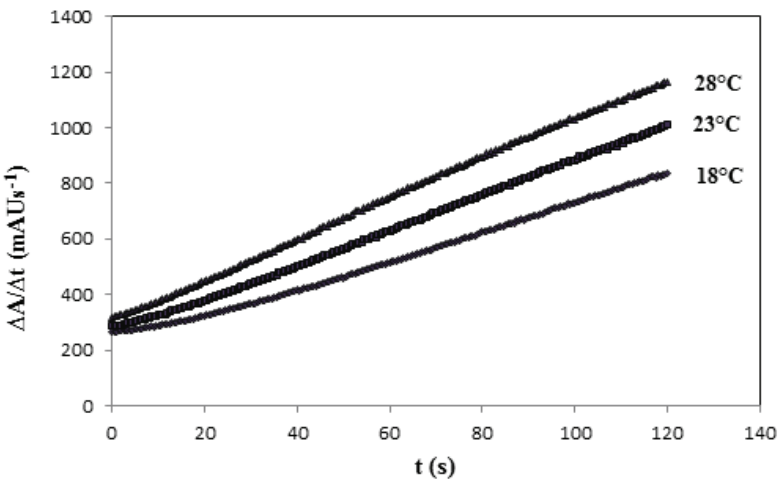

Figure 1. Temperature influence on reaction rate.

Calibration curve

Based on experimental data obtained for dependence of reaction rate on aspartame concentration, calibration curve was constructed (Figure 2).

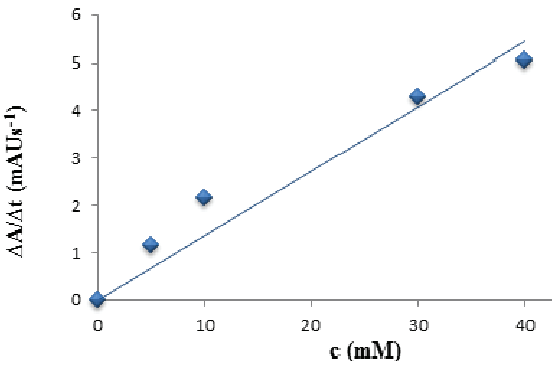

Figure 2. Calibration curve.

Equation of the calibration curve:

$$\frac{\Delta A}{\Delta t}[\text{mA s}^{-1}] = (0.14 \pm 0.013)c\,,\ R^2 = 0.9690 \qquad (4)$$

Standard solution analysis

In order to check the accuracy of developed assay, the concentration of aspartame in solutions of known concentrations was determined. The results are shown in Table 3.

The limit of detection (LOD) for the developed assay was calculated as follows:

$$LOD = \frac{3.3S_a}{b} \qquad (5)$$

where S_a stands for standard deviation of the response, while b stands for the slope of the calibration curve.

The value for *LOD* was found to be 9.9 mM. Results clearly indicate that this assay needs further improvement towards lowering the detection limit using a more sensitive technique, such as fluorimetry or chemiluminescence.

Table 3. Analysis of standard solutions

Taken, mM	Found, mM
1.00	1.52
2.00	3.75
7.00	11.74
15.00	22.44
25.00	31.09
35.00	36.25

Reproducibility of the results

Table 4 presents results for 10 consecutive measurements of the 15 mM aspartame solution.

The mean reaction rate, calculated from experimental results, was 2.98±0.087 mA s^{-1} (n= 10).

Determination of aspartame in real food samples

After basic development and optimization of the assay, an attempt was made to determine the aspartame concentration in commercial products Coca-Cola Zero and Canderel sweetener pills. Main problem that occurred was low concentration of aspartame in the sample. It was hard to obtain accurate signal as the aspartame concentration was close to the detection limit (9.9 mM). Namely, proposed method requires relatively high aspartame concentration in sample, in

Table 4. Reproducibility of the results for the 15 mM aspartame solution

No of measurement	Reaction rate ± *SE*, mA s^{-1}	Correlation coefficient, R^2
1	2.928±0.009	0.998
2	2.925±0.008	0.998
3	2.845±0.008	0.998
4	2.906±0.009	0.997
5	3.087±0.007	0.999
6	3.039±0.009	0.998
7	2.936±0.008	0.998
8	3.053±0.008	0.998
9	3.105±0.009	0.998
10	2.952±0.008	0.998

order to get the measurable response, as can be seen from analysis of standard solutions. Thus, preparation of 33.3 mM aspartame Canderel solution requires dissolution of 24 Canderel pills in 20 mL of deionized water. Additionally, in order to get rid of the interference of caramel color of Coca-Cola it was necessary to dilute samples at 1:5. In this way, aspartame concentration was even lower, so it could not be measured spectrophotometrically.

CONCLUSION

The determination of aspartame, particularly in food products, is mandatory from health and legal aspects. Therefore, the development of new assay for aspartame determination is highly recommended. The proposed method showed good results in samples containing high aspartame concentrations. However, for the samples containing lower aspartame content, the method requires further optimization. That could be achieved through enhancing the sensitivity of the detection. For that purpose, chemiluminescence as method for detection could provide good results, as it can go down to 10 nM [16].

Acknowledgements

Work is performed within LeanGreenFood Marie Curie Initial Training Network funded by FP7/2007--2013 under grant agreement No. 238084; FP7-REGPOT 2009-1 Project Nanotech FTM, under grant agreement No.245916, as well as Ministry of Education, Science and Technological Development, Republic of Serbia, Project No. III46010, 2011-2014.

REFERENCES

[1] R.G. Ranney, J.A. Operman, E. Muldoon, F.G. McMahon. Comperative metabolism of aspartame in experimental animals and humans. J. Toxicol. Environ. Health **2** (1976) 441–451.

[2] D. Odaci, S. Timur, A. Telefoncu, Carboxyl esterase-alcohol oxidase based biosensor for the aspartame determination, Food Chem. **84** (2004) 493–496.

[3] L.F. Capitan-Vallvey, M.C. Valencia, E.A. Nicolas, Flow-through spectrophotometric sensor for the determination of aspartame in low-calorie and dietary products, Anal. Sci. **20** (2004) 1437–1442.

[4] FAO/WHOEC, Aspartame: Specifications for Identity and Purity of Carrier Solvents, Emulsifier and Stabilizers, Enzyme Preparations, Flavoring Agents, Food Colors, Sweetening Agents and Other Food Additives, Rome, 1982.

[5] European Commission, Directive 2006/52/EC of European Parliament and of the Council of 5 July 2006 amending Directive 95/2/EC on food additives other than colors and sweeteners and Directive 94/35/EC on sweeteners for use in foodstuffs, Off. J. Eur. Un. **L024** (2004) 10.

[6] A. Zygler, A. Wasik, J. Namiesnik, Analytical methodologies for determination of artificial sweeteners in foodstuffs, Trend Anal. Chem. **28** (2009) 1082–1102.

[7] E. Dinckaya, M. Cagin, A. Telefoncu, Enzymatic method for the spectrophotometric determination of aspartame, Food Chem. **50** (1994) 95–97.

[8] V. Pereira, O. Fatibello-Filho, Flow-injection spectrophotometric determination of L-ascorbic acid in pharmaceutical formulations with on-line solid-phase reactor containing copper (II) phosphate, Anal. Chim. Acta **366** (1998) 55–62.

[9] K. Wrabel, K. Wrabel, Determination of aspartame and phenylalanine in diet soft drinks by high-performance liquid chromatography, J. Chromatogr., A **773** (1997) 163–167.

[10] O.W. Lau, S.F. Luk, W.M. Chan, Spectrophotometric determination of aspartame in soft-drinks with ninhydrin as reagent, Analyst **113** (1988) 765–768.

[11] S. Motellier, I.W. Wainer, Direct stereochemical resolution of aspartame stereoisomers and their degradation products by high-performance liquid chromatography on a chiral crown ether-based stationary phase, J. Chromatogr. **516** (1990) 365–373.

[12] I.C. Vieira, O. Fatibello-Filho, Determinação espectrofotométrica de aspartame em produtos dietéticos

usando ninidrina como reagent, Quim. Nova **18** (1995) 250–254.

[13] U.V. Prasad, T.E. Divakar, C.S.P. Sastry, M.V.Rao, O.P. Kapur, New methods for determination of aspartame, Food Chem. **28** (1988) 269–278.

[14] C.I.C. Silvestre, P.C.A.G. Pinto, M.A. Segundo, M.L. M.F.S. Saraiva, J.L.F.C. Lima, Enzyme based assays in a sequential injection format: A review, Anal. Chim. Acta **689** (2011) 160–177.

[15] A.M.G. Vasilarou, C.A. Georgiou, Enzymatic spectrophotometric reaction rate determination of glucose in fruit drinks and carbonated beverages. An analytical chemistry laboratory experiment for food science--oriented students, J. Chem. Edu. **77** (2000) 1327–1329.

[16] E.G. Vasiliou, Y.M. Makarovska, I.A. Pneumatikos, N.V. Lolis, E.A. Kalogeratos, E.K. Papadakis, C.A. Georgiou, Hydrogen peroxide assessment in exhaled breath condensate: condensing equipment – rapid flow injection chemiluminescence method, J. Braz. Chem. Soc. **18** (2007) 1040–1047.

IZVOD

ENZIMATSKO–SPEKTROFOTOMETRIJSKI TEST ZA ODREĐIVANJE ASPARTAMA

Kata T. Trifković[1], Lucyna Łękawska-Andrinopoulou[2], Branko M. Bugarski[1], Constantinos A. Georgiou[2]

[1]*Tehnološko–metalurški fakultet, Univerzitet u Beogradu, Beograd, Srbija*
[2]*Chemistry Laboratory, Agricultural University of Athens, Athens, Greece*

(Naučni rad)

Aspartam je veštački zaslađivač niske kalorijske vrednosti, približno 200 puta slađi od saharoze. Aspartam se trenutno koristi u industriji hrane i pića kao zamena za šećer u preko 90 zemalja u svetu, pa je stoga nužno imati razvijenu metodologiju i dobru analitiku za njegovo određivanje. Metode koje se najčešće koriste za određivanje aspartama su obično dugotrajne, skupe i zahtevaju značajna ulaganja u opremu, kao i komplikovan pred-tretman uzoraka. Stoga je neophodno razviti brz, ekonomičan, osetljv i precizan test za njegovu detekciju. U ovom radu je predložen test za određivanje aspartama koji se zasniva na nizu reakcija katalizovanih upotrebom tri enzima: *α*-himotripsin, alkoholna oksidaza i peroksidaza iz rena. Tokom reakcione kaskade dolazi do transformacije aspartama u tri reakciona koraka, od kojih je svaki enzimski katalizovan, α-himotripsinom, alkoholnom oksidazom i peroksidazom iz rena, redom. Preko nekoliko reakcionih međuproizvoda (methanol i vodonik-peroksid) aspartam se transformiše do obojenog produkta, čije se formiranje prati spektrofotometrijski, a zatim se na osnovu apsorbance obojenja dalje preračunava koncentracija aspartama prisutna u ispitivanom uzorku. Eksperimentalni postupak je jednostavan i efikasan, a njegova preciznost dobra. Optimizacija predloženog testa izvršena je u cilju određivanja optimalne: *i*) aktivnosti *α*-himotripsina; *ii*) vremena pre-inkubacije; *iii*) temperature pri kojoj se odvija reakcija. Predloženi test ocenjen je određivanjem sadržaja aspartama u dijetalnim pićima (Coca-Cola Diet) i veštačkim zaslađivačima (Candarel tablete), kao i procenom njegovog praga osetljivosti. Dobijeni rezultati ukazuju na neophodnost optimizacije metode detekcije, u cilju omogućavanja određivanja nižih koncetracija aspartama prisutnih u uzorku.

Ključne reči: Određivanje aspartama • Enzimatska metoda • *α*-Himotripsin

The improved photostability of naproxen in the inclusion complex with 2-hydroxypropyl-β-cyclodextrin

Snežana S. Ilić-Stojanović[1], Vesna D. Nikolić[1], Ljubiša B. Nikolić[1], Aleksandar S. Zdravković[2], Agneš J. Kapor[3], Mirjana M. Popsavin[4], Slobodan D. Petrović[5]

[1]*University of Niš, Faculty of Technology, Leskovac, Serbia*
[2]*College of Textile, Leskovac, Serbia*
[3]*University of Novi Sad, Faculty of Sciences, Department of Physics, Novi Sad, Serbia*
[4]*University of Novi Sad, Faculty of Sciences, Department of Chemistry, Novi Sad, Serbia*
[5]*University of Belgrade, Faculty of Technology and Metallurgy, Belgrade, Serbia*

Abstract
The aim of this work was the preparation of the inclusion complex of naproxen with 2-hydroxypropyl-β-cyclodextrin (HP-β-CD) in order to improve the physical and chemical properties of naproxen. The molecular inclusion complexes of naproxen with HP-β-CD were prepared by using the co-precipitation method in the solid state with the molar ratio of 1:1. The structure of the obtained complex was characterized by using FTIR, ^{1}H NMR, UV-Vis and XRD methods. The testing of naproxen photostability by the UV-Vis method indicated the degradation to aromatic ketone, 2-acetyl-6-methoxynaphthalene. FTIR analysis showed that the degradation has started 15 days after the exposure of naproxen to daylight while the inclusion complex of naproxen:2-hydroxypropyl-β-cyclodextrin was photostable for a period of 30 days.

Keywords: naproxen, photodegradation, 2-hydroxypropyl-β-cyclodextrin, inclusion complex.

Available online at the Journal website: http://www.ache.org.rs/HI/

SCIENTIFIC PAPER

UDC 615:547:543.5

Hem. Ind. **69** (4) 361–370 (2015)

doi: 10.2298/HEMIND131128050I

Naproxen, (+)-(*S*)-2-(6-methoxynaphthalen-2-yl)-propanoic acid, is a derivative of 2-arylpropionic acids (profen drugs) which, in therapeutic doses, reduces the biosynthesis of prostaglandin and fever [1]. It exhibits anti-inflammatory and analgesic effects, relieves the symptoms of rheumatic diseases and other conditions accompanied by inflammation and the acute pain of moderate severity. Of two enantiomers of naproxen only the *S*-form is active.

Naproxen is a photosensitive and low soluble molecule which can be degraded under the influence of light by giving pharmacologically inactive products. A great number of published works were presented in the ways to improve the solubility of naproxen. For the improved solubility Mura and colleagues developed solid naproxen and chitosan systems [2,3] and triple systems of naproxen, amino acids and hydroxypropyl-β-cyclodextrin [4]. Various synthetic polymers were used as drug carriers in order to achieve the efficient and targeted delivery systems for a satisfactory therapeutic application. Agglomerated crystals of naproxen with hydroxypropyl cellulose improved the compactness [5]. A diblock copolymer of poly(ethylene-β-methacrylic acid) (PEO-β-PMAA) was synthesized by the atom transfer radical polymerization and applied to the pH-dependent release of naproxen embedded into the core of the micelle [6]. The obtained results provided the potential use of the PEO-β-PMAA micelle system for a targeted delivery of various hydrophobic drugs in the small intestine. The interactions of poly(vinylpyrrolidone) (PVP) with ibuprofen and naproxen were also studied [7]. The influence of the drug on the glass transition, solubility and specific types of hydrogen bonding interactions were analyzed [8].

Cyclodextrins and their derivatives are suitable drug carriers because their molecule can host another substance in its cavity. The inclusion complex of naproxen with β-cyclodextrin increased the solubility and the drug release rate [9,10]. The interactions in inclusion complexes of α-cyclodextrin, β-cyclodextrin, γ-cyclodextrin and dimethyl-β-cyclodextrin with naproxen, ibuprofen and panadol were examined [11]. The inclusion complexes of cyclodextrin and its derivatives were used to improve the physical and chemical properties of the drugs (solubility, vapor, odor, stability, etc.). A great number of researches proved that the solubility and stability of the drugs are increased, *e.g.*, atenolol [12–14], nifedipine, nicardipine [15–17], amlodipine [18,19] and allicin [20]. The solubility of the usnic acid was improved by complexation with β-cyclodextrin (β-CD:UA) which is incorporated in liposomes [21].

It was observed that naproxen absorbed UV irradiation up to 360 nm and, in the presence of oxygen, lead

Correspondence: S.S. Ilić-Stojanović, Faculty of Technology, University of Niš, Bulevar oslobođenja 124, 16000 Leskovac, Serbia.
E-mail: ilic.s.snezana@gmail.com; ilicsnezana@tf.ni.ac.rs
Paper received: 28 November, 2013
Paper accepted: 17 June, 2014

to its direct degradation. As a result of photodegradation, the obtained molecules were more hydrophobic with the increased toxicity which, compared to naproxen [22], reduced the pharmacological activity and safety of the drug administration. Photodegradation products of naproxen include 4-isobutylacetophenone, 1-(6-methoxy-2-naphthyl)ethanol and 2-acetyl-6-methoxynaphthalene. Both keto analogues of naproxen belonged to the group of aromatic ketones, that presence increases the rate of photodegradation during the light exposure. Aromatic ketones moved the molar absorptivity towards higher wavelengths and consequently acted as more photosensitive agents [23]. A recent research showed the improved photostability of the usnic acid and piroxicam in the inclusion complexes with 2-hydroxypropyl-β-cyclodextrin (HP-β-CD) [24,25].

The aim of this work was the preparation of the inclusion complex of naproxen with HP-β-CD, its structural characterization and the naproxen photosensitivity enhancement. The molecular inclusion complex based on naproxen and HP-β-CD, as a complexing agent, was prepared by the chemical co-precipitation method in the solid state and in the molar ratio of 1:1. For the structural characterization of the complex, a complexing agent, naproxen, the corresponding physical mixture of naproxen and HP-β-CD, the methods of nuclear magnetic resonance (^{1}H-NMR), X-Ray diffraction (XRD) and Fourier transform infrared spectrometry (FTIR) were used. For the investigation of the impact in the photostability of naproxen, the FTIR method and ultraviolet and visible spectroscopy (UV–Vis) were used for the analysis of photosensitive groups of naproxen in a pure and complexed form.

EXPERIMENTAL

Material and methods

Naproxen was supplied from Megafine Pharma Ltd. (99.67% purity), while 2-hydroxypropyl-β-cyclodextrin (97%) and potassium bromide (spectroscopic grade) were supplied from Merck, Darmstadt. Other solvents and reagents used were of p.a. purity.

Preparation of inclusion complex

The inclusion complex of naproxen:2-hydroxypropyl-β-cyclodextrin was obtained by the co-precipitation method with the molar ratio of the reactants 1:1. The measured amounts of naproxen (230.259 mg) and 2-hydroxypropyl-β-cyclodextrin (1541.54 mg) were suspended in distilled water (150 cm^3). The solution was mixed at room temperature for 48 h, protected from the light. In order to carry out the dissolution and due to the poor solubility of naproxen, the prepared solution was then subjected to ultrasound for 1 h. The ultrasound device Sonic (Niš, Serbia), and an ultrasonic bath with the dimensions A:B:H = 300 mm×151 mm×200 mm, with 8 dm^3 volume, were used under the following conditions: the temperature 30 °C, the ultrasound wave frequency 40 kHz and the power of 150 W, the total nominal power of 3×50 W. After the treatment by ultrasound, this solution was evaporated in a vacuum evaporator at 50 °C protected from the light, to the volume of approximately 20 cm^3, and then dried in a desiccator above the concentrated sulfuric acid at 25 °C. After drying, a white crystalline complex was obtained and as such it was used for further investigations in this work.

Preparation of physical mixture

Physical mixtures were prepared by simple mixing of naproxen with 2-hydroxypropyl-β-cyclodextrin as complex agents in the mole ratio of 1:1.

Fourier transform infrared spectrometry (FTIR)

FTIR spectra of the samples were recorded by using the technique of thin transparent pills with potassium bromide, spectroscopic purity, under vacuum at the pressure of 200 MPa. Using this method, the following was analyzed: naproxen, 2-hydroxypropyl-β-cyclodextrin, the inclusion complex naproxen:2-hydroxypropyl-β-cyclodextrin and a physical mixture of naproxen and 2-hydroxypropyl-β-cyclodextrin with the measured 150 mg KBr and 0.2 mg samples. KBr tablets, with naproxen and the complex naproxen:2-hydroxypropyl-β-cyclodextrin, were exposed to daylight and, in certain time intervals, FTIR spectra were recorded.

For all the samples, the recording was carried out in the area of wave numbers from 4000 to 400 cm^{-1} on the FTIR spectrophotometer Bomem Hartmann & Braun MB-series. The spectra were processed by using the Win-Bomem Easy software.

Nuclear magnetic resonance spectrometry (^{1}H-NMR)

^{1}H-NMR spectra of the samples of the inclusion complex naproxen:hydroxypropyl-β-cyclodextrin, 2-hydroxypropyl-β-cyclodextrin and naproxen were made on the Bruker AC 250 E NMR spectrometer with operating frequencies of 250 MHz, in a 5 mm diametar glass cuvette at room temperature. D_2O was used as a solvent.

X-ray diffraction (XRD)

X-ray diffraction was performed on the Phillips PW 1030 powder diffractometer by exposing the samples to monochrome CuKα radiation, λ = 1.54178 Å, and analyzed under the angle 2θ between 5 and 45° with 0.05° increments and recording time, τ = 5 s. The voltage and the strength of the electric current were 40 kV and 20 mA, respectively.

Ultraviolet and visible spectrophotometry (UV–Vis)

The sample was prepared by dissolving 2.5 mg of naproxen in 10 cm^3 of distilled water. The quartz glass cuvette of dimensions 1 cm×1 cm×4.5 cm was used. The recordings were performed in the wavelength range of 200–800 nm using the Varian Cary 100 spectrophotometer while distilled water was used as a blind test.

RESULTS AND DISCUSSION

The structural characterization of the obtained molecular inclusion complex naproxen:2-hydroxypropyl-β-cyclodextrin, a complexing agent, naproxen and the corresponding physical mixtures were carried out by FTIR, ^{1}H-NMR, XRD and UV–Vis methods. For monitoring the formed photodegradation products of naproxen, FTIR and UV–Vis methods were applied. XRD diffraction patterns of naproxen, 2-hydroxypropyl-β-cyclodextrin, the physical mixture and the inclusion complex naproxen:2-hydroxypropyl-β-cyclodextrin are shown in Figure 1.

The comparative analysis of XRD diffraction patterns (Fig. 1) was used to observe the difference at some peaks in the diffraction patterns of the complex naproxen:2-hydroxypropyl-β-cyclodextrin, naproxen, 2-hydroxypropyl-β-cyclodextrin and the physical mixture of naproxen and 2-hydroxypropyl-β-cyclodextrin. Diffractogramm of 2-hydroxypropyl-β-cyclodextrin (Fig. 1, data d) had two wide peaks with the maxima at 11.7 and 18.5° which did not show clearly defined reflections and the disordered crystal structure corresponded to the amorphous structure. The presence of well-structured sharp peaks with the maxima at 6.5, 12.6, 13.4, 16.6, 18.0, 18.8, 19.9, 20.6, 22.1, 22.5, 23.5, 23.9 and 28.2° with clearly defined reflections in the XRD diffractogram of naproxen (Fig. 1, data c) confirmed its crystalline structure. In the XRD diffractogram of the physical mixture of naproxen and 2-hydroxypropyl-β-cyclodextrin (Fig. 1, data a) characteristic peaks of naproxen with the maxima at 6.6, 12.6, 18.9, 20.6, 22.5 and 23.5° and wide peaks with the maximum at 11.7 and 18.5° derived from 2-hydroxypropyl-β-cyclodextrin were present. The results of the physical mixture indicated that there was no molecular interaction between the molecules of the guest and the host, *i.e.*, the diffraction of the physical mixture presented the sum of diffraction patterns of naproxen and 2-hydroxypropyl-β-cyclodextrin. The diffraction pattern of the inclusion complex of naproxen:2-hydroxypropyl-β-cyclodextrin did not contain the peaks that are characteristic for diffractograms of naproxen and HP-β-CD. The loss of the peaks at 6.5, 13.4, 16.6, 18.0, 19.9, 21.1, 23.9 and 28.2°, and the peaks with the reduced intensity present at 12.6, 18.8, 20.6, 22.5 and 23.5°, which originated from naproxen in the diffraction pattern of the inclusion complex of naproxen:2-hydroxypropyl-β-cyclodextrin (Fig. 1, data b), indicated that the drug molecules were protected from X-rays by the inclusion of the guest molecules in the hydrophobic cavities of the host molecule.

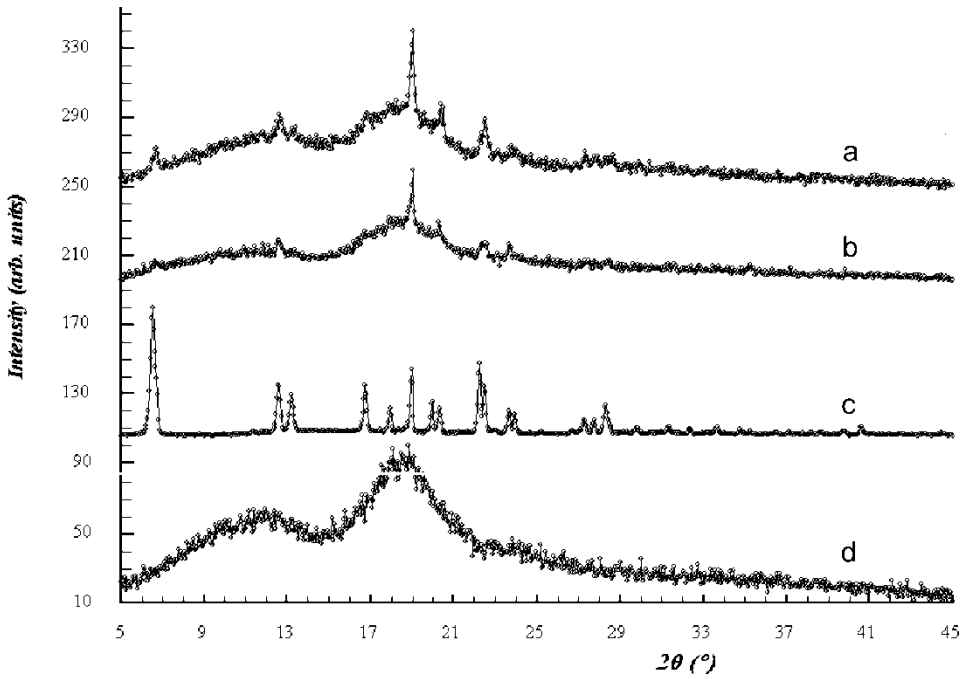

Figure 1. XRD diffraction: physical mixture of naproxen and 2-hydroxypropyl-β-cyclodextrin (a), inclusion complex naproxen:2-hydroxypropyl-β-cyclodextrin (b), naproxen (c) and 2-hydroxypropyl-β-cyclodextrin (d).

The numbering of C atoms at naproxen and glucopyranose units of 2-hydroxypropyl-β-cyclodextrin was shown in Fig. 2, while the results of ^{1}H-NMR analysis are given in Table 1.

The ^{1}H-NMR analysis of the complex of naproxen:2--hydroxypropyl-β-cyclodextrin (Table 1) showed the presence of a multiplet at δ 7.0 to 7.85 ppm which originated from the proton of naphthalene in the naproxen structure, but of a significantly lower intensity. The signal at δ 1.52 ppm assigned to protons in the position 3 of the CH_3 groups of naproxen is also present in the ^{1}H-NMR spectrum of the complex, but of lower intensity and shifted for +0.08 towards higher values of δ units. On the other hand, all of the signals originating from the protons of 2-hydroxypropyl-β-cyclodextrin glucopyranose units are present in the spectrum complex. The triplet at δ 3.975 ppm assigned to H_3 protons and the doublet at δ 1.125 assigned to H_9 protons from 2-hydroxypropyl-β-cyclodextrin complex, are moved to higher values of δ units (Table 1), to +0.045 and +0.065, respectively. The greatest displacement ($\Delta\delta$ = –0.1 ppm) in the spectrum of the complex showed the signals at δ 3.9 ppm, which corresponds to H_6 protons of 2-hydroxypropyl-β-cyclodextrin glucopyranose units. Compared to naproxen and 2-hydroxypropyl-β-cyclodextrin, these movements in the ^{1}H-NMR spectrum of the naproxen:2-hydroxypropyl-β-cyclodextrin complex indicated that there were non-covalent interactions between H_3 protons of the guest molecules and H_3, H_6 and H_9 protons of the host molecules, *i.e.*, there was a formation of a supramolecular structure by the type of the inclusion.

In the FTIR spectrum of naproxen (Fig. 3, curve a) there was a wide absorption band of the medium intensity with the maximum at 3215 cm^{-1} attributed to the valence vibrations of OH groups from carboxylic acids, ν(OH).

The weak absorption band at 3002 cm^{-1} originated from CH valence vibrations of the aromatic part of the structure. In the FTIR spectrum of naproxen (Fig. 3, curve a), the characteristic band with a very high intensity and the maximum at 1727 cm^{-1} was the result of the valence vibration of C=O group from carboxylic acids, ν(C=O), which is consistent with the investigations of other authors [8,26]. The weak band at 1416 cm^{-1} and the medium intensity band with the maximum at 1267 cm^{-1} in the spectrum were caused by coupling between C–O valence vibrations and the OH deformation vibration in the plane. The existence of the condensed polycyclic aromatic structure (naphthaene) confirmed the bands of C=C valence vibrations, ν(C=C), which occurred in the range of 1600–1450 cm^{-1} and were present in the spectrum with the maximal peaks at 1605, 1505, 1484 and 1458 cm^{-1}. OH deformation vibrations in the plane, δ(OH), and out of the plane, γ(OH), in the spectrum of naproxen (Fig. 3), provide the bands with the maximum at 1393 and 672 cm^{-1}, respectively [7]. The medium strength band at

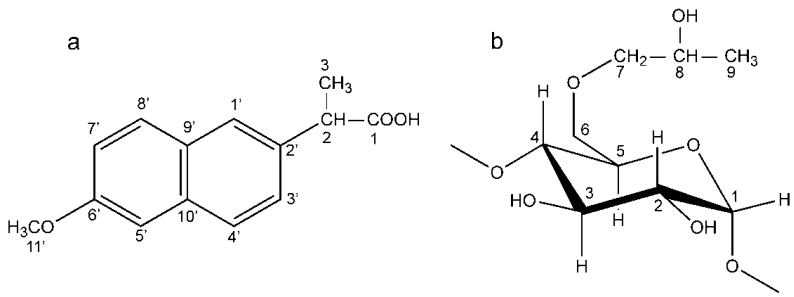

Figure 2. The numbering of C atoms with naproxen (a) and glucopyranosyl unit 2-hydroxypropyl-β-cyclodextrin (b).

Table 1. Chemical shifts (δ / ppm) of protons in the ^{1}H-NMR spectrum of naproxen, 2-hydroxypropyl-β-cyclodextrin and inclusion complex naproxen:2-hydroxypropyl-β-cyclodextrin and changes in chemical shift ($\Delta\delta$ / ppm); s – singlet, d – doublet, dd – doublet of doublets, t – triplet, q – quartet, m – multiplet, HP-β-CD – 2-hydroxypropyl-β-cyclodextrin

C-atom	Naproxen	Complex	$\Delta\delta$	C-atom	HP-β-CD	complex	$\Delta\delta$
1'	7.25 (*s*, 1H)	7.25 (*s*, 1H)	–	1	5.15 (*d*, 1H)	5.15 (*d*, 1H)	–
2	3.84 (*q*, 1H)	–	–	2	3.62 (*t*, 1H)	3.62 (*t*, 1H)	–
3	1.52 (*d*, 3H)	1.6 (*d*, 3H)	+0.08	3	3.975 (*t*, 1H)	4.02 (*t*, 1H)	+0.045
3'	7.13 (*dd*, 1H)	–	–	4	3.46–3.53 (*m*, 1H)	–	–
4'	7.71 (*d*, 1H)	7.71 (*d*, 1H)	–	5	–	–	–
5'	7.68 (*s*, 1H)	7.68 (*s*, 1H)	–	6	3.9 (*s*, 2H)	3.8 (*s*, 2H)	–0.1
7'	7.4 (*dd*, 1H)	7.4 (*dd*, 1H)	–	7	–	–	–
8'	7.76 (*d*, 1H)	7.76 (*d*, 1H)	–	8	–	–	–
11'	3.92 (*s*, 3H)	–	–	9	1.125 (*d*, 3H)	1.19 (*d*, 3H)	+0.065

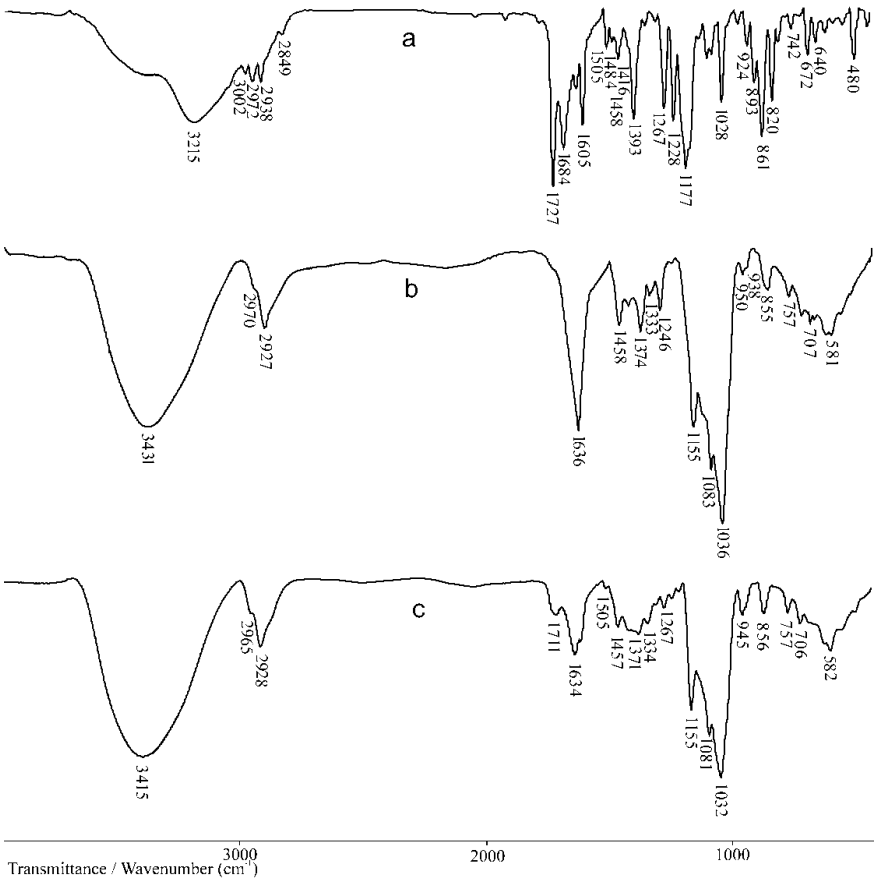

Figure 3. FTIR spectrum of naproxen (a), 2-hydroxypropyl-β-cyclodextrin (b) and inclusion complex of naproxen:2-hydroxypropyl-β--cyclodextrin (c).

924 cm^{-1}, which also originating from the OH group out-of-plane deformation vibration, indicates the possibility of dimeric forms of naproxen.

The FTIR analysis of the spectrum of 2-hydroxypropyl-β-cyclodextrin (Fig. 3, curve b) showed the characteristic wide band of high intensity with the maximum at 3431 cm^{-1}, which originated from the valence vibration of OH groups, ν(OH). The bands of valence vibrations of CH groups, ν(CH), in the of 2-hydroxypropyl-β-cyclodextrin were present at 2970 and 2927 cm^{-1}, while the bands of deformation vibrations in the plane, δ(CH), appeared at 1458 and 1374 cm^{-1}. The intensive band with the maximum at 1155 cm^{-1} was the result of valence vibrations of C–O–C bond, and this is the characteristic of saturated cyclic ethers. In the range of 1200–1000 cm^{-1} there was a complex band with the maxima at 1155, 1083 and 1036 cm^{-1} resulting from the coupling of asymmetric valence vibrations C–O, C–O–C, C–C–O and C–C–C bonds. In the FTIR spectrum of the host (Fig. 3, curve b) the existence of glucopyranose units was confirmed by the bands in the area of 700–1000 cm^{-1}, whereas the C1 of chairs conformation indicated the bands appearing in the spectrum at 950 and 855 cm^{-1}.

The analysis of the FTIR spectrum of the inclusion complex naproxen:2-hydroxypropyl-β-cyclodextrin (Fig. 3, curve c) showed that there was a difference in comparison to the FTIR spectra of naproxen (Fig. 3, curve a) and 2-hydroxypropyl-β-cyclodextrin (Fig. 3, curve b). The band of OH group valence vibrations, ν(OH), from 2-hydroxypropyl-β-cyclodextrin in the spectrum of the complex (Fig. 3, curve c) at 3415 cm^{-1} was shifted to lower wave numbers by 16 units, compared to the position of the same band in the spectrum of the host. This band covers the band of OH group valence vibrations from carboxyl groups of naproxen. In the spectrum of the complex, the valence vibrations of C=O group of naproxen provided a low intensity band with the maximum at 1711 cm^{-1}, the centroid of which was shifted towards smaller wave numbers by 16 units, compared to naproxen. This shift may indicate a non-covalent interaction of the host molecule with the guest molecule. In the spectrum of the complex, there was a characteristic band from the condensed polycyclic aromatic structure of naproxen, as a single band of low intensity which occurred at 1505 cm^{-1}. In the spectrum of the complex there was also a low intensity band with the maximum at 1267 cm^{-1}, which was the result of coupling between the valence vibration of C–O

groups and the deformation vibrations of OH groups from naproxen. Compared to the same bands in 2-hydroxypropyl-β-cyclodextrin spectrum (2970 and 2927 cm^{-1}), the medium intensity band with the maxima at 2965 and 2928 cm^{-1}, which were attributed to CH valence vibrations, showed a movement of the centroid towards smaller wave numbers for 5 and 1 units, respectively. This shift may be the result of establishing a hydrogen bond between the CH groups of complexing agents which are proton donors and the guest molecules.

The differences in the FTIR spectra indicated the formation of supramolecular structures by the type of inclusions and they were in compliance with the investigations of ^{1}H-NMR and XRD analysis.

Marrota *et al*. studied the photosensitivity of naproxen and kinetics of photodegradation. In the aqueous medium, 2-acetyl-6-methoxynaphthalen and 1-(6-methoxy-2-naphthyl)ethanol were determined as the main photodegradation products [27]. The scheme of photolytic degradation of naproxen is given in Fig. 4 [23].

Naproxen is a photosensitive molecule that, in the presence of oxygen, gives two degradation products, aromatic alcohol and ketone (Fig. 4). By decarboxylation of naproxen (**I**) a product is formed (**II**), *i.e*., 1-(6-methoxy-2-naphthyl) ethanol. By further oxidation of the resulting alcohol the photodegradation product (**III**), 2-acetyl-6-methoxynaphthalen was obtained, which may be derived directly from naproxen. By photodegradation of naproxen, the molecules with higher toxicity of naproxen which reduce the pharmacological activity and the safety of the drug application were obtained [23].

In these investigations the photostability of naproxen in the pure state and in the complex was monitored by FTIR spectroscopy during 30 days of exposure to daylight. The structure change of naproxen under the influence of daylight was monitored using UV–Vis spectrophotometry. The results of this testing are given in Fig. 5.

In the UV–Vis spectrum of naproxen, which was not exposed to daylight (Fig. 5, curve a), three absorption maxima at 208, 256 and 328 nm originating from the $\pi \rightarrow \pi^*$ transitions of naphthalene were found. The

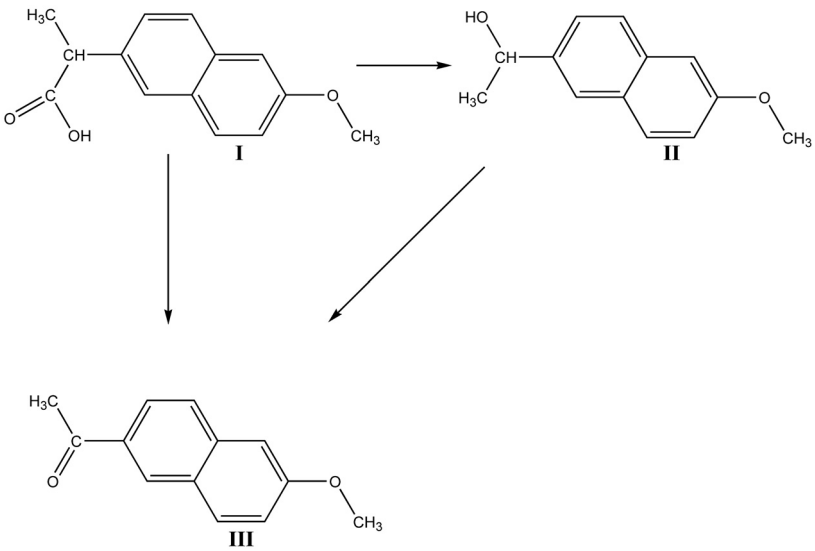

Figure 4. Photodegradation route of naproxen.

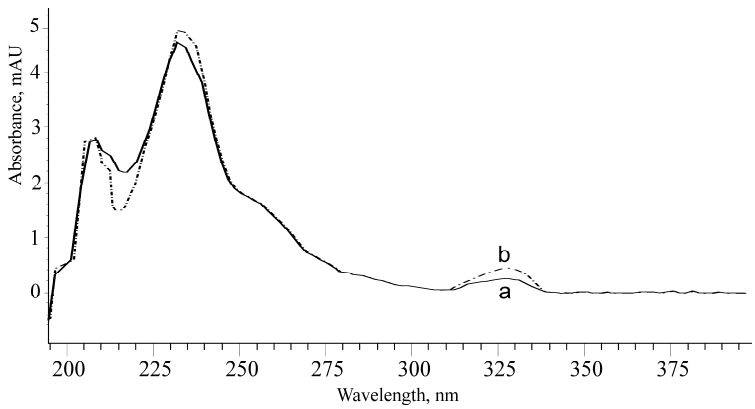

Figure 5. UV–Vis spectrum of naproxen not exposed to daylight (a) and after exposure to 30 days (b).

presence of C=O of carboxyl group in naproxen which originated from the n→π* transitions was confirmed by the maximum absorbance at 232 nm. In the UV–Vis spectrum of naproxen which was exposed to daylight for 30 days (Fig. 5, curve b) the absorption maxima at the same wavelengths as naproxen were observed but of a bit greater intensity. These maxima corresponded to π→π*and n→π* transitions of naphthalene and keto groups, respectively, which means that these functional groups were retained in the photodegradation product of naproxen. Based on the UV–Vis analysis it can be concluded that under the influence of daylight naproxen most probably formed aromatic ketone, 2-acetyl-6-methoxynaphthalen (**III**), which is in accordance with the studies of other authors [23].

FTIR spectra naproxen and naproxen which was exposed to daylight for a period of 30 days are given in Fig. 6.

The comparative analysis of the FTIR spectra of naproxen (Fig. 6, curve a) and naproxen exposed to daylight (Fig. 6, curve b) showed that in the spectrum of naproxen exposed to daylight for 15 days (Fig. 6, curve b) bands at 3213, 1393 and 924 cm^{-1} from the OH valence and deformation vibration were observed, which were less intensive than in the spectrum of naproxen (Fig. 6, curve a). The centroid of the band attributed to valence vibrations of OH group (3213 cm^{-1}) in the spectrum of naproxen which was exposed to daylight for 15 days was shifted to lower wave numbers by 2 units. These changes in the spectrum might indicate that a certain extent of naproxen was succumbed to photodegradation.

It is evident that there is no loss of the band from C=O valence vibrations in the spectrum of naproxen which is exposed to daylight for 15 days, which leads to the conclusion that in the structure of photodegradation products a keto group, C=O is still present. According to the studies of other researchers this corresponds to the photodegradation products **III** [23] (Fig. 4). The spectrum of naproxen which is continuously exposed to daylight for 30 days (Fig. 6, curve c) showed the additional reduction of the band intensity with the maxima at 3216, 1393, 924 and 672 cm^{-1}, while the band of the C=O group at 1727 cm^{-1} remained unchanged, compared to the same band in the spectrum of naproxen and naproxen exposed to daylight for 15 days. Based on the obtained results it can be suggested that photodegradation is heading towards the product **III,** *i.e.*, 2-acetyl-6-methoxynaphthalen, which is consistent with the UV–Vis analysis in this paper.

In order to determine the stability of naproxen in the inclusion complex with 2-hydroxypropyl-β-cyclodextrin, the change of the bands using the FTIR spectra was monitored for 30 days. Periodical recording was carried out and the results are shown in Fig. 7.

Comparing the FTIR spectra of the inclusion complex which was not exposed to daylight (Fig. 7, curve a) and the inclusion complex which was exposed to daylight for 30 days (Fig. 7, curve b), it is evident that there is no loss of the bands as well as their changes in

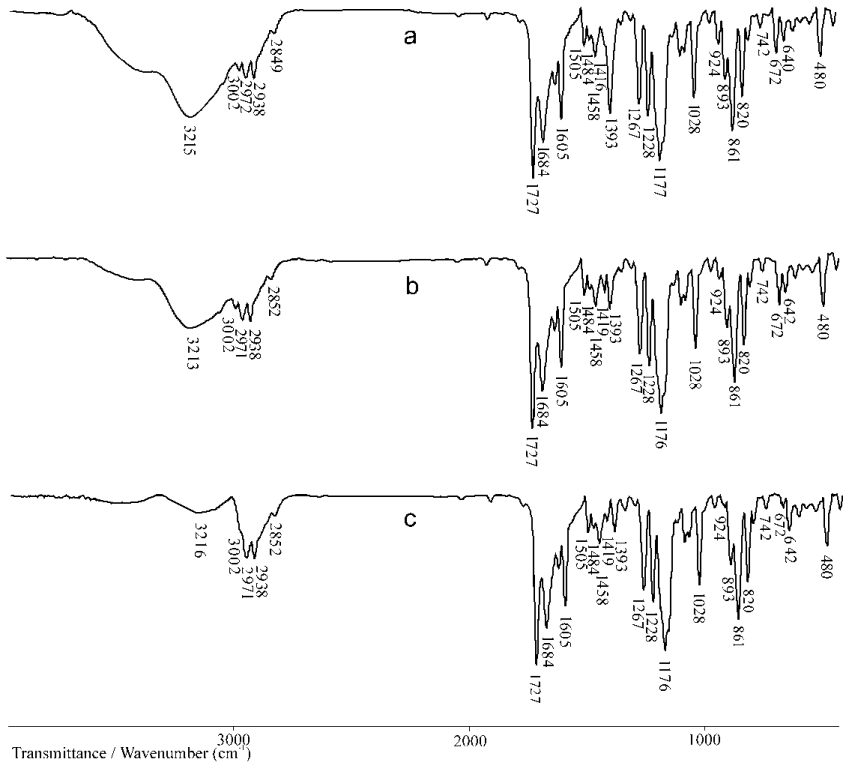

Figure 6. FTIR spectrum of naproxen not exposed to daylight (a) and after exposure to daylight for 15 (b) and 30 days (c).

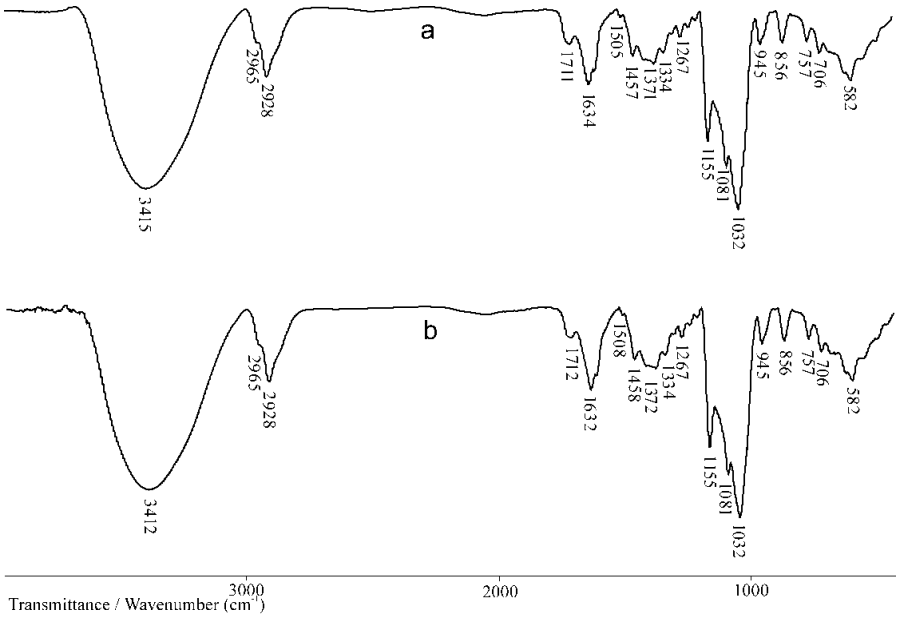

Figure 7. FTIR spectrum of the inclusion complex of naproxen:2-hydroxypropyl-β-cyclodextrin not exposed to daylight (a) and after exposure to 30 days (b).

the intensity and position or the appearance of new bands. These results indicate that the inclusion complex of naproxen:2-hydroxypropyl-β-cyclodextrin is photostabile and preserves naproxen for 30 days, while the uncomplexed naproxen is largely degraded for the same period.

CONCLUSION

The molecular inclusion complex was prepared by the co-precipitation method in the solid state at 1:1 molar ratio of the reactants. The loss of peaks in the complex naproxen:2-hydroxypropyl-β-cyclodextrin at 6.5, 13.4, 16.6, 18, 19.9, 22.1, 23.9 and 28.2°, which is a characteristic of naproxen in the XRD diffractogram, indicates that the drug is sheltered from the X-rays and shows that there was an inclusion of the drug in the hydrophobic cavity of 2-hydroxypropyl-β-cyclodextrin. Chemical shifts of the signals from H_3, H_6 and H_9 protons of glucopyranose units, as well as the signals of protons from CH_3 group of naproxen at position 3 in the ^{1}H-NMR spectrum of the complex, suggest the presence of non-covalent interactions of the host molecule with the guest molecule. The loss of characteristic bands in the FTIR spectrum of naproxen:2-hydroxypropyl-β-cyclodextrin also demonstrates the formation of supramolecular structures, which is consistent with the results of the previous analysis. The results of the investigation of photodegradation of naproxen by FTIR and UV–Vis methods show that naproxen is photo-unstable and that the main degradation product is the aromatic ketone, 2-acetyl-6-methoxynaphthalen (**III**). The inclusion complex of naproxen:2-hydroxypropyl-β-cyclodextrin showed the increased photostability of naproxen, compared to the uncomplexed naproxen.

Acknowledgement

This work is a part of the research done within the project TR 34012. The authors would like to thank to the Ministry of Education, Science and Technological Development, Republic of Serbia.

REFERENCES

[1] A. Bruke, E.M. Smzth, G.A. FitzGerald, in: L. Brunton, J. Lazo, K. Parker (Eds.), Goodman & Gilman's The pharmacological basis of therapeutics, 11th ed., The McGraw-Hill Companies, New York, 2005, pp. 687–733.

[2] P. Mura, N. Zerrouk, N. Mennini, F. Maestrelli, C. Chemtob, Development and characterization of naproxen–chitosan solid systems with improved drug dissolution properties, Eur. J. Pharm. Sci. **19** (2003) 67–75.

[3] N. Zerrouk, N. Mennini, F. Maestrelli, C. Chemtob, P. Mura, Comparison of the effect of chitosan and polyvinylpyrrolidone on dissolution properties and analgesic effect of naproxen, Eur. J. Pharm. Biopharm. **57** (2004) 93–99.

[4] P. Mura, F. Maestrelli, M. Cirri, Ternary systems of naproxen with hydroxypropyl-β-cyclodextrin and amino-acids, Eur. J. Pharm. Sci. **260** (2003) 293–302.

[5] M. Maghsoodi, D. Hassan-Zadeh, M. Barzegar-Jalali, A. Nokhodchi, G. Martin, Improved Compaction and Packing Properties of Naproxen Agglomerated Crystals Obtained by Spherical Crystallization Technique, Drug Dev. Ind. Pharm. **33** (2007) 1216–1224.

[6] G-V. Jin, X.Y. Ji, J.S. Choi, Preparation of Naproxen-Loaded Poly(ethylene oxide-β-methacrylic acid) Micelle

and Its pH-dependent Drug Release Behavior, Bull. Korean Chem. Soc. **30** (2009) 931–934.

[7] S. Bogdanova, I. Pajeva, P. Nikolova, I. Tsakovska, B. Müller, Interactions of Poly(vinylpyrrolidone) with Ibuprofen and Naproxen: Experimental and Modeling Studies, Pharm. Res. **22** (2005) 806–815.

[8] R. Nair, N. Nyamweya, S. Gönen, L.J. Martínez-Miranda, S.W. Hoag, Influence of various drugs on the glass transition temperature of poly(vinylpyrrolidone): a thermodynamic and spectroscopic investigation, Int. J. Pharm. **225** (2001) 83–96.

[9] N. Erdena, N. Çelebi, A study of the inclusion complex of naproxen with β-cyclodextrin, Eur. J. Pharm. Sci. **48** (1988) 83–89.

[10] J. Wang, I.M. Warner, Studies of the Naproxen:β-Cyclodextrin Inclusion Complex, Microchem. J. **48** (1993) 229–239.

[11] S.E. Brown, J.H. Coates, C.J. Easton, S.F. Lincoln, Y. Luo, A.K.W. Stephens, Cyclodextrin Inclusion Complexes of Two Non-Steroidal Antiinflammatory Drugs and of an Analgesic Drug, Aust. J. Chem. **4** (1991) 855–862.

[12] V. Nikolić, Lj. Nikolić, M. Stanković, A. Kapor, M. Popsavin, D. Cvetković, A molecular inclusion complex of atenolol with 2-hydroxypropyl-β-cyclodextrin; the production and characterization thereof, J. Serb. Chem. Soc. **72** (2007) 737–746.

[13] R. Ficarra, P. Ficarra, M.R. Di Bella, D. Raneri, S. Tommasini, M.L. Calabro, M.C. Gamberini, C. Rustichelli, Study of β-blockers/β-cyclodextrins inclusion complex by NMR, DSC, X-ray and SEM investigation, J Pharm Biomed. Anal. **23** (2000) 33–40.

[14] R. Ficarra, P. Ficarra, M.R. Di Bella, D. Raneri, S. Tommasini, M.L. Calabro, A. Villari, S. Coppolino, Study of the inclusion complex of atenolol with β-cyclodextrins, J. Pharm. Biomed. Anal. **23** (2000) 232–236.

[15] V. Nikolić, D. Ilić, Lj. Nikolić, M. Stanković, M. Cakić, Lj. Stanojević, A. Kapor, M. Popsavin, The protection of Nifedipin from photodegradation due to complex formation with β-cyclodextrin, Cent. Eur. J. Chem. **8** (2010) 744–749.

[16] J. Mielcarek, Photochemical stability of the inclusion complexes of nicardipine with α-, γ-cyclodextrin, methyl-β-cyclodextrin, hydroxypropyl-β-cyclodextrins in the solid state and in solution, Pharmazie **51** (1996) 477–479.

[17] K.L.A. Chan, S.G. Kazarian, FTIR spectroscopic imaging of dissolution of a solid dispersion of nifedipine in poly-(ethylene glycol), Mol. Pharm. **1** (2004) 331–335.

[18] A. Kapor, V. Nikolić, Lj. Nikolić, M. Stanković, M. Cakić, Lj. Stanojević, D. Ilić, Inclusion complexes of amlodipine besylate and cyclodextrins, Cent. Eur. J. Chem. **8** (2010) 834–841.

[19] J. Mielcarek, A. Czernielewska, B. Czarczynska, Inclusion Complexes of Felodipine and Amlodipine with Methyl-β-cyclodextrin, J. Incl. Phenom. Macrocycl. Chem. **54** (2006) 17–21.

[20] V. Nikolić, M. Stanković, A. Kapor, Lj. Nikolić, D. Cvetković, J. Stamenković, Allylthiosulfinate; β-cyclodextrin inclusion complex: preparation, characterization and microbiological activity, Pharmazie **59** (2004) 845–848.

[21] M.C.B. Lira, M.S. Ferraz, D.G.V.C. da Silva, M.E. Cortes, K.I. Teixeria, N.P. Caetano, R.D. Sinisterra, G. ponchel, N.S. Santos-Magalhes, Inclusion complex of usnic acid with β-cyclodextrin: characterization and nanoencapsulation into liposomes, J. Incl. Phenom. Macrocycl. Chem. **64** (2009) 215–224.

[22] L.J. Martínez, J.C. Scaiano, Characterization of the transient intermediates generated from the photoexcitation of nabumetone: a comparison with naproxen, Photochem. Photobiol. **68** (1998) 646–651.

[23] W. Cory, A. DeSantis, C. Ulmer, Photodegradation of Naproxen and Ibuprofen and the Formation of Ecotoxic Photoproducts in Natural Water Systems, IWA Specialty Conference on natural Organic Matter, Costa Mesa, CA, July 27-29, 2011.

[24] V. Nikolić, S. Ilić-Stojanović, Lj. Nikolić, M. Cakić, A. Zdravković, A. Kapor, M. Popsavin, Photostability of piroxicam in the inclusion complex with 2-hydroxypropyl--β-cyclodextrin, Hem. Ind. **68** (2014) 107–116.

[25] V. Nikolić, M. Stanković, Lj. Nikolić, G. Nikolić, S. Ilić-Stojanović, M. Popsavin, S. Zlatković, T. Kundaković, Inclusion complexes with cyclodextrin and usnic acid, J. Incl. Phenom. Macrocycl. Chem. **76** (2013) 173–182.

[26] N. Tiong, A.A. Elkordy, Effects of liquisolid formulations on dissolution of naproxen, Eur. J. Pharm. Biopharm. **73** (2009) 373–384.

[27] R. Marotta, D. Spasiano, I. Di Somma, R. Andreozzi,: Photodegradation of naproxen and its photoproducts in aqueous solution at 254 nm: A kinetic investigation. Water Res. **47** (2013) 373–383.

IZVOD

POBOLJŠANA FOTOSTABILNOST NAPROKSENA U INKLUZIONOM KOMPLEKSU SA 2-HIDROKSIPROPIL-β-CIKLODEKSTRINOM

Snežana S. Ilić-Stojanović[1], Vesna D. Nikolić[1], Ljubiša B. Nikolić[1], Aleksandar S. Zdravković[2], Agneš J. Kapor[3], Mirjana M. Popsavin[4], Slobodan D. Petrović[5]

[1]*Univerzitet u Nišu, Tehnološki fakultet, Leskovac, Srbija*
[2]*Visoka strukovna škola za tekstil, Leskovac, Srbija*
[3]*Univerzitet u Novom Sadu, Prirodno-matematički fakultet, Departman za Fiziku, Novi Sad, Srbija*
[4]*Univerzitet u Novom Sadu, Prirodno-matematički fakultet, Departman za Hemiju, Novi Sad, Srbija*
[5] *Univerzitet u Beogradu, Tehnološko-Metalurški fakultet, Beograd, Srbija*

(Naučni rad)

Naproksen, (+)-(*S*)-2-(6-metoksinaftalen-2-il)propionska kiselina, je derivat 2-arilpropionske kiseline (profena) iz grupe nesteroidnih antiinflamatornih lekova koji u terapijskim dozama smanjuje biosintezu prostaglandina i snižava povišenu telesnu temperaturu. Ovaj slabo rastvoran i fotoosetljiv molekul se transformiše pod uticajem svetlosti dajući farmakološki neaktivne proizvode. Cilj ovog rada je priprema inkluzionog kompleksa naproksena sa 2-hidroksipropil-β-ciklodekstrinom (HP-β-CD) u cilju poboljšanja fizičko-hemijskih svojstava naproksena. Molekulski inkluzioni kompleks naproksena i HP-β-CD pripremljen je metodom koprecipitacije u čvrstom stanju u molskom odnosu 1:1. Za strukturnu karakterizaciju kompleksa, kompleksirajućeg agensa, odgovarajuće fizičke smeše i naproksena, korišćene su metode protonske nuklearne magnetne rezonance (^{1}H-NMR), difrakcije rendgenskih zraka (XRD) i infracrvene spektrofotometrije sa Furijeovom transformacijom (FTIR). FTIR i UV–Vis metode korišćene su za analizu fotoosetljivih grupa naproksena u čistom i kompleksiranom obliku radi ispitivanja uticaja na fotostabilnost naproksena. Difraktogram inkluzionog kompleksa naproksen:2-hidroksipropil-β-ciklodekstrin ne sadrži pikove koji su karakteristični za difraktograme naproksena i HP-β-CD. Ovo ukazuje da je naproksen zaklonjen u šupljine domaćina prilikom molekularne inkapsulacije. Odsustvo karakterističnih pikova naproksena u FTIR spektru kompleksa ukazuje na formiranje supramolekularne strukture po tipu inkluzije. Hemijska pomeranja u ^{1}H-NMR spektru nakon inkluzije naproksena u šupljine HP-β-CD, posebno H_3, H_6 i H_9 protona i vodonika iz CH_3 u HP-β-CD takođe ukazuju na formiranje molekulskog inkluzionog kompleksa. Ispitivanje fotostabilnosti naproksena, pomoću UV-Vis metode, ukazuje na degradaciju do aromatičnog ketona, 2-acetil-6-metoksinaftalena. FTIR analiza je pokazala da degradacija naproksena počinje nakon 15 dana izlaganja dnevnoj svetlosti i da je molekularnom inkapsulacijom on zaštićen od fotodegradacije za vremenski period od 30 dana.

Ključne reči: Naproksen • Fotodegradacija • 2-hidroksipropil-β-ciklodekstrin • Inkluzioni kompleks

Površinski napon i suspenzibilnost radnih tečnosti fungicida, insekticida i nepesticidnih supstanci zavisno od kvaliteta vode

Slavica M. Vuković, Dušanka V. Inđić, Sonja M. Gvozdenac

Univerzitet u Novom Sadu, Poljoprivredni fakultet, Novi Sad

Izvod

Cilj rada je bio određivanje površinskog napona i suspenzibilnosti radnih tečnosti fungicida (Quadris i Dithane M-70), insekticida (Actara 25-WG i Cipkord 20-EC) i njihovih mešavina sa nepesticidnim supstancama (komleksno đubrivo – Mortonjic plus; ađuvant – Sillwet L-77), zavisno od kvaliteta vode (bunarska, česmenska ili površinska), koje se koriste u poljoprivredi (navodnjavanje i primena agrohemikalija). Sve ispitane vode su imale visok površinski napon (63,8–68,7 mJ/m²). Smanjenje istog za oko 50%, u odnosu na kontrolne vode, ostvareno je ađuvantom (Sillwet L-77) i preparatom formulisanim kao koncentrat za emulziju (Cipkord 20-EC) dodavanjem u radne tečnosti pesticida i nepesticidnih supstanci, a smanjenje za oko 2/3 je registrovano u vodi iz reke Save. Evidentno je smanjenje suspenzibilnosti upotrebom česmenske vode za razliku od ostalih voda, ali i u mešavinama koje sadrže Dithane M-70.

Ključne reči: površinski napon, suspenzibilnost, fungicidi, insekticidi, nepesticidne komponente, mešavine, kvalitet vode.

Dostupno na Internetu sa adrese časopisa: http://www.ache.org.rs/HI/

STRUČNI RAD

UDK 628:631.67:544

Hem. Ind. **69** (4) 371–380 (2015)

doi: 10.2298/HEMIND140303051V

Primena pesticida u zaštiti bilja protiv štetnih organizama je nužnost savremene poljoprivrede, uslovljena potrebom za očuvanjem prinosa i proizvodnjom sve većih količina hrane. Veliki broj pesticida u zaštiti bilja, zavisno od oblika formulacije, primenjuje se uz prethodno razređenje vodom. Svojstva vode kao što su pH, elektroprovodljivost i tvrdoća, mogu uticati na kvalitet i efekat primene kako pojedinačnih pesticida tako i njihovih mešavina, kao i pri mešanju pesticida i nepesticidnih supstanci (kompleksna đubriva, ađuvanti i protektanti), što za posledicu ima povećanje rizika primene istih [1]. Pomenuta svojstva vode mogu prouzrokovati ubrzanu razgradnju aktivne supstance, promene u suspenzibilnosti ili ne retko i u biološkom efektu (antagonizam, aditivni efekat i sinergizam), pa i nepoželjne, toksične promene na biljkama. Navedena svojstva vode su promenljiva i zavise od sezonskih i klimatskih kolebanja, a nekada i elementarnih nepogoda [2].

Poljoprivreda je jedan od najznačajnijih korisnika vodnih resursa, s obzirom da se veliki procenat gajenih biljaka navodnjava, ali i da se priprema radnih tečnosti pesticida ili kompleksnih đubriva, obavlja korišćenjem podzemnih ili površinskih voda [3], a u skorije vreme sve više i česmenske vode.

Imajući u vidu izneto, od velikog značaja su saznanja o kvalitetu vode i njen uticaj na fizičko-hemijske promene radnih tečnosti pesticida u cilju što uspešnije zaštite bilja i što racionalnije poljoprivredne proizvodnje. Kako u našoj zemlji tako i u svetu, istraživanja iz ove oblasti su vrlo retka i pružaju veoma malo informacija, te su ova ispitivanja usmerena u pravcu verifikacije fizičko–hemijskih svojstava odnosno, površinskog napona i suspenzibilnosti radnih tečnosti pesticida zavisno od kvaliteta vode u kojoj se razređuju. Površinski napon se kreće od 72,7 mJ/m² (voda na 20 °C) za polarne tečnosti pa do 20 mJ/m² za nepolarne tečnosti (destilat petroleuma). Što je vrednost površinskog napona viša, to je kvašljivost radnih tečnosti pesticida manja [4]. Svojstvo kvašljivosti radnih tečnosti pesticida je veoma važno, jer za primenu većine sredstava za zaštitu bilja, pokrovnost biljnih delova tankim slojem ili finom pesticidnom prevlakom, garancija je većeg uspeha pri primeni istih. Kvašljivost se određuje merenjem površinskog napona radne tečnosti pesticida, i predstavlja količinu energije potrebnu da se površina tečnosti poveća za jedinicu (1 m^2), odnosno to je sila koja deluje tangencijalno na jedinicu dužine linije na graničnoj površini tečnosti i u obrnutoj je zavisnosti od kvašljivosti.

Suspenzibilnost ili postojanost suspenzije je svojstvo radnih tečnosti pesticida uslovljeno finoćom i oblikom čestica, ali i specifičnom masom, čija je veličina u suspenziji do 10 μm [4]. Po pripremi radnih tečnosti, suspenzibilnost se procenjuje najpre vizuelno, evidentiraju se moguće pojave kao što su aglomeracija, kristalizacija i sedimentacija, a i merenjem posle 30 min. Promene u suspenzibilnosti mogu nastati pri mešanju različitih ili istih formulacija pesticida, kao i istih s nepesticidnim supstancama [5,6]. Imajući u vidu napred izneto, cilj rada je bio odrediti površinski napon i suspenzibilnost radnih tečnosti fungicida, insekticida i njihovih meša-

Prepiska: S.M. Vuković, Departman za fitomedicinu i zaštitu životne sredine, Poljoprivredni fakultet, Univerzitet u Novom Sadu, Trg Dositeja Obradovića 8., 21000 Novi Sad, Srbija.

E-pošta: vukovic@polj.uns.ac.rs

Rad primljen: 3. mart, 2014

Rad prihvaćen: 17. jun, 2014

vina sa nepesticidnim supstancama zavisno od kvaliteta vode (bunarska, česmenska ili površinska).

EKSPERIMENTALNI DEO

Ispitivanja površinskog napona i suspenzibilnosti pesticida zavisno od kvaliteta vode za tretiranje, obavljena su u laboratorijama Deprtmana za fitomedicinu i zaštitu životne sredine, Poljoprivredni fakultet, Novi Sad. Kvalitet voda određen je u Laboratoriji za ispitivanje prehrambenih proizvoda i hrane za životinje, Tehnološki fakultet, Novi Sad.

Vode uključene u ispitivanja

Izabrano je pet voda od čega su dve bunarske (lokaliteti Bečej i Adice), jedna česmenska (Novi Sad) i dve površinske vode (reke Karaš i Sava).

Kvalitet voda

Kvalitet voda (pH, tvrdoća, elektroprovodljivost, hloridi, nitriti, nitrati, amonijak, kalcijum i gvožđe) određen je po standardnim metodama (tabela 1).

Pesticidi, kompleksno đubrivo, ađuvant i njihove mešavine

U tabeli 2 su prikazani fungicidi, insekticidi, kompleksno đubrivo (u daljem tekstu: M+), ađuvant, njihove dvojne i trojne mešavine, i primenjene količine u eksperimentima.

Određivanje površinskog napona

Površinski napon je određen pomoću tenziometra (Lecomte du Nouy) po metodi iz literature [4] i izražen je u mJ/m^2 sa tačnošću ±0,1 mJ/m^2.

Određivanje suspenzibilnosti

Kao fizičko–hemijska osobina radnih tečnosti, preparata formulisanih kao kvašljivi prašak (WP), koncentrovana suspenzija (SC), vododisperzibilne granule (WG) i mešavine koje ih sadrže, određena je standardnom metodom CIPAC MT 15 [7]. Suspenzibilnost je izražena u procentima (%) a donja propisana granica za pesticide je 60%.

Tabela 2. Insekticidi, fungicidi, kompleksno đubrivo, ađuvant, njihove mešavine i primenjene količine
Table 2. Insecticides, fungicides, complex fertilizer, ađuvant, their mixtures and application rates

Redni broj	Preparat	Primenjene količine (kg, l/ha)/300 L vode
1.	Quadris	0,75 l/ha
2.	Dithane M-70	2,5 kg/ha
3.	Actara 25-WG	0,07 kg/ha
4.	Cipkord 20-EC	0,3 l/ha
5.	Mortonijc plus (M^+)	3 kg/ha
6.	Sillwet L-77	0,1 l/ha
7.	Quadris +Cipkord 20-EC	0,75 l/ha+0,3 l/ha
8.	Quadris +Actara 25-WG	0,75 l/ha+ 0,07 kg/ha
9.	Dithane M-70+Cipkord 20-EC	2,5 kg/ha+0,3 l/ha
10.	Dithane M-70+Actara 25-WG	2,5 kg/ha+0,07 kg/ha
11.	Cipkord 20-EC+ Mortonijc plus	0,3 l/ha+3,0 kg/ha
12.	Quadris+ Mortonijc plus	0,75 l/ha+3,0 kg/ha
13.	Dithane M-70+ Mortonijc plus	2,5 kg/ha+3,0 kg/ha
14.	Actara 25-WG+ Mortonijc plus	0,07 kg/ha+3,0 kg/ha
15.	Quadris+ Silwett L-77	0,75 l/ha+0,1 l/ha
16.	Dithane M-70+ Silwett L-77	2,5 kg/ha+0,1 l/ha
17.	Cipkord 20-EC+Silwett L-70	0,3 l/ha+0,1 l/ha
18.	Actara 25-WG+Silwett L-77	0,07 kg/ha+0,1 l/ha
19.	Quadris+Cipkord 20-EC + Mortonijc plus	0,75 l/ha+0,3 l/ha+3,0 kg/ha

Tabela 1. Kvalitet voda korišćenih u ogledu
Table 1. The quality of water used in the experiment

Lokalitet sa kojeg je uzorkovana voda (GPS)	pH	Tvrdoća d°H	Elektroprovodljivost µS/cm	Cl	NO_2^-	NO_3^-	NH_3	Ca^{2+}	$Fe^{2+,3+}$
				mg/l					
Bunarske vode									
Bečej (N 45°37,329' Eo 20°2,155')	7,90	9,20	2200	61,5	0,05	6,0	16,9	37,5	0,768
Adice (N 45°13,868' Eo19°46,870')	7,55	34,7	1470	61,2	2,5	36,0	0,0	74,8	<0,05
Česmenska voda									
Novi Sad (N 45°14,833' Eo 19°51,132')	7,42	15,4	641	26,0	0,002	2,8	0,01	78,4	0,02
Površinske vode									
Karaš (N 44° 57,733' Eo 21°19,012')	8,10	12,9	463	7,9	0,3	16,0	0,0	82,5	0,100
Sava, Sr. Mitrovica (N 44° 58,477' Eo 19°35,629')	8,15	11,7	415	7,4	0,18	15,6	0,93	67,3	<0,3
II klasa vode[a]	**6,8–8,5**	[b]	**2500**	**200**	**0,03**	**50**	**0,1**	**200**	**0,3**

[a]Maksimalno dozvoljene vrednosti za kvalitet vode II klase [22]; [b]skala za tvrdoću vode: 0–4 vrlo meka; 4–8 slabo meka; 8–16 slabo tvrda; 16–30 tvrda; preko 30 jako tvrda)

Tabela 2. Nastavak
Table 2. Continued

Redni broj	Preparat	Primenjene količine u 300 L vode
20.	Quadris+ Actara 25-WG+ Mortonijc plus	0,75 l/ha+0,07 kg/ha+3,0 kg/ha
21.	Dithane M-70+ Cipkord 20-EC+ Mortonijc plus	2,5 kg/ha+0,3 l/ha+3,0 kg/ha
22.	Dithane M-70+ Actara 25-WG+ Mortonijc plus	2,5 kg/ha+0,07 kg/ha+3,0 kg/ha
23.	Quadris+Cipkord 20-EC+ Silwett L-77	0,75 l/ha+0,3 l/ha+0,1 l/ha
24.	Quadris+Actara 25 WG+ Silwett L-77	0,75 l/ha+0,07 kg/ha+0,1 l/ha
25.	Dithane M-70+ Cipkord 20-EC+ Silwett L-77	2,5 kg/ha+0,3 l/ha+0,1 l/ha
26.	Dithane M-70+ Actara 25-WG+ Silwett L-77	2,5 kg/ha+0,07 kg/ha+0,1 l/ha

REZULTATI

Površinski napon radnih tečnosti zavisno od kvaliteta vode

Svih pet ispitivanih voda u kontroli, imale su površinski napon 63,8–68,7 mJ/m² na početku eksperimenta (slike 1–5). Merenjem posle 24 h kod četiri vode je registrovano smanjenje površinskog napona, a povećao se jedino kod vode iz reke Karaš.

Površinski napon bunarske vode iz Bečeja je 68 mJ/m², a posle 24 h je 54,3 mJ/m². Radne tečnosti fungicida su ispoljile smanjenje površinskog napona u odnosu na samu vodu, i on se kretao od 51,2–53,7 mJ/m² po mešanju, odnosno 53,8–60,3 mJ/m² posle 24 h (sl. 1). Kod radne tečnosti preparata Actara 25-WG površinski napon je iznosio 45,7 mJ/m² po mešanju, a 53,2 mJ/m posle 24 h, a kod preparata Cipkord 20-EC 32,5 mJ/m² po mešanju, a 33,7 mJ/m² posle 24 h. Kompleksno đubrivo M+ je ispoljilo visok površinski napon 60,3–63,8 mJ/ m², kako po mešanju, tako i posle 24 h što je više nego u kontroli, dok je Sillwet L-77 odmah po mešanju smanjio površinski napon za preko 50% (33,8 mJ/m²), a posle 24 h za preko 40% u odnosu na kontrolu. Sve radne tečnosti nezavisno od pesticidnih komponenata, koje sadrže površinski aktivnu komponentu (Sillwet L-77) ili preparat EC formulacije (Cipkord 20-EC) su smanjile površinski napon za oko 30 mJ/m², kako po mešanju tako i posle 24 h u odnosu na kontrolne vode. Smanjenje površinskog napona za 10–20 mJ/m² u odnosu na kontrolu je izmereno kod radnih tečnosti koje ne sadrže ađuvant i insekticid Cipkord 20-EC. Kod svih radnih tečnosti evidentiran je porast, površinskog napona posle 24 h, iako neznatno u odnosu na vrednosti koje su izmerene odmah po mešanju, osim kod varijanti Cipkord 20-EC+Sillwet L-77, Quadris+Cipkord 20-EC+M+ i Dithane M-70+Actara 25-WG+M+ gde je isti smanjen posle 24 h. Na osnovu iznetog može se konstatovati da površinski napon radnih tečnosti zavisi od komponenti i vremena stajanja.

Površinski napon bunarske vode iz Adica (slika 2) u kontroli je iznosio 68,7, a 63 mJ/m² posle 24 h, odnosno

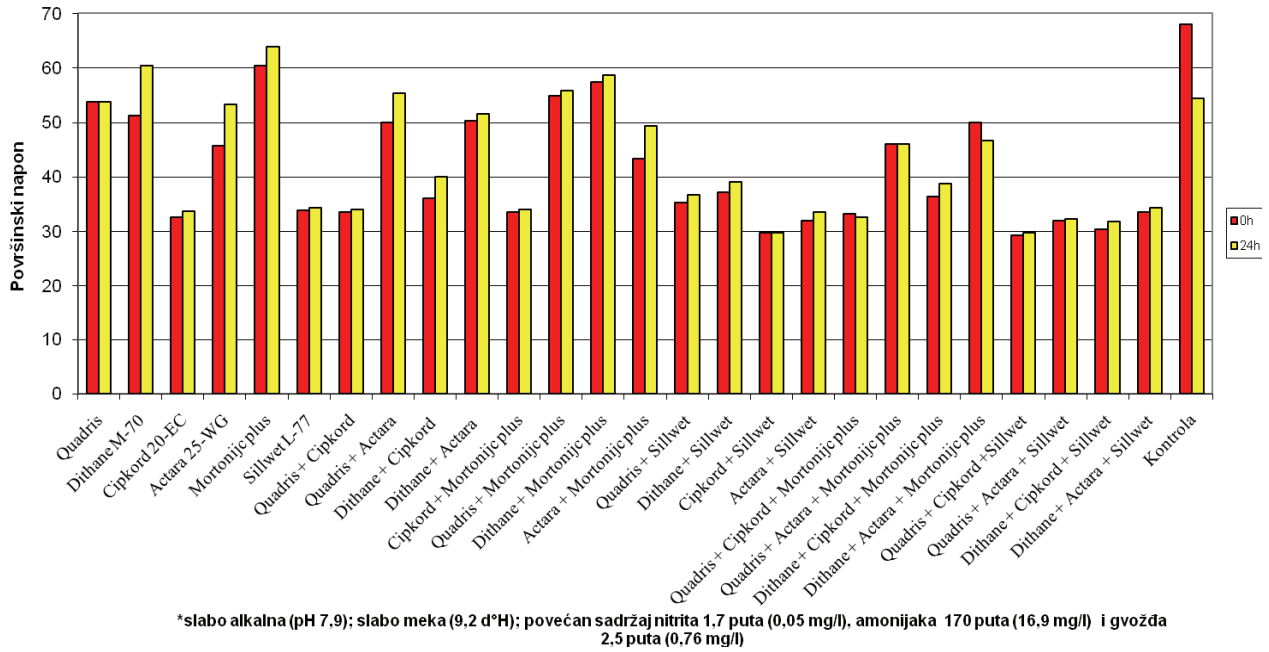

Slika 1. Površinski napon (mJ/m²) radnih tečnosti fungicida, insekticidai nepesticidnih supstanci (kompleksno đubrivo i ađuvant) i njihovih smeša, odmah po pripremi i posle 24 h u bunarskoj vodi Bečej.
Figure 1. Surface tension (mJ/m²) of spray liquides of fungicides, insecticides and non-pesticide substances (complex fertilizer and ađuvant) and their mixtures immediately after preparation and after 24 h in well water from Bečej.

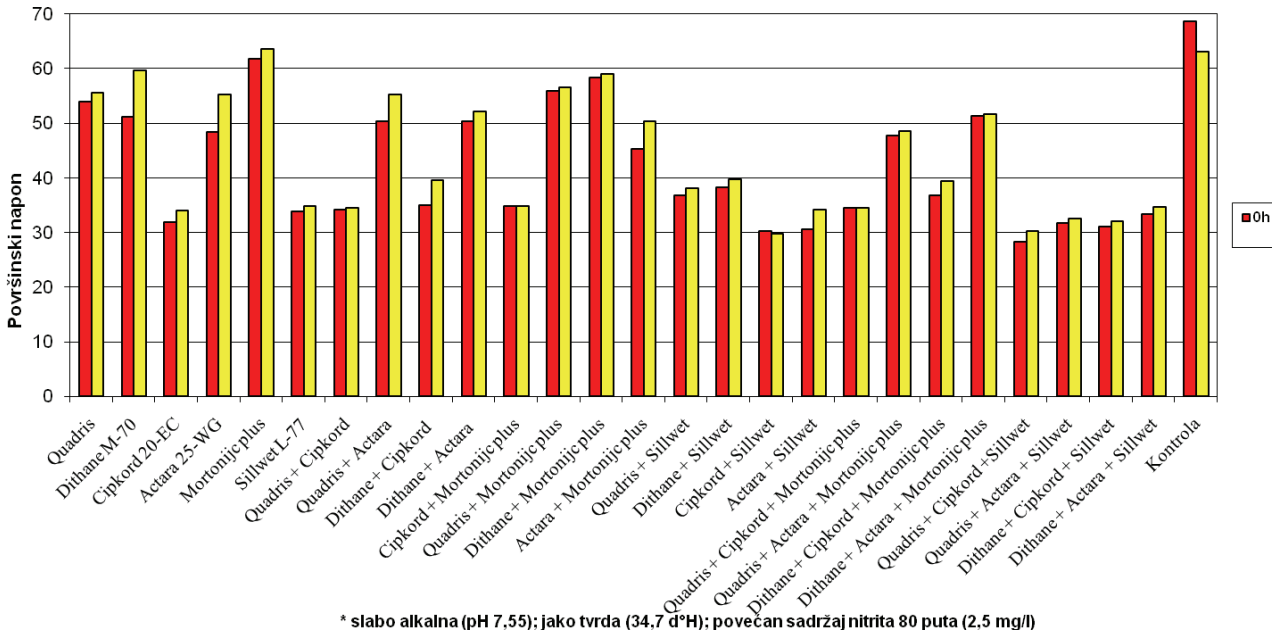

Slika 2. Površinski napon (mJ/m²) radnih tečnosti fungicida, insekticida i nepesticidnih supstanci (kompleksno đubrivo i ađuvant) i njihovih smeša, odmah po pripremi i posle 24 h u bunarskoj vodi Adice.
Figure 2. Surface tension (mJ/m²) of spray liquides of fungicides, insecticides and non-pesticide substances (complex fertilizer and ađuvant) and their mixtures immediately after preparation and after 24 h in well water from Adice.

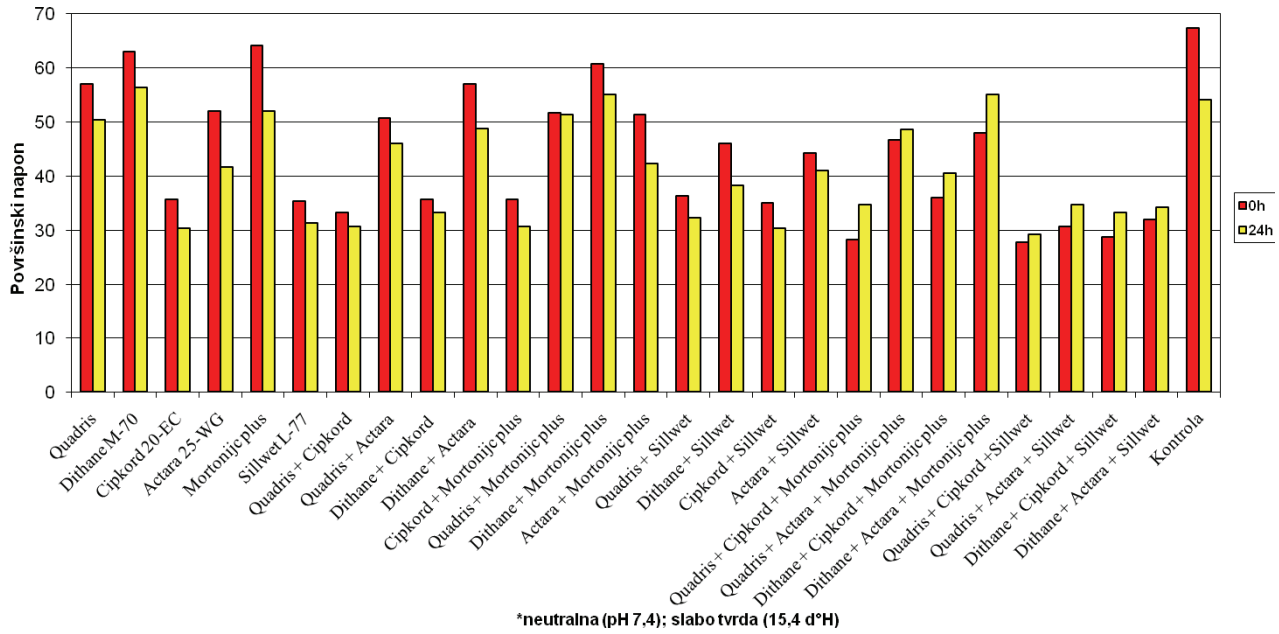

Slika 3. Površinski napon (mJ/m²) radnih tečnosti fungicida, insekticidai nepesticidnih supstanci (kompleksno đubrivo i ađuvant) i njihovih smeša, odmah po pripremi i posle 24 h u česmenskoj vodi Novi Sad
Figure 3. Surface tension (mJ/m²) of spray liquides of fungicides, insecticides and non-pesticide substances (complex fertilizer and ađuvant) and their mixtures immediately after preparation and after 24 h in tap water from Novi Sad.

smanjio se. Kod radnih tečnosti preparata Quadris i Dithane M-70 je smanjen površinski napon u odnosu na kontrolu, i iznosio je 51,2–54,0 mJ/m² po mešanju i 55,5–59,7 mJ/m² posle 24 h. Izmeren površinski napon radne tečnosti preparata Actara 25-WG je bio 48,3 mJ/m² po mešanju, a posle 24 h 55,2 mJ/m², a kod preparata Cipkord 20-EC 31,8 mJ/m² po mešanju, a posle 24 h je iznosio 34,0 mJ/m². Kompleksno đubrivo M+ je neznatno smanjilo površinski napon (61,7 mJ/m²) odmah po mešanju, a posle 24 h je bio na nivou sa kontrolom. Ađuvant je i u ovoj vodi smanjio površinski napon za oko 50% (33,8 mJ/m²) po mešanju, a posle 24

h za oko 45% u odnosu na kontrolu. Kod svih radnih tečnosti koje sadrže komponentu Sillwet L-77 i/ili Cipkord 20-EC, površinski napon je smanjen u odnosu na kontrolu za oko 30 mJ/m² ili oko 50% kako po mešanju tako i posle 24 h. Sve radne tečnosti su ispoljile neznatan porast površinskog napona posle 24 h od pripreme, u odnosu na vrednosti koje su ostvarene odmah po mešanju, osim smeše Cipkord 20-EC+ Sillwet L-77 kod koje je došlo do neznatnog smanjenja površinskog napona posle 24 h. Na osnovu navedenog može se konstatovati da površinski napon radnih tečnosti u bunarskoj vodi Adice zavisi od komponenti i vremena stajanja istih što ukazuje na neophodnu primenu pomenutih kombinacija ispitivanih jedinjenja odmah po mešanju da ne bi došlo do smanjenja kvašljivosti.

Na slici 3 je prikazan površinski napon česmenske vode iz Novog Sada i on je iznosio 67,3 mJ/m², a posle 24 h je 54 mJ/m², to jest smanjivao se. Kod radnih tečnosti fungicida (Quadris i Dithane M-70) površinski napon je iznosio 57–63 mJ/m² odmah po mešanju, a smanjen je posle 24 h na 50,3–56,3 mJ/m² respektivno. Radne tečnosti insekticida Actara 25-WG su imale površinski napon 52,0 mJ/m² po mešanju, a posle 24 h je došlo do smanjenja na 41,7 mJ/m². Za preparat Cipkord 20-EC površinski napon je iznosio 35,7 mJ/m² po mešanju, a posle 24 h stajanja 30,3 mJ/m² i znatno je smanjen i u odnosu na kontrolu. Kompleksno đubrivo M+ je ispoljilo visok površinski napon 64,0 mJ/ m², kako odmah po mešanju, tako i posle 24 h i iznosio je 52,0 mJ/m², dok je ađuvant Sillwet L-77 ispoljio znatno smanjenje površinskog napona (31,3 mJ/m²) u odnosu na kontrolnu vodu. Sve mešavine koje sadrže ađuvant i/ili insekticid Cipkord 20-EC, to jest formulaciju koncentrat za emulziju, površinski napon je smanjen (29,3–38,3 mJ/m²) za skoro 50% u odnosu na površinski napon u kontroli (67,3 mJ/m²), dok druge pojedinačne komponente (52–63 mJ/m²) kao i mešavina koje ih ne sadrže (42,3–56,3 mJ/m²), kako po mešanju tako i posle 24 h imale su znatno viši površinski napon odnosno njihova kvašljivost se smanjila. U česmenskoj vodi sve radne tečnosti su ispoljile smanjenje površinskog napona posle 24 h od pripreme, u odnosu na vrednosti koje su ostvarene po mešanju, osim radnih tečnosti koje sadrže tri komponente, gde je došlo do povećanja površinskog napona. Na osnovu ostvarenih rezultata evidentno je da se površinski napon radnih tečnosti menja zavisno od komponenti i vremena stajanja.

Površinski napon vode Karaš je 63,8 mJ/m², a posle 24 h se neznatno povećao i iznosio je 65,5 mJ/m². Kod radnih tečnosti fungicida površinski napon je povećan u odnosu na kontrolnu vodu i iznosio je 66,2–68,8 mJ/m² po mešanju, dok je posle 24 h smanjen (63,8–64,5 mJ/m²) u odnosu na kontrolu (slika 4). Za insekticid Actara 25-WG, površinski napon radne tečnosti odmah po pripremi je iznosio 51,0 mJ/m², a posle 24 h je 50,8 mJ/m², dok je za Cipkord 20-EC iznosio 35,3 mJ/m² kako po mešanju tako i posle 24 h. Površinski napon kompleksnog đubriva M+ je 64,2 mJ/m² po mešanju, a posle 24 h se smanjuje na 61,8 mJ/m². Ađuvant je i u ovoj vodi znatno smanjio površinski napon u odnosu na

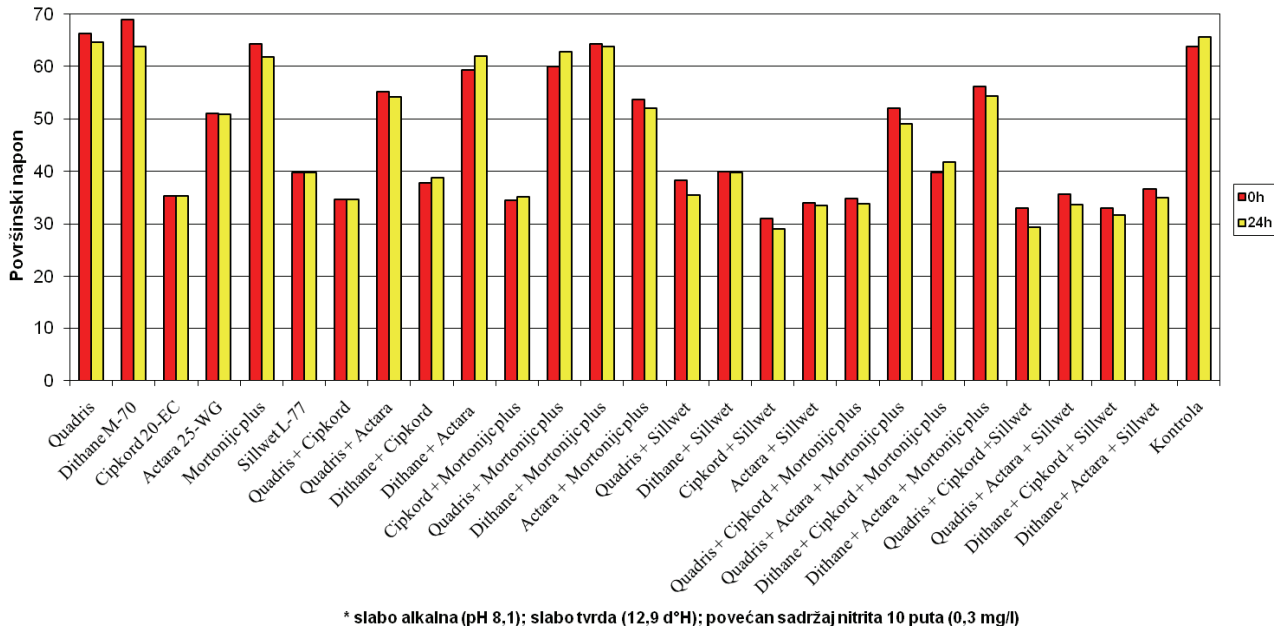

Slika 4. Površinski napon (mJ/m²) radnih tečnosti fungicida, insekticida i nepesticidnih supstanci (kompleksno đubrivo i ađuvant) i njihovih smeša, odmah po pripremi i posle 24 h u površinskoj vodi Karaš.
Figure 4. Surface tension (mJ/m²) of spray liquides of fungicides, insecticides and non-pesticide substances (complex fertilizer and ađuvant) and their mixtures immediately after preparation and after 24 h in surface water from Karaš.

vodu u kontroli i iznosio je 39,7 mJ/m². U svim smešama u čiji sastav ulaze Cipkord 20-EC i/ili Sillwet L-77 površinski napon je smanjen za oko 50% u odnosu na kontrolu, radne tečnosti fungicida i smeše u čiji sastav nisu uključeni pomenuta dva preparata. Pojedinačne komponente i mešavine su ispoljile neznatano smanjenje površinskog napona posle 24 h od pripreme, u odnosu na vrednosti koje su ostvarene po mešanju, osim radnih tečnosti Cipkord 20-EC, Sillwet L-77, Quadris+Cipkord 20-EC i Dithane M-70+Sillwet L-77, gde je ostao nepromenjen. Kod radnih tečnosti Dithane M-70+Cipkord 20-EC, Dithane M-70+Actara, Quadris+M+, Cipkord 20-EC+M+ i Dithane M-70+Cipkord 20-EC+M+ došlo je do povećanja površinskog napona posle 24 h. Na osnovu ostvarenih rezultata za površinski napon radnih tečnosti pripremljenih u površinskoj vodi iz reke Karaš može se konstatovati da se isti menja zavisno od komponenti i vremena stajanja.

Površinski napon vode iz reke Sava je 63,8 mJ/m² na početku eksperimenta, a posle 24 h se smanjuje i iznosio je 51,8 mJ/m². Kod radnih tečnosti fungicida površinski napon je znatno smanjen u odnosu na kontrolnu vodu i iznosio je 52,3–55,7 mJ/m² po mešanju, a posle 24 h je 41,3–50,0 mJ/m² (slika 5). Kod radne tečnosti preparata Actara 25-WG je iznosio 39,0 odmah po mešanju i 37,7 mJ/m², a posle 24 h, a za preparat Cipkord 20-EC je 32,3 po mešanju i 32,5 mJ/m² posle 24 h. Površinski napon kompleksnog đubrivo M+ je smanjen u odnosu na kontrolnu vodu i iznosio je 52,3 mJ/m² odmah po mešanju, a posle 24 h je 43,7 mJ/m², dok je za ađuvant svega 19,7 mJ/m² po mešanju, i posle 24 h, što je skoro za 2/3 manje u odnosu na isti u kontrolnoj vodi. U vodi iz Save Sillwet L-77 i Cipkord 20-EC su smanjili površinski napon za skoro 2/3 u odnosu na kontrolu, što je više nego u drugim ispitivanim vodama. Kod svih radnih tečnosti površinski napon je smanjen posle 24 h od pripreme, u odnosu na vrednosti koje su ostvarene odmah po mešanju, osim smeša Dithane M-70+Sillwet L-77, Cipkord 20-EC+Sillwet L-77 i Dithane M-70+Actara 25-WG+Sillwet L-77, kod kojih je došlo do povećanja površinskog napona posle 24 h.

Na osnovu ostvarenih rezultata sve ispitane vode su imale visok površinski napon, a smanjenje površinskog napona se postiže dodavanjem ađuvanta i preparata formulisanog kao koncentrat za emulziju. U ispitivanju je potvrđeno da se površinski napon smanjuje u mešavinama, to jest dodavanjem radnim tečnostima ađuvanta Sillwet L-77 i preparata Cipkord 20-EC formulisanog kao koncentrat za emulziju, u svim vodama, približno za oko 50% ili više (u vodi iz Save) u odnosu na: kontrolne vode, pojedinačne komponente fungicida i kompleksnog đubriva, kao i smeše koje ne sadrže ađuvant i insekticid Cipkord 20-EC. Na osnovu iznetog može se konstatovati da površinski napon radnih tečnosti zavisi od kvaliteta vode, komponenti i vremena stajanja istih.

Suspenzibilnost radnih tečnosti zavisno od kvaliteta vode

Suspenzibilnost ili stabilnost preparata formulisanih kao SC, WP i WG, je svojstvo radne tečnosti u kojoj se nalaze u vodi nerastvorene fine čestice aktivne sup-

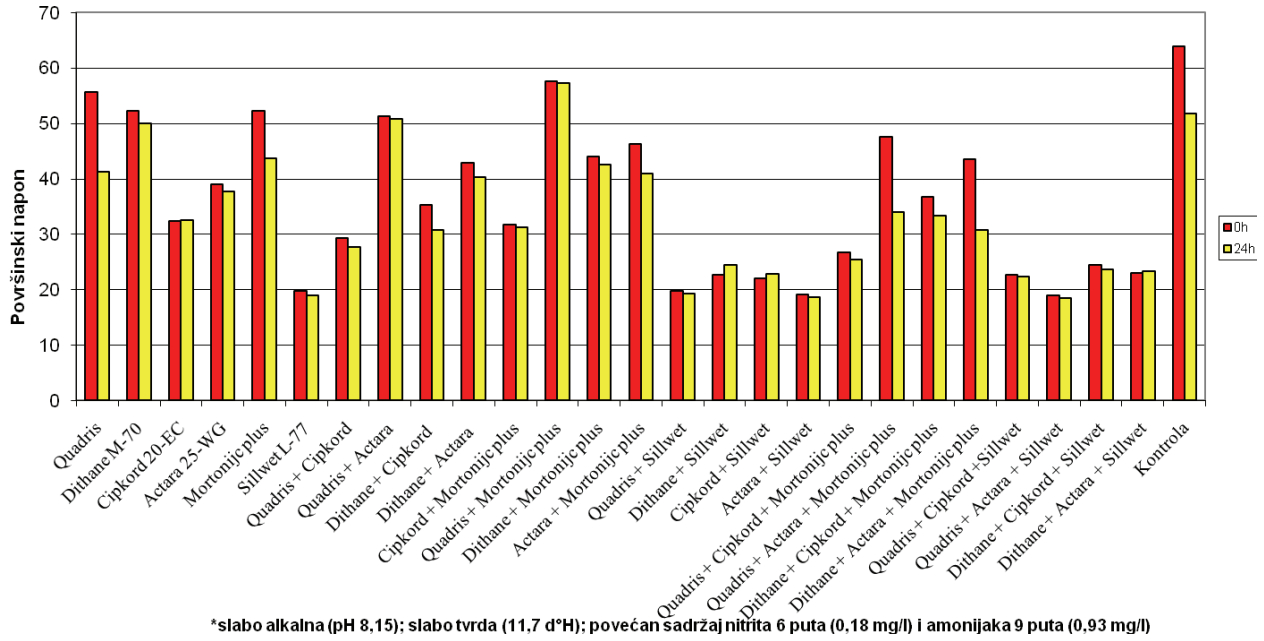

Slika 5. Površinski napon (mJ/m²) radnih tečnosti fungicida, insekticida i nepesticidnih supstanci (kompleksno đubrivo i ađuvant) i njihovih smeša, odmah po pripremi i posle 24 h u površinskoj vodi Sava.
Figure 5. Surface tension (mJ/m²) of spray liquides of fungicides, insecticides and non-pesticide substances (complex fertilizer and ađuvant) and their mixtures immediately after preparation and after 24 h in surface water from Sava.

stance i druge komponente preparata, da se što je moguće duže održe u suspenziji [4]. Donja propisana granica suspenzibilnosti je 60% [8]. Radne tečnosti fungicida, insekticida, njihove mešavine i mešavine sa nepesticidnim supstancama (kompleksno đubrivo, ađuvant) u svim ispitivanim vodama, ostvarile su suspenzibilnost u dozvoljenim granicama koja je u svim slučajevima bila iznad 60% (tabela 3). Suspenzibilnost preparata Quadris, formulisan kao koncentrovana suspenzija u svim ispitivanim vodama je veoma visoka 99,0–99,8 %, kao i mešavina koje ga sadrže 97,1–99,8%, nezavisno od komponenata u smeši. Preparat Dithane M-70, formulisan kao kvašljivi prašak, ostvario je smanjenu suspenzibilnost u odnosu na preparate Quadris i Actara 25-WG, ali u granicama dozvoljenog. Suspenzibilnost preparata Dithane M-70, zavisno od kvaliteta vode, znatno je bila veća u bunarskim i površinskim vodama (80,5–85,5%), nego u česmenskoj (69,3%). Posmatrano u celini kod svih varijanti koje sadrže Dithane M-70 kao komponentu smanjena je suspenzibilnost u odnosu na suspenzibilnost samog preparata Dithane M-70 u svim vodama. Promena, to jest najveća učestalost smanjenja suspenzibilnosti ispod 70 %, evidentna je kod česmenske vode za razliku od ostalih. Kod nas u praktičnoj primeni u najvećem broju slučajeva se koristi česmenska voda, a na osnovu iznetih rezultata proizilazi da je u ovoj vodi najizraženije smanjenje suspenzibilnosti, iako ne ispod donje propisane granice, i to samo u prisustvu preparata Dithane M-70, što može biti posledica primene ovog preparata u količini (2,5 kg/ha) koja je u odnosu na ostale daleko veća. Ovakva promena bi se mogla prevazići upotrebom opreme gde je obezbeđeno konstantno mešanje radne tečnosti u rezervoaru ili zamenom WP formulacije nekom od savremenijih. Radne tečnosti preparata Actara 25-WG, ispoljile su dobru suspenzibilnost u svim vodama koja je iznosila 98,0–99,2%, kao i u ostalim mešavinama gde je prisutan izuzimajući one gde je uključen preparat Dithane M-70. Pomenutom svojstvu odnosno, dobroj suspenzibilnosti preparata Actara 25-WG verovatno doprinosi relativno mala količina za praktičnu primenu (70 g/ha), za razliku od preparata Ditahane M-70, koji

Tabela 3. Suspenzibilnost (%) radnih tečnosti fungicida (SC, WP), insekticida (WG) i istih sa nepesticidnim materijama (kompleksno đubrivo i ađuvant) u vodama različitog kvaliteta
Table 3. Suspensibility (%) of spray liquids of fungicides (SC, WP), insecticide (WG) and their mixtures with non-pesticide substances (complex fertilizer and ađuvant) in waters of different quality

fungicidi, insekticidi, kompleksno đubrivo, ađuvant i mešavine	Tip vode				
	Bunarska Bečej[a]	Bunarska Adice[b]	Česmenska Novi sad[c]	Površinska Karaš[d]	Površinska Sava[e]
Quadris (SC)	99,5	99,2	99,8	99,5	99,0
Dithane M-70 (WP)	81,5	80,1	69,3	80,2	85,5
Actara 25-WG (WG)	98,5	98,0	99,2	98,7	98,5
Quadris+Cipkord 20-EC	98,7	99,3	98,5	99,2	98,7
Quadris+Actara 25-WG	98,2	98,8	99,5	99,7	98,5
Dithane M-70 +Cipkord 20-EC	79,0,6	74,5	68,5	72,2	81,0
Dithane M-70 +Actara 25-WG	77,2	75,8	73,6	81,7	82,5
Quadris+Mortonijc plus	98,2	98,5	99,5	99,7	98,2
Dithane M-70+Mortonijc plus	69,9	70,1	71,9	72,3	71,0
Actara 25-WG+Mortonijc plus	99,0	99,3	99,5	99,7	99,0
Quadris+Sillwet L-77	98,2	97,8	99,8	99,4	98,2
Dithane M-70+Sillwet L-77	76,8	77,3	69,1	80,4	76,8
Actara 25-WG+Sillwet L-77	98,3	99,1	82,3	97,5	98,3
Quadris+Cipkord 20-EC+Mortonijc plus	97,9	97,5	99,5	99,7	97,9
Quadris+Actara 25-WG+Mortonijc plus	99,0	98,0	98,5	98,5	99,0
Dithane M-70+Cipkord 20-EC+Mortonijc plus	68,2	67,5	69,6	71,6	70,5
Dithane M-70+Actara 25-WG+Mortonijc plus	70,7	71,7	71,3	71,4	72,0
Quadris+Cipkord 20-EC+Sillwet L-77	98,3	99,0	99,6	99,5	98,3
Quadris+Actara 25-WG+Sillwet L-77	97,1	97,7	98,5	99,0	98,0
Dithane M-70+Cipkord 20-EC+Sillwet L-77	75,3	74,3	71,5	70,6	71,3
Dithane M-70+Actara 25-WG+Sillwet L-77	72,0	71,8	69,2	74,2	73,5

[a]Slabo alkalna (pH 7,9), slabo meka (9,2 d°H) sa povećanim sadržajem nitrita (0,05 mg/l), amonijaka (16,9 mg/l) i gvožđa (0,76 mg/l); [b]slabo alkalna (pH 7,55), jako tvrda (34,7 d°H) sa povećanim sadržajem nitrita (2,5 mg/l); [c]neutralna (pH 7,42), slabo tvrda (15,4 d°H); [d]slabo alkalna (pH 8,1), slabo tvrda (12,9 d°H) sa povećanim sadržajem nitrita (0,3 mg/l); [e]slabo alkalna (pH 8,15), slabo tvrda (11,7 d°H) sa povećanim sadržajem nitrita (0,18 mg/l) i amonijaka (0,93 mg/l)

se primenjuje u u količini većoj za 37 puta u odnosu na gore pomenuti. Suspenzibilnost radnih tečnosti fungicida, insekticida i njihovih mešavina sa nepesticidnim supstancama u svim ispitivanim vodama, je iznad 60 % (67,5–99,5%). Međutim, suspenzibilnost preparata Dithane M-70 razlikovala se zavisno od kvaliteta vode i u česmenskoj vodi je iznosila 69,3%, a u ostalim 80,1––85,5%.

DISKUSIJA

Podataka o kvalitetu vode za pripremu radnih tečnosti pesticida kako kod nas tako i u svetu veoma je malo. Međutim daleko manje podataka je o uticaju kvaliteta vode na efekte pesticida i oni se uglavnom odnose na stabilnost pesticida zavisno od pH i tvrdoće vode ili se samo navode razlike u biološkim efektima pesticida zavisno od upotrebljenih voda kao što su bunarska, tehnička i česmenska [9,10].

Uticaj površinskog napona ili kvašljivost zavisi od svojstava tretirane površine (dlakava, voskasta, glatka, naborana), temperature radne tečnosti, međumolekularnih sila tečnosti pri čemu polarne tečnosti (voda) imaju veći površinski napon od nepolarnih [4]. Ađuvanti su površinski aktivne supstance koje se dodaju pesticidima da olakšaju mešanje, nanošenje ili efikasnost istih [11]. Na osnovu rezultata Janků i sar. [12] maksimalno smanjenje površinskog napona vode je ostvareno dodavanjem ađuvanta Syllwet L-77 i Break Superb. Površinski napon radnih tečnosti imidakloprida, pirimifos-metila, propineba i mankozeba se smanjuje u odnosu na površinski napon same vode, a posebno kod pirimifos-metila, što ukazuje na povećanje kvašljivosti [13,14]. Slični rezultati dobijeni su i za smešu radnih tečnosti cipermetrina (EC formulacija) sa mankozebom, metiramom, folpetom i hlorpirifosom (EC formulacija) sa istim fungicidima u standardno tvrdoj vodi, destilovanoj, vodi iz gradskog vododvoda i bunarskoj vodi [15,16]. Ispitivanjem uticaja kvaliteta vode na fizičke osobine radnih tečnosti pojedinačnih preparata i njihovih mešavina, konstatovano je sniženje površinskog napona radnih tečnosti u bunarskoj u odnosu na česmensku vodu, osim radne tečnosti preparata Mankogal-80, gde je površinski napon povećan u bunarskoj vodi u odnosu na česmensku [17]. Površinski napon mešavina (Pyrinex 48-EC+ Polyram-DF, Pyrinex 48--EC+Folpan WP-50, Pyrinex 48-EC+Ridomil MZ-72 WP) je na nivou površinskog napona emulzije preparata Pyrinex 48-EC, nezavisno od kvaliteta vode ili fungicida, a u odnosu na površinski napon same vode smanjen je skoro za polovinu [15].

Na osnovu rezultata Klokočar-Šmit i sar. [15], utvrđeno je da je suspenzibilnost radne tečnosti Mankogal--80+Sucip 20-EC značajno smanjena u tehničkoj vodi u poređenju sa vrednostima ostvarenim u vodi iz vodovoda, takođe je smanjena i u odnosu na suspenzibilnost samog fungicida u tehničkoj vodi, što je verovatno posledica, kako kvaliteta vode tako i izbora preparata u smeši. Pomenuta tehnička voda odlikovala se većom: tvrdoćom, sadržajem kalcijumovih jona i ukupnih jona gvožđa, amonijačnog i nitritnog jona i alkalnom reakcijom. Kod većine radnih tečnosti insekticida (pirimifos-metil i imidakloprid) i fungicida (propineb i mankozeb) u bunarskoj vodi suspenzibilnost je snižena u odnosu na iste suspenzije u česmenskoj vodi, što ukazuje na zavisnost suspenzibilnosti pesticida od kvaliteta vode kao i od izbora tank-miks komponente [18]. Na osnovu rezultata Savoy i sar. [19], suspenzibilnost radnih tečnosti pesticida zavisi od tvrdoće vode. Ovim je ukazano na promene u suspenzibilnosti prouzrokovane kako kvalitetom vode za tretiranje tako i izborom komponenata u smeši [20,21].

ZAKLJUČAK

Na osnovu izvedenih ispitivanja i ostvarenih rezultata o uticaju kvaliteta vode na površinski napon i suspenzibilnost radnih tečnosti pesticida mogu se izvesti sledeći zaključci:

- Ispitivane vode su ispoljile visok površinski napon (63,8–68,7 mJ/m²), a dodatkom ađuvanta Sillwet L-77 i preparata Cipkord 20-EC, je približno smanjen za oko 50% u odnosu na kontrolnu vodu i sve varijante koje ih ne sadrže, a u vodi iz Save površinski napon je smanjen za oko 2/3 u odnosu na kontrolu, što je dokaz o uticaju vode na površinski napon radnih tečnosti pesticida.
- Suspenzibilnost radnih tečnosti fungicida, insekticida i njihovih mešavina sa nepesticidnim supstancama u svim ispitivanim vodama, je iznad 60% (67,5––99,5%). Međutim suspenzibilnost preparata Dithane M-70 razlikovala se zavisno od kvaliteta vode i u česmenskoj vodi je iznosila 69,3%, a u ostalim vodama 80,1–85,5%.

Zahvalnica

Istraživanje je finansirano od strane Ministarstva prosvete, nauke i tehnološkog razvoja Republike Srbije (projekat III43005).

LITERATURA

[1] D. Inđić, Z. Klokočar-Šmit, M. Ignjatov, S. Belić, Fizičke osobine insekticida i fungicida u mešavini zavisno od kvaliteta vode, Letopis naučnih radova **23** (1999) 229––241.

[2] B. Dalmacija, I. Ivančev-Tumbas, Analiza vode – kontrola kvaliteta, tumačenje rezultata. Univerzitet u Novom Sadu, Prirodno-matematički fakultet, Departman za hemiju, Novi Sad, 2004.

[3] S. Lazić, D. Šunjka, M. Pucarević, N. Grahovac, S. Vuković, D. Inđić, S. Jakšić, Monitoring atrazina i njegovih

metabolita u podzemnim vodama Republike Srbije, Hem. Ind. **67** (2013) 513–523.

[4] R. Šovljanski, Z. Klokočar Šmit, S. Lazić, Praktikum iz opšte fitofarmacije – za studente Poljoprivrednog fakulteta, Poljoprivredni fakultet, Novi Sad, 2002.

[5] M. Maceljski, O utjecaju nekih faktora na delovanje pesticida, Zbornik radova saopštenih na X jubilarnom savetovanju o primeni pesticida, Poreč, 1980, str. 43–49.

[6] N. Ostojić, Mogućnosti i granice primene pesticida pri gajenju biljaka u zaštićenom prostoru, Biljni lekar **2** (1996) 167–169.

[7] W. Dobrat, A. Martijn (Eds.), CIPAC Handbook F, MT 15, Suspensibility of wettable powders in water, Herb AL5 2HG, Collaborative International Pesticides Analytical Council Limited, Harpenden, 2007, pp. 45–52.

[8] Pravilnik o metodama za ispitivanje pesticida, Sl. list SRJ, 63/2001.

[9] S. Vuković, D. Inđić, V. Bursić, D. Šunjka, B. Brestovac, Kvalitet voda u AP Vojvodini koje se koriste pri primeni pesticida, Biljni lekar **5** (2008) 343–351.

[10] S. Vuković, D. Inđić, V. Bursić, D. Šunjka, Biological effects of insecticide, fungicide and complex fertilizer combinations depending on water quality, Acta Horticulture **2** (2009) 577–583.

[11] J. Janků, L. Bartovská, J. Soukup, M. Jursík, K. Hamouzová, Density and surface tension of aqueous solutions of ađuvants used for tank-mixes with pesticides, Plant Soil Environ. **58** (2012) 568–572.

[12] M. Czarnota, P. Thomas, Using Surfactants, Wetting Agents, and Ađuvants in the Greenhouse, The University of Georgia, Bulletin 1314, 2012 (http://extension.uga.edu/publications/detail.cfm?number=B1319).

[13] Z. Perović, Kompatibilnost insekticida, fungicida i mineralnih hraniva zavisno od kvaliteta voda u proizvodnji povrća, Magistarska teza, Poljoprivredni fakultet Novi Sad, 2006.

[14] Z. Perović, D. Inđić, S. Vuković, Z. Klokočar-Šmit, S. Lazić, Surface tension of spray liquids (fungicides, insecticides and mineral fertilizers) depending on the components and water quality, in Proceedings of 8th Slovenian Conference on plant protection, Radenci, Slovenija, 2007, pp. 261–266.

[15] Z. Klokočar-Šmit, D. Inđić, S. Belić, E. Erdelji, Bilogical properties of chlorpyrifos and cypermethrin in tank mix with some fungicides, in Proceedings of 2nd International Plant Protection Symposium, Debrecen, Hungary, 2000, p. 32.

[16] Z. Klokočar-Šmit, D. Inđić, S. Belić, E. Erdelji, Biološki efekat hlorpirifosa i cipermetrina u mešavini sa fungicidima zavisno od kvaliteta vode za tretiranje, Pesticidi **16** (2001) 93–101.

[17] Z. Klokočar-Šmit, D. Inđić, S. Belić, M. Mitar, M. Petrov, Biološki efekti pesticida u zavisnosti od kvaliteta vode u suspenzijama za zaštitu povrća, Savremena poljoprivreda **1–2** (2001) 193–198.

[18] Z. Perović, D. Inđić, Z. Klokočar-Šmit, S. Lazić, Stabilnost mešavina fungicida, insekticida i mineralnih hraniva zavisno od kvaliteta vode, Pesticidi i fitomedicina **20** (2005) 247–254.

[19] V.L.T. Savoy, M.F. Piedade, R.C.B. Prisco, Water hardness effect on the physical chemical characteristics of wettable powder fungicide (http://www.cipac.org/document/presentation_poster/2012/Poster/Savoy_WATER%20HARDNESS%20EFFECT%20ON%20THE%20PHYSICAL%20CHEMICAL.pdf).

[20] S. Vuković, D. Inđić, M. Grahovac, S. Gvozdenac, V. Bursić, D. Šunjka, Suspenzibilnost radnih tečnosti fungicida, insekticida i nepesticidnih materija zavisno od kvaliteta vode, u Yborniku radova sa XI Savetovanja o zaštiti bilja, Zlatibor, 2011, pp. 166–167.

[21] S. Vuković, Biološki efekti pesticida zavisno od kvaliteta vode za tretiranje, Doktorska disertacija, Univerzitet u Novom Sadu, Poljoprivredni fakultet, Novi Sad, 2011.

[22] Kvalitet voda, Sl. list SRJ, 42/1998.

SUMMARY

SURFACE TENSION AND SUSPENSIBILITY OF SPRAY LIQUIDS OF FUNGICIDES, INSECTICIDES AND NON-PESTICIDE SUBSTANCES DEPENDING ON WATER QUALITY

Slavica M. Vukovic, Dušanka V. Inđić, Sonja M. Gvozdenac

University of Novi Sad, Faculty of Agriculture, Novi Sad, Serbia

(Professional paper)

The aim of this work was to determine the surface tension and suspensibility of spray liquids of fungicides (Quadris and Dithane M-70), insecticides (Actara WG-25 and Cipkord EC-20) and two and/or three component mixtures with non-pesticide substances (complex fertilizer – Mortonjic plus and ađuvant – Sillwet L-77), depending on water quality. For this work the following waters were used: well water from Bečej (slightly alkaline, slightly soft), well water from Adice (slightly alkaline, very hard), tap water from Novi Sad (neutral, slightly hard) and surface water from Sava and Karaš rivers (slightly alkaline, slightly hard). Surface tension of fungicide and insecticide spray liquids and their mixtures in mentioned waters was determined using tensiometer and suspensibility according to a standard method (CIPAC MT 15). The surface tension of all tested waters was high. However, the reduction of surface tension by 50% (or more in water from Sava river) compared to the control waters, was achieved by adding the ađuvant (Sillwet L-77) and insecticide formulated as emulsifiable concentrate (Cipkord EC-20). Surface tension was slightly decreased in a single component spray liquids of fungicides and the complex fertilizer, as well as in mixtures that did not contain ađuvant and/or Cipkord EC-20, regardless on water quality. Suspensibility of all spray liquids, regardless on tested water was above the lower limit (60%). In general, the suspensibility in case of all mixtures containing Dithane M-70 was reduced compared to Dithane M–70 spray liquid, in all tested waters. The most pronounced decrease in suspensibility, below 70%, was registered in the case of spray liquids with tap water, compared to others (99.8%).

Keywords: Surface tension • Suspensibility • Fungicide • Insecticide • Non-pesticide substances • Mixtures • Quality water

Composition, antioxidant and antimicrobial activity of the essential oil of *Achillea collina* Becker growing wild in western Romania

Călin Jianu[1], Corina Mişcă[1], Simona Gabriela Muntean[2], Alexandra Teodora Gruia[3]

[1]*Faculty of Food Processing Technologies, Banat's University of Agricultural Sciences and Veterinary Medicine "King Michael I of Romania" at Timişoara, Timişoara, Romania*
[2]*Institute of Chemistry Timişoara of Romanian Academy, Timişoara, Romania*
[3]*Center for Transplant Immunology, County Hospital Timişoara, Timişoara, Romania*

Abstract
The investigation of the chemical composition, antioxidant and antimicrobial properties of the essential oil of *Achillea collina* Becker growing wild in western Romania was the aim of this study. The chemical composition of the essential oil was evaluated by GC–MS. The major compounds identified were chamazulene (38.89%), germacrene D (12.90%), β-caryophyllene (11.52%) and β-pinene (10.66%). The antimicrobial activity was assessed by the diffusimetric method against seven common food-related bacteria. No effects were observed against *Clostridium perfringens* and *Streptococcus pyogenes*. The antioxidant activity was evaluated using the DPPH test, the essential oil (IC_{50} = 25.03±0.12 μg/ml) demonstrated a stronger scavenging effect than BHA and lower than that of ascorbic acid and propyl gallate. The results reveal strong antimicrobial and antioxidant properties of the essential oil tested and contribute to future research to find new sources of natural antiseptics and antioxidants: a viable and safe alternative to reduce the use of synthetic additives.

Keywords: *Achillea millefolium* ssp. *collina* Becker, essential oil, GC–MS analysis, antimicrobial activity, antioxidant activity.

Available online at the Journal website: http://www.ache.org.rs/HI/

SCIENTIFIC PAPER

UDC 582.998.1:615.322(498)

Hem. Ind. **69** (4) 381–386 (2015)

doi: 10.2298/HEMIND140329052J

The genus *Achillea* belongs to Asteraceae family (Compositae), this large family is represented in the Romanian spontaneous flora by 23 species and 10 varieties or subspecies, spread across all types of landforms [1]. Yarrow inflorescences (Romanian name: *coada șoricelului*) are known as a widely used Romanian traditional remedy, with antispasmodic, bitter tonic and antihemorrhagic actions [2].

The whole plant contains essential oil (EO), but for its isolation the inflorescences are preferred [3], the minimum EO content in the dried plant product being 2 mL/kg [4]. The major components of the yarrow EO are chamazulene, sabinene, germacrene D, β-pinene, 1,8-cineole, linalool, α- and β-thujone, *cis*- and *trans*-β-ocimene, myrcene, camphor, ascaridole, β-caryophyllene, *p*-cymene, bornyl acetate, camphene, limonene, γ-terpinene, caryophyllene oxide, α-phellandrene, β-eudesmol and α-bisabolol [5–9].

According to the European Pharmacopoeia 7.0 (Ph. Eur. 7.0) [4], the content of chamazulene in yarrow, dried plant, must be minimum 0.02%. However, the accumulation of azulenogenic compounds is not a common characteristic of all members of the genus *Achillea*, this property being closely related to the chromosome number in the plant [10]. According to Nemeth and Bernath [10], the accumulation of chamazulene is a characteristic of the members of the group *Millefolium*, in particular of *Achillea asplenifolia* Vent, *Achillea roseo-alba* Ehrend. and *Achillea collina* Becker, native species in the Romanian wild flora [1].

The increasing trend in the last decades for the applications of EOs in the food and pharmaceutical industries prompted the investigation on the biological activities of the members of the genus *Achillea*. Various studies have reported notable antimicrobial properties of extracts and EOs obtained from various species of *Achillea* [5,11–13], together with a good antioxidant potential [5,11,14,15]. Although these results suggest the potential applications as antioxidant or antiseptic for the yarrow EO, it is currently only used in the food industry for flavoring certain alcoholic beverages [16].

To date, based on our knowledge, only the chemical composition of the EO isolated from *Achillea collina* Becker originating in Romania was the subject of a small number of studies [17,18], while information on the *in vitro* antimicrobial and antioxidant activity has not been reported. The purpose of this study is to investigate the chemical composition, antimicrobial properties and antioxidant potential of the EO isolated

Correspondence: C. Jianu, Faculty of Food Processing Technologies, Banat's University of Agricultural Sciences and Veterinary Medicine "King Michael I of Romania" at Timişoara, Calea Aradului 119, RO-300645 Timişoara, Romania.
E-mail: calin.jianu@gmail.com
Paper received: 29 March, 2014
Paper accepted: 27 June, 2014

by steam distillation from *A. collina* Becker growing wild in western Romania, in order to identify new sources of natural additives (antioxidants and antiseptics) with applicability in the food and pharmaceutical industries.

MATERIALS AND METHODS

Collection of raw material

The used inflorescences of *A. collina* Becker were collected in July 2012, in the Hunedoara county – the Orăştioara de Sus commune, village of Ludeştii de Jos (45°43'5"N 23°10'21"E), at their maximum flowering stage. A voucher specimen (V.FPT-278) was deposited in the Herbarium of the Faculty of Pharmacy, Victor Babeș University of Medicine and Pharmacy, Timișoara, Romania. After harvesting the material was dried in natural conditions (away from direct sunlight) and stored in double paper bags at temperatures of 3–5 °C.

Isolation of the essential oil

The dried plant material was subjected to steam distillation, according to the method previously described by Craveiro [19]. The EO was separated from water by decantation, dried over anhydrous sodium sulfate and stored for analysis in hermetically sealed amber glass vials at a temperature of 4 °C.

Physical analysis

The specific gravity and the refractive index of the EO were measured according to the method described by the Food Chemical Codex [20]. To determine the specific gravity a 2-mL Gay-Lussac pycnometer (Duran) was used, and a DR6100 digital refractometer (Krüss Optronic GmbH, Germany) was used for the refraction index. The tests were performed in triplicate at the temperatures of 20 °C (refraction index) and 25 °C (specific gravity), respectively.

Free radical-scavenging activity: DPPH assay

The radical scavenging activity was determined by the DPPH assay, as previously described by Brand-williams [21]. Briefly, 3 mL of methanolic stock solution of yarrow oil (1 mg/mL) were prepared, and then diluted to different concentrations (0.01–0.5 mg/mL). 0.5 mL of each diluted sample was mixed with 5 mL methanolic solution of DPPH 0.06 mM. The mixtures were shaken and held in the dark for 15 min. The same procedure was repeated for butylated hydroxylanisole (BHA), propyl gallate, and ascorbic acid (Sigma-Aldrich Chemie GmbH), used as positive controls. The decrease in the DPPH absorbance was measured at 517 nm using a Cecil UV/Vis spectrophotometer (model CE 7200, Milton, England). The methanolic solution of DPPH 0.06 mM was used as negative control and methanol (99.8%) as blank. The DPPH free radical inhibition as a percentage (*I%*) was calculated according to the following equation:

$$I\% = 100(A_{blank} - A_{sample}/A_{blank}) \quad (1)$$

where A_{blank} is the absorbance of the control, and A_{sample} is the absorbance of the test sample. Each test was performed in triplicate. IC_{50} was obtained using the BioDataFit 1.02 software (Chang Broscience Inc, Castro Valley, CA, USA).

Gas chromatography–mass spectrometry

The oil samples were analyzed by gas chromatography with a HP6890 gas chromatograph, coupled with a HP 5973 mass spectrometer. The gas chromatograph has a split/splitless injector and a Factor Four™ VF-35ms capillary column, 35% phenylmethyl phase, 30 m×0.25 mm, 0.25 µm film thickness. The gas chromatography conditions include a temperature range of 50 to 250 °C with a slope of 4 °C/min, with a solvent delay of 5 min. The temperature of the injector was maintained at 250 °C. The inert gas was helium at a flow of 1.0 mL/min, and the volume of injected sample in the splitless mode was 2 µL. The MS conditions were the following: ionization energy, 70 eV; quadrupole temperature, 100 °C; scanning velocity, 1.6 scan/s; weight range, 40–500 amu. The percent composition of the essential oils was calculated. The qualitative analysis was based on the percent area of each peak of the sample compounds. The mass spectrum of each compound was compared with the mass spectrum from the spectra library NIST 98 (USA National Institute of Science and Technology software).

Determination of antimicrobial activity

The antimicrobial activity was determined against seven common food-related bacteria: *Shigella flexneri* (ATCC 12022), *Klebsiella pneumoniae* (ATCC 13882), *Salmonella typhimurium* (ATTC 14028), *Staphylococcus aureus* (ATCC 25923), *E. coli* (ATCC 25922), *Streptococcus pyogenes* (ATTC 19615) and *Clostridium perfringens* (ATCC13124), using the diffusimetric method [22]. Briefly, a suspension of the tested microorganism (10^6 cells mL^{-1}) was spread on the solid media plates (Mueller–Hinton agar). The paper discs, 6 mm in diameter (Whatman No. 1), impregnated with 20µL EO were placed in the centre of the plates. A disc containing 10 µL of sterile broth medium was used as the negative control and as positive control was used rifampicin (5 µg/disk) (Oxoid, UK). After 1 h at room temperature to allow the EO to diffuse across the surface, the plates were sealed with sterile parafilm and incubated at 37 °C for 24–48 h. After incubation, the diameters of the inhibition zones were measured (in mm). Each test was performed in triplicate on at least three separate experiments. The results are presented as means ± *SD*.

Statistical methods

Data were expressed as means and standard deviations. One-way ANOVA test (Bonferroni correction) was used to assess the mean differences of continuous measurements between groups. StataIC 11 statistical software (StataCorp. LP, College Station, TX, USA, version 2009) was used for data analysis. A p-value < 0.05 was considered statistically significant.

RESULTS AND DISCUSSIONS

The physical properties and yield of the EO of *A. collina* Becker are shown in Table 1. In the analyzed sample thirty components were identified, representing 99.92% of the EO analyzed (Table 2). The major components were chamazulene (38.89%), germacrene (12.90%), caryophyllene (11.52%) and β-pinene (10.66%), suggesting that the EO analyzed belongs to

Table 1. Yield, physical properties and antioxidant activity of the essential oil of A. collina Becker grown in western Romania; values are mean values and standard deviations (SD, n = 3)

Parameter	Essential oil	Ascorbic acid	BHA	Propyl gallate
Yield, %	0.47	–	–	–
Refractive index (20 °C)	1.515±0.001	–	–	–
Specific gravity (25 °C)	0.912±0.000	–	–	–
DPPH, IC_{50} / μg mL^{-1}	25.03±0.12	23.56±0.12	35.04±0.15	2.1±0.13

Table 2. Composition of the essential oil obtained from A. collina Becker grown in western Romania; compounds are listed in the order of elution from the VF 35 MS column

No.	Compound	R.T. / min	% Of total
1	α-Thujene	5.454	0.16
2	α-Pinene	5.689	2.40
3	Camphene	6.253	0.10
4	Sabinene	6.806	4.87
5	β-Pinene	6.970	10.66
6	α-Terpinene	7.830	0.15
7	Limonene	8.104	0.63
8	1,8-Cineole	8.586	3.99
9	γ-Terpinene	9.004	0.27
10	Terpineol	9.544	0.17
11	Chrysanthenol	11.817	1.43
12	Camphor	12.605	0.25
13	Borneol	12.649	0.06
14	α-Pinocarvone	13.045	0.30
15	*p*-Menth-1-en-8-ol	13.128	0.74
16	Verbenyl acetate	13.700	0.29
17	Lavandulyl acetate	14.655	0.79
18	α-Copaene	16.007	0.10
19	β-Bourbonene	16.359	0.56
20	β-Elemene	16.483	0.39
21	2-Methylbicyclo[4.3.0]non-1(6)-ene	16.559	1.13
22	1*H*-Cycloprop[e]azulene	16.882	0.07
23	Caryophyllene E	17.405	11.52
24	β-Farnesene	17.775	0.73
25	Germacrene D	18.921	12.90
26	γ-Cadinene	19.755	0.38
27	Naphthalene, 1,2-dihydro-3,5,8-trimethyl	20.513	1.02
28	1*H*-Cycloprop[e]azulen-4-ol	21.753	2.51
29	Caryophyllene oxide	21.794	2.46
30	Chamazulene	25.754	38.89
Identified from total area			99.92

the chamazulene chemotype. At the same time, the presence in the composition of the tested EO of a high content of β-pinene, besides chamazulene, points to tetraploid species [5]. Compared with the results obtained, Gherase [17] reports a content below 53% chamazulene in the EO of the same species in Romania, while Nemeth [18] identifies a content of 57.7% chamazulene in the analyzed samples from Romania. The presence of chamazulene as the major compound was also recorded in oils obtained from *A. collina* Becker from Hungary (30.5–67.1%) [18] and Serbia (19.42%) [5], respectively.

The antioxidant capacity of the yarrow EO and the three standard references used, BHA, propyl gallate and ascorbic acid, was determined by the DPPH assay (Table 1). The yarrow EO demonstrated stronger scavenging effects than BHA and lower than that of ascorbic acid and propyl gallate. The literature in this area contains little data on the active compounds responsible for the antioxidant capacity of EOs. However, a number of studies report the antioxidant potential of chamazulene, the constituent with the highest share in the composition of the EO analyzed in this study [15,23,24]. Previously, Bozin [5], seeking to identify the most active constituents of the EO isolated from *A. collina* Becker, responsible for the radical scavenging capacity, indicated chamazulene, the mixture of mono- and sesquiterpene hydrocarbons and camphor. At the same time, a series of studies reported the interdependence between the antioxidant capacity and the presence of phenolic compounds in the composition of extracts of *A. collina* Becker [14,25], their accumulation being influenced by climatic conditions [25].

The results of antimicrobial activity determined by the diffusimetric method (Table 3 and Figure 1) demonstrate that the EO analyzed inhibits most strongly the

Table 3. Antimicrobial activity of the A. collina Becker essential oil, and rifampicin as positive control; inhibitions are expressed as diameter of inhibition zone in mm and include the diameter of the paper disc (6 mm). Data distributions were expressed as mean values and standard deviations (SD, n = 9). Rifampicin (5 µg/disk) was used as positive control; n.a.: no activity

No.	Test microorganism	Antioxidant	
		EO	Rifampicin
1.	*Shigella flexneri* (ATCC 12022)	11.05 (0.13)	14.05 (0.1)
2.	*Klebsiella pneumoniae* (ATCC 13882)	10.94 (0.21)	14.04 (0.06)
3.	*Salmonella typhimurium* (ATTC 14028)	10.14 (0.19)	14.02 (0.07)
4.	*Staphylococcus aureus* (ATCC 25923)	8.98 (0.13)	14.09 (0.08)
5.	*Escherichia coli* (ATCC 25922)	12.97 (0.19)	18.05 (0.07)
6.	*Streptococcus pyogenes* (ATTC 19615)	n.a.	13.03 (0.07)
7.	*Clostridium perfringens* (ATCC13124)	n.a.	12.06 (0.06)

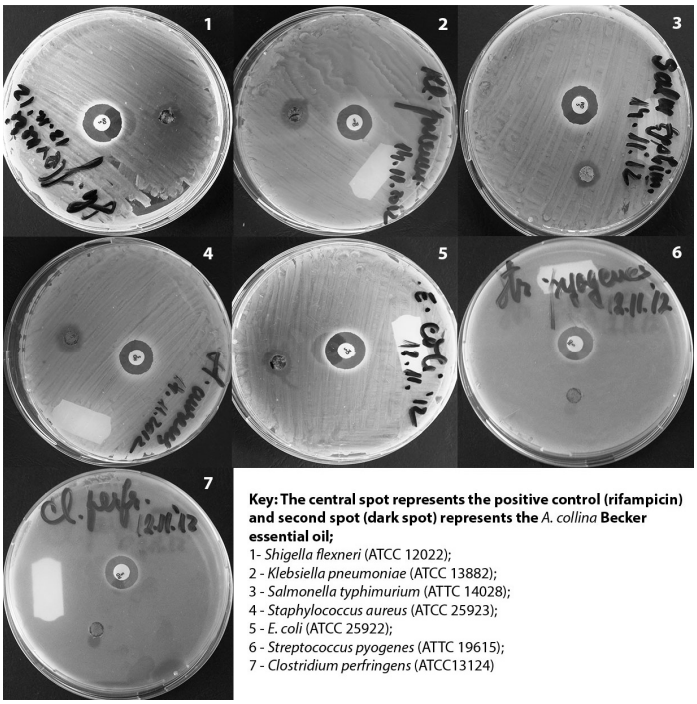

Figure 1. Agar plates showing the growth inhibition zones by A. collina Becker EO against bacterial strains tested.

development of *E. coli*, followed by *Shigella flexneri* > *Klebsiella pneumoniae* > *Salmonella typhimurium* > *Staphylococcus aureus*. There was a statistically significant difference between the mean values of the analyzed groups ($p < 0.0001$, one-way ANOVA test). The pairwise comparisons showed statistical differences between all groups ($p < 0.001$), except *Shigella flexneri* – *Klebsiella pneumoniae*. No effects were observed against *Clostridium perfringens* and *Streptococcus pyogenes*.

The antimicrobial activity of the analyzed oil is comparable to that reported for the EO of *A. collina* Becker originating from Serbia, except in the case of *Streptococcus pyogenes*, on which the latter exerts a strong inhibitory effect [5]. A possible explanation for the antimicrobial activity recorded could be the inhibitory effects exhibited by the major constituents of the EO analyzed: chamazulene [5], along with caryophyllene [26,27] and β-pinene [28]. Also noteworthy is the presence of certain minor components of the EO, known for their strong antimicrobial activity, such as limonene, α-pinene, 1,8-cineole, etc [28,29]. However, various studies have reported, in addition to the synergistic effect of minor components in the chemical composition of EOs, also additive and antagonistic effects, respectively [29–31]. These findings confirm the assumption that along with the major compounds, the total composition should be taken into consideration because of the synergistic role of the constituents, which can modify the biological activity of the oil [10].

CONCLUSIONS

We have investigated the chemical composition, antimicrobial properties and antioxidant potential of the EO of *A. collina* Becker growing wild in western Romania. Thirty components were identified by GC–MS analysis, chamazulene (38.89%), germacrene D (12.90%), β-caryophyllene (11.52%) and β-pinene (10.66%) being the major constituents. The analyzed sample showed comparable scavenging effects with the most used food antioxidants (BHA, propyl gallate and ascorbic acid) and inhibits foodborne pathogens such as: *E. coli*, *Shigella flexneri*, Klebsiella pneumoniae, *Salmonella typhimurium* and *Staphylococcus aureus*. The study complements the existing data in the literature on the biological activity of the EO isolated from *A. collina* Becker and contributes to future research to find new sources of natural antiseptics and antioxidants: a viable and safe alternative to reduce the use of synthetic additives.

REFERENCES

[1] E. Ghişa, Flora Republicii Populare Române: IX. 'Cucurbitaceae', 'Campanulaceae', 'Lobeliaceae', 'Compositae', Vol. 9, Academy of R.S. România Publishing House, Bucharest, 1964 (in Romanian).

[2] V. Cucu, C. Bodea, C. Cioacă, Plante medicinale şi aromatice, Academy of R.S. România Publishing House, Bucharest, 1982 (in Romanian).

[3] V. Eliu-Ceauşescu, Gh. Rădoiaş, T. Cădariu, Odorante și aromatizante chimie, tehnologie, aplicații, Tehnic Publishing House, Bucharest, 1988 (in Romanian).

[4] Eur.Phar.Com., European Pharmacopoeia, 7th ed., VII ed. Council of Europe, Strasbourg, 2007.

[5] B. Bozin, N. Mimica-Dukic, M. Bogavac, L. Suvajdzic, N. Simin, I. Samojlik, M. Couladis, Chemical composition, antioxidant and antibacterial properties of *Achillea collina* Becker ex Heimerl s.l. and *A. pannonica* Scheele essential oils, Molecules **13** (2008) 2058–2068.

[6] O. Gudaitytė, P.R. Venskutonis, Chemotypes of *Achillea millefolium* transferred from 14 different locations in Lithuania to the controlled environment, Biochem. Sys. Ecol. **35** (2007) 582–592.

[7] E. Nemeth, Essential oil composition of species in the Genus *Achillea*, J. Essent. Oil Res. **17** (2005) 501–512.

[8] F. Rauchensteiner, Nejati, S, Saukel, J, The *Achillea millefolium* group (Asteraceae) in Middle Europe and Balkans a diverse source for crude drug Herba Millefolii, J. Trad. Med. **21** (2004) 113-119.

[9] A.S. Shawl, S.K. Srivastava, K.V. Syamasundar, S. Tripathi, V.K. Raina, Essential oil composition of *Achillea millefolium* L. growing wild in Kashmir, India, Flavour Frag. J. **17** (2002) 165–168.

[10] E. Nemeth, J. Bernath, Biological activities of yarrow species (Achillea spp.), Curr. Pharm. Des. **14** (2008) 3151–3167.

[11] F. Candan, M. Unlu, B. Tepe, D. Daferera, M. Polissiou, A. Sokmen, H.A. Akpulat, Antioxidant and antimicrobial activity of the essential oil and methanol extracts of *Achillea millefolium* subsp. millefolium Afan. (Asteraceae), J. Ethnopharmacol. **87** (2003) 215–220.

[12] G. Stojanovi, Y. Asakawa, R. Pali, N. Radulovi, Composition and antimicrobial activity of *Achillea clavennae* and *Achillea holosericea* essential oils, Flavour Frag. J. **20** (2005) 86–88.

[13] G. Stojanovic, N. Radulovic, T. Hashimoto, R. Palic, *In vitro* antimicrobial activity of extracts of four *Achillea* species: the composition of *Achillea clavennae* L. (Asteraceae) extract, J. Ethnopharmacol. **101** (2005) 185–190.

[14] A. Giorgi, R. Bombelli, A. Luini, G. Speranza, M. Cosentino, S. Lecchini, M. Cocucci, Antioxidant and cytoprotective properties of infusions from leaves and inflorescences of *Achillea collina* Becker ex Rchb, PTR **23** (2009) 540–545.

[15] N.V. Sizova, Composition and antioxidant activity of essential oils containing azulene derivates, Khim. Farm. Zh. **46** (2012) 369–371.

[16] G.A. Burdock, Fenaroli's Handbook of flavor ingredients, 5rd ed., Taylor & Francis, New York, 2004.

[17] F. Gherase, A. Spac, V. Dorneanu, U. Stanescu, E. Grigorescu, Pharmacognostic research of some species of Achillea. Note 1. Volatile oils analysis, Revista medico-chirurgicala a Societaţii de Medici şi Naturalişti din Iaşi **107** (2003) 188–191 (in Romanian).

[18] E. Nemeth, J. Bernáth, G. Tarján, Quantitative and qualitative studies of essential oils of Hungarian *Achillea* populations. J. Herbs Spices Med. Plants **13** (2007) 57–69.

[19] A.A. Craveiro, J.W. Alencar, F.J.A. Matos, A simple and inexpensive steam generator for essential oils extraction, J. Chem. Educ. **53** (1976) 652.

[20] FCC, Food Chemicals Codex, 5rd ed., National Academies Press, Washington, DC, 2003.

[21] W. Brandwilliams, M.E. Cuvelier, C. Berset, Use of a free-radical method to evaluate antioxidant activity, Food Sci. Technol.-Lebensmitt.-Wiss. Technol. **28** (1995) 25–30.

[22] C. Jianu, G. Pop, A.T. Gruia, F.G. Horhat, Chemical composition and antimicrobial activity of essential oils of lavender (*Lavandula angustifolia*) and lavandin (*Lavandula x intermedia*) grown in Western Romania, Int. J. Agric. Biol. **15** (2013) 772–776.

[23] M. Burits, K. Asres, F. Bucar, The antioxidant activity of the essential oils of *Artemisia afra*, *Artemisia abyssinica* and *Juniperus procera*, PTR **15** (2001) 103–108.

[24] E.A. Rekka, P. Kourounakis, P.N. Kourounakis, Investigation of the effect of chamazulene on lipid peroxidation and free radical processes, Res. Commun. Mol. Pathol. Pharmacol. **92** (1996) 361–364.

[25] A. Giorgi, M. Madeo, G. Speranza, M. Cocucci, Influence of environmental factors on composition of phenolic antioxidants of *Achillea collina* Becker ex Rchb. Nat. Prod. Res. **24** (2010) 1546–1559.

[26] D. Azaz, F. Demirci, F. Satil, M. Kurkcuoglu, K.H.C. Baser, Antimicrobial activity of some Satureja essential oils, ZNaturforsch(C) **57** (2002) 817–821.

[27] M. Ozturk, M.E. Duru, F. Aydogmus-Ozturk, M. Harmandar, M. Mahhch, U. Kolak, A. Ulubelen, GC-MS analysis and antimicrobial activity of essential oil of *Stachys cretica* subsp smyrnaea, Nat. Prod. Commun. **4** (2009) 109–114.

[28] H.J.D. Dorman, S.G. Deans, Antimicrobial agents from plants: antibacterial activity of plant volatile oils, J. Appl. Microbiol. **88** (2000) 308–316.

[29] E.R. Hendry, T. Worthington, B.R. Conway, P.A. Lambert, Antimicrobial efficacy of eucalyptus oil and 1,8-cineole alone and in combination with chlorhexidine digluconate against microorganisms grown in planktonic and biofilm cultures, J. Antimicrob. Chemother. **64** (2009) 1219–1225.

[30] A. Mourey, N. Canillac, Anti-Listeria monocytogenes activity of essential oils components of conifers, Food Control **13** (2002) 289–292.

[31] A.O. Gill, P. Delaquis, P. Russo, R.A. Holley, Evaluation of antilisterial action of cilantro oil on vacuum packed ham, Int. J. Food Microbiol. **73** (2002) 83–92.

IZVOD

SASTAV, ANTIOKSIDATIVNA I ANTIMIKROBNA AKTIVNOST ETARSKOG ULJA DIVLJE HAJDUČKE TRAVE *Achillea collina* Becker POREKLOM IZ ZAPADNE RUMUNIJE

Călin Jianu[1], Corina Mişcă[1], Simona Gabriela Muntean[2], Alexandra Teodora Gruia[3]

[1]*Faculty of Food Processing Technologies, Banat's University of Agricultural Sciences and Veterinary Medicine "King Michael I of Romania" at Timișoara, Timișoara, Romania*
[2]*Institute of Chemistry Timișoara of Romanian Academy, Timișoara, Romania*
[3]*Center for Transplant Immunology, County Hospital Timișoara, Timișoara, Romania*

(Naučni rad)

Cilj ovog rada bio je da se ispita hemijski sastav, antioksidativna i antimikrobna svojstava etarskog ulja divlje hajdučke trave *Achillea collina* Becker poreklom iz zapadne Rumunije. Hemijski sastav etarskog ulja određen je GC–MS analizom. Kao glavni sastojci identifikovani su: kamazulen (38,89%), germacren D (12,90%), β-kariofilen (11,52%) i β-pinen (10,66%). Antimikrobna aktivnost testirana je difuzionim metodom na sedam vrsta bakterija, koje se mogu naći u hrani. Nije zapažen antimikrobni efekat prema vrstama bakterija *Clostridium perfringens* i *Streptococcus pyogenes*. Antioksidativna aktivnost je određena DPPH testom, koji je pokazao, da etarsko ulje (IC_{50} = 25.03±0.12 μg/ml) ima jači efekat sakupljanja slobodnih radikala od BHA, ali manji od askorbinske kiseline i propil galata. Rezultati su pokazali, da ispitivano etarsko ulje poseduje jaka antimikrobna i antioksidativna svojstva, što omogućava da se u budućim istraživanjima pronađu nova prirodna antiseptična i antioksidativna sredstva: održiva i bezbedna alternativa da se smanji primena sintetičkih aditiva.

Ključne reči: *Achillea millefolium* ssp. *collina* Becker • etarsko ulje • GC–MS analiza • antimikrobna aktivnost • antioksidativna aktivnost

Spektroskopsko ispitivanje ikone slikane na drvenom nosiocu

Sofija R. Stojanović[1], Maja D. Gajić-Kvaščev[2], Ljiljana S. Damjanović[1]

[1]*Univerzitet u Beogradu, Fakultet za fizičku hemiju, Beograd, Srbija*
[2]*Univerzitet u Beogradu, Institut za nuklearne nauke "Vinča", Beograd, Srbija*

Izvod

U ovom radu analizirana je ruska ikona slikana na drvenom nosiocu, darivana manastiru Pokrova Presvete Bogorodice kod Paraćina, nepoznatog porekla i autora. Slične ikone često se sreću na našim prostorima. U cilju karakterizacije korišćenih pigmenata i tehnike izrade, ikona je analizirana energetski disperzivnom rendgenskom fluorescentnom spektroskopijom (EDXRF) i mikro-ramanskom spektroskopijom. Potvrđena je upotreba olovo bele, vermiliona, minijuma, ultramarina, smeđih i zelenih zemljanih pigmenata i srebra u kombinaciji sa žutim organskim lakom, što je ikonopiscu poslužilo kao imitacija pozlate. Kao punilac podloge ikone korišćena je kreda (kalcijum-karbonat). Plavi pigment ultramarin je najverovatnije korišćen kako za plavu boju tako i za postizanje određenih tonova u većem delu bojenog sloja. Ovo može da bude značajan podatak za dalja ispitivanja koja se tiču određivanja porekla i ikonopisne škole u okviru koje je ikona rađena. Korišćeni materijali tipični su za ruski ikonopis 19. veka.

Ključne reči: ikona na drvenom nosiocu, EDXRF, mikro-ramanska spektroskopija, pigmenti.

Dostupno na Internetu sa adrese časopisa: http://www.ache.org.rs/HI/

NAUČNI RAD

UDK 75:543.424.2

Hem. Ind. **69** (4) 387–393 (2015)

doi: 10.2298/HEMIND140430053S

Istoričari umetnosti i konzervatori-restauratori, tradicionalno, koriste vizuelnu i mikroskopsku analizu za karakterizaciju umetničkih dela, pri tom se fokusirajući na tehniku, stil, boje i trenutno stanje umetničkog dela. Savremeni pristup podrazumeva kombinovanje ovih informacija sa rezultatima fizičko–hemijskih metoda analize [1]. Bliska saradnja naučnika iz oblasti prirodnih nauka, istoričara umetnosti i konzervatora-restauratora omogućava identifikaciju materijala koji su korišćeni pri izradi umetničkog dela, što je od izuzetnog značaja za rekonstrukciju "životne priče" samog dela. Na taj način se utvrđuje tehnologija izrade, proverava autentičnost i poreklo i doprinosi očuvanju kulturne baštine i izboru najpogodnijih procedura restauracije. Istovremeno se dobijaju dragocene informacije o vezama između naroda, trgovinskim putevima i migracijama kulturnih grupa.

Kod ovog tipa ispitivanja uvek je prisutan problem uzorkovanja jer je neophodno izbeći oštećenja umetničkih dela. Odnos između rizika od mogućeg oštećenja dela i značaja informacija koji se dobijaju u toku analiza se mora pažljivo optimizirati pri svakom ispitivanju [2,3]. Značajan napredak u tom smislu je postignut razvojem nedestruktivnih analitičkih tehnika koje ne oštećuju ispitivane umetničke predmete i mogu se koristiti *in situ*, u slučajevima kada je nemoguće pomeranje ispitivanih predmeta [4].

U ovom radu primenom dve mikro-analitičke tehnike, energetski disperzivne rendgenske fluorescentne spektroskopije (EDXRF) i mikro-ramanske spektroskopije, ispitivana je ikona koja je darivana manastiru Pokrova Presvete Bogorodice kod Paraćina 2007. godine. Ikona je poklon našeg državljanina koji je neko vreme živeo u Rusiji, odakle je ikonu i doneo. Fizičko–hemijska karakterizacija ikone ispitivane u ovom radu je značajna iz aspekta istorije umetnosti jer ne postoji dokumentacija o tome u kojoj je radionici ikona nastala, u kom vremenskom periodu, niti ko je bio autor. Istoričari umetnosti i konzervatori-restauratori su ikonu svrstali u grupu ikona slikanih u manastirskim radionicama koje su bile veoma popularne u Rusiji, a često se sreću na našim prostorima, gde su pristizale putem kupovine ili prilozima vernika. Jedan broj sličnih ikona doneli su ruski emigranti posle 1918. godine. Stil ikonopisa odgovara rešenjima iz 16. i 17. veka, s tim da se on na manastirskim ikonama ne menja sve do 20. veka. Na osnovu programa ikone, prikazane na sl. 1., ona se može svrstati u kategoriju tzv. Minejske ikone (u sredini je Vaskrsenje Hristovo, a okolo su Veliki praznici).

Publikacije u kojima su prezentovane fizičko–hemijske analize istočnohrišćanskih religioznih slika su malobrojne. Pored toga što je značaj ovih umetničkih dela svetski priznat većina studija je orijentisana ka njihovim istorijskim i estetskim kvalitetima. Istorijski dokumenti u kojima su dati opisi materijala i tehnika korišćenih pri stvaranju ikona različitih stilova u različitim vremenskim periodima su sačuvani i dostupni istraživačima, međutim oni su često nepotpuni ili komplikovani za interpretaciju, pa je egzaktno utvrđivanje materijala i tehnika izrade ovih umetničkih dela veoma važno [5,6].

Prepiska: Lj. Damjanović, Univerzitet u Beogradu, Fakultet za fizičku hemiju, Studentski trg 12, p.pr. 47, 11158 Beograd, PAK: 105305, Srbija.
E-pošta: ljiljana@ffh.bg.ac.rs
Rad primljen: 30. april, 2014
Rad prihvaćen: 27. jun, 2014

Slika 1. Analizirana ikona.
Figure 1. Investigated icon.

Glavni cilj ovog rada bio je karakterizacija pigmenata ispitivane ikone što će omogućiti adekvatnu restauraciju i konzervaciju ikone, a od izuzetnog je značaja jer se ikone ovog tipa nalaze u mnogim našim crkvama.

EKSPERIMENTALNI DEO

Opis ikone

Dimenzije ispitivane ikone su 44,0 cm×34,0 cm×2,5 cm. Ikona je rađena tehnikom tempere na drvetu, koje je najverovatnije lipa. Daska je sastavljena iz dva dela zalepljena tutkalom, koje je vremenom popustilo pa se razdvojila. Sudeći po zakrivljenosti dasaka delovi su razdvojeni duže vreme. Nije ugrožena od crvotočine i u prilično je dobrom stanju. Na dasku je tutkalom nalepljeno platno, nakon čega je nanet sloj podloge. Poznato je da je za izradu podloga za ikone najčešće korišćen gips [5], i konzervatori su pretpostavili da je reč o levkasu (ruski naziv za gips koji je često u upotrebi [7]) u koji je urezan pripremni crtež koji se na pojedinim mestima vidi. Uočeno je da je bojeni sloj oštećen i da ima na sebi naslage prljavštine. Na pojedinim mestima bojeni sloj je još uvek prekriven slojem laka za koji su konzervatori imali dve pretpostavke: žuti šelak (njime su premazivane ikone u 19. veku, a često je korišćen u kombinaciji sa srebrom jer daje vizuelni efekat zlata) ili gold-lak (ćilibar ili šafran nanesen na srebro). Na osnovu izgleda drveta na kome je ikona rađena procenjeno je da potiče iz 19. veka. Ovo se podudara sa vremenom nastanka ikona sličnih po tipu od kojih se jedna čuva u Čeljabinskoj zavičajnoj galeriji slika u Rusiji. Ta ikona je rađena u okviru Nevjanske škole koja je svoj procvat doživela krajem 18. i u prvoj polovini 19. veka [8].

Analitičke tehnike

EDXRF spektroskopija predstavlja najčešće korišćenu instrumentalnu tehniku za nedestruktivno ispitivanje predmeta kulturnog nasleđa. U ovom radu izvršena je kvalitativna analiza elementnog sastava podloge i pigmenata na bojenom sloju. Za analizu je korišćen mobilni spektrometar koji se sastoji od katodne cevi sa rodijumskom anodom (Oxford, maksimalnog napona 50 kV i maksimalne struje 1 mA) koja je opremljena posebno konstruisanim tačkastim kolimatorom pobudnog X-zračenja za njegovo što efikasnije fokusiranje na mernu tačku. Katodna cev je smeštena u kućište koje sprečava moguće rasejanje pobudnog X-zračenja u okolinu. Na ovo kućište montirani su Si-PIN detektor X-zraka (6 mm^2/500 µm, sa Be prozorom 12,5 µm debljine) sa jedinicom za digitalnu akviziciju podataka (Amptek Inc., X123) i dva laserska pokazivača namenjena vizuelizaciji mernog mesta. Ovako dizajnirano kućište smešteno je na motorizovanoj platformi koja omogućava njegovo jednostavno i precizno kretanje duž sve tri ose. Spektrometar su konstruisali i opremili saradnici Laboratorije za hemijsku dinamiku Instituta za nuklearne nauke "Vinča". Eksperimentalni parametri za sva merenja su bili sledeći: rastojanje između površine ikone i vrha katodne cevi je bilo 22 mm i ugao između ose detektora i upadnog snopa X-zračenja 45°, napon katodne cevi je bio 40 kV, struja 800 µA i vreme snimanja 120 s. Ukupno su analizirane 23 tačke. Svi spektri snimani su direktno sa ikone.

Za dobijanje mikro-ramanskih spektara je korišćen Thermo Scientific DXR ramanski spektrometar opremljen mikroskopom. Eksperimentalni uslovi su bili: ekscitaciono lasersko zračenje talasne dužine 532 nm, vreme ekspozicije, t = 2 s, broj ekspozicija 15. Korišćena je rešetka sa 1800 ureza/mm, Olympus optički mikroskop aperture 25 µm, rezolucije 2 cm^{-1}. Spektri su snimani u opsegu 50–1800 cm^{-1}, na sobnoj temperaturi. Kako je tokom rada fluorescencija bila veoma izražena, korišćena je opcija svetlosnog izbeljivanja, u trajanju od 1 i 2 min. Identifikacija pigmenata izvršena je poređenjem snimljenih spektara sa spektrima čistih pigmenata iz baze podataka koja je napravljena na Fakultetu za fizičku hemiju ili sa spektrima dostupnim u literaturi [9].

REZULTATI I DISKUSIJA

Drveni nosioc ispitivane ikone je razdvojen na dve polovine, što se može videti na sl. 1. Preliminarnim EDXRF spektroskopskim ispitivanjima su dobijeni identični rezultati za levu i desnu polovinu ikone, pa je

detaljno ispitivana samo leva strana ikone. Na slici 2 prikazana su mesta EXDRF merenja. Analizirano je šest karakterističnih partija bojenog sloja u više tačaka (crvena, bela, braon, zelena, plava i ljubičasta), "pozlata" i podloga. Snimani su spektri za tačke koje se nalaze na 3 kompozicije od ukupno 13 (jedna centralna i 12 koje je okružuju). Analizirane su i tačke na slikanom okviru, na kojem su uočeni ispisani nazivi kompozicija i floralni motivi.

Slika 2. Mesta EDXRF merenja na levoj polovini ikone.
Figure 2. Positions on the left half of the icon where EXDRF measurements were performed.

Rezultati EDXRF ispitivanja pigmenata na ikoni dati su u Tabeli 1. EDXRF spektar snimljen u tački 12 crvene partije bojenog sloja prikazan je na slici 3.

Na tri EDXRF spektra snimljena u tačkama na crvenim partijama bojenog sloja identifikovana je živa, što je potvrda korišćenja jarko crvenog pigmenta vermiliona (HgS). Vermilion se dobija od minerala cinabarita i jedini je crveni pigment koji u svom sastavu ima živu. Analizom EDXRF spektra snimljenog u tački 23 može se identifikovati intenzivan pik olova koji ukazuje na korišćenje minijuma (Pb_3O_4).

EDXRF spektri snimljeni u tačkama na belim partijama bojenog sloja pokazuju intenzivan signal olova na osnovu čega je moguće identifikovati olovo belu kao beli pigment. Ovaj pigment korišćen je pri slikanju ispitivane ikone i kao osnovna boja i za nijansiranje drugih boja, jer je znatno većeg intenziteta u spektrima snimljenim u tačkama svetlijih tonova određene boje.

Vrlo intenzivni signali gvožđa dobijeni su EDXRF analizom braon partija bojenog sloja ukazujući na korišćenje smeđih zemljanih pigmenata. Karakteristični elementi u tragovima (Tabela 1) omogućavaju precizniju identifikaciju korišćenog pigmenta, tj. crvenog okera, Fe_2O_3. U analiziranim tačkama zelenog dela detektovani pik gvožđa je jedini koji može da ukaže na korišćeni pigment. Potvrda da je korišćena zelena zemlja su detektovani signali elemenata koji su u tragovima pratioci ovog pigmenta, a to su Cr, Mn, Ti+Ba [5,10]. Zemljani pigmenti imaju složeni hemijski sastav i vrlo često su korišćeni u mešavinama različitih odnosa. Za njihovo precizno određivanje neophodno je korišćenje drugih analitičkih tehnika i uzimanje uzorka sa ispitivanog predmeta [5].

EDXRF spektri plave boje snimljeni su u ukupno šest tačaka: pet tačaka plave partije bojenog sloja i jednoj tački na plavoj liniji sa okvira ikone. Na pet EDXRF spektara snimljenih u tačkama plave partije bojenog sloja najintenzivniji je signal olova, dok je na EDXRF spektru snimljenom sa okvira ikone dominantan signal kalcijuma. Nije detektovan nijedan element koji bi

Tabela 1. Rezultati EDXRF analize pigmenata ispitivane ikone
Table 1. Results obtained by EDXRF analysis of pigments on investigated icon

Boja	Analizirana tačka	Detektovani elementi[a]	Identifikovani pigmenti
Crvena	1, 2, 12	Hg, S (Ca, Sr, Ba, Fe)	Vermilion (HgS)
	23	Pb (Ca, Fe, Sr, Ba)	Minijum (Pb_3O_4)
Bela	4, 13	Pb (Fe, Ca, Sr, Ba, Cu)	Olovo bela ($2PbCO_3 \cdot Pb(OH)_2$)
Braon	3, 5, 16	Fe (Ca, Ti+Ba, Cr, Pb,Sr)	Zemljani pigment-crveni oker (Fe_2O_3)
Zelena	14,15	Fe (Cr, Mn, Ti+Ba, Sr)	Zelena zemlja
Plava	6, 7, 9, 10, 11, 18	Pb, Ca, Fe, Ba, Sr	–
Ljubičasta	8	Pb (Ca, Fe, Ba, Sr)	Minijum (Pb_3O_4)
"Pozlata"	17, 19, 22	Ag (Ca, Fe, Sr, Mn)	Srebro

[a]U zagradama su dati elementi identifikovani u spektrima, ali koji ne potiču od pigmenta koji je određen na datom bojenom sloju (ovi elementi mogu da potiču od primesa, nečistoća, iz podloge ili sloja prepature, a mogu da budu i iz pigmenta sa kojim je pigment osnovnog tona mešan da bi se dobila željena boja ili ton; informacije dobijene na ovaj način mogu da ukažu na slikarsku tehniku)

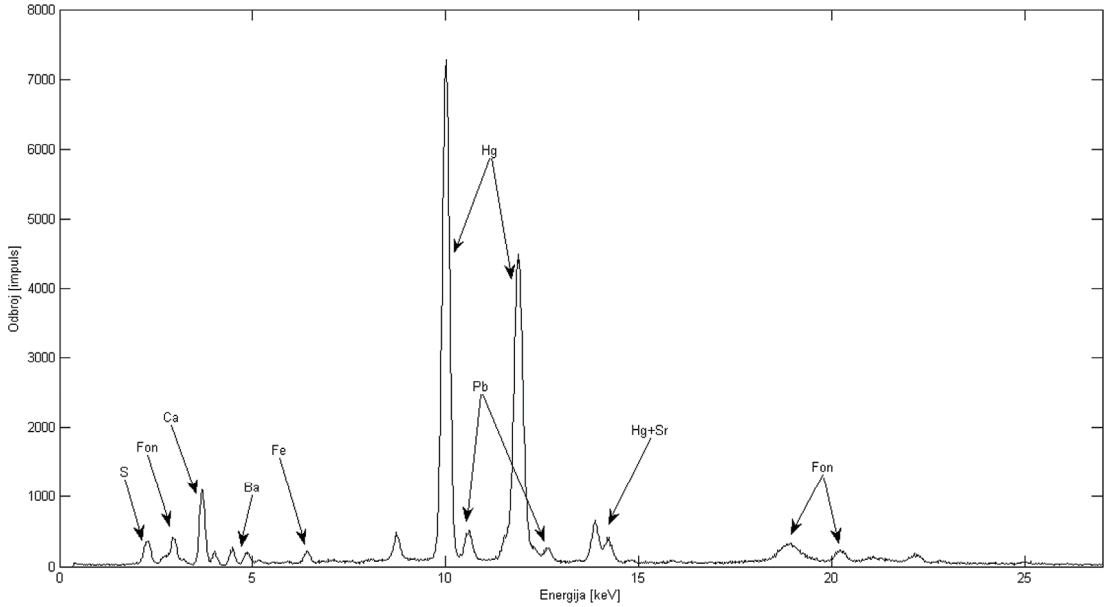

Slika 3. EDXRF spektar snimljen u tački 12 crvene partije bojenog sloja.
Figure 3. EDXRF spectrum recorded at the spot 12 on the red part of paint layer.

omogućio preciznu identifikaciju plavog pigmenta, već samo elementi iz podloge, podslika (premaz podloge, nanosi se pre bojenog sloja) ili mešavine sa plavom. Na osnovu detektovanog signala olova, sigurno je korišćeni plavi pigment mešan sa olovo belom radi nijansiranja. S obzirom da nije detektovan nijedan karakterističan element za plave pigmente, može se pretpostaviti da je korišćen ili ultramarin ili indigo jer su u EDXRF spektrima detektovani signali elemenata (Tabela 1) koji često prate ova dva pigmenta [5].

Radi identifikacije korišćenog plavog pigmenta, uzeta je mala količina uzorka plave boje sa oštećenog dela bojenog sloja ikone i analizirana mikro-ramanskom spektroskopijom. Dobijeni ramanski spektar plave boje prikazan je na slici 4. Poređenjem sa referentnim spektrom utvrđeno je da je korišćeni plavi pigment ultramarin ($Na_4Al_3Si_3S_2O_{12}$). Ramanskom spektroskopijom se ne može utvrditi da li se radi o prirodnom ili sintetičkom ultramarinu [11], što bi bilo od značaja za utvrđivanje radionice u kojoj je ikona nastala, već je neophodno koristiti druge analitičke metode.

EDXRF analizom jedne tačke ljubičaste partije bojenog sloja identifikovana je olovo bela, minijum i mala količina vermiliona, na osnovu čega se može zaključiti da je ljubičasta boja dobijena mešanjem belog, crvenog i plavog pigmenta.

EDXRF analiza "pozlate" vršena je u tri tačke. U dva EDXRF spektra (tačke 17 i 19) detektovano je srebro. Ovaj rezultat potvrđuje pretpostavku konzervatora da je efekat pozlate postignut premazivanjem organskog laka ili boje, jer EDXRF metodom nije moguće detektovati jedinjenja organskog porekla.

Pri analizi podloge, snimani su EDXRF spektri na oštećenim delovima gde nije bilo bojenog sloja. EDXRF

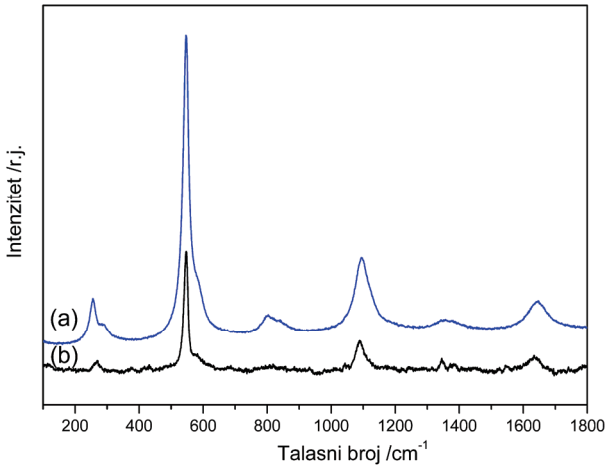

Slika 4. Ramanski spektri: a) čistog ultramarina iz baze podatka napravljene na Fakultetu za fizičku hemiju i b) uzorka plave boje sa ikone.
Figure 4. Raman spectra of: a) pure ultramarine from home made database and b) blue coloured sample taken from the icon.

spektar podloge snimljen u tački 20 prikazan je na slici 5. Signal kalcijuma je dominantan na oba EDXRF spektra podloge (tačke 20 i 21). Takođe, signal kalcijuma je prisutan u svim snimljenim EDXRF spektrima (23 ispitivane tačke). EDXRF spektroskopija pruža informacije o elementnom sastavu površine, ali kada se radi o višeslojnim uzorcima karakteristično X-zračenje može poticati iz više slojeva. U slučaju ispitivane ikone, može se u EDXRF spektrima očekivati pojava signala ne samo bojenog sloja već i podloge. Poznato je da se kao podloga za izradu ikona mogu koristiti kreda ili gips (kalcijum-karbonat ili kalcijum-sulfat) [5]. Signal kalcijuma koji je detektovan u svim snimljenim EDXRF spektrima

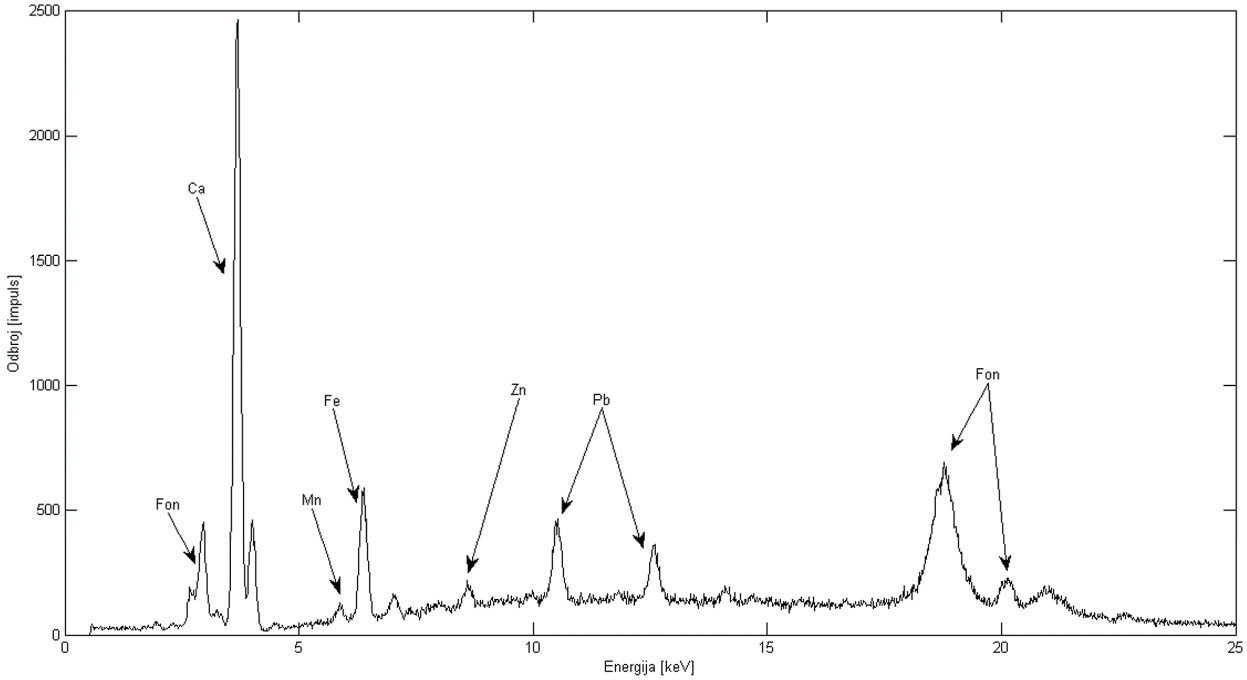

Slika 5. EDXRF spektar podloge snimljen u tački 20.
Figure 5. EDXRF spectrum of ground layer recorded at the spot 20.

potiče od podloge, ali je ovom metodom nemoguće utvrditi o kojem se tačno jedinjenju radi.

Radi identifikacije jedinjenja korišćenog za podlogu snimljen je ramanski spektar uzorka podloge, slika 6, i na osnovu prisustva karakterističnih traka [9] utvrđeno je da je kao podloga korišćen kalcijum-karbonat, što opovrgava polaznu pretpostavku o sastavu podloge koju su dali konzervatori.

Signal gvožđa nije registrovan samo na jednom EDXRF spektru snimljenom u tački bele partije bojenog sloja. Ovaj rezultat ukazuje na to da je zemljani pigment koji u svom sastavu ima gvožđe korišćen za premazivanje podloge. Detekcija mangana na EDXRF spektrima (slika 5), koji je pratilac gvožđa u umbri, omogućila je preciznu identifikaciju zemljanog pigmenta koji je korišćen kao podslik.

U EDXRF spektrima 16 tačaka bojenog sloja (od 18 snimljenih) detektovan je barijum. U EDXRF spektrima podloge i "pozlate" barijum nije detektovan, što ukazuje da je barijum verovatno korišćen u vidu belog pigmenta barita ($BaSO_4$) za postizanje određenih tonova.

U svim snimljenim EDXRF spektrima je detektovan signal stroncijuma. U tačkama bojenog sloja detektovani stroncijum je verovatno prisutan kao stroncijum-sulfat koji se javlja kao primesa barita. Međutim, ostaje otvoreno pitanje prisustva stroncijuma u tačkama u kojima nije registrovano prisustvo barijuma. Stroncijum-sulfat se može javiti u podlozi ikone pomešan sa kalcijum-sulfatom koji u ovom radu nije detektovan. Pitanje porekla stroncijuma prisutnog na ikonima je

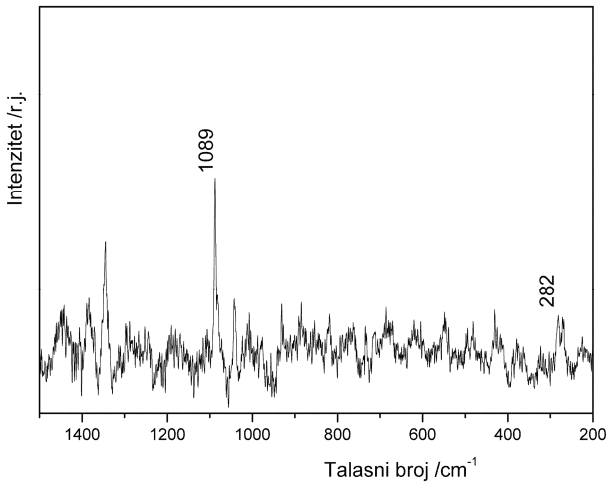

Slika 6. Ramanski spektar podloge; obeležene su karakteristične trake kalcijum-karbonata.
Figure 6. Raman spectrum of ground layer; positions of characteristic peaks for calcium-carbonate are marked.

otvoreno ranije u literaturi [12] i predmet je daljih istraživanja.

Dobijeni rezultati ukazuju da je u izradi ispitivane ikone korišćen materijal karakterističan za ruski ikonopis 19. veka.

ZAKLJUČAK

Analizirana je ruska ikona iz 19. veka, nepoznatog porekla i autora, kombinacijom EDXRF spektroskopije i mikro-ramanske spektroskopije. Utvrđeno je da su pri

izradi ikone korišćeni sledeći pigmenti: vermilion, minijum, olovo bela, ultramarin, barit i pretežno zemljani pigmenti za braon (crveni oker) i zelenu boju. Zemljani pigment umbra je korišćen i za premazivanje podloge što je po pravilu rađeno u okviru nekih ikonopisnih škola. Kao podloga korišćen je kalcijum-karbonat. U EDXRF spektru "pozlate'' detektovano je srebro koje je verovatno premazano žutim organskim lakom.

Dobijeni rezultati mogu poslužiti za izbor najadekvatnije procedure restauracije, ali i istoričarima umetnosti u daljim istraživanjima. Interesantna činjenica da je za plavu boju kao i za dobijanje drugih boja (na pr. ljubičasta) korišćen ultramarin može biti značajan podatak za određivanje porekla ikone i radionice u kojoj je nastala.

Zahvalnica

Autori duguju zahvalnost Ministarstvu prosvete, nauke i tehnološkog razvoja Republike Srbije za finansijsku podršku (projekti OI 177021 i OI 177012), dr Danici Bajuk-Bogdanović za pomoć pri snimanju ramanskih spektara, kao i dr Danieli Koroliji-Crkvenjakov konzervatoru-restauratoru Galerije Matice srpske, profesoru dr Nenadu Makuljeviću sa Odseka za Istoriju umetnosti Filozofskog fakulteta Univerziteta u Beogradu i konzervatoru-restauratoru Istorijskog muzeja Srbije gospodinu Bobanu Veljkoviću i kolegi Veliboru Andriću, dipl. fizikohemičaru, na korisnim diskusijama u toku realizacije rada.

LITERATURA

[1] P. Ward, The Nature of Conservation: The Race against Time, The Getty Conservation Institute, Los Angeles, CA, 1989.

[2] M. Ortega-Avilés, P. Vandenabeele, D. Tenorio, G. Murillo, M. Jiménez-Reyes, N. Gutérrez, Spectroscopic investigation of a “Virgin of Sorrows” canvas painting: A multi-method approach, Anal. Chim. Acta **550** (2005) 164–172.

[3] P. Dredge, R. Wuhrer, M.R. Phillips, Monet’s Painting under the Microscope, Microsc. Microanal. **9** (2003) 139–143.

[4] A. Adriaens, Non-destructive analysis and testing of museum objects: An overview of 5 years of research, Spectrochim. Acta, B **60** (2005) 1503–1516.

[5] D. Korolija-Crkvenjakov, V. Andrić, M. Marić-Stojanović, M. Gajić-Kvaščev, J. Gulan, N. Marković, Ikonostas crkve manastira Krušedola, Galerija Matice srpske, Univerzitet u Beogradu, Institut za nuklearne nauke “Vinča”, Beograd, 2012.

[6] S. Sotiropoulou, S. Daniilia, Material Aspects of Icons. A Review on Physicochemical Studies of Greek Icons, Acc. Chem. Res. **43** (2010) 877–887.

[7] I.C.A. Sandu, S. Bracci, I. Sandu, M. Lobefaro, Integrated Analytical Study for the Authentication of Five Russian Icons (XVI–XVII centuries), Micros. Res. and Tech. **72** (2009) 755–765.

[8] Uralьskaя istoričeskaя эnciklopediя — UrO RAN, Institut istorii i arheologii, Akademkniga, Ekaterinburg, 2000.

[9] I.M. Bell, R.J.H. Clark, P.J. Gibbs, Raman spectroscopy library of natural and synthetic pigments (pre- ~1850 AD), Spectrochim. Acta, A **53** (1993) 2159–2179.

[10] D. Hradil, T. Grygar, J. Hradilova, P. Bezdička, Clay and iron oxide pigments in the history of painting, Appl. Clay Sci. **22** (2003) 223–236.

[11] I. Osticioli, N.F.C. Mendes, A. Nevin, Francisco P.S.C. Gil, M. Becuccia, E. Castellucci, Spectrochim. Acta, A **73** (2009) 525–531.

[12] L. Burgio, R.J.H. Clark, K. Theodoraki, Raman microscopy of Greek icons: identification of unusual pigments, Spectrochim. Acta, A **59** (2003) 2371–2389.

SUMMARY

SPECTROSCOPIC STUDY OF AN ICON PAINTED ON WOODEN PANEL

Sofija R. Stojanović[1], Maja D. Gajić-Kvaščev[2], Ljiljana S. Damjanović[1]

[1]*University of Belgrade, Faculty of Physical Chemistry, Belgrade, Serbia*
[2]*University of Belgrade, Vinča Institute of Nuclear Sciences, Belgrade, Serbia*

(Scientific paper)

Russian icon painted on wooden panel analyzed in this work is interesting for art historians because there is no precise information in which workshops it was made or who the author was. Similar icons are often found in churches and monasteries in our region. In order to obtain information about materials used for creation of investigated icon two micro-analytical techniques were used: Energy-Dispersive X-Ray Fluorescence spectroscopy (EDXRF) and micro-Raman spectroscopy. Obtained results confirmed presence of following materials: lead-white, vermilion, minium, ultramarine, brown and green earth pigments and silver in combination with yellow organic varnish, which served to an iconographer for gilding. Ground layer was made of calcite. Blue pigment ultramarine was probably used for blue colour as well as for obtaining particulars hues in several parts of the paint layer. This can be important information for further research concerning particular workshop in which the icon was made. Identified materials are typical for Russian iconography of the 19th century.

Keywords: Icon on a wooden panel • EDXRF • Micro-Raman spectroscopy • Pigments

Comparative analysis of milling results on the tail-end reduction passages of the wheat flour milling process: Conventional *vs.* eight-roller milling system

Aleksandar Z. Fišteš

Department of Carbohydrate Food Engineering, Faculty of Technology, University of Novi Sad, Serbia

Abstract

Introduction of the eight-roller mill into the wheat flour milling process significantly reduces the investment costs and overall energy requirements compared to the conventional milling system. However, the conditions for controlled milling are less favorable and could result in deterioration of flour yield and quality. Paper compares milling results obtained using a conventional process and process with an eight-roller mill employed on the tail-end passages of the reduction system. At the same roll gap and under the same sieving conditions, the flour release was lower in the process with the eight-roller mill compared to the conventional milling system. By decreasing the roll gap and increasing the upper size limit (granulation) of flour in the process with the eight-roller mill it is possible to increase flour yield and decrease milling energy consumption per unit mass of flour produced. This can be achieved without deterioration of flour quality as determined by ash content.

Keywords: wheat flour milling, conventional system, eight-roller mill, tail-end passages.

Available online at the Journal website: http://www.ache.org.rs/HI/

SCIENTIFIC PAPER

UDC 664.71–11:655.11

Hem. Ind. **69** (4) 395–403 (2015)

doi: 10.2298/HEMIND140211055F

The aim of the wheat flour milling process is to obtain the best possible dissociation of the starchy endosperm from the other parts of the grain and to achieve as high as possible flour extraction with the lowest contamination of bran and germ that increase the ash content [1]. It is a gradual reduction process consisting of sequential and consecutive size reduction (roller mills) and separation (plansifters). Roller mills break the wheat kernel such that particles of different sizes also vary in botanical origin and composition [2]. They tend to keep the bran layers relatively intact as large particles, while shattering the endosperm into small particles so they can be separated from bran [3]. This is possible due to differences in the structural characteristics between the anatomic parts of the wheat kernel. These differences are exaggerated by adding water to the wheat prior to milling in process known as conditioning.

The process involves breaking open the kernel, scraping the endosperm from the bran and germ, and gradually reducing the chunks of endosperm into flour [4]. Breaking the wheat kernel is affected by corrugated cast steel rolls that gradually separate the endosperm, bran and germ. The break system has two parts: the head break which releases relatively pure particles of endosperm and tail break, which cleans up the remaining endosperm from bran and releases smaller endosperm particles along with finer pieces of bran and germ [5]. The objective of grinding in the sizing system is to detach the bran pieces attached to endosperm particles (large middlings), while minimizing flour production [5]. Reduction of relatively pure endosperm to flour is achieved by using smooth rolls. Segregation between the kernel parts occurs in plansifters, where sieves separate particles of different size, and in purifiers, where sieves and air-flow separate particles of different size, with specific gravity and shape [6].

The milling industry is also very conservative. After more than 100 years, roller mills and plansifters still remain the primary machines used in the process. Of course, the equipment has been redesigned to such an extent that it has been possible to multiply the throughputs of these machines, but flour process technology has not changed fundamentally [7]. Millers always sought out for possibilities to simplify the process and make it more efficient in terms of reducing the investment, operating and maintaining costs as long as the quantity and quality of the finished products are not affected [8]. Over the years, rationalization of the process has been achieved by increasing the roll velocities, using drum detachers and bran finishers while grinding has been supported with impact milling (intensive detachers) making the shorter roll surface a reality [5,9]. Also, the use of debranning machines to remove the bran ahead of the first break can simplify break and reduction steps of conventional milling [4,10].

Also, the traditional wisdom in flour milling is that after every grinding step the ground material should be

Correspondence: Department of Food Engineering, Faculty of Technology, University of Novi Sad, Bulevar Cara Lazara 1, 21000 Novi Sad, Serbia.

E-mail: fistes@uns.ac.rs

Paper received: 11 February, 2014

Paper accepted: 4 July, 2014

sieved and the undersize material should be removed before regrinding. This is the reason why the double grinding of intermediate streams before sieving has been one of the most notable process developments in flour milling [11]. Eight-roller mill (a total of 8 rolls in one housing) provides two grinding passages without any intermediate sifting. Introduction of the eight-roller mill into the milling flowsheet provides significant advantages compared to a conventional process. Double grinding without intermediate sifting means that pneumatic conveying of the stock from the roll to the sifter is necessary only after the lower pair of rolls. Fewer pneumatic suction lifts reduce the investment costs and the time needed for the installation of the pneumatic conveying system. Lower pneumatic air requirements result in lower power requirements for the fan and lower filter surface for cleaning the conveying air. There is a significant reduction of sifter surface, less number of roll stands, less spouting and auxiliary components. With less equipment there is less cleaning and maintenance and less space for their installation is required resulting in lower building costs with less area to keep clean and fumigate. Also, within existing limited building space, by replacing the four-roller mills with eight-roller mills, the roll length and therefore the grinding capacity can be significantly increased without need for changing existing sifter passages and pneumatic lifts [5,7–9,12–14].

On the other hand, the eight-roller mill ignores the basic milling principle that after grinding coarse material is separated from the fines. Some of the intermediate materials produced on the upper rolls, normally are not sent to the lower rolls (next grinding passage), which are not designed to mill them. Flour produced in the upper rolls is fed to the lower rolls instead of being sent to the collecting flour conveyor. Also, the material from the upper rolls almost immediately enters the grinding zone of the lower rolls without any cooling (normally occurs in the pneumatic suction lift). The temperature of the stock following the lower rolls could be high and harmful to flour quality and even cause condensation problems in the milling equipment [15]. There are less flour streams to be selected for specialty flours [14].

Number of authors [8,14,16–19] stated that when the first and second breaks are combined into a twin passage there is a shift in particle size distribution compared to a conventional single break system. Eight-roller mill produces more break flour and fine middlings and less coarse middlings and sizings. The flour granulation is finer with the use of the eight-roller mill because the flour released through the first passage is regrinded. The finer flour could also produce whiter flour. With double grinding on smooth rolls the bran particles are more flattened, due to their plasticity and intense compressive forces, and therefore it is easier to separate them from flour [9,14].

Most of the research considering the factors that affect the milling results using the eight-roller mills are focusing on the break system [17,19,20], while relatively little research has been done considering the effects of using this technique in the reduction system. Fistes *et al*. [21] compared the effect that roll gap changes have on the milling results obtained using a conventional process and process with an eight-roller mill employed on the front passages of the reduction system. The results showed that it is possible to achieve similar results to the ones obtained in the conventional process with appropriate adjustment of the roll gap and micron size of the bolting cloths. In contrast to head-end passages, streams that are sent to the tail-end passages of the reduction system are much finer in particle size and contain a large portion of bran with relatively little endosperm mainly from the outer portion of the endosperm. Also, in the wheat flour milling process the set of roll parameters are constantly changing from the beginning to the end of the process. Therefore, findings from the head-end passages cannot be directly transferred to the tail-end passages of the reduction system. These are the reasons why this paper is focusing on the possibilities of using the eight-roller mill on the tail-end passages of the reduction system.

MATERIALS AND METHODS

Material

A sample of the total mass of about 50 kg was obtained from an industrial mill (120 t/day), having five break (1Bk–5Bk), four sizing (1R–4R) and six reduction passages (1M–6M). The stream, which according to the mill flow sheet would have been sent to the 5M, was intercepted end employed in the experiments. It comprises the streams leaving the 5Bk (250/150 μm), 2nd vibro-sifter (>236 μm) and 4M (530/132 μm). Moisture and ash contents of the sample, determined according to ICC standard methods no. 110/1 [22] and 104/1 [23], were 12.8 and 2.22(%)$_{dm}$, respectively.

Milling procedure

The sample was separated into 0.5 kg batches using the automatic sampler divider (Gompper–Maschinen KG). The batches were milled on a Variostuhl (model C Ex 2) laboratory roll stand (Miag). Smooth rolls 0.1 m in length and 0.25 m in diameter were used. Table 1 summarizes the experimental range of variables tested (chosen to be near the ranges likely to be encountered commercially).

The experiments were designed to compare the performance of conventional and eight-roller milling systems employed on the tail-end passages of the red-

Table 1. Summary of experimental range of variables tested

Milling system	Roll surface	Roll gap combinations, mm	Feed rate, kg/cm^{-1} min^{-1}	Differential	Fast roll speed, m/s
Conventional	Smooth	5M-0.08; 6M-0.05	5M-0.14; 6M-0.10[a]	1.25	5
		5M-0.08; 6M-0.04			
		5M-0.08; 6M-0.03			
Eight-roller		5M-0.05; 6M-0.04	5M-0.14; 6M-0.14		
		5M-0.05; 6M-0.03			
		5M-0.04; 6M-0.03			

[a]The slower feed rate on 6M corresponds to the amount of flour removed by intermediate sifting of the stock leaving 5M

uction system (5M and 6M passages in this particular mill). For the conventional milling system the entire stock following 5M was sieved for 3 min on a laboratory sifter (model MLU-300, Bühler) and the part of the stock held on the sieve fitted with 150 µm bolting cloth was milled on 6M. For the eight-roller milling system the entire stock following 5M was milled on 6M without intermediate sifting. Two samples were milled and sifted at the same conditions and a total of 72 grinding runs were performed, 36 on each 5M and 6M.

Milling results

Sieve analysis of the stock following 6M in conventional system was performed using the sieve openings of 350, 250 and 150 µm, along with the bottom collecting pan. For the sieve analysis of the stock following 6M in the eight-roller milling system, two different stacks of sieves were used. The first stack was the same as that mentioned above. In the second, the sieve with the 150 µm bolting cloth was replaced with a sieve having 180 µm bolting cloth. The stock held on each sieve and pan was weighed.

Flour yield, F (%), in the eight-roller and conventional milling systems was calculated from Eqs. (1) and (2), respectively:

$$F(\%) = 100\frac{m_{6M}}{M} \tag{1}$$

$$F(\%) = 100\frac{m_{5M} + m_{6M}}{M} \tag{2}$$

The energy consumption per unit mass of flour produced, E (kJ/kg), in the conventional and eight-roller milling systems were calculated by Eqs. (3) and (4) respectively:

$$E = \frac{P_{5M} - P_{5M}^*}{m_{5M}} t_{5M} + \frac{P_{6M} - P_{6M}^*}{m_{6M}} t_{6M} \tag{3}$$

$$E = \frac{(P_{5M} - P_{5M}^*) + (P_{6M} - P_{6M}^*)}{m_{6M}} (t_{5M} + t_{6M}) \tag{4}$$

Here t (s) is the time of the grinding run determined by the chronometer. The symbols m and M stand for the weights (kg) of the flour and native feed, respectively. Power readings, P (kW) and P^* (kW), correspond to operation with and without the material flow, respectively. The subscripts indicate the milling passage (5M or 6M).

The ash content in flour and other size fractions of the milling output have been determined according to ICC standard method No.104/1 [23]. The analyses were done in two replicates.

Statistical analysis

The significance of the differences between milling results (flour yield, flour ash content and milling energy consumptin) obtained using investigated milling systems have been tested by the paired Student's t-test. The significant level was established at $p < 0.05$.

One-way ANOVA was used to ascertain whether the different roll gap settings significantly affect the ash content and milling energy consumption. Means were compared using the Tukey test at the 95% significance level.

RESULTS AND DISCUSSION

In a roller mill, particles are subjected to shear and compressive forces. The roll parameters such as: the roll gap, the roll differential, the roll velocities, the feed rate, and the type and condition of roll surface, influence the magnitude of the stress and relative contributions of compressive and shearing forces [24]. Also, the nature of deformation (ductile or brittle) depends not only on the applied stresses, but as well on the particle components upon which the stresses act. Compressive stresses are more effective in causing the disintegration of the brittle endosperm material, while bran particles being tough and fibrous are more prone to fracture imparted by shear forces. Under industrial conditions, during the flour milling process, only the roll gap can be adjusted (feed rate to a limited degree) while the other roll parameters remain the same. At the same time, the roll gap is the parameter with the biggest influence on milling results. A number of earlier papers [25–30] showed that the particle size distribution, resulting from milling a particular feed size, critically depends on the ratio of roll gap to input particle size. Changes in the particle size distribution of the stock leaving 6M in the conventional process (Fig.

1a) and the eight-roller milling system (Fig. 1b), brought about by the decrease of the roll gap, followed the same trends.

By decreasing the roll gap, the quantity of material >150 μm tends to decrease while the flour yield (<150 μm) increased. Considering that the 6M feeds were different for the two milling systems, this cumulative size distributions are not to be compared and serve merely to show the trends. By decreasing the roll gap greater compressive forces are imposed, thereby increasing the number of endosperm fractures creating more flour. At the same time, the tougher branny particles are flattened and remain in coarser size fractions of the milling output. The material feeding the rolls of the tail-end passages of the reduction system normally contains a large portion of bran with relatively little endosperm mainly from the outer portion of the endosperm. These branny particles absorb the big portion of the stresses in the grinding zone so there is only a slight increase of the flour yield. The gradient of ash increases from center to the outer layers of wheat kernel [31], so the increase of the ash content indicates the higher contamination of the stock with the bran and germ. By decreasing the roll gap, on both passages and in both milling systems investigated, the flour ash content practically remained the same (there is only slight change without some general trend) but there is a significant increase of the ash content of the coarsest fraction of the stock (Table 2).

This proves the previous conclusion that branny particles absorb the stresses in the grinding zone but they don't pass into the flour because of predominant compressive forces under present grinding conditions (smooth rolls, 1.25 roll differential and small roll gaps), which create more endosperm fractures while flattening the branny particles. With the same gap setting on the 6M in the conventional system, higher flour release is obtained with the bigger roll gap on the 5M because the material entering the 6M, after flour removal by intermediate sifting, contains more endosperm as a result of smaller compressive forces and therefore less number of endosperm fractures.

At the same roll gap setting and under the same sieving conditions, the flour release was lower in the process with the eight-roller mill compared to the conventional milling system (Fig. 2) and the difference is statistically significant ($p < 0.05$).

This is similar to the results obtained in the study of the effects of using the eight-roller mill on the front passages of the reduction system [21]. The flour particles, which are removed from the stock by intermediate sifting in the conventional process, remain in the material feeding the lower pair of rolls of the eight-roller mill. They take on some of the stresses in the grinding zone which otherwise would be used to reduce the remaining coarse particles of the stock. This causes the lower flour yield and the finer flour granulation as a result of further grinding of flour particles. Posner and

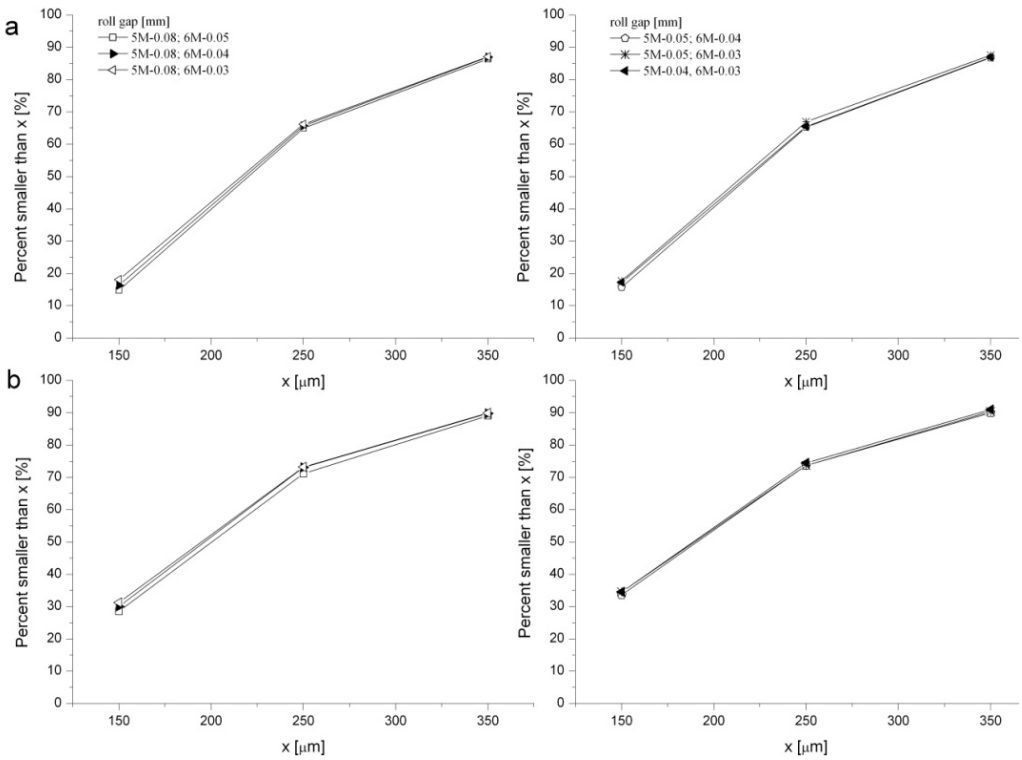

Figure 1. Cumulative size distributions of the stocks following 6M milled through different roll gaps in the a) conventional milling system and b) eight-roller mill system.

Table 2. Ash content in the size fractions of the stock following 5M and 6M in the conventional and eight-roller milling systems; values for a particular column, milling system and grinding passage differ significantly when followed by different letters

Milling system	Grinding passage	Roll gap, mm	Ash content, $(\%)_{dm}$			
			>350 µm	350/250 µm	250/150 (180[a]) µm	<150 (180[a]) µm
Conventional	5M	0.08	4.08 a	3.37 a	1.73 a	1.04 a
		0.05	4.20 b	3.39 a	1.81 b	1.03 a
		0.04	4.26 b	3.46 b	1.87 b	1.04 a
Conventional	6M	5M-0.08; 6M-0.05	4.31 a	3.53 a	2.10 a	1.44 a
		5M-0.08; 6M-0.04	4.35 b	3.56 a	2.13 ab	1.45 a
		5M-0.08; 6M-0.03	4.39 c	3.56 a	2.19 ab	1.41 b
		5M-0.05; 6M-0.04	4.43 d	3.55 a	2.23 b	1.45 a
		5M-0.05; 6M-0.03	4.44 d	3.55 a	2.24 b	1.40 b
		5M-0.04; 6M-0.03	4.45 d	3.52 a	2.23 b	1.40 b
Eight-roller	6M	5M-0.08; 6M-0.05	4.13 a	3.55 a	1.89 a (2.15 a)	1.14 a (1.16 c)
		5M-0.08; 6M-0.04	4.22 b	3.52 a	1.94 ab (2.16 ab)	1.13 a (1.11 b)
		5M-0.08; 6M-0.03	4.36 c	3.54 a	1.98 b (2.14 a)	1.14 a (1.11 b)
		5M-0.05; 6M-0.04	4.38 c	3.54 a	2.08 c (2.22 bc)	1.17 a (1.12 b)
		5M-0.05; 6M-0.03	4.40 c	3.56 a	2.07 c (2.19 abc)	1.19 a (1.20 a)
		5M-0.04; 6M-0.03	4.42 c	3.53 a	2.06 c (2.23 c)	1.13 a (1.15 c)

[a]In the second stack of sieves for the eight-roller milling system, the sieve with the 150 µm bolting cloth was replaced with a sieve having 180 µm bolting cloth

Hibbs [5] also observed this reduced grinding efficiency and stated that the lower pair of rolls should be considered to be 0.75 of their actual length because regrinding material made up of significantly different particle sizes and quality is less effective.

The other probable cause of lower flour yield in the eight-roller milling process is underbolting. This is a condition that occurs when insufficient sifter area is allocated for the separation and the material that passes over the screen contains particles smaller than the sieve aperture [5]. The absence of intermediate sifting between two grinding operations increases the amount of material on 6M and therefore the load of the sifter surface is higher compared to a conventional system. Also, the amount of flour in the stock following 6M is considerably higher in the eight-roller milling process while the granulation of flour is finer (because of regrinding) which makes it harder to be sifted.

The problem of underbolting led to a construction of eight-roller mills which include some intermediate sifting. The first solution is based on the fact that the heavy material exiting from the nip of the upper pair of rolls is thrown farther than the flour and light material. A baffle arrangement below the upper rolls separates the fines and therefore they bypass the lower rolls. The second solution is a centrifugal sifter below the upper rolls to separate the fines to bypass the lower rolls [5].

The savings with the eight-roller mill can be fully exploited only if it is possible to achive similar milling results to those obtained with a conventional mill. By decreasing the gap setting on the eight-roller mill on both 5M and 6M, without changing the sieving conditions, it is possible to achieve flour yield similar to the one obtained with the conventional milling system (Fig. 2: conventional: 5M-0,08 mm, 6M-0,05 mm; eight-roller 5M-0,05 mm, 6M-0,04 mm; conventional: 5M-0,08 mm, 6M-0,04 mm; eight-roller 5M-0,05 mm, 6M-0,03 mm or 5M-0,04 mm and 6M-0,03 mm). This had no influence on ash content of the flour and there is no statistically significant difference ($p > 0.05$) compared to the ash content in the total amount of flour following 6M in the conventional system (Table 3).

It needs to be pointed out that even though there is no significant difference between two milling system considering the ash content in the total amount of flour, there is a significant difference between the ash content of the flour streams following 5M and 6M in the conventional milling system (Table 2). Pojić *et al.* [32] also observed significant difference between the ash content in the tail-end reduction flours. These flour streams are mixed together in the process with the eight-roller mill therefore reducing the number of flour streams that could be selected for flour blending.

It is obvious that in the area of very tight roll gaps (0.03–0.05 mm), decrease of the roll gap setting is not followed with noticeable increase of the flour yield (Fig. 2). Considering the relatively short duration of the grinding runs (21–23 s) and the long interval between them, heating of the rolls did not take place even when the roll gaps were very tight. However, in the industrial conditions the undesirable heating of the rolls could occur especially in the cases of tight roll gaps and increased feed rate to the rolls (increased friction between particles and between roll surface and particles). This

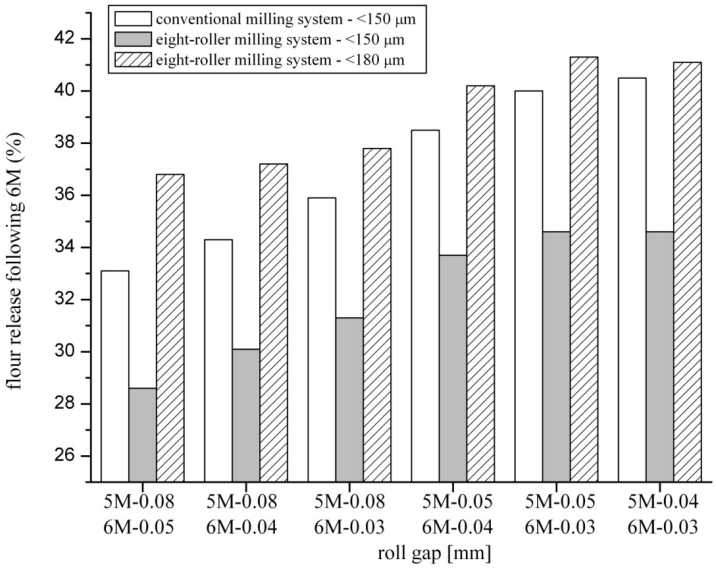

Figure 2. Flour release following 6M in the conventional and eight-roller milling system.

Table 3. Ash content in the total amount of flour and milling energy consumption following 6M in the conventional and eight-roller milling systems; values for a particular milling result differ significantly when followed by different letter

Roll gap, mm	Ash content, $(\%)_{dm}$			Milling energy consumption, kJ/kg		
	Conventional system	Eight-roller system		Conventional system	Eight-roller system	
	< 150 µm	< 150 µm	< 180 µm	< 150 µm	< 150 µm	< 180 µm
5M-0.08; 6M-0.05	1.15 abc	1.14 ab	1.18 bc	50.7 a	51.9 a	35.2 j
5M-0.08; 6M-0.04	1.16 abc	1.13 ab	1.11 a	58.1 b	59.0 bg	53.4 ak
5M-0.08; 6M-0.03	1.15 abc	1.14 ab	1.11 a	65.4 cd	73.8 h	57.3 kb
5M-0.05; 6M-0.04	1.16 abc	1.16 abc	1.12 a	67.6 d	76.2 h	62,6 gc
5M-0.05; 6M-0.03	1.15 abc	1.18 bc	1.18 bc	85.2 e	87.8 e	75.1 h
5M-0.04; 6M-0.03	1.15 abc	1.13 ab	1.15 abc	96.9 f	102.3 i	87.1 e
5M-0.08; 6M-0.05	1.15 abc	1.14 ab	1.18 bc	50.7 a	51.9 a	35.2 j

problem is present in the conventional process as well, but is even more likely to occur in the eight-roller milling system. The material from the upper rolls of the eight-roller mill almost immediately enters the grinding zone of the lower rolls without any cooling. The higher temperature of the rolls and therefore the increased temperature of the stock in the grinding zone of the lower rolls could change the nature of deformation (shift from brittle to ductile) and decrease the milling efficiency.

Previous considerations along with the inefficient sifting in the process with the eight-roller suggested that appropriate changes of the sieving conditions are necessary in order to increase flour release in the process with the eight-roller mill. Sifting efficiency depends on a number of different factors such as disposable sifter area, cloth tension, number of gyrations per min, feed rate to the sifter, flour flowability, etc. [33–35]. Increase of disposable sifter area in the process with the eight-roller mill in order to increase sifting efficiency is not a solution especially considering that a significant reduction of sifter surface is one of the main advantages of eight-roller milling system compared to a conventional system. Under industrial conditions, replacement of the sieves in the plansifter (changing the sieve aperture) is probably the easiest way to change the sieving conditions and therefore influence the sifting efficiency. However, the flour quality must not be affected by these changes. Replacing the 150 µm sieve with the sieve having 180 µm bolting cloth resulted in a significant increase in the flour yield (Fig. 2). It is evident that the increase in the flour yield, as a result of increasing the sieve aperture in the process with the eight-roller mill, is much noticeable at bigger roll gaps with flour release (<180 µm) significantly higher compared to flour release in conventional system (<150 µm). In the area of tight roll gaps flour release in the process with the eight-roller mill is similar to the flour release in conventional process. This confirms the previous statement that in the area of extremely tight roll gaps milling efficiency decreases. Changing the sieve size from 150 to 180 µm increases the upper size limit

of flour while the flour ash content was not affected (Table 3).

However, there is significant increase of the ash content of the size fraction 250/180 μm compared to the size fraction 250/150 μm (Table 2). This proves that the particles in the size range 180/150 μm are similar to those smaller than 150 μm. However, it also points out that on the end passages of the reduction system replacement of the sieves should be done carefully in order not to increase flour ash content.

Variostuhl laboratory roll stand has a relatively short roll length compared to roll stands used in commercial mills. This makes it easier to reproduce the certain feed rate to the rolls. Constant feed rate is very important considering the power readings and reliable energy consumption data. In both milling systems, as roll gap decreased milling energy consumption rose (Table 3). By decreasing the roll gap the flour yield increased. This contributes to the reduction of milling energy consumption because Eqs. (3) and (4) define energy consumption relative to the mass of flour obtained. On the other hand, decrease of the roll gap increases the power requirements in the operation with the material flow and as a result the milling energy consumption grows. Scanlon *et al.* [26] also reported that energy consumption is significantly related to roll gap setting.

At the same roll gap setting and under the same sieving conditions milling energy consumption in the eight-roller mill process is slightly higher compared to that in the conventional milling system (Table 3). It is mainly due to the lower flour yield in the eight-roller mill process. The heavier load to 6M rolls in the process with eight-roller mill (no intermediate sifting and flour removal) increases the power requirements and also contributes to higher energy consumption. Increasing the flour release, by increasing the sieve openings from 150 to 180 μm or decreasing the roll gap, it is possible to significantly reduce energy consumption in the process with the eight-roller mill (Table 3).

CONCLUSION

Introduction of the eight-roller mill into the wheat flour milling flow sheet significantly reduces production costs. These advantages can be fully exploited only if it is possible to achieve milling results close to those obtained in the conventional system. Under the same set of roll and sieving parameters, the eight-roller mill employed on the tail-end passages of the reduction system produces less flour compared to a conventional approach. By decreasing the roll gap setting and especially by increasing the upper size limit of flour it is possible to increase flour release in the process with the eight-roller mill. This way the actual energy consumption per unit mass of flour produced is decreasing. However, in the area of extremely tight roll gaps increase of the flour yield, brought about by the increase of the uper size limit of flour, is small. At the same time there is a significant increase in milling energy consumption as a result of increase in power requirements. Adjustments of the sieve aperture were not followed by increase of the flour ash content. The streams which are usually sent to the tail-end passages of the reduction system contain a large portion of the kernel outer layers and they can be designated as relatively low quality streams compared to the streams on other milling passages. This is the reason why these changes of the sieving conditions are limited in order to avoid deterioration of flour quality as determined by ash content.

Acknowledgment

The author highly appreciate financial support of the Ministry of Education, Science and Technological Development of the Republic of Serbia, project No. 031014.

REFERENCES

[1] C. Antoine, S. Peyron, V. Lullien-Pellerin, J. Abecassis, X. Rouau, Wheat bran tissue fractionation using biochemical markers, J. Cereal Sci. **39** (2004) 387–393.

[2] F. Mateos-Salvador, J. Sadhukhan, G.M. Campbell, The Normalised Kumaraswamy Breakage Function: A simple model for wheat roller milling, Powder Technol. **208** (2011) 144–157.

[3] G.M. Campbell, in: A.D. Salman, M. Ghadiri, M.J. Hounslow (Eds.), Roller Milling of Wheat: Handbook of Particle Breakage, Elsevier, Oxford, 2007, pp. 383–419.

[4] J.E. Dexter, P.J. Wood, Recent applications of debraning of wheat before milling, Trends Food Sci. Tech. **7** (1996) 35–41.

[5] E.S. Posner, A.N. Hibbs, Wheat Flour Milling, 2nd ed., AACC, St.Paul, MN, 2005.

[6] E.S. Posner, in: K. Kulp, J.G. Ponte (Eds.), Wheat: Handbook of Cereal Science and Technology, CRC Press, Taylor and Francis Group, New York, 2000, pp. 1–30.

[7] W. Baltensperger, State-of-the-Art Grain Milling Technology, Association of Operative Millers-Bulletin, 2001, pp. 7583–7591.

[8] W. Baltensperger, New Development in the Mill Flow Charts Grinding Process Using Eight-Roller Mills, Association of Operative Millers-Bulletin, 1993, pp. 6327––6332.

[9] H. Wanzenried, Benefits and results with 8-roller mill, model MDDL, Association of Operative Millers-Bulletin, 1991, pp. 5977–5981.

[10] Q. Lin, L. Liu, Y. Bi, Z. Li, Effects of different debranning degrees on the qualities of wheat flour and Chinese steamed bread, Food Bioprocess Tech. **5** (2012) 648––656.

[11] W.G. Owens, in: W.G. Owens (Ed.), Wheat, corn and coarse grains milling: Cereals Processing Technology, Woodhead Publishing Ltd., Cambridge, 2001, pp. 27–52.

[12] W. Baltensperger, Particle Size of Semolinas for Pasta Production, Association of Operative Millers-Bulletin, 1997, pp. 6879–6884.

[13] W. Eugster, Advances in Process Technology, Association of Operative Millers-Bulletin, 2001, pp. 7706–7707.

[14] V.C. Tegeler, Eight-High Roller Mills *vs*. Four-High Roller Mills The Pros and Cons, Association of Operative Millers-Bulletin, 1999, pp. 7229–7230.

[15] R. Flamer, Developments in Flour Milling, Milling J. (2008) 14–16.

[16] H. Zwingelberg, Verschiedene Walzenstuhlbeschüttungen und deren Auswirkungen auf Produktanfall und Mineralstoffgehalt Teil 2: Versuche an nicht geputztem Grieß als Einzel- und Doppelvermahlung, Mühle Mischfuttertech. **20** (1998) 649–654.

[17] H. Zwingelberg, B. Arzt, Verschiedene Walzenstuhlbeschüttungen und deren Auswirkungen auf Produktanfall und Mineralstoffgehalt Teil 1: Versuche beim I. Schrot und als Doppelvermahlung beim I. Und II. Schrot, Mühle Mischfuttertech. **18** (1998) 593–595.

[18] B. Handreck, L. Pötschke, C. Senge, Intensives Aufschroten von Weizen im Achtwalzenstuhl, Mühle Mischfuttertech. **26** (1999) 818–826.

[19] C. Willm, Studium eines französischen Weizenmühlen-Diagrammes, Mühle Mischfuttertech. **14** (2003) 417–425.

[20] D.A. Zhygunov, A comparative study of various structures of grinding process on the head break system, in Proceedings of 6th Central European Congress on Food, Novi Sad, Serbia, 2012, pp. 607–611.

[21] A. Fistes, G. Tanović, J. Mastilović, Using the eight-roller mill on the front passages of the reduction system, J. Food Eng. **85** (2008) 296–302.

[22] Determination of Moisture Content of Cereals and Cereal Products (Practical Method), ICC Standard Method No.110/1, International Association for Cereal Science and Technology, Vienna, 1976.

[23] Determination of Ash in Cereals and Cereal Products, ICC Standard Method No. 104/1, International Association for Cereal Science and Technology, Vienna, 1990.

[24] E. Haque, Application of Size Reduction Theory to Roller Mill Design and Operation, Cereal Foods World **36** (1991) 368–374.

[25] F.H. Hsieh, D.G. Martin, H.C. Black, K.H. Tipples, Some factors affecting the first break grinding of Canadian wheat, Cereal Chem. **57** (1980) 217–223.

[26] M.G. Scanlon, J.E. Dexter, C.G. Biliaderis, Particle-Size Related Physical Properties of Flour Produced by Smooth Roll Reduction of Hard Red Spring Wheat Farina, Cereal Chem. **65** (1988) 486–492.

[27] Y.Z. Li, E.S. Posner, The Influence of kernel size on wheat millability, Association of Operative Millers-Bulletin, 1987, pp. 5089–5098.

[28] C. Fang, G.M. Campbell, Stress-strain analysis and visual observation of wheat kernel breakage during roller milling using fluted rolls, Cereal Chem. **79** (2002) 511–517.

[29] G.M. Campbell, C. Webb, On predicting roller milling performance Part I: The breakage equation, Powder Technol. **115** (2001) 234–242.

[30] G.M. Campbell, P.J. Bunn, C. Webb, S.C.W. Hook, On predicting roller milling performance Part II: The breakage function, Powder Technol. **115** (2001) 243–255.

[31] J.J.C. Hinton, The distribution of the ash in wheat kernel, Cereal Chem. **36** (1959) 19–31.

[32] M.M. Pojić, N.B. Spasojević, M.Đ. Atlas, Chemometric approach to characterization of flour mill streams: chemical and rheological properties, Food Bioprocess Tech. **7** (2014) 1298–1309.

[33] S. Curran, W. Eustace, J. Gwirtz, The effect of cloth tension on sifting performance, Association of Operative Millers-Bulletin, 1994, 6379–6381.

[34] J. Wingfield, A. Ferrer, Multiple sieve sifter performance using various combinations of feed rates, circles and speeds, J. Food Process Eng. **7** (1984) 91–110.

[35] D.V. Neel, R.C. Hoseney, Sieving characteristics of soft and hard wheat flours, Cereal Chem. **61** (1984) 259–261.

IZVOD

UPOREDNA ANALIZA POKAZATELJA EFEKTIVNOSTI USITNJAVANJA OSEVAKA NA POSLEDNJIM PROLAZIŠTIMA IZMELJAVANJA U KLASIČNOM I POSTUPKU SA PRIMENOM OSMOVALJNE STOLICE

Aleksandar Z. Fišteš

Katedra za inženjerstvo ugljenohidratne hrane, Tehnološki fakultet, Univerzitet u Novom Sadu, Srbija

(Naučni rad)

Uključivanjem osmovaljne stolice u tehnološki postupak mlevenja pšenice ostvaruju se, u poređenju sa klasičnim mlevnim postupkom, višestruke investicione, energetske i operativne uštede u potrebnom prostoru u objektu, pneumatskom transportu međuproizvoda mlevenja, potrebnoj sejnoj i filtracionoj površini, elementima gravitacionog trasporta, troškovima održavanja i dr. Sa druge strane, primenom osmovaljne stolice, pogoršavaju se uslovi za efikasnost i selektivnost usitnjavanja što potencijalno može imati negativne posledice na prinos, asortiman i kvalitet brašna i iskorišćenje zrna. Pomenuto ukazuje na potrebu optimizacije parametara usitnjavanja i prosejavanja mliva u postupku sa osmovaljnom stolicom. U radu je data uporedna analiza efekata usitnjavanja ostvarenih na poslednjim prolazištima mlevenja osevaka primenom klasičnog i postupka sa osmovaljnom stolicom. Pri istom vođenju valjaka i pri upotrebi istog sloga sita za prosejavanje mliva, u postupku sa osmovaljnom stolicom ostvaruje se manji prinos brašna nego u klasičnom postupku. Nižim vođenjem valjaka i korekcijom sloga sita u postupku sa osmovaljnom stolicom (povećanje veličine otvora sejnog tkiva na kome se brašno izdvaja kao propad) povećava se prinos brašna u pomenutom postupku usled čega se smanjuje specifični utrošak energije po jedinici mase brašna. Pri tome ne dolazi do promene sadržaja pepela u brašnu. Odgovarajućim vođenjem valjaka i prilagođavanjem veličine otvora sejnih tkiva u slogu sita mogu se u postupku sa osmovaljnom stolicom ostvariti efekti usitnjavanja bliski efektima u klasičnom postupku, a istovremeno se ostvaruju značajne investicione i energetske uštede što doprinosi racionalizaciji proizvodnje.

Ključne reči: Mlevenje pšenice • Klasičan postupak • Osmovaljna stolica • Mlevenje osevaka

Synthesis, characterization and pharmacological evaluation of substituted phenoxy acetamide derivatives

Priyanka Rani[1], Dilip Kumar Pal[2], Rahul Rama Hegde[3], Syed Riaz Hashim[4]

[1]*Department of Chemistry, School of Sciences, IFTM University Moradabad, Uttar Pradesh, India*
[2]*Department of Chemistry, Institute of Pharmaceutical Sciences, Guru Ghasidas Viswavidyalaya, Bilaspur, Chhattisgarh, India*
[3]*Department of Pharmaceutics, School of Pharmaceutical Sciences, IFTM University Moradabad, Uttar Pradesh, India*
[4] *Department of Chemistry, School of Pharmaceutical Sciences, IFTM University Moradabad, Uttar Pradesh, India*

Abstract

A novel series of 2-(substituted phenoxy)-*N*-(1,7,7-trimethylbicyclo[2.2.1]heptan-2-yl)acetamide and *N*-(2-bromocyclohexyl)-2-(substituted phenoxy)acetamide derivatives having cyclohexyl nucleus as common in both types were synthesized and assessed for their anti-inflammatory activity by a carrageenan induced rat paw oedema method, analgesic activity by Eddy's hot plate method and antipyretic activity by brewer's yeast induced pyrexia method. All the novel derivatives have been synthesized by the reaction of camphor and similar ketone having cyclohexane nucleus (*e.g.*, 2-bromocyclohexanone) with ammonium carbonate and formic acid resulting in the formation of aromatic amines **1a** and **1b**. These amines on further chloroacetylation with chloroacetylchloride give compounds **2a** and **2b**. Compounds **2a** and **2b** are converted to 2-(substituted phenoxy)-*N*-(1,7,7-trimethylbicyclo[2.2.1]heptan-2-yl) acetamide and *N*-(2-bromocyclohexyl)-2-(substituted phenoxy)-acetamide derivatives on treatment with substituted phenol. Among the series **3a**–**f**, **3i**, **3k** and **3l** compounds showed significant anti-inflammatory activity as compared to the standard drug diclofenac sodium and also compounds **3a**–**f**, **3h**, **3j** and **3k** exhibit significant analgesic activity as compared to the standard drug. Compounds **3a**–**f** and **3k** showed antipyretic activity nearly to the standard drug indomethacin. Compounds **3a**–**f** and **3k** possess anti-inflammatory, analgesic and antipyretic activities near to the standard.

Keywords: 2-(substituted phenoxy)-*N*-(1,7,7-trimethylbicyclo[2.2.1]heptan-2-yl)acetamide, *N*-(2-bromocyclohexyl)-2-(substituted phenoxy)acetamide, anti-inflammatory activity, analgesic activity, antipyretic activity.

Available online at the Journal website: http://www.ache.org.rs/HI/

SCIENTIFIC PAPER

UDC 547.057:615

Hem. Ind. **69** (4) 405–415 (2015)

doi: 10.2298/HEMIND140330057R

Inflammation is a complicated process, but it may be explained as a complex reaction in the form of body's response of local tissues to inactivate injurious agents, such as microbes and to remove dead cells and tissues and to initiate the process of healing [1]. This complex reaction consists of series of events such as vascular responses, migration and activation of leucocytes, and systemic reactions. Body's first inflammatory response is the change in blood circulation. During this event, smooth muscle cells regulate the flow of blood into the capillaries and relaxation of smooth muscle cells allows blood to rush into the capillaries. This results in the redness and heat. Increased pressure is transmitted from capillaries to venules. This results in the plasma filtration through the vessel wall and finally oedema formation [2]. Body's second response is adhesion of leucocytes to the surface of venules by the surface adhesion molecules. During inflammation these are activated by mediators of inflammation. Body's third response is the change in vessel wall permeability. There are various mediators of inflammation such as chemical mediators, biogenic amines, peptides and arachidonic acid derivatives [3,4]. Out of these arachidonic acid derivatives play an important role as mediators of inflammation. There are four main symptoms of inflammation namely redness, swelling, heat and pain. These symptoms can be essentially targeted to examine analgesic and antipyretic activities of the synthesized compounds. Arachidonic acid is synthesized from cell membrane phospholipids by the action of phospholipases [5]. Further prostaglandin and 5-HPETE (hydroperoxy-eicosatetraenoic acids) are synthesized by the action of cyclooxygenase and 5-lipoxygenase respectively on the arachidonic acid. There are five types of PGs synthesized from arachidonic acid. These PGs are PGD_2, PGE_2, PGI_2 (prostacyclin), TXA_2 (thromboxane A_2) and $PGF_{2\alpha}$. These PGs are involved in skin inflammation where PGs activate the inflammatory action of platelet activating factor (PAF). PGS are effected plysiologically by G-protein-coupled prostanoid receptors (GPCRs). These

Correspondence: P. Rani, Department of Chemistry, School of Sciences, IFTM University Moradabad, Uttar Pradesh, India.
E-mail: skiftm@gmail.com
Paper received: 30 March, 2014
Paper accepted: 23 June, 2014

GPCRs comprise of nine members (DP, EP1-4, FP, IP, TP and CRTH-2). TP is thromboxane A_2 (TXA_2) receptor. TXA_2 act as mediator to change in the shape of platelet and aggregation of platelet. DP and CRTH-2 are PGD_2 receptors. PGD_2 act as a mediator for smooth muscle contraction and relaxation. EP1-4 are PGE_2 receptors. PGE_2 plays a protective role for gastrointestinal mucosa. IP is PGI_2 receptor. PGI_2 increases the microvascular permeability. FP is $PGF_{2\alpha}$ receptor. $PGF_{2\alpha}$ facilitates the inflammatory pain and transmission of pain. Hence for non-steroidal anti-inflammatory drugs (NSAIDs), the most important mechanism of action is forbiddance of the synthesis of prostaglandin and 5-HPETE [6,7]. NSAIDs are the most widely prescribed worldwide. These are used in various inflammatory diseases including rheumatoid and osteoarthritis. However, their therapeutic use is often limited by common side effects, such as gastrointestinal bleeding and ulceration [8]. In addition, there is evidence to suggest that leukotriene promotes gastric ulceration, which limits the therapeutic utilization of these drugs [9]. In spite of many NSAIDs, there is still need to develop new drugs that have potent anti-inflammatory effect with minimum side effects [10,11].

Compounds with a 2-phenoxy-*N*-phenylacetamide core structure have attracted considerable research interest as these entities established a long range of pharmacological activities such as anti-inflammatory [12], antibacterial [13], antiparasitic [14], anticancer [15], antiviral [1] and antihypoglycemic [16] effects. This enhances the chemotherapeutic utilization [17]. Recently, in a program of high throughput screening for biological evaluation, the hit compound methyl 2-(4-(2-(2,4-dimethylphenoxy)acetamido)phenoxy) acetate (**I**, Figure 1) [18] was reported to possess potent anti-tuberculosis activity, which indicates that 2-phenoxy-*N*-phenylacetamide (**II**, Figure 1) may be a promising scaffold for develop novel anti-inflammatory agents. The synthetic ease of the 2-phenoxy-*N*-phenylacetamide scaffold provides a strong motivation for the development of effective and affordable anti-inflammatory agents. To date there have been no reports describing the synthesis and anti-inflammatory assessment of its derivatives. In the vision of above facts, a novel class of titled compounds has been synthesized. In extension of our research plan on synthesis and pharmacological importance of various phenoxy acetamide derivatives, now we are reporting the synthesis, anti-inflammatory, analgesic and antipyretic activity of titled derivatives. Compounds which showed significant activities in acute anti-inflammatory, analgesic and antipyretic model were mentioned in the result and discussion part. The structural assignments of the new compounds were based on their spectral (IR, ^{1}H-NMR, ^{13}C-NMR and mass) data. The characterization data of all the new compounds have been given in the experimental part.

EXPERIMENTAL

General considerations. All research chemicals were purchased from CDH (Central Drug House P. Ltd., New Delhi, India) and used as such for the reactions. Solvents without laboratory reagent mark were dehydrated and purified according to the literature whenever necessary. Purification of the compounds was carried out by the recrystallization with appropriate solvent in case of solids but by distillation in case of liquids. Purity of the compounds and completion of reactions were monitored by thin layer chromatography (TLC) on silica gel plates and spots were visualized by exposure to iodine vapor.

Melting points were determined in open capillaries on Thomas Hoover apparatus and are uncorrected. IR spectra were recorded on a Shimadzu IR-435 spectrophotometer using KBr pellets, ^{1}H-NMR and ^{13}C-NMR spectra were recorded on a Bruker Avance II 400 NMR spectrometer (Bruker Corporation, Billerica, MA, USA) instrument using tetramethylsilane (TMS) as an internal standard and DMSO-d_6 as a solvent. Mass spectra were

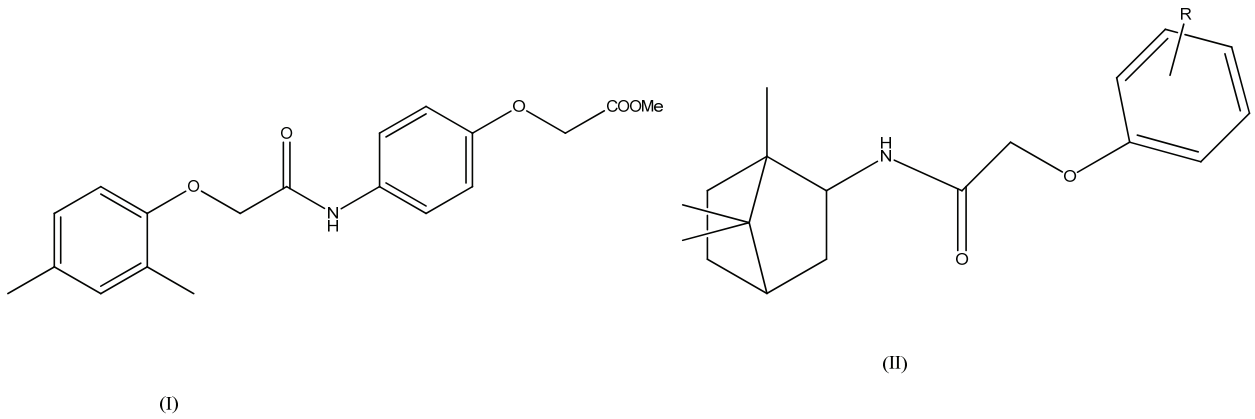

*Figure 1. The chemical structures of methyl 2-(4-(2-(2,4-dimethylphenoxy)acetamido) phenoxy)acetate (**I**) 2-(substituted phenoxy)-N-(1,7,7-trimethylbicyclo[2.2.1]heptan-2-yl)acetamide (**II**) derivatives.*

recorded on Micromass Q-Tof Micro (Waters Corporation Milford, MA, USA). Chemical shifts are given in ppm. The anti-inflammatory and analgesic screening is carried out at Pharmacology laboratory of School of Pharmaceutical Sciences, IFTM University, Moradabad. The anti-inflammatory activity was carried out using digital plethysmometer. All the animal experiments were approved by Institutional Animal Ethical Committee (IAEC). Elemental analysis was carried out using Elementar Vario EL III, elementar Analysensysteme GmbH, Hanau, Germany.

Synthesis of 2-bromocyclohexanone from cyclohexanone [19]. Cyclohexanone (5.3 ml, 0.05 mol) and water (30 ml) are placed in a three necked flask equipped with a stirrer and a dropping funnel. Bromine (2.58 ml, 0.05 mol) is added dropwise during 1 h at 5 °C to the mixture while stirring. After the addition is complete, the stirring is complete at room temperature until the reaction mixture becomes colorless (about 1 h). The reaction mixture is allowed to warm during this period. The upper layer of bromo-cyclohexanone is separated by ether extraction (3×20 ml). The ether extract is washed with water, saturated sodium chloride solution and dried (anhydrous sodium sulphate). Then, the ether is distilled. 2-Bromocyclohexanone is collected by distillation in vacuum.

*General method for the synthesis of 1,7,7-trimethylbicyclo[2.2.1]heptan-2-amine (**1a**) and 2-bromocyclohexylamine (**1b**) starting from camphor and 2-bromocyclohexanone*. This procedure of Leuckart reaction [19] was followed for the preparation of amines from ketones. Ammonium carbonate (215 g, 4 mol) was placed in a 1-l three necked round bottom flask, fitted with a thermometer, a dropping funnel and a bent tube attached for distillation to a short condenser. Formic acid (98%, 109 ml) was taken in the dropping funnel and added drop wise. When the reaction subsided, the mixture was heated slowly until the temperature increased to about 165 °C. The ketone (1 mol) was added in one lot and the temperature was slowly raised to 180–185 °C. Water, ammonia, carbon dioxide and some of the ketone distilled over. The distilled ketone was separated and returned to the reaction mixture. The mixture which gradually became homogenous was maintained at 180–18 °C (for 2-bromocyclohexanone) and at 160–165 °C (for camphor) for 4–5 h. Deposited camphor in the condenser was scratched with glass rod at 15 min interval and returned to the reaction mixture. When the reaction was complete, the mixture was cooled and stirred thoroughly with twice its volume of water. The aqueous layer was separated and the formyl derivative of the amine so obtained was refluxed with 100–150 ml of concentrated hydrochloric acid for 2–3 h. After the hydrolysis, the reaction mixture was cooled and extracted with ether to remove any unreacted ketone. The aqueous solution was made strongly alkaline with 30% sodium hydroxide solution and the separated amine was extracted with ether. The ethereal extract was dried over anhydrous sodium sulphate and after removal of the solvent, the product distilled under reduced pressure.

Amines 1,7,7-trimethylbicycloheptan-2-amine (**1a**) and 2-bromocyclohexylamine (**1b**) are synthesized by the above reaction from camphor and 2-bromocyclohexanone respectively.

*General method for the synthesis of 2-chloro-N--1,7,7-trimethylbicyclo[2.2.1]heptan-2-yl)acetamide (**2a**) and N-(2-bromocyclohexyl)-2-chloroacetamide (**2b**) from **1a** and **1b**, respectively*. To an ice-cooled aqueous solution of sodium hydroxide (50 ml, 10%) taken in two different well-corked conical flask, 0.1 mol of synthesized compounds **1a** and **1b** was added in both the flasks followed by addition of chloroacetyl chloride (11.93 ml, 0.15 mol) with constant stirring and shaking. The reaction was vigorously shaken until odour of chloroacetylchloride disappeared. The pH of reaction mixture was kept around 9–10 by the addition of sodium hydroxide solution. The solid amides **2a** and **2b** that formed was collected by filtration and washed thoroughly with water, dried and recrystallized from ethanol.

*2-Chloro-N-1,7,7-trimethylbicyclo[2.2.1]heptan-2--yl)acetamide (**2a**).* Yield 78%; M.p.: 102–104 °C. IR (KBr) cm^{-1}: 3275, 3050, 2875, 1680.

*N-(2-bromocyclohexyl)-2-chloroacetamide (**2b**)*. Yield 69%; M.p.: 91–93 °C. IR (KBr) cm^{-1}: 3215, 2910, 1735.

*General method for the synthesis of 2-(substituted phenoxy)-N-1,7,7-trimethylbicyclo[2.2.1]heptan-2-yl)-acetamides (**3a**–**3f**) and N-(2-bromocyclohexyl)-2-(substituted phenoxy)acetamides (**3g**–**3l**) from **2a** and **2b**, resrespectively*. Phenoxy acetamide derivatives were prepared by reacting **2a** and **2b** (0.01 mol) with different substituted phenols (0.01 mol) in presence of anhydrous potassium carbonate (0.01 mol) and catalytic amount of potassium iodide in refluxing dry acetone. In some cases unreacted phenol was removed from the final product by treating the substance with 10%, *w*/*V*, sodium carbonate solution in water. The compound was then filtered and washed thoroughly with water and recrystallised from appropriate solvent. The completion of the reaction was monitored by TLC.

*2-Phenoxy-N-(1,7,7-trimethylbicyclo[2.2.1]heptan-2--yl)acetamide (**3a**)*. Colourless crystals, $C_{18}H_{25}NO_2$, yield 58.6%. M.p.: 178–180 °C. IR (KBr) cm^{-1} : 3210, 3150, 3010, 2930, 1775, 1640, 1315, 1270. ^{1}H-NMR (400 MHz, DMSO-d_6, δ / ppm): 8.90 (*s*, 1H, NH), 7.41 (*t*, *J* = = 7.4 Hz, 2H, H-3'', H-5''), 7.30–6.90 (*m*, 3H, H-2'', H-4'', H-6''), 4.28 (*s*, 2H, CH_2-2), 3.50 (*t*, *J* = 7.2 Hz, 1H, CH-2'), 2.82–2.55(*m*, 2H, CH_2-3'), 2.48–2.30 (*m*, 5H,

CH-4′, CH_2-5′, CH_2-6′), 1.56 (*s*, 3H, CH_3-1′), 1.11 (*s*, 6H, $(CH_3)_2$-7′). ^{13}C-NMR (DMSO-d_6, δ / ppm): 167.1 (C=O, NHCO), 157.9 (C, C-1′′), 128.1 (C, C-3′′,C-5′′), 122.1 (C, C-4′′), 115.8 (C, C-2′′,C-6′′), 68.1 (CH_2), 58.1 (CH, C-2′), 49.4 (C, C-1′), 48.1 (C, C-7′), 44.5 (CH, C-4′), 37.1 (CH_2, C-3′), 33.4 (CH_2, C-6′), 26.1 (CH_2, C-5′), 19.1 (2XCH_3, $(CH_3)_2$-C7′), 13.8 (CH_3, CH_3-C1′). mass: m/z 287 (M^+), 288 (M +1, 20.1%), 289 (M +2 , 1.5%). Anal. Calc. for $C_{18}H_{25}NO_2$: C 75.22, H 8.77, N 4.87, O 11.13. Found: C 75.15, H 8.62, N 4.80, O 10.95.

*2-(4-Bromophenoxy)-N-(1,7,7-trimethylbicyclo[2.2.1]-heptan-2-yl)acetamide (**3b**)*. Colourless amorphous powder, $C_{18}H_{24}BrNO_2$, yield: 61.0%. M.p.: 110–112 °C. IR (KBr) cm^{-1}: 3305, 3120, 3000, 2875, 1690, 1600, 1345, 1050. ^{1}H-NMR (400 MHz, DMSO-d_6, δ / ppm): 9.10 (*s*, 1H, NH), 7.32 (*d*, *J* = 1.5 Hz, 2H, H-3′′, H-5′′), 6.86 (*d*, *J* = 1.5 Hz, 2H, H-2′′, H-6′′), 4.31 (*s*, 2H, CH_2-2), 3.15 (*t*, *J* = 7.2 Hz, 1H, CH-2′), 2.75–2.47 (*m*, 2H, CH_2-3′), 2.30–2.15 (*m*, 5H, CH-4′, CH_2-5′, CH_2-6′), 1.61 (*s*, 3H, CH_3-1′), 1.12 (*s*, 6H, $(CH_3)_2$-7′). ^{13}C-NMR (DMSO-d_6, δ / ppm): 168.4 (C=O, NHCO), 156.2 (C, C-1′′), 131.2 (C, C-3′′,C-5′′), 116.9 (C, C-2′′,C-6′′), 114.4 (C, C-4′′), 67.8 (CH_2), 59.2 (CH, C-2′), 48.6 (C, C-1′), 47.3 (C, C-7′), 44.8 (CH, C-4′), 36.4 (CH_2, C-3′), 33.9(CH_2, C-6′), 25.8 (CH_2, C-5′), 19.7 (2×CH_3, $(CH_3)_2$-C7′), 12.2 (CH_3, CH_3-C1′). MS: *m/z* 365 (M^+), 367 (M+2, 97.6%), 366 (M+1, 19.8%). Anal. Calcd. for $C_{18}H_{24}BrNO_2$: C 59.02, H 6.60, Br 21.81, N 3.82, O 8.74. Found: C 58.94, H 6.51, Br 21.89, N 3.91, O 8.68.

*2-(4-Nitrophenoxy)-N-(1,7,7-trimethylbicyclo[2.2.1]-heptan-2-yl)acetamide (**3c**)*. Very light yellow amorphous powder, $C_{18}H_{24}N_2O_4$, yield: 57.8%. M.p.: 165–167 °C. IR (KBr) cm^{-1}: 3265, 3200, 3075, 2805, 1715, 1575, 1535, 1220, 1095. ^{1}H-NMR (400 MHz, DMSO-d_6, δ / ppm): 8.55 (*d*, *J* = 1.5 Hz, 2H, H-3′′, H-5′′), 8.42 (*s*, 1H, NH), 7.34 (*d*, *J* = 1.5 Hz, 2H, H-2′′, H-6′′), 4.20 (*s*, 2H, CH_2-2), 3.26 (*t*, *J* = 7.2 Hz, 1H, CH-2′), 2.80–2.49 (*m*, 2H, CH_2-3′), 2.41–2.23 (*m*, 5H, CH-4′, CH_2-5′, CH_2-6′), 1.54 (*s*, 3H, CH_3-1′), 1.22 (*s*, 6H, $(CH_3)_2$-7′). ^{13}C-NMR (DMSO-d_6, δ / ppm): 168.9 (C=O, NHCO), 163.3 (C, C-1′′), 138.1 (C, C-4′′), 125.1 (C, C-3′′,C-5′′), 113.6 (C, C-2′′,C-6′′), 67.1 (CH_2, C-2), 56.8 (CH, C-2′), 48.4 (C, C-1′), 47.8 (C, C-7′), 43.1 (CH, C-4′), 37.9 (CH_2, C-3′), 31.1 (CH_2, C-6′), 26.1 (CH_2, C-5′), 18.9 (2XCH_3, $(CH_3)_2$-C7′), 12.8 (CH_3, CH_3-C1′). MS: *m/z* 332 (M^+), 333 (M+1, 19.6%), 334 (M+2, 2.4%). Anal. Calcd. for $C_{18}H_{24}N_2O_4$: C 65.04, H 7.28, N 8.43, O 19.25. Found: C 65.11, H 7.15, N 8.56, O 19.31.

*2-(4-(tert-Butyl)phenoxy)-N-(1,7,7-trimethylbicyclo-[2.2.1]heptan-2-yl)acetamide (**3d**)*. White crystals, $C_{22}H_{33}NO_2$, yield: 70.0%. M.p.: 105–107 °C. IR (KBr) cm^{-1}: 3280, 3195, 2990, 2800, 1735, 1505, 1293, 1155. ^{1}H-NMR (400 MHz, DMSO-d_6, δ / ppm): 8.27 (*s*, 1H, NH), 7.30 (*d*, *J* = 1.5 Hz, 2H, H-3′′, H-5′′), 6.81 (*d*, *J* = 1.5 Hz, 2H, H-2′′, H-6′′), 4.13 (*s*, 2H, CH_2-2), 3.41 (*t*, *J* = 7.2 Hz, 1H, CH-2′), 2.78–2.34 (*m*, 2H, CH_2-3′), 2-14–1.42 (*m*, 2H, CH_2-5′), 1.31 (*s*, 9H, $(CH_3)_3$), 1.29–1.25 (*m*, 3H, CH-4′, CH_2-6′), 1.21 (*s*, 3H, CH_3-1′), 1.18 (*s*, 6H, $(CH_3)_2$-7′). ^{13}C-NMR (DMSO-d_6, δ / ppm): 167.1 (C=O, NHCO), 162.8 (C, C-1′′), 137.9 (C, C-4′′), 124.7 (C, C-3′′,C-5′′), 112.4 (C, C-2′′,C-6′′), 67.9 (CH_2), 55.6 (CH, C-2′), 48.1 (C, C-1′), 46.9 (C, C-7′), 44.2 (CH, C-4′), 38.4 (CH_2, C-3′), 34.9 (C, C–$(CH_3)_3$), 31.9 (CH_2, C-6′), 29.1 (3×CH_3, $(CH_3)_3$–C–C4′′)), 26.7 (CH_2, C-5′), 19.1 (2×CH_3, $(CH_3)_2$-C7′), 12.1 (CH_3, CH_3-C1′). MS: *m/z* 343 (M^+), 344 (M+1, 24.2%), 345 (M+2, 3.1%). Anal. Calcd. for $C_{22}H_{33}NO_2$: C 76.92, H 9.68, N 4.08, O 9.32. Found: C 76.81, H 9.75, N 4.19, O 9.22.

*2-(4-Methoxyphenoxy)-N-(1,7,7-trimethylbicyclo-[2.2.1]heptan-2-yl)acetamide (**3e**)*. White amorphous powder, $C_{19}H_{27}NO_3$, yield: 67.4%. M.p.: 170–172 °C. IR (KBr) cm^{-1}: 3275, 3125, 2975, 2915, 2795, 1655, 1560, 1200, 1125. ^{1}H-NMR (400 MHz, DMSO-d_6, δ / ppm): 9.13 (*s*, 1H, NH), 7.41 (*s*, 4H, H-2′′, H-3′′, H-5′′, H-6′′), 4.46 (*s*, 2H, CH_2-2), 3.81(*s*, 3H, OCH_3), 3.35 (*t*, *J* = 7.2 Hz, 1H, CH-2′), 2.71–2.45 (*m*, 2H, CH_2-3′), 2.35–2.12 (*m*, 5H, CH-4′, CH_2-5′, CH_2-6′), 1.34 (*s*, 3H, CH_3-1′), 1.24 (*s*, 6H, $(CH_3)_2$-7′). ^{13}C-NMR (DMSO-d_6, δ / ppm): 166.8 (C=O, NHCO), 150.2 (C, C-4′′), 149.3 (C, C-1′′), 127.2 (C, C-3′′,C-5′′), 112.8 (C, C-2′′, C-6′′), 68.4 (CH_2), 56.1 (CH, C-2′), 54.1 (CH_3, O–CH_3), 48.9 (C, C-1′), 48.4 (C, C-7′), 43.9 (CH, C-4′), 36.2 (CH_2, C-3′), 31.8 (CH_2, C-6′), 27.8 (CH_2, C-5′), 18.6 (2×CH_3, $(CH_3)_2$-C7′), 13.9 (CH_3, CH_3-C1′). MS: *m/z* 317 (M^+), 318 (M+1, 21.1%), 319 (M+2, 2.3%). Anal. Calcd. for $C_{19}H_{27}NO_3$: C 71.89, H 8.57, N 4.41, O 15.12. Found: C 71.96, H 8.64, N 4.58, O 15.27.

*2-(2-nitrophenoxy)-N-(1,7,7-trimethylbicyclo[2.2.1]-heptan-2-yl)acetamide (**3f**)*. Pale yellow crystals, $C_{18}H_{24}N_2O_4$, yield: 62.0%. M.p.: 210–212 °C. IR (KBr) cm^{-1}: 3205, 2990, 3010, 2895, 1785, 1570, 1490, 1275, 1215. ^{1}H-NMR (400 MHz, DMSO-d_6, δ / ppm): 8.75 (*d*, 1H, H-3′′), 8.30 (*s*, 1H, NH), 7.37 (*t*, *J* = 7.2 Hz, 1H, H-5′′), 7.21 (*t*, *J* = 7.4 Hz, 1H, H-2′′), 6.87 (*d*, *J* = 1.5 Hz, 1H, H-6′′), 4.45 (*s*, 2H, CH_2-2), 3.42 (*t*, *J* = 7.4 Hz, 1H, CH-2′), 2.55–2.31 (*m*, 2H, CH_2-3′), 2.22–2.16 (*m*, 5H, CH-4′, CH_2-5′, CH_2-6′), 1.24 (*s*, 3H, CH_3-1′), 1.10 (*s*, 6H, $(CH_3)_2$-7′). ^{13}C-NMR (DMSO-d_6, δ / ppm): 167.1 (C=O, NHCO), 162.8 (C, C-1′′), 139.8 (C, C-2′′), 130.1 (C, C-5′′), 126.5 (C, C-3′′), 122.2 (C, C-4′′), 115.9 (C, C-6′′), 67.8 (CH_2), 57.9 (CH, C-2′), 48.8 (C, C-1′), 46.4 (C, C-7′), 43.7 (CH, C-4′), 36.8 (CH_2, C-3′), 32.6 (CH_2, C-6′), 26.9 (CH_2, C-5′), 16.8 (2×CH_3, $(CH_3)_2$-C7′), 13.1 (CH_3, CH_3-C1′). MS: *m/z* 332 (M^+), 333 (M+1, 19.9%), 334 (M+2, 2.5%). Anal. Calcd. for $C_{18}H_{24}N_2O_4$: C 65.04, H 7.28, N 8.43, O 19.25. Found: C 65.19, H 7.17, N 8.36, O 19.37.

*N-(2-Bromocyclohexyl)-2-phenoxyacetamide (**3g**)*. White crystals, $C_{14}H_{18}BrNO_2$, yield: 57.0%. M.p.: 189–191 °C. IR (KBr) cm^{-1}: 3285, 3050, 2930, 2075, 1660, 1600, 1250, 1050. ^{1}H-NMR (400 MHz, DMSO-d_6, δ / ppm): 8.13 (*s*, 1H, NH), 7.41 (*t*, *J* = 7.2 Hz, 2H, H-3′′,

H-5''), 7.30–7.05 (*m*, 3H, H-2'', H-4'', H-6''), 5.14 (*s*, 2H, CH_2-2), 4.12–3.23 (*m*, 2H, CH-1', CH-2'), 2.83–2.67 (*m*, 2H, CH_2-3'), 2.55–2.45 (*m*, 2H, CH_2-6'), 2.39–2.12 (*m*, 2H, CH_2-4'), 1.93–1.52 (*m*, 2H, CH_2-5'). ^{13}C-NMR (DMSO-d_6, δ ppm): 167.4 (C=O, NHCO), 157.6 (C, C-1''), 127.4 (C, C-3'',C-5''), 120.1 (C, C-4''), 110.5 (C, C-2'',C-6''), 69.4 (CH_2), 60.7 (CH, C-2'), 58.4 (CH, C-1'), 34.8 (CH_2, C-3'), 31.3 (CH_2, C-6'), 23.1 (CH_2, C-4'), 21.5 (CH_2, C-5'). MS: *m/z* 311 (M^+), 313 (M+2, 97.3%), 312 (M+1, 15.3%). Anal. Calcd. for $C_{14}H_{18}BrNO_2$: C 53.86, H 5.81, Br 25.59, N 4.49, O 10.25. Found: C 53.98, H 5.72, Br 25.68, N 4.61, O 10.39.

*N-(2-bromocyclohexyl)-2-(4-bromophenoxy)acetamide (**3h**)*. Pale yellow amorphous powder, $C_{14}H_{17}Br_2NO_2$, yield: 66.2%. M.p.: 205–207 °C. IR (KBr) cm^{-1}: 3290, 3055, 2925, 2875, 1655, 1550, 1250, 1055. ^{1}H-NMR (400 MHz, DMSO-d_6, δ / ppm): 8.20 (*s*, 1H, NH), 7.46 (*d*, *J* = 2.0 Hz, 2H, H-3'', H-5''), 7.07 (*d*, *J* = 2.0 Hz, 2H, H-2'', H-6''), 5.35 (*s*, 2H, CH_2-2), 4.05–3.14 (*m*, 2H, CH-1', CH-2'), 2.15–2.11 (*m*, 2H, CH_2-3'), 2.07–1.98 (*m*, 2H, CH_2-6'), 1.87–1.76 (*m*, 2H, CH_2-4'), 1.71–1.68 (*m*, 2H, CH_2-5'). ^{13}C-NMR (DMSO-d_6, δ / ppm): 169.1 (C=O, NHCO), 156.9 (C, C-1''), 126.3 (C, C-3'',C-5''), 119.4 (C, C-4''), 110.8 (C, C-2'',C-6''), 71.4 (CH_2), 61.4 (CH, C-2'), 59.6 (CH, C-1'), 37.3 (CH_2, C-3'), 32.4 (CH_2, C-6'), 24.8 (CH_2, C-4'), 21.9 (CH_2, C-5'). MS: *m/z* 390 (M^+), 388 (M–2, 51.2%), 392 (M+2 , 49.0%). Anal. Calcd. for $C_{14}H_{17}Br_2NO_2$: C 42.99, H 4.38, Br 40.86, N 3.58, O 8.18. Found: C 42.81, H 4.24, Br 40.71, N 3.70, O 8.35.

*N-(2-bromocyclohexyl)-2-(4-nitrophenoxy)acetamide (**3i**)*. Pale yellow crystals, $C_{14}H_{17}BrN_2O_4$, yield: 64.1%. M.p.: 155–157 °C. IR (KBr) cm^{-1}: 3325, 3060, 3025, 2900, 1670, 1580, 1525, 1250, 1075. ^{1}H-NMR (400 MHz, DMSO-d_6, δ / ppm): 8.34 (*d*, *J* = 2.0 Hz, 2H, H-3'', H-5''), 8.12 (*s*, 1H, NH), 7.18 (*d*, *J* = 2.0 Hz, 2H, H-2'', H-6''), 5.30 (*s*, 2H, CH_2-2), 4.28–3.14 (*m*, 2H, CH-1', CH-2'), 2.13-2.02 (*m*, 2H, CH_2-3'), 1.91–1.77 (*m*, 2H, CH_2-6'), 1.62–1.43 (*m*, 2H, CH_2-4'), 1.41–1.36 (*m*, 2H, CH_2-5'). ^{13}C-NMR (DMSO-d_6, δ / ppm): 164.3 (C=O, NHCO), 154.6 (C, C-1''), 135.4 (C, C-4''), 130.2 (C, C-3'',C-5''), 111.5 (C, C-2'',C-6''), 68.6 (CH_2), 61.6 (CH, C-2'), 57.8 (CH, C-1'), 33.9 (CH_2, C-3'), 31.8 (CH_2, C-6'), 22.8 (CH_2, C-4'), 20.7 (CH_2, C-5'). MS: *m/z* 356 (M^+), 358 (M+2, 99.2%), 357 (M+1, 15.5%). Anal. Calcd. for $C_{14}H_{17}BrN_2O_4$: C 47.07, H 4.80, Br 22.37, N 7.84, O 17.92. Found: C 47.18, H 4.67, Br 22.51, N 7.65, O 17.79.

*N-(2-bromocyclohexyl)-2-(4-(tert-butyl)phenoxy)-acetamide (**3j**).* Colourless crystals, $C_{18}H_{26}BrNO_2$, yield: 68.0%. M.p.: 195–197 °C. IR (KBr) cm^{-1}: 3360, 3025, 3000, 2955, 2925, 1600, 1575, 1260, 1080. ^{1}H-NMR (400 MHz, DMSO-d_6, δ / ppm): 8.45 (*s*, 1H, NH), 7.68 (*d*, *J* = 2.0 Hz, 2H, H-3'', H-5''), 7.44 (*d*, *J* = 2.0 Hz, 2H, H-2'', H-6''), 5.21 (*s*, 2H, CH_2-2), 4.05–3.15 (*m*, 2H, CH-1', CH-2'), 2.92–2.76 (*m*, 2H, CH_2-3'), 2.68–2.37 (*m*, 2H, CH_2-6'), 2.22–1.87 (*m*, 2H, CH_2-4'), 1.81 (*s*, 9H, $(CH_3)_3$), 1.54–1.31 (*m*, 2H, CH_2-5'). ^{13}C-NMR (DMSO-d_6, δ / ppm): 166.9 (C=O, NHCO), 151.4 (C, C-1''), 145.1 (C, C-4''), 126.4 (C, C-3'',C-5''), 115.4 (C, C-2'', C-6''), 68.1 (CH_2), 61.6 (CH, C-2'), 57.1 (CH, C-1'), 35.6 (CH_2, C-3'), 33.3 (C, C-$(CH_3)_3$), 30.6 (3×CH_3, $(CH_3)_3$-C-C4''), 29.8 (CH_2, C-6'), 24.8 (CH_2, C-4'), 20.1 (CH_2, C-5'). MS: *m/z* 367 (M^+), 369 (M+2, 97.2%), 368 (M+1, 19.6%). Anal. Calcd. for $C_{18}H_{26}BrNO_2$: C 58.70, H 7.12, Br 21.69, N 3.80, O 8.69. Found: C 58.57, H 7.29, Br 21.81, N 3.69, O 8.78.

*N-(2-bromocyclohexyl)-2-(4-methoxyphenoxy)acetamide (**3k**).* Pale yellow needles, $C_{15}H_{20}BrNO_3$, yield: 61.0%. M.p.: 220–222 °C. IR (KBr) cm^{-1}: 3200, 2920, 2900, 2810, 2055, 1655, 1550, 1300, 1050. ^{1}H-NMR (400 MHz, DMSO-d_6, δ / ppm): 8.56 (*s*, 1H, NH), 7.82 (*s*, 4H, H-2'', H-3'', H-5'', H-6''), 5.32 (*s*, 2H, CH_2-2), 4.12–3.23 (*m*, 2H, CH-1', CH-2'), 3.18 (*s*, 3H, OCH_3) 2.21–2.06 (*m*, 2H, CH_2-3'), 1.91–1.82 (*m*, 2H, CH_2-6'), 1.78–1.63 (*m*, 2H, CH_2-4'), 1.54-1.48 (*m*, 2H, CH_2-5'). ^{13}C NMR (DMSO-d_6, δ / ppm): 169.4 (C=O, NHCO), 154.3 (C, C-4''), 152.7 (C, C-1''), 110.8 (C, C-2'',C-3'',C-5'',C-6''), 66.1 (CH_2), 61.8 (CH, C-2'), 53.9 (CH_3, O–CH_3), 53.1 (CH, C-1'), 35.6 (CH_2, C-3'), 31.8 (CH_2, C-6'), 27.4 (CH_2, C-4'), 25.2 (CH_2, C-5'). MS: *m/z* 341 (M^+), 343 (M+2, 97.3%), 342 (M+1, 16.3%). Anal. Calcd. for $C_{15}H_{20}BrNO_3$: C 52.64, H 5.89, Br 23.35, N 4.09, O 14.03. Found: C 52.81, H 5.97, Br 23.51, N 3.94, O 14.15.

*N-(2-bromocyclohexyl)-2-(2-nitroyphenoxy)acetamide (**3l**)*. Pale yellow amorphous powder, $C_{14}H_{17}BrN_2O_4$, yield: 67.0%. Mp: 115–117 °C. IR (KBr) cm^{-1}: 3205, 3115, 3000, 2995, 1705, 1550, 1515, 1305, 1090. ^{1}H-NMR (400 MHz, DMSO-d_6, δ / ppm): 8.55 (*d*, *J* = 2.0 Hz, 1H, H-3''), 8.30 (*s*, 1H, NH), 7.41(*t*, *J* = 7.2 Hz, 1H, H-5''), 7.33 (*t*, *J* = 7.2 Hz, 1H, H-4''), 6.92 (*d*, *J* = 2.0 Hz, 1H, H-6''), 5.22 (*s*, 2H, CH_2-2), 4.06–3.10 (*m*, 2H, CH-1', CH-2'), 2.65–2.47 (*m*, 2H, CH_2-3'), 2.39–2.07 (*m*, 2H, CH_2-6'), 1.78–1.64 (*m*, 2H, CH_2-4'), 1.33–1.16 (*m*, 2H, CH_2-5'). ^{13}C-NMR (DMSO-d_6, δ / ppm): 165.3 (C=O, NHCO), 158.1 (C, C-1''), 145.1 (C, C-2''), 130.4 (C, C5''), 127.8 (C, C-3''), 122.7 (C, C-4''), 116.1 (C, C-6''), 68.7 (CH_2), 61.7 (CH, C-2'), 59.8 (CH, C-1'), 33.9 (CH_2, C-3'), 32.3 (CH_2, C-6'), 23.9 (CH_2, C-4'), 20.4 (CH_2, C-5'). MS: *m/z* 356 (M^+), 358 (M+2, 99.1%), 357 (M+1, 15.2%). Anal. Calcd. for $C_{14}H_{17}BrN_2O_4$: C 47.07, H 4.80, Br 22.37, N 7.84, O 17.92. Found: C 46.92, H 4.91, Br 22.46, N 7.59, O 17.79.

Pharmacological screening

Animals. Wistar albino rats of either sex weighing 140–180 g were obtained. The animals were divided into several groups of five each. All the animals were housed under standard ambient conditions of temperature (25±2 °C) and relative humidity of 50±5%. A 12:12 h light:dark cycle was maintained. All the animals were allowed to have free access to water and standard palletized laboratory animal diet 12 h prior to pharmaco-

logical studies. All the experimental procedures and protocols used in this study were reviewed and approved by the institutional Animal Ethical Committee (IAEC).

Preparation of test compounds. Test samples and the reference drugs were prepared as a suspension in 1% Tween 80. Group one (control) received 0.1 ml of tween 80 suspension orally. Group second (standard) was treated by suspension of diclofenac sodium with a dose of 50 mg/kg. Test groups were administered with a dose of 150 mg/kg of final synthesized compounds.

Acute toxicity. The acute toxicity study was carried out as per OECD guidelines [20] to found the successful dose of the test compounds after getting ethical clearance. Wistar albino rats of either sex weighing between 140–170 g were divided into several groups of 5 animals each. Animals were starved for 12 h with water ad libitum prior to test. On the day of the experiment, animals were treated with different compounds to different groups in an increasing order of 10, 20, 100, 200, 1000 and 1500 mg/kg body weight orally. The animals were then observed continuously for 3 h for common behavioral, neurological, autonomic profiles and then every 30 min for next 3 h and finally for next 24 h or till death.

From above toxicity test, it was observed that animals were found to be secure up to a highest dose of 1500 mg/kg body weight. But few changes were found in the behavioral reaction like touch response, alertness, and restlessness. As a result, 1/10th of the highest tolerated dose, *i.e.*, 150 mg/kg body weight (b.w.) was chosen for the studies.

Anti-inflammatory activity. Carrageenan induced rat paw edema method [21] was employed for screening of the anti-inflammatory activity of the synthesized compounds listed in Table 1. The animals were divided into fourteen groups of five each.

One hour after oral administration of the drug, acute inflammation was produced by preparing aqueous suspension of carrageenan (1%, *w*/*V*, 0.1 ml) which was injected in the right hind paw in the subplantar region of each rat.

A mark was applied on the leg at the malleolus to facilitate subsequent readings. The paw volume was measured plethysmometrically at 30 min, 2 and 4 h after the injection of carrageenan. The %Inhibition was calculated by applying Newbould formula [22]:

$$\%\text{Inhibition} = 100(1 - Vt/Vc)$$

where *Vt* and *Vc* are the mean change in paw volume of treated and control rats respectively.

Analgesic activity. The compounds exhibited an important analgesic profile measured by the Eddy's hot plate method [23,24]. Animals were individually placed on a hot plate maintained at a constant temperature (55 °C) and the reaction of animals, such as paw licking or jump response (whichever appears first) was taken as the end point. A cut-off time of 15 s was taken as

*Table 1. Characterization data of 2-(substituted phenoxy)-N-(1,7,7-trimethylbicyclo[2.2.1]heptan-2-yl)acetamide and N-(2-bromocyclohexyl)-2-(substituted phenoxy)acetamide derivatives. *Recrystallization with ethanol. # Stationary phase: Silica gel, Mobile phase: n-Hexane: ethyl acetate (1:1), Iodine vapors as visualizing agent*

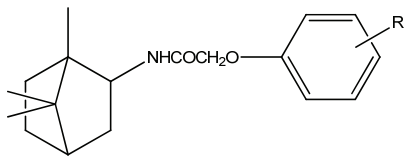

3a–f

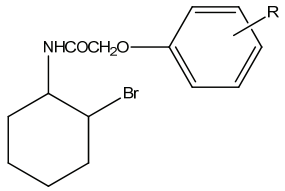

3g–l

Compound	R	Yield, %	Melting point range[a], °C	*Rf* Value[b]	Molecular formula
3a	H	58.6	178–180	0.47	$C_{18}H_{25}NO_2$
3b	4-Br	61.0	110–112	0.41	$C_{18}H_{24}BrNO_2$
3c	4-NO_2	57.8	165–167	0.39	$C_{18}H_{24}N_2O_4$
3d	4-C-$(CH_3)_3$	70.0	105–107	0.44	$C_{22}H_{33}NO_2$
3e	4-OCH_3	67.4	170–172	0.41	$C_{19}H_{27}NO_3$
3f	2-NO_2	62.0	210–112	0.47	$C_{18}H_{24}N_2O_4$
3g	H	57.0	189–191	0.38	$C_{14}H_{18}BrNO_2$
3h	4-Br	66.2	205–207	0.45	$C_{14}H_{17}Br_2NO_2$
3i	4-NO_2	64.1	155–157	0.44	$C_{14}H_{17}BrN_2O_4$
3j	4- C-$(CH_3)_3$	68.0	195–197	0.39	$C_{18}H_{26}BrNO_2$
3k	4-OCH_3	61.0	220–222	0.35	$C_{15}H_{20}BrNO_3$
3l	2-NO_2	67.0	115–117	0.44	$C_{14}H_{17}BrN_2O_4$

[a]Recrystallization with ethanol; [b]stationary phase: silica gel, mobile phase: *n*-hexane:ethyl acetate (1:1), iodine vapors as visualizing agent

maximum analgesic response to avoid injury to the paws. The reference group was administered with a dose of 50 mg/kg of the suspension of diclofenac sodium (standard). The reaction time for each animal was noted on the hot plate at 30, 60 and 90 min after the drug administration.

Antipyretic activity. The antipyretic activity of the test compounds on the feverish body temperature was determined following a reported process [25,26]. Groups of five fasted rats (12 h) were injected subcutaneously with brewer's yeast in physiological saline at a dose of 150 mg/kg body weight. After 17 h, the initial body temperature was measured and the test compounds were administered orally. The body temperature was recorded after 1, 2 and 4 h from the administration of the test compounds.

Statistical analysis

The results of anti-inflammatory activity and analgesic activity are shown in the Tables 2 and 3, respectively. The results were expressed as mean ± *SEM* and were analyzed using one-way analysis of variance (ANOVA) followed by Dunnett's *t*-test. The probability of 0.05 or less was considered statistically significant. Statistical analysis of the results was performed using one way ANOVA or Dunnett's test followed by least significant difference test. Statistical analysis was computed with the GraphPad Prism software version 5.01, GraphPad Software Inc., USA.

RESULTS AND DISCUSSION

A series of titled derivatives 2-(substituted phenoxy)-*N*-(1,7,7-trimethylbicyclo[2.2.1]heptan-2-yl)acetamide and *N*-(2-bromocyclohexyl)-2-(substituted phenoxy) acetamide derivatives **3a**–**l** were synthesized as per scheme in Figure 2. Camphor and 2-bromocyclohexanone were separately treated with ammonium carbonate and formic acid resulting in the formation of amines **1a** and **1b**, respectively. These amines on chloroacetylation with chloroacetyl chloride at 0°C at 10% sodium hydroxide medium gives chloro compounds **2a** and **2b** which converted to **3a**–**l** by the reaction with different substituted phenols in presence of potassium iodide and potassium carbonate in dry acetone as a solvent. The structure of newly synthesized compounds was confirmed by spectral data (IR, ^{1}H-NMR,^{13}C-NMR and MS). Table 1 shows the physical data of compounds **3a**–**l**.

IR spectrum of compounds **2a** and **2b** showed strong absorption bands at 3275/3215 cm^{-1} (due to NH) and 1680/1735 cm^{-1} (characteristic of C=O). This indicates the presence of linkage. Further IR spectrum of compounds **3a**–**l** showed characteristic absorption bands at range of 3205–3310cm^{-1} was attributed to NH, 1600–1785 cm^{-1} accounting for C=O of amide group and 1490–1640 cm^{-1} for C=C in the aromatic ring. Two peaks at range of 1200–1345 cm^{-1} and 1050––1270 cm^{-1} indicates the presence of C–O–C linkage. The structure of compounds was further supported by mass spectral data.

All compounds **3a**–**l** were subjected for preliminary toxicity test as per Organization for Economic Co-operation and Development [20] guidelines in rats. Compounds were found to be safe up to 1500 mg/kg b.w. Hence 1/10th of highest tolerated dose, *i.e*., 150 mg/kg was used as therapeutic dose.

*Table 2. Results of anti-inflammatory activity of compounds (**3a**–**l**) against carrageenan induced rat paw edema model in rats; data analyzed by one-way ANOVA followed by Dennett's test (n = 5); *p < 0.05 significant from control.; **p < 0.01 significant from control*

Compound	Mean values ± *SEM* of oedema volume			Anti-inflammatory activity (% inhibition)		
	30 min	2 h	4 h	30 min	2 h	4 h
Control	0.600±0.004	0.500±0.006	0.400±0.005	–	–	–
Diclofenac sodium	0.090±0.010	0.100±0.015	0.140±0.009	85.00±0.53	80.00±0.50	65.00±0.53
3a**	0.192±0.004	0.292±0.004	0.292±0.004	68.00±0.62	51.33±0.62	51.33±0.62
3b**	0.094±0.002	0.291±0.004	0.192±0.004	84.33±0.41	51.33±0.62	68.00±0.62
3c**	0.304±0.005	0.204±0.005	0.204±0.005	49.33±0.85	66.00±0.85	66.00±0.85
3d**	0.302±0.007	0.204±0.005	0.204±0.005	49.67±1.11	66.00±0.85	66.00±0.85
3e**	0.204±0.005	0.304±0.005	0.204±0.005	66.00±0.85	49.33±0.85	66.00±0.85
3f**	0.304±0.005	0.302±0.006	0.204±0.005	49.33±0.85	49.66±0.97	66.00±0.85
3g*	0.308±0.004	0.404±0.000	0.304±0.005	48.66±0.62	32.67±0.85	49.33±0.85
3h*	0.204±0.005	0.204±0.005	0.204±0.005	66.00±0.85	66.00±0.85	66.00±0.85
3i**	0.304±0.005	0.204±0.005	0.204±0.005	49.33±0.85	66.00±0.85	66.00±0.85
3j*	0.404±0.005	0.304±0.005	0.304±0.005	32.66±0.85	49.33±0.85	49.33±0.85
3k**	0.304±0.005	0.404±0.005	0.406±0.007	49.33±0.85	32.66±0.85	32.33±1.13
3l**	0.308±0.004	0.204±0.005	0.204±0.005	48.66±0.62	66.00±0.85	66.00±0.85

*Table 3. Results of analgesic activity of compounds **3a–l***

Compound	Reaction time, s, after drug administration (mean ± *SEM*)			%Inhibition		
	30 min	60 min	90 min	30 min	60 min	90 min
Control	2.690±0.020	2.700±0.023	2.720±0.027	–	–	–
Diclofenac sodium	5.100±0.030	5.400±0.019	5.800±0.014	79.03±0.214	69.62±0.217	55.70±1.620
3a**	5.627±0.015	6.110±0.032	6.643±0.023	60.07±0.214	43.33±0.214	27.51±0.214
3b**	6.743±0.023	6.943±0.023	6.943±0.023	18.44±0.214	12.59±0.214	14.27±0.211
3c**	5.640±0.021	5.913±0.009	6.523±0.018	59.33±0.214	50.74±0.214	31.92±0.214
3d**	6.027±0.015	6.200±0.012	6.320±0.012	45.32±0.329	39.87±0.329	39.29±0.199
3e**	6.802±0.015	6.900±0.021	7.113±0.015	15.84±0.217	14.07±0.214	10.48±0.326
3f**	6.540± 0.021	6.743±0.023	7.047± 0.026	25.50±0.214	19.98±0.217	12.80±0.211
3g*	4.903±0.015	5.900±0.017	6.217±0.009	86.47±0.214	51.11±0.214	44.32±1.190
3h**	6.743±0.023	6.820± 0.015	7.050±0.029	18.07±0.217	17.03±0.214	12.44±0.211
3i*	5.023±0.015	6.357±0.329	7.197±0.026	81.63±0.217	34.07±0.214	7.270±0.199
3j**	6.513±0.019	6.940±0.021	7.090± 0.021	26.62±0.217	12.59±0.214	10.97±0.211
3k**	5.207±0.012	5.630±0.021	6.023±0.015	74.94±0.214	61.11±0.214	50.30±0.211
3l*	6.003±0.023	6.993±0.015	7.200±0.012	45.20±0.214	10.93±0.185	6.800±0.323

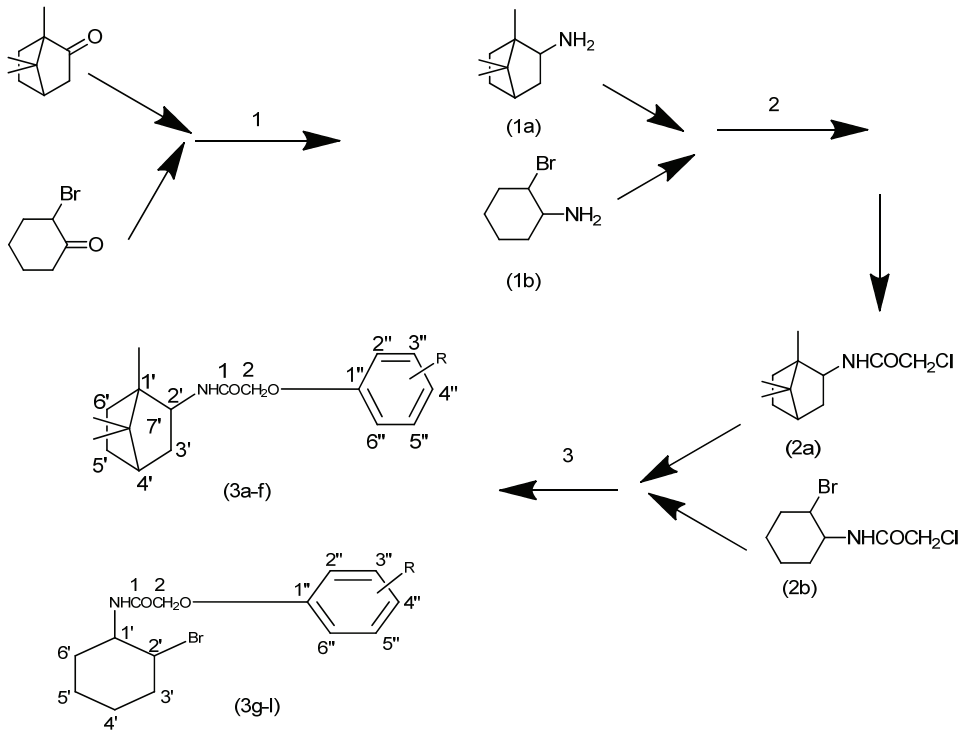

*Figure 2. Synthesis of 2-(substituted phenoxy)-N-(1,7,7-trimethylbicyclo[2.2.1]heptan-2-yl)acetamide **3a–f** and N-(2-bromocyclo-hexyl)-2-(substituted phenoxy)acetamide **3g–l** derivatives. Reagents and conditions: 1) ammonium carbonate and formic acid, heat very slowly heating to 165 °C → ketone, heat,4–5 h, 180–185 °C → reflux, concentrated hydrochloric acid, 2–3 h, water bath → extraction, diethylether → strongly alkaline, 30% sodium hydroxide → extraction, diethylether; 2) chloroacetyl chloride, 10% sodium hydroxide, ice bath, pH 9–10; 3) substituted phenols, dry acetone, potassium carbonate, potassium iodide, reflux, 30–40 h.*

Acute anti-inflammatory activity was performed by carrageenan induced rat paw edema method by Winter and his co-workers [21]. Diclofenac sodium was used as a reference standard. Compounds **3a–f**, **3i**, **3k** and **3l** exhibited significant anti-inflammatory activity similar to the standard, table 2 and Figure 3. The analgesic effects of compounds **3a–f**, **3h**, **3j** and **3k** were found to be nearly of diclofenac sodium, table 3 and Figure 4. Compounds **3a–f** and **3k** were found to exhibit potent antipyretic activity.

Compounds **3a–f** and **3k** were found to possess anti-inflammatory, analgesic and antipyretic activities nearly to the standard because of the presence of nitro and bromo groups on ortho and para positions on the

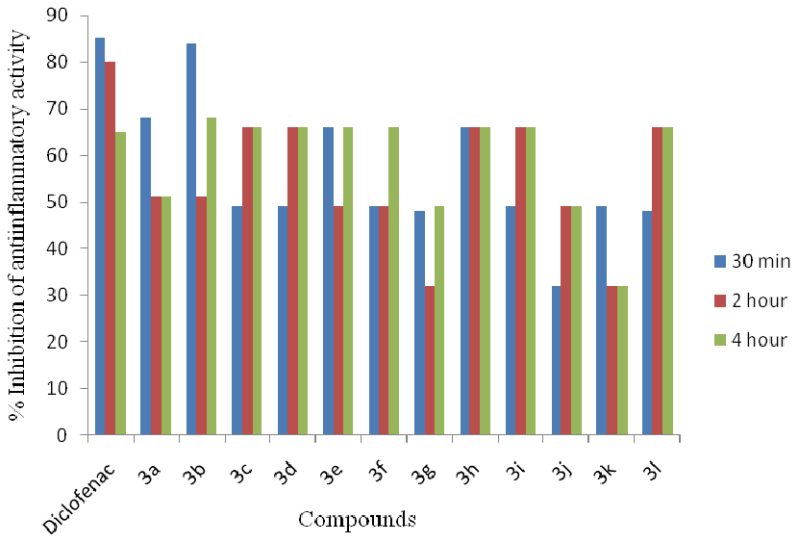

Figure 3. Graphical representation of (% inhibition) of anti-inflammatory activity.

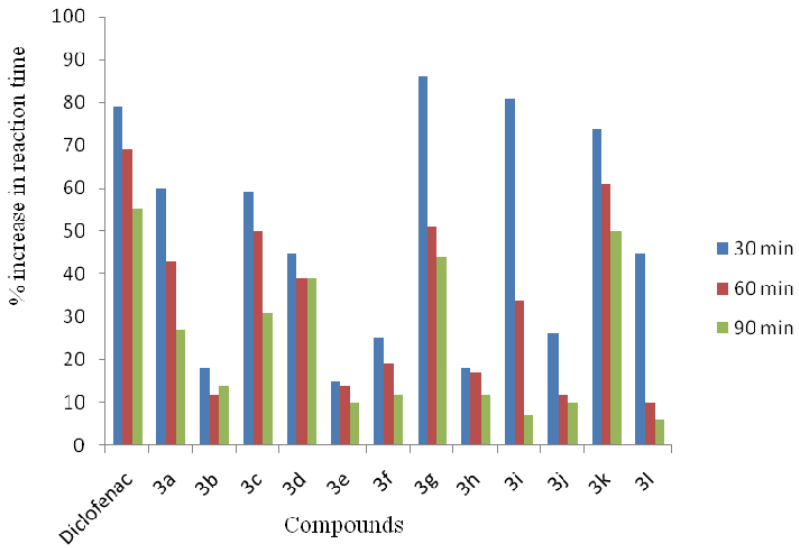

Figure 4. Graphical representation of % increase in reaction time for analgesic activity.

benzene ring. 2-Phenoxy-*N*-phenylacetamide is an intermediate in the synthesis of potent antiinflammatory drug diclofenac sodium, and its antiinflammatory activity is mainly due to the intermediate. Camphor and cyclohexanone derivative compounds are also known to show the antiinflammatory activity, and so we have attached camphor and bromocyclohexane to *N*-phenylacetamide to evaluate the antiinflammatory activity. When camphor was used as starting material, its all compounds showed anti-inflammatory, analgesic and antipyretic activities. But when 2-bromocyclohexanone was used as starting material, only compound **3k** was found to exhibit all the activities.

Compounds **3a–f** and **3k** exhibited significant antipyretic activity nearly to the standard (Table 4).

*Table 4. Results of antipyretic activity of compounds **3a–l***

Compound	Body temperature ± *SEM*, °C			
	0	1 h	2 h	4 h
Control	38.20±0.023	38.18±0.012	38.17±0.005	38.18±0.021
Indomethacin	38.21±0.010	37.42±0.011	36.35±0.016	36.23±0.069
3a	38.11±0.044	37.44±0.011	36.16±0.013	36.71±0.007
3b	38.27±0.014	37.51±0.064	36.55±0.023	36.43±0.020

Table 4. Continued

Compound	Body temperature ± *SEM*, °C			
	0	1 h	2 h	4 h
3c	38.24±0.069	37.28±0.024	37.14±0.009	36.71±0.013
3d	38.22±0.114	37.44±0.032	36.85±0.021	36.76±0.069
3e	38.23±0.320	37.45±0.041	37.38±0.008	36.22±0.021
3f	38.17±0.014	37.33±0.018	36.57±0.030	36.64±0.180
3g	38.24±0.019	37.71±0.078	37.18±0.013	37.16±0.019
3h	38.15±0.032	38.14±0.009	38.17±0.390	38.15±0.012
3i	38.18±0.031	37.78±0.018	37.28±0.011	37.68±0.023
3j	38.26±0.069	37.82±0.078	37.35±0.120	37.84±0.019
3k	38.24±0.014	37.44±0.016	37.13±0.039	36.25±0.011
3l	38.17±0.015	38.12±0.009	37.87±0.007	37.76±0.021

CONCLUSION

From the comprehensive analysis of the results in current studies, we conclude that synthesized compounds have anti-inflammatory and analgesic activities because of the presence of camphor and 2-bromocyclohexanone as basic rings. In analysis of these observations, we conclude that this series **3a–l** could be developed and explored as a novel class of NSAIDs. However, further detailed pharmacological program is required to recognize the potent molecule without various side effects.

Acknowledgement

Authors are grateful to Prof. R.M. Dubey, Vice Chancellor of IFTM University, for providing necessary facilities for this research work.

REFERENCES

[1] L.K. Hedstrom, B. Striepen, IMP dehydrogenase inhibitors for treating mammalian gastrointestinal parasitic infections, WO2007143557 (2007).

[2] O. Morteau, Prostaglandins and Inflammation: the Cyclooxygenase Controversy, Arch Immunol. Ther. Ex. **48** (2000) 473–480.

[3] E. Ricciotti, G.A. FitzGerald, Prostaglandins and Inflammation, Arterioscler. Thromb.Vasc. Biol. **31** (2011) 986––1000.

[4] C. Nathan, Points of control in inflammation, Nature **420** (2002) 846–885.

[5] N.M. Davies, J.L. Wallac, Nonsteroidal anti-inflammatory drug-induced gastrointestinal toxicity: New insights into an old problem, J. Gasteroenterol. **32** (1997) 127–133.

[6] J. Andraos, Reaction intermediates in organic chemistry — The big picture, Can. J. Chem. **83** (2005)1415–1431.

[7] G. Lombardino, Nonsteroidal Antiinflammatory Drugs. Wiley Interscience, New York, 1985, pp. 3–15.

[8] M.D. Mullican, M.W. Wilson, D.T. Connor, C.R. Kostlan, D.J. Schrier, D. Dyer, Design of 5-(3,5-di-tert-butyl-4--hydroxyphenyl)-1,3,4-thiadiazoles, 1,3,4-oxadiazoles, and 1,2,4-triazoles as orally active, nonulcerogenic anti-inflammatory agents, J. Med. Chem. **36** (1993) 1090––1099.

[9] M. Osiri, L.W. Moreland, Specific Cyclooxygenase 2 Inhibitors: A New Choice of Nonsteroidal Anti-Inflammatory Drug Therapy, Arthitis Care Res. **12** (1999) 351–362.

[10] M. Baggiolini, B. Dewald, B. Moser. Interleukin-8 and related chemotactic cytokines – CXC and CC chemokines, Adv. Immunol. **55** (1994) 97–179.

[11] E.A. Garcia-Zepeda, C. Combadiere, M.E. Rothenberg, M.N. Sarafi, F. Lavigne, Q. Hamid, P.M. Murphy, A.D. Luster, Human monocyte chemoattractant protein (MCP)-4 is a novel CC chemokine with activities on monocytes, eosinophils, and basophils induced in allergic and nonallergic inflammation that signals through the CC chemokine receptors (CCR)-2 and -3, J. Immunol. **157** (1996) 5613–5626.

[12] P.M. Chandrika, T. Yakaiah, A.R.R. Rao, N.C. Narsaiah Reddy, V. Sridhar, J.V. Rao, Synthesis of novel 4,6-disubstituted quinazoline derivatives, their anti-inflammatory and anti-cancer activity (cytotoxic) against U937 leukemia cell lines, Eur. J. Med. Chem. **43** (2007) 846–852.

[13] D. Kohli, S.R. Hashim, S. Vishal, M. Sharma, A.K. Singh, Synthesis and antibacterial activity of Quinazolinone Derivatives, Int. J. Pharm. Pharm. Sci. **1** (2009) 163–169.

[14] S.K. Tipparaju, S.P. Muench, E.J. Mui, S.N. Ruzheinikov, J.Z. Lu, S.L. Hutson, M.J. Kirisits, S.T. Prigge, C.W. Roberts, F.L. Henriquez, A.P. Kozikowski, D.W. Rice, R.L. McLeod, Identification and development of novel inhibitors of toxoplasma gondii enoyl reductase, J. Med. Chem. **53** (2010) 6287–6300.

[15] A. Sun, A. Prussia, W. Zhan, E.E. Murray, J. Doyle, L.T. Cheng, J.J. Yoon, E.V. Radchenko, V.A. Palyulin, R.W. Compans, D.C. Liotta, R.K. Plemper, J.P. Snyder, Non-peptide inhibitors of measles virus entry, J. Med. Chem. **49** (2006) 5080–5092.

[16] A.P.G. Nikalje, D. Deshpande, H.D. Une, Facile synthesis and *in vivo* hypoglycemic activity of novel 2,4-thiazolidinedione derivatives, Eur. J. Exp. Biol. **2** (2012) 343––353.

[17] L.P. Carrod, F.D. Grady, Antibiotics and Chemotherapy, 3rd ed., Churchill Livingstone, Edinburgh, , 1972, pp. 477.

[18] S. Ananthan, E.R. Faaleolea, R.C. Goldman, J.V. Hobrath, C.D. Kwong, B.E. Laughon, J.A.Maddry, A. Mehta, L. Rasmussen, R.C. Reynolds, J.A. 3rd Secrist, N. Shindo, D.N. Showe, M.I. Sosa, W.J. Suling, E.L. White, High--throughput screening for inhibitors of Mycobacterium tuberculosis H37Rv, Tuberculosis **89** (2009) 334–353.

[19] M.M. Faul, L.L. Winneroski, C.A. Krumrich, A new one step synthesis of maleimides by condensation of glyoxylate esters with acetamides, Tetrahedron Lett. **40** (1999) 1109–1112.

[20] OCED/OCDC, OECD, October 2000. Guidelines for testing of chemicals, revised draft guidelines 423, Acute oral toxicity class method, revised document.

[21] C.A. Winter, E.A. Risley, G.A. Nuss, Carrageenin-induced edema in hind paw of the rat as an assay for antiiflammatory drugs, Proc. Soc. Exp. Biol. Med. **3** (1962) 544––547.

[22] B.B. Newbould, Chemotherapy of Arthritis Induced In Rats By Mycobacterial Adjuvant, Brit. J. Pharmacol. **21** (1963) 127–136.

[23] N.B. Eddy, D.J. Leimbach, Synthetic analgesics II. Dithienylbutenyl and dithienylbutylamines, J. Pharmacol. Exp. Ther. **107** (1953) 385–393.

[24] V. Mathew, J. Keshavayya, V.P. Vaidya, D. Giles, Studies on synthesis and pharmacological activities of 3,6-disubstituted-1,2,4-triazolo[3,4-*b*]-1,3,4-thiadiazoles and their dihydro analogues, Eur. J. Med. Chem. **42** (2007) 823–840.

[25] R. Ochi, K. Suemaru, H. Kawasaki, H. Araki, Effect of Brewer's yeast-induced pyrexia on aminophylline-elicited convulsions in mice, Acta Med. Okayama **63** (2009) 273–280.

[26] A. Patra, S. Jha, P. Narasimha Murthy, V.D. Aher, P. Chattopadhyay, G. Panigrahi, D. Roy, Anti-Inflammatory and Antipyretic Activities of *Hygrophila spinosa* T. Anders Leaves (Acanthaceae), Trop. J. Pharm. Res. **8** (2009) 133–137.

IZVOD

SINTEZA, KARAKTERIZACIJA I FARMAKOLOŠKA EVALUACIJA SUPSTITUISANIH DERIVATA FENOKSIACETAMIDA

Priyanka Rani[1], Dilip Kumar Pal[2], Rahul Rama Hegde[3], Syed Riaz Hashim[4]

[1]*Department of Chemistry, School of Sciences, IFTM University Moradabad, Uttar Pradesh, India*
[2]*Department of Chemistry, Institute of Pharmaceutical Sciences, Guru Ghasidas Viswavidyalaya, Bilaspur, Chhattisgarh, India*
[3]*Department of Pharmaceutics, School of Pharmaceutical Sciences, IFTM University Moradabad, Uttar Pradesh, India*
[4]*Department of Chemistry, School of Pharmaceutical Sciences, IFTM University Moradabad, Uttar Pradesh, India*

(Naučni rad)

Nove serije 2-(supstituisanih fenoksi)-*N*-(1,7,7-trimetilbiciklo[2.2.1]heptan-2--il)acetamida i derivata *N*-(2-bromocikloheksil)-2-(supstituisanih fenoksi)acetamida koji sadrže cikloheksanski prsten su sintetizovane i ispitivane u cilju određivanja njihove antiinflamatorne aktivnosti, analgetske aktivnosti i antipiretičkog dejstva. Sva nova jedinjenja su sintetizovana reakcijom kamfora ili sličnih ketona, koji sadrže cikloheksanski prsten (na primer 2-bromocikloheksanon), sa amonijum-karbonatom i mravljom kiselinom, pri čemu su se kao krajnji proizvod dobili aromatični amini **1a** i **1b**. Ovi amini su hloroacetilovanjem pomoću hloroacetilhlorida dali jedinjenja **2a** i **2b**. Jedinjenja **2a** i **2b** su prevedena u 2-(supstituisane fenoksi)-*N*-(1,7,7-trimetilbiciklo[2.2.1]heptan-2-il)acetamide i *N*-(2-bromocikloheksil)-2-(supstituisane fenoksi)acetamid derivate reakcijom sa supstituisanim fenolom. Jedinjenja **3a**–**f**, **3i**, **3k** i **3a** su pokazala značajnu antiinflamatornu aktivnost u poređenju sa standardnim lekom natrijum-diklofenakom, dok su jedinjenja **3a**–**f**, **3h**, **3j** i **3k** pokazala značajnu analgetsku aktivnost u poređenju sa standardnim lekovima. Jedinjenja **3a**–**f** i **3k** su pokazala antipiretičku aktivnost skoro kao i standardni lek indometacin. Jedinjenja **3a-f** i **3k** poseduju i antiinflamatornu, analgetsku i antipiretičku aktivnost kao odgovarajući standard.

Ključne reči: 2-(Supstituisani fenoksi)-*N*--(1,7,7-trimetilbiciklo[2.2.1]heptan-2-il)-acetamid • *N*-(2-Bromocikloheksil)-2--(supstituisani fenoksi)acetamid • Antiinflamatorna aktivnost • Analgetska aktivnost • Antipiretička aktivnost

The content of essential and toxic elements in wheat bran and flour

Gordana I. Ludajić[1], Lato L. Pezo[2], Nada K. Filipović[3], Jelena N. Filipović[4]

[1]*Technical College of Applied Sciences in Zrenjanin, Zrenjanin, Serbia*
[2]*University of Belgrade, Institute of General and Physical Chemistry, Belgrade, Serbia*
[3]*University of Novi Sad, Faculty of Technology, Novi Sad, Serbia*
[4]*University of Novi Sad, Institute for Food Technology, Novi Sad, Serbia*

Abstract

The research was conducted with the aim of examining the presence of toxic elements (Pb, Cd, As and Hg) and essential elements (Zn, Cu, Fe and Mn) in selected samples of wheat flour and bran by Inductively Coupled Plasma Mass Spectrometry. The principal component analysis has been used for assessing the variety of samples. Quality results show that the first two principal components, accounting for 84.22% of the total variability, can be considered sufficient for data representation and the first two principal components for toxic elements and essential microelements. Zn (16.38%), Mn (16.19%), Cu (15.73), Fe (15.44%) and Cd (14.99%) have been found the most influential for the first factor coordinate calculation, while the contribution of Hg (89.09%) has been the most important variable for the second factor coordinate calculation.

Keywords: microelements, wheat bran, flour, principal component analysis.

Available online at the Journal website: http://www.ache.org.rs/HI/

SCIENTIFIC PAPER

UDC 664.641.12:664.764:543

Hem. Ind. **69** (4) 417–423 (2015)

doi: 10.2298/HEMIND140322056L

Wheat is one of the most important crops in the world and is grown in different climates. The importance of wheat lies in the fact that wheat crop covers the largest area in the world of agricultural production. The most important step in wheat processing is milling which produces different types of flour as well as different by-products such as bran, and shorts and also impurities extracted from the process of preparing [1].

In addition to nutrients (high level of vitamins, minerals and dietary fibers), wheat grain also contains a number of elements (Cu, Zn, Fe, Ni and Mn) vital to our biological functions, but hazardous to our health in high concentrations [2–4]. It also may contain certain toxic elements (As, Pb, Hg and Cd) which CERCLA Priority List [5] rated as the first, second, third and seventh in toxicity.

Both nutritional essentiality and toxicity of an element depend on its concentration and dietary intake [6].

Mineral fertilizers and pesticides used in wheat production may be contaminated with insecticides based on toxic elements: Pb, Cd or As. Due to the slow Pb, Cd, As and Hg excretion from organisms, carcinogenic and mutagenic effects caused by chronic toxicity may occur [7], along with acute intoxication caused by toxic doses taken over an extended period of time (six months to two years).

Correspondence: G.I. Ludajić, Technical College of Applied Sciences in Zrenjanin, Djordja Stratimirovica 23, 23000 Zrenjanin, Serbia.
E-mail: gludajic@gmail.com
Paper received: 22 March, 2014
Paper accepted: 9 July, 2014

The quality of bread, pastries and other wheat products depends primarily on the quality of the flour as the basic ingredient, *i.e.*, the quality of the wheat variety as the basic raw material. Considering that bread is consumed on a daily basis, the emphasis should be put on its healthy production. If there are undesirable substances present in bread, there is a risk to human health [8]; thus, wheat-based products have received considerable attention in view of their potential role in transporting of microelements into the human diet [9].

According to the current Regulation on the quantities of pesticide, metals, metalloids and other toxic substances, drugs, anabolic and other substances that could be present in foodstuffs [10], the maximum permissible concentration levels of Pb, Cd, Hg and As in flour are 0.4, 0.1, 0.05 and 1 mg/kg of dry matter, respectively, while the maximum permissible concentration of Cd in bran is 0.05 mg/kg of dry matter.

In addition to Cd, Pb, Hg, and As, Cu, Zn, Fe and Mn were selected for this study, as the consumption of wheat products is also an important source of dietary intake of these essential trace elements and can also influence trace element reference values in the tissues of the world's population [11].

The objective of this research is to test the presence of toxic elements (Pb, Cd, As and Hg) and essential elements (Zn, Cu, Fe and Mn) in flour and bran obtained by milling wheat grown in Banat, Serbia. The results will provide information about the position of the accumulation of the studied elements in certain parts of the grain, and thus enable the production of safe food and prevent these elements from entering the food chain.

MATERIAL AND METHODS

Material

Wheat samples were collected from ten locations in the whole territory of Banat (the region in Serbia's northern province of Vojvodina; geographic coordinates of Vojvodina: latitude 45.3167° N, longitude 19.8500° E). 30 individual samples were taken from each site and they were mixed to obtain a representative sample for each site. In this way, ten representative samples of wheat were obtained out of 300 individual samples.

Bran and flour of 60% extraction were obtained by milling the representative samples of wheat in the mill Quadrumat Senior.

Preparation and analysis of the wheat bran and flour

The wheat bran and flour samples were prepared in the following way: A 0.5 g sample was dissolved in 10 ml of concentrated HNO_3 and heated under reflux. After dissolution, 10 ml of concentrated perchloric acid was added and heated until the formation of nitrous fumes stopped. The digestion temperature did not exceed 85 °C to prevent loss of As and Hg (the temperature range was from 70 to 85 °C). The solution was placed in a 50 ml volumetric flask and made up to volume with deionized water (18.2 Ω).

Samples were analyzed depending on the type of elements and their concentration by inductively coupled plasma mass spectrometry (Nexion 300 ICP-MS, Perkin Elmer).

Appropriate quality assurance procedures and precautions were carried out to ensure the reliability of the results. Samples were generally carefully handled to avoid contamination. Glassware was properly cleaned and the reagents were of analytical grade. Reagent blank determinations were used to calibrate the instrument readings. A recovery study of the analytical procedure was carried out by spiking and homogenizing several previously analyzed samples with varied amounts of standard solutions of the metals. Recoveries ranged from 97% for Hg and Fe to 102% for Cu and Cd. It is evident that the determined concentrations of toxic elements agreed well with the reported certified values, confirming the accuracy of the procedure applied.

Toxic element index (*TEI*) and essential microelement index (*EMI*)

Central tendency is the most widely used to compare the toxic element and essential microelement content of complex samples determined using multiple assays [12], where samples are ranked based on the mean value and standard deviation of the assays used. Since the units and the scale of the data from various assays are different, the data in each data set should be transformed into standard scores, a dimensionless quantity derived by subtracting the minimum from the raw data divided by the difference of maximum and minimum values, according to the following equation (for both *TEI* and *EMI*):

$$\overline{x}_i = \frac{\max\limits_i x_i - x_i}{\max\limits_i x_i - \min\limits_i x_i}, \quad \forall i \tag{1}$$

where x_i represents the raw data. When averaged, the standard scores of a sample for different assays give a single unitless value termed as: toxic element index (*TEI*), for toxic elements (Pb, Cd, As and Hg) and essential microelement index (*EMI*), for essential elements (Zn, Cu, Fe and Mn), which is a specific combination of data from different chemical assays with no unit limitation and no variance among the methods.

Statistical analysis

All the experiments were performed with 24 repetitions. Descriptive statistical analyses for calculating the means and the standard error of the mean were performed using the StatSoft Statistica 10 software. All the results obtained were expressed as the mean ± standard deviation (*SD*). The evaluation of correlation matrix and the principal component analyses (PCA) of the results obtained were performed using the StatSoft Statistica 10 software.

RESULTS AND DISCUSSION

Toxic and essential microelement content in the wheat bran and flour

The concentrations of analyzed microelements in the collected wheat bran and flour samples are shown in Table 1.

Cd content in the analyzed samples of flour ranged between 0.094 and 0.113 mg/kg (Table 1), which is a concentration four times higher than the concentrations found in the tests reported by Tejera *et al.* [13] where the total content of Cd found in the flour samples was 0.023–0.027 mg/kg.

The concentration of Cd found in the bran (0.109–0.138 mg/kg) was higher than the maximum permissible concentration level (0.05 mg/kg) due to phosphate fertilizers used in agricultural production.

Pb content in the flour ranged from 0.076 to 0.122 mg/kg. The mean values of Pb were 0.107±0.010 mg/kg. The results show that Pb concentration in the analyzed flour was higher than the concentrations found in the tests reported by Tejera *et al.* [8], where the total content of Pb found in the flour samples was 0.037-0.056 mg/kg, and also higher than the concentrations found in the tests performed by Zhange *et al*.

Table 1. Descriptive statistics data for toxic element and essential microelement content (mg/kg) in the bran and the flour

Parameter	Pb	Cd	Hg	As	Zn	Cu	Fe	Mn
				Bran				
Average	0.143	0.121	0.008	0.028	68.545	9.017	104.23	164.665
St.Dev.	0.046	0.006	0.002	0.014	13.471	2.231	36.508	29.858
Min.	0.105	0.109	0.004	0.014	46.043	1.439	12.045	121.738
Max.	0.290	0.138	0.011	0.074	99.985	13.265	240.48	235.850
Variance	0.002	0.000	0.000	0.000	181.468	4.976	1332.85	891.495
				Flour				
Average	0.107	0.105	0.007	0.015	6.342	1.465	9.392	11.302
St.Dev.	0.010	0.004	0.002	0.008	1.688	0.350	2.461	3.734
Min.	0.076	0.094	0.003	0.009	3.200	0.987	6.764	6.150
Max.	0.122	0.113	0.010	0.045	13.070	2.944	20.098	26.829
Variance	0.000	0.000	0.000	0.000	2.849	0.122	6.054	13.943

[13], where Pb concentration was 0.0351 mg/kg. However, the tests carried out by Doe *et al.* [14] and Locatelli [15] showed Pb concentrations in the flour which ranged from 0.22 to 0.34 mg/kg and from 0.49 to 0.89 mg/kg, respectively, which are the concentrations much higher than the ones found in the results obtained in this study.

Pb, As and Hg contents found in the analyzed samples of bran and flour (Table 1) indicate that the average content range of these toxic elements was within permissible limits prescribed by the Regulations [10]. Having in mind that the toxic and cumulative effects which these elements may have on human organism, it is necessary to permanently monitor and determine their content. The results show that Zn concentration found in the flour (Table 1) is 11 times lower than in the bran, which complies with the results obtained by Cubadda *et al.* [16]. Zn concentration is equalized between the concentrations found in the tested flour samples and the concentrations found in previously performed tests [8], where the average Zn content in wheat flour was 6.154±0.313 mg/kg.

According to the obtained results, the content of Fe found in the bran varied between 12.45 and 240.48 mg/kg (Table 1), while in the wheat flour it was between 6.76 and 20.09 mg/kg.

The results show that Fe concentration found in the bran was higher than the concentration found in the flour, which complies with the results obtained by Milivojević *et al*. [17] who investigated the reactions of different wheat genotypes which were results of application of different types of fertilization and concluded that the mineral nutrition significantly affected the concentration of Fe in the grain.

Analyzing deficiencies in human nutrition, the World Health Organization (WHO) and nutritionists stress the important role of dietary fibers in health maintenance. Pastry products are consumed on a daily basis, which makes them suitable to compensate for fiber deficiency in food. Being rich in dietary fibers, wheat bran is used in bread and pastry production; therefore, monitoring of the content of toxic elements in both flour and bran is required to ensure production of safe and healthy food and to prevent them from entering the food chain.

TEI and *EMI* calculations

TEI and *EMI* score results, calculated using Eq. (1), for the bran and flour samples are presented in Fig. 1. Positive scores in Fig. 1 show increased toxic element and essential microelement content, and these values belong to areas close to larger towns, *i.e.*, areas with higher population density.

The positive *TEI* values indicate higher levels of toxic elements mainly due to the high level of Pb content (0.29 mg/kg) and of Cd content whose average concentration is 2.4 times higher than the maximum permissible concentration prescribed in the regulations [10].

The results (Fig. 1) show that the concentrations of tested elements are the highest in peripheral parts of the grain, *i.e.*, in the bran, which is especially significant for production of either whole meal bread or bread with added bran.

The positive *EMI* values account for high concentrations of essential microelements due to high levels of Zn, Fe and Mn concentrations.

Correlation analysis

The data in Table 2 show a correlation between toxic element and essential microelement assays in the bran and the flour samples. These data showed that the contents of Pb, Zn, and Cu found in the flour are independent from the contents of these metals found in the bran. As and Fe contents in the flour are even negatively correlated to the contents of these metals in the bran. Cd and Hg contents in the flour are positively correlated to the contents of these metals in the bran,

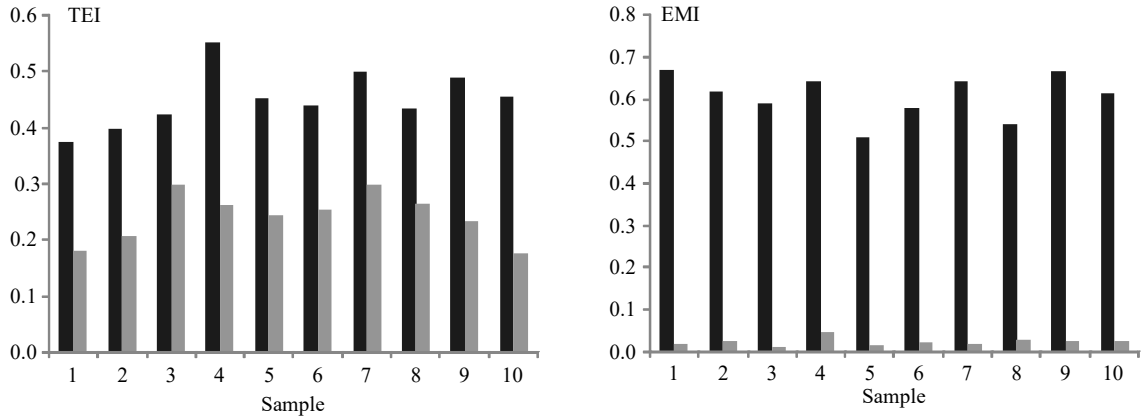

Figure 1. TEI and EMI score results for bran (■) and flour (■).

*Table 2. Pearson's correlation coefficients between toxic element and essential microelement assays in the bran and flour samples, with statistical significance expressed as p-level values, written in small parentheses; * – significant at p < 0.05 level, ** – significant at p < 0.10 level; unmarked correlation coefficients were statistically insignificant*

		Flour							
		Pb	Cd	Hg	As	Zn	Cu	Fe	Mn
Bran	Pb	0.27	–0.03	**0.42***	–0.05	–0.14	–0.26	–0.17	–0.17
		(0.145)	(0.887)	**(0.022)**	(0.794)	(0.451)	(0.159)	(0.382)	(0.35)
	Cd	–0.16	**0.48***	–0.24	0.06	0.33**	0.25	0.31**	0.19
		(0.395)	**(0.007)**	(0.211)	(0.749)	(0.078)	(0.188)	(0.096)	(0.32)
	Hg	–0.04	0.12	**0.65***	0.33**	–0.25	–0.16	–0.23	–0.28
		(0.836)	(0.512)	**(0.000)**	(0.078)	(0.188)	(0.413)	(0.227)	(0.13)
	As	0.14	0.23	0.04	–0.10	–0.01	0.13	–0.06	–0.12
		(0.446)	(0.222)	(0.825)	(0.595)	(0.940)	(0.496)	(0.736)	(0.54)
	Zn	0.05	0.01	–0.30	–0.19	0.26	0.17	0.06	–0.10
		(0.787)	(0.973)	(0.102)	(0.303)	(0.159)	(0.374)	(0.739)	(0.61)
	Cu	–0.10	–0.14	–0.23	–0.22	–0.01	0.13	0.03	–0.10
		(0.613)	(0.459)	(0.227)	(0.237)	(0.974)	(0.502)	(0.885)	(0.59)
	Fe	–0.24	0.07	–0.05	–0.03	–0.05	–0.07	–0.06	**–0.38***
		(0.204)	(0.719)	(0.788)	(0.864)	(0.779)	(0.701)	(0.736)	**(0.03)**
	Mn	0.09	0.05	–0.03	0.10	0.33**	0.36**	0.28	0.36**
		(0.645)	(0.791)	(0.871)	(0.584)	(0.077)	(0.054)	(0.131)	(0.05)

0.48 and 0.65, (statistically significant at $p < 0.05$ level, 95% confidence limit), which indicates that the contents of Cd and Hg in the flour are directly related to their contents in the bran. The content of Cd and Hg in the bran and flour may be associated with their content in the soil where wheat is grown. Correlation between Mn content in the flour and bran is statistically significant at $p < 0.10$ level.

The correlation between Hg in the flour and Pb in the bran, and also between Mn in the flour and Fe in the bran were observed, statistically significant at $p < 0.05$ level. Cd content in the bran correlates Zn and Fe contents in the flour samples, statistically significant at $p < 0.10$ level, while Hg content in the bran correlates As content in the flour samples, at $p < 0.10$ level. Mn content in the bran correlates both Zn and Cu contents in the flour at $p < 0.10$ level.

Principal component analyses (PCA)

The PCA allows a considerable reduction in a number of variables and the detection of a structure in the relationship between measuring parameters that give complimentary information. The eigenvalues for successive factors are displayed on a so-called "scree-plot", Fig. 2. The number of factors retained in the model for proper classification of experimental data, in original matrix into loading (bran and flour samples) and score (toxic element and essential microelement content) matrices were determined by application of Kaiser and Rice's rule [18]. This criterion retains only principal components with eigenvalues > 1. All samples

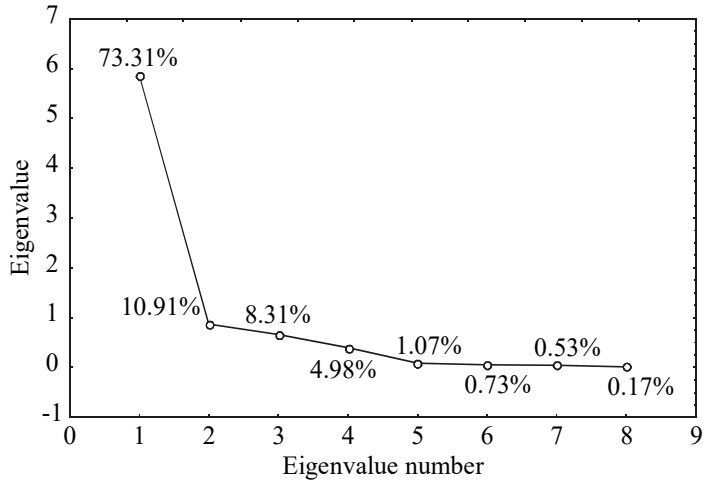

Figure 2. Scree-plot.

having different toxic elements and essential microelement content are shown by descriptive analysis (Table 1) and predicted by the PCA score plot (Fig. 3). The full auto scaled data matrix consisting of different bran and flour samples is submitted to the PCA.

For visualizing the data trends and the discriminating efficiency of the descriptors used, a scatter plot of samples using the first two principal components (PCs) issued from the PCA of the data matrix is obtained (Fig. 3). As can be seen, there is a neat separation of the observed samples, according to the assays used. Quality results show that the first two principal components, accounting for 84.22% of the total variability, can be considered sufficient for data representation and the first two principal components for toxic elements and essential microelements. Zn (16.38%), Mn (16.19%), Cu (15.73), Fe (15.44%) and Cd (14.99%) have been found the most influential for the first factor coordinate calculation, while the contribution of Hg (89.09%) has been the most important variable for the second factor coordinate calculation.

The influence of toxic elements and essential microelements can be observed in Fig. 3, with higher Cd, Zn, Cu, Mn and Fe contents, and on the left side of the graphic. The PCA graphic showed good discrimination characteristics between the bran and flour samples, which were found different mostly due to the contents of Cd, Zn, Cu, Mn and Fe. The samples having the highest *TEI* and *EMI* content are located on the left side of PCA biplot graphic.

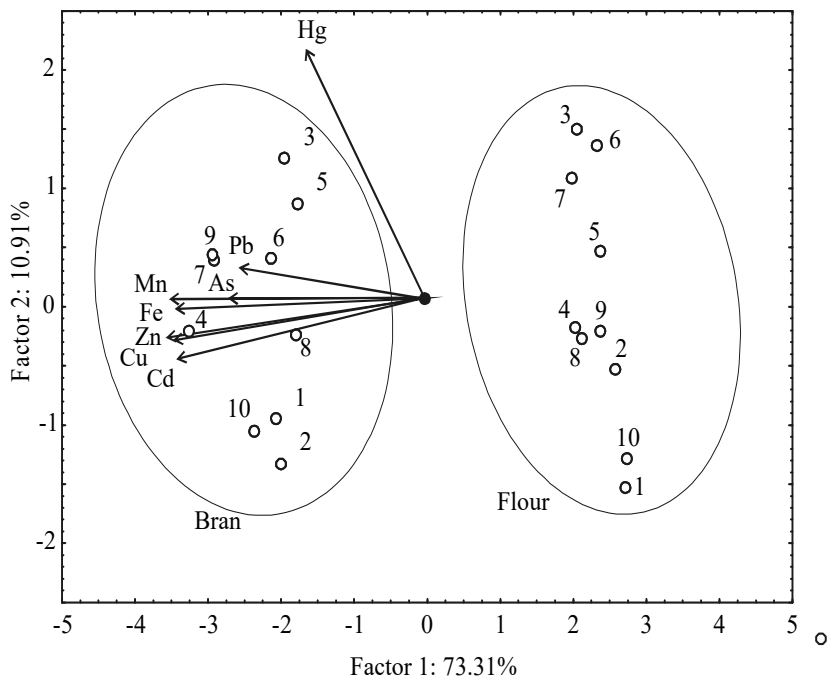

Figure 3. Biplot for toxic element and essential microelement content in the bran and flour.

CONCLUSION

Considering the results of the analysis of toxic elements and essential microelements in the wheat bran and flour, the following could be concluded:

The Pearson table is a useful tool for showing correlation between chemical elements in the bran compared to the content of the elements analyzed in the flour. The content of Cd and Hg in the flour is positively correlated to the content of these metals in the bran, 0.48 and 0.65, which indicates that the content of Cd and Hg in the flour is directly related to their content in the bran.

The Cd concentrations found in the bran, 0.109–0.138 mg/kg, are higher than the maximum permissible concentration levels prescribed by the Serbian legislation (0.05 mg/kg).

The content of Fe in the bran varied between 12.45 and 240.48 mg/kg, while in the wheat flour it ranged between 6.76–20.09 mg/kg. Since the content of this metal, whose role is very important in human nutrition, is less in the flour than in the bran, it would be advisable to fortify the flour used in bread production with iron by adding wheat bran safe from toxic elements.

According to the PCA analysis it has been found that there is a far less quantity of analyzed elements in the wheat bran than in the flour. The factor axes indicate the samples with increased content of certain elements. Quality results show that the first two principal components, accounting for 84.22% of the total variability, can be considered sufficient for data representation and the first two principal components for toxic elements and essential microelements. Zn (16.38%), Mn (16.19%), Cu (15.73), Fe (15.44%) and Cd (14.99%) have been found the most influential for the first factor coordinate calculation, while the contribution of Hg (89.09%) has been the most important variables for the second factor coordinate calculation.

Monitoring of the content of toxic elements in flour and bran is required to ensure production of safe and healthy food, particularly if wheat bran is used for fiber deficiency compensation in wheat based products.

Acknowledgements

These results are part of the project supported by the Ministry of Education, Science and Technological Development of the Republic of Serbia, TR 31055.

REFERENCES

[1] E.J. Pyler, L.A. Gorton, Baking Science and Technology, Fourth ed. Sosland Publ. Co., Kansas City, MO, 2008.

[2] Z. Nan, C. Zhao, J. Li, F. Chen, W. Sun, Relations between soil properties and elected heavy metal concentrations in spring wheat (*Triticum aestivum* L.) grown in contaminated soils, Water Air Soil Pollut. **133** (2002) 205–213.

[3] A.A. Carbonell-Barrachina, E. Garcia, J. Sanchez Soriano, P. Aracil, F. Burlo, Effects of raw materials, ingredients and production lines on arsenic and copper concentrations in confectionery products, J. Agric. Food Chem. **50** (2002) 3738–3742.

[4] E.E. Santos, D.C. Lauria, C.L. Porto da Silveira, Assessment of daily intake of trace elements due to consumption of foodstuffs by adult inhabitants of Rio de Janeiro city, Sci. Total Environ. **327** (2004) 69–79.

[5] CERLA Priority List of Hazardous Substances. 2003 (available from http://www.atsdr.cdc.gov).

[6] B. Škrbić, N. Đurišić-Mladenović, J. Cvejanov, Principal Component Analysis of Trace Elements in Serbian Wheat, J. Agric. Food Chem. **53** (2005) 2171–2175.

[7] P.W. Abrahams, Soils: their implications to human health, Sci. Total Environ. **291** (2002) 1–32.

[8] R. Tejera, G. Luis, D. González-Weller, J. M. Caballero, Á. J. Gutiérrez, C. Rubio, A. Hardisson, Metals in wheat flour; comparative study and safety control, Nutr. Hosp. **28** (2013) 506–513.

[9] B. Škrbić, A. Onjia, Multivariate analyses of microelement contents in wheat cultivated in Serbia (2002), Food Control **18** (2007) 338–345.

[10] Serbian Regulations for the Content of Pesticides, Metals, Metalloids and Other Toxic Substances in Food, **5** (1992) 67–85 (in Serbian).

[11] C. Minoia, E. Sabbioni, A. Ronchi, A. Gatti, R. Pietra, A. Nicolotti, S. Fortaner, C. Balducci, A. Fonte, C. Roggi, Trace element reference values in tissues from inhabitants of the European Community, Sci. Total Environ. **141** (1994) 181–195.

[12] T. Sun, C.T. Ho, Antiradical efficiency of tea components, J. Food Lip. **8** (2001) 231–238.

[13] Z.W. Zhang, T. Watanabe, S. Shimbo, K. Higashikawa, M. Ikeda, Lead and cadmium contents in cereals and pulses in northeastern China, Sci. Total Environ. **220** (1998) 137–145.

[14] E.D. Doe, A.K. Awua, O.K. Gyamfi, N.O. Bentil, Levels of selected heavy metals in wheat flour on the ghanaian market: a determination by atomic absorption spectrometry, Am. J. Appl. Chem. **1** (2013) 17–21.

[15] C. Locatelli, Heavy metals in matrices of food interest: Sequential voltammetric determination at trace and ultra-trace level of copper, lead, cadmium, zinc, arsenic, selenium, manganese and iron in meals, Electroanal. **16** (2004) 1478–1486.

[16] F. Cubadda, M. Baldini, M. Carcea, L.A. Pasqui, A. Raggi, P. Stacchini, Influence of laboratory homogenization procedures on trace element content of food samples: an ICP-MS study on soft and durum wheat, Food Addit. Contam. **18** (2001) 778–787.

[17] J. Milivojević, M. Jakovljević, M. Jelić, Lj. Bošković- Rakočević, Investigation of methods for Fe, Mn and Zn solubility in the smonitza of Serbia, J. Agric. Sci. **47** (2002) 9–18.

[18] M. Otto, Chemometrics Statistics and Computer Application in Analytical Chemistry. Wiley-VCH, Weinheim, 1999.

IZVOD

SADRŽAJ ESENCIJALNIH I TOKSIČNIH ELEMENATA U PŠENIČNIM MEKINJAMA I BRAŠNU

Gordana I. Ludajić[1], Lato L. Pezo[2], Nada K. Filipović[3], Jelena N. Filipović[4]

[1]*Visoka tehnička škola strukovnih studija u Zrenjaninu, Zrenjanin, Serbia*
[2]*Univerzitet u Beogradu, Institut za opštu i fizičku hemiju, Beograd, Srbija*
[3]*Univerzitet u Novom Sadu, Tehnološki fakultet, Novi Sad, Srbija*
[4]*Univerzitet u Novom Sadu, Naučni institut za prehrambene tehnologije, Novi Sad, Srbija*

(Naučni rad)

Žitarice, brašno i hleb predstavljaju, direktno ili indirektno, jednu od osnovnih komponenti ljudske ishrane, pa je i njihov uticaj na zdravlje ljudi veliki. Zbog značaja koje ove namirnice imaju u ljudskoj ishrani, potrebno je znati njihov mineralni sastav koji je i direktan indikator hranljive vrednosti ovih proizvoda kao i eventualnog zagađenja ovih proizvoda kao posledica zagađenja životne sredine ili posledica primenjenih agrotehničkih mera. Istraživanje je sprovedeno sa ciljem ispitivanja prisustva toksičnih elemenata (Pb, Cd, As i Hg) kao i esencijalnih elemenata (Zn, Cu, Fe i Mn) na odabranim uzorcima pšeničnih mekinja i brašna primenom metode ICP-MS. Praćena je korelacija između sadržaja toksičnih mikroelemenata u pšeničnim mekinjama i brašnu. Rezultati pokazuju statistički značajnu korelaciju (na nivou značajnosti $p < 0,05$) između Cd (0,48), kao i Hg (0,65) u brašnu i mekinjama. Izmerene koncentracije Cd u mekinjama, 0,109–0,138 mg/kg, su veće od maksimalno dozvoljene, koja je propisana Pravilnikom RS (naveden u literaturi) (0,05 mg/kg). Sadržaj Fe u mekinjama se kretao od 12,45–240,48 mg/kg, a u pšeničnom brašnu od 6,76–20,09 mg/kg. Kako je sadržaj ovog, u ishrani ljudi važnog metala, manji u brašnu u poređenju sa mekinjama može se preporučiti da se prilikom prozvodnje hleba vrši njegovo obogaćivanje gvožđem korišćenjem pšeničnih mekinja ili celih zrna pšenice. Analiza glavnih komponenata pokazuje da je samo jedna faktorska koordinata dovoljna za opisivanje 73,31% ukupne varijanse, a da druga faktorska koordinata opisuje 10,91% varijabilnosti sistema. Pošto ove dve koordinate opisuju zajedno 84,22% ukupne varijanse, sistema može se smatrati da one opisuju sistem na zadovoljavajućem nivou.

Ključne reči: Mikroelementi • Mekinje • Brašno • Analiza glavnih komponenti

Size distribution of fullerenol nanoparticles in cell culture medium and their influence on antioxidative enzymes in Chinese hamster ovary cells

Branislava U. Srdjenovic[1], Marija N. Slavić[2], Karmen M. Stankov[3], Nebojša V. Kladar[1], Danica S. Jović[4], Mariana N. Seke[5], Višnja V. Bogdanović[6]

[1]*University of Novi Sad, Faculty of Medicine, Department of Pharmacy, Novi Sad, Serbia*
[2]*Institute for Biological Research "Siniša Stanković", Belgrade, Serbia*
[3]*University of Novi Sad, Faculty of Medicine, Clinical Center of Vojvodina, Novi Sad, Serbia*
[4]*University of Novi Sad, Faculty of Science, Department of Chemistry, Biochemistry and Environmental Protection, Novi Sad, Serbia*
[5]*University of Belgrade, Vinča Institute of Nuclear Science, Belgrade, Serbia*
[6]*Institute of Oncology, Department for Experimental Oncology, Sremska Kamenica, Serbia*

Abstract

Fullerenol ($C_{60}(OH)_{24}$) nanoparticles (FNP) have a significant role in biomedical research due to their numerous biological activities, some of which have cytoprotective and antioxidative properties. The aim of this study was to measure distribution of fullerenol nanoparticles and zeta potential in cell medium RPMI 1640 with 10% fetal bovine serum (FBS) and to investigate the influence of FNP on Chinese hamster ovary cells (CHO-K1) survival, as well as to determine the activity of three antioxidative enzymes: superoxide-dismutase, glutathione-reductase and glutathione-S-transferase in mitomycin C-treated cell line. Our investigation implies that FNP, as a strong antioxidant, influences the cellular redox state and enzyme activities and thus may reduce cell proliferation, which confirms that FNP could be exploited for its use as a cytoprotective agent.

Keywords: fullerenol, mytomocine C, antioxidative enzyme, CHO K1 cell line.

Available online at the Journal website: http://www.ache.org.rs/HI/

SCIENTIFIC PAPER

UDC 615:616–085:547

Hem. Ind. **69** (4) 425–431 (2015)

doi: 10.2298/HEMIND131218054S

With the rapid development of nanotechnology, many kinds of nanomaterials have been and are being used in fields of industry and scientific researches. A wide range of engineered nanoparticles, ranging from 1–100 nm, have been proposed to be used in nanomedicine due to their unique physical and chemical characteristics. Fullerenols are polyhydroxylated fullerenes $C_{60}(OH)_x$ (between $2 > x < 44$). Fullerenol $C_{60}(OH)_{24}$ has a diameter of approximately 1 nm with symmetrically arranged hydroxyl groups on the C_{60} sphere [1]. Fullerenol dissolved in water forms polyanion nanoparticles of size mostly between 3 and 100 nm [2,3]. Polyhydroxylated fullerenes, including $C_{60}(OH)_{24}$, have demonstrated high antioxidative activity in many chemical, *in vivo* and *in vitro* studies [4–7]. Mrdjanovic *et al*. confirmed the antigenotoxic effect of FNP on mitomycin-damaged CHO-K1 cells [8]. *In vitro* and *in vivo* studies have proved fullerenol's tissue-protective effect in irradiated human erythroleukemia cell line K562 and organs of rats, due to its antioxidative and radical scavenging activity [9,10]. Results of studies on healthy and tumor-bearing rats, treated with a single high dose of doxorubicin (DOX), imply the potential tissue-protective role of FNP [11–18].

Internalization of nanoparticles into live cells is closely related to their potential application, function and cytotoxicity. It is known that cellular uptake and the processes of cellular delivery are influenced by various factors, such as: physicochemical properties of nanoparticles (chemical composition, size, shape and surface charge), concentration of nanoparticles, incubation time, the type of cells, etc. [19].

Mitomycin C (MMC) is an antitumor quinone that undergoes reductive metabolism to generate reactive electrophilic species, which can then alkylate cellular nucleophiles. It also acts as a DNA cross-linking agent [20].

The aim of this study was to measure distribution of FNP by volume and number, as well as zeta potential of particles, in aqueous solution and in RPMI 1640 with 10% FBS in dark on 37 °C during 24 h, which are basically used to treat the particles in cell culture. Based on the above mentioned fact concerning numerous biological activities of FNP, our additional goal was to test *in vitro* influence of FNP on cell's survival and activity of three antioxidative enzymes: total superoxide-dismutase (SOD), glutathione–reductase (GR) and glutathione-S-transferase (GST), in both, mitomycin C-treated CHO-K1 cells and control untreated groups of CHO-K1 cell line.

Correspondence: B. Srdjenovic, Department of Pharmacy, Faculty of Medicine, University of Novi Sad, Hajduk Veljkova 3, 21000 Novi Sad, Serbia.
E-mail: srdjbr@yahoo.com
Paper received: 18 December, 2013
Paper accepted: 3 July, 2014

MATERIALS AND METHODS

Fullerenol nanoparticle synthesis

Fullerenol $C_{60}(OH)_{24}$ was synthesized in alkaline media by complete substitution of bromine atoms from $C_{60}Br_{24}$. Briefly, the polybromine derivative $C_{60}Br_{24}$ was synthesized through catalytical ($FeBr_3$) reaction of C_{60} in Br_2 [21]. 50 mg of $C_{60}Br_{24}$ was mixed in 5ml of NaOH pH 10 for 2 h at room temperature. After the reaction was completed, the solvent was evaporated at 40 °C, and the mixture was rinsed five times with 10 ml portions of 80% ethanol. The aqueous solution of fullerenol (20 ml) with residual amounts of NaOH and NaBr was applied on the top of the combined ion-exchange resin DOWEX MB50 QC121815 R1 (20 g) and eluted with demineralized water until discoloration. The solution of fullerenol (pH 7) was evaporated under low pressure; a dark brown powder substance remained. Analysis: FTIR $C_{60}(OH)_{24}$: 3427, 1627, 1419, 1080 cm^{-1}; ^{13}C-NMR (D_2O) reaction mixture: singlet peaks at δ 77.7 ppm and multiplet at δ 140 ppm, ^{13}C-NMR (D_2O) $C_{60}(OH)_{24}$: singlet peaks δ 169.47 ppm and multiplet peak δ 160–110 ppm; MALDI (matrix α-cyano-4-hydroxycinnamic acid) (*m*/*z*): 720 (C_{60}^+), 721 ($C_{60}H^+$), 722 ($C_{60}H_2^+$), 737 ($C_{60}(OH)^+$), 808 ($C_{60}(OH)_5^+$), 839 ($C_{60}(OH)_7^+$), 856 ($C_{60}(OH)_8^+$), 1009 ($C_{60}(OH)_{17}^+$), 1026 ($C_{60}(OH)_{18}^+$) and minor peak 1128 ($C_{60}(OH)_{24}^+$); DTG, DTA, TG reveal two thermal changes, in temperature of 120–395 °C, corresponding to the loss of mass of 35.7% (23.7 OH groups) and at the temperature of 430 °C loss of mass was 64.3% (this was the temperature of sublimation of C_{60}). Elementary analysis of fullerenol provided the following: C, 63.00%; H, 2.00% calc.: C, 63.83%; H, 2.13%.

Size distribution of nanoparticles

In order to obtain results for distribution of particles by volume and number, as well as zeta potential of particles, high performance analyzer Zetasizer Nano ZS (Malvern Instruments) was used. Prior to measurement, samples were tempered at 37 °C for 24 h and stored in the dark.

Scanning electron microscopy (SEM)

Scanning electron microscopy (SEM) was performed with a JEOL JSM 6460 LV scanning microscope (300000× magnification). The 10 ppm aqueous solution of fullerenol was placed on a conductive carbon tape, evaporated under reduced pressure and covered with a thin gold layer about 5 nm.

Cell line treatment

All the experiments were performed on Chinese hamster ovary cell line CHO-K1, ATCC CCL61 (American Type Culture Collection Catalogue of Cell Lines and Hybridomas, 6th ed., 1988). CHO-K1 cells were cultured as a tightly flask-bonded monolayer in RPMI 1640 medium (Sigma), supplemented with 10% FCS (Veterinary institute Novi Sad, NIVNS), 2 mM L-glutamine, penicillin (100 IJ/mL) and streptomycin (100 µg/mL, Galenika) at 37 °C in fully humified atmosphere with 5% CO_2. Single-cell suspension was obtained with 0.25% trypsin or trypsin in EDTA (Sigma). Cells were passaged twice a week in concentration of 50000–100000 cells/ml.

CHO-K1 sample cells were plated in sterile cultivation plates (Costar, 6 well) in concentration of 200000/ml and treated as follows:

Control – untreated cells

MMC – mitomycin C 0.1 µg/ml

F1 – FNP 0.025 mg/ml

F3 – FNP 0.125 mg/ml

F1 + MMC – FNP 0.025 mg/ml 30 min before MMC 0.1 µg/ml

F3 + MMC – FNP 0.125 mg/ml 30 min before MMC 0.1 µg/ml.

FNP was dissolved in bi-distilled water and added in the cell culture in two final concentrations: 0.025 and 0.125 mg/ml in a 3- and 24-hour treatment.

Mitomycin C was dissolved in distilled water and added in cell culture samples in final concentration of 0.1 µg/ml in a 3- and 24-hour treatment.

In FNP pretreated samples, FNP was added half an hour before MMC.

Dye exclusion test (DET) with Trypan blue was used to monitor the cell survival [22]. The DET test was performed by mixing 50 µl of cell suspension with 200 µl of 0.1% Trypan blue solution in 0.9% NaCl. After 2 min of incubation at a room temperature, the number of viable cells (unstained cells) was determined using a Burker-Turk hemocytometer.

Survival rate was calculated according to formula:

Survival rate (%) = 100×(Total number of viable cells in experimental group / Total number of viable cells in control group)

All enzyme activity assays were performed in cytosolic cell fraction, in supernatant obtained by ultrasonication (Soniprep 150 MSE) (10 min at 10000 rpm at 4 °C) and kept at –80 °C. All spectrophotometric measurements were carried out in triplicates (Agilent 8453 UV/Vis spectrophotometer with thermostatted multicell position sample system).

Superoxide dismutase assay

Total (Cu–Zn and Mn) superoxide dismutase (SOD) activity measuring method was based on the ability of superoxide dismutase to inhibit the auto-oxidation of epinephrine [23]. One unit of activity was defined as the amount of enzyme necessary to decrease by 50% the rate of adrenalin auto-oxidation at pH 10.2 and 480 nm. The results were expressed as $U/10^6$ of cells.

Glutathione reductase assay

Glutathione reductase (GR) was determined measuring the reduction rate of oxidized glutathione with NADPH as suitable enzyme substrate at 340 nm [24]. Activity of GR was defined as nmol of NADPH/min per 10^6 of cells.

Glutathione-S-transferase assay

Glutathione-S-transferase (GST) was based on conjugation of –SH group of reduced glutathione with 1-chloro-2,4-dinitrobenzene (CDNB) [24]. Absorbance of the conjugate CDNB–glutathione was measured at 340 nm. Activity of GST was expressed as nmol of CDNB-glutathione conjugate/min per 10^6 of cells.

Statistical analysis

The data were analyzed by Multivariate analysis of variance (MANOVA) followed by Duncan test at 0.05 significance level to compare the means using SPSS 13.0 for Windows.

RESULTS AND DISCUSSION

Results for size distribution of particles by volume (Fig. 1a) put an emphasis on inhomogeneity of the analyzed samples. In all samples can be noticed the presence of particles of dimensions within 2–30 nm, with the maximum at 5 nm. Fullerenol nanoparticles in aqueous solution are mostly within 2–8 nm, while in samples containing fetal bovine serum size varies within 2–30 nm. Addition of FNP in the cell culture medium with 10% FBS has not influenced the size distribution of nanoparticles by volume.

Figure 1b presents nanoparticle's size distribution by number in which particles are classified into a family within 2–9 nm, with the maximum at approx. 5 nm. It can be concluded that addition of FNP in the culture medium with 10% FBS has not induced changes in the size of particles.

In Figure 2, SEM image of the fullerenol nanoparticles studied in this work shows the particles size from 30–80 nm. These findings are in accordance with DLS and AFM measurements conducted before [25].

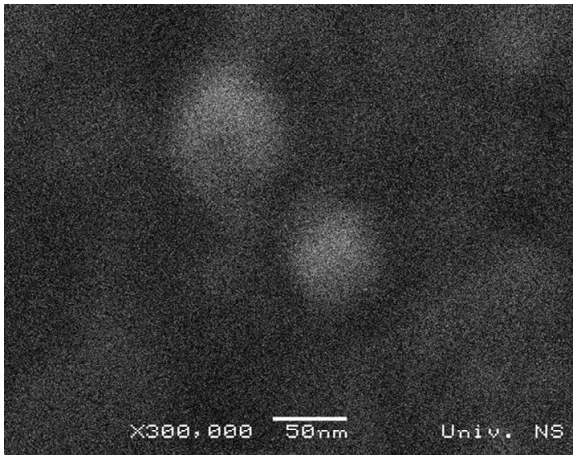

Figure 2. SEM image of film resulted from a 10 ppm aqueous solution of fullerenol.

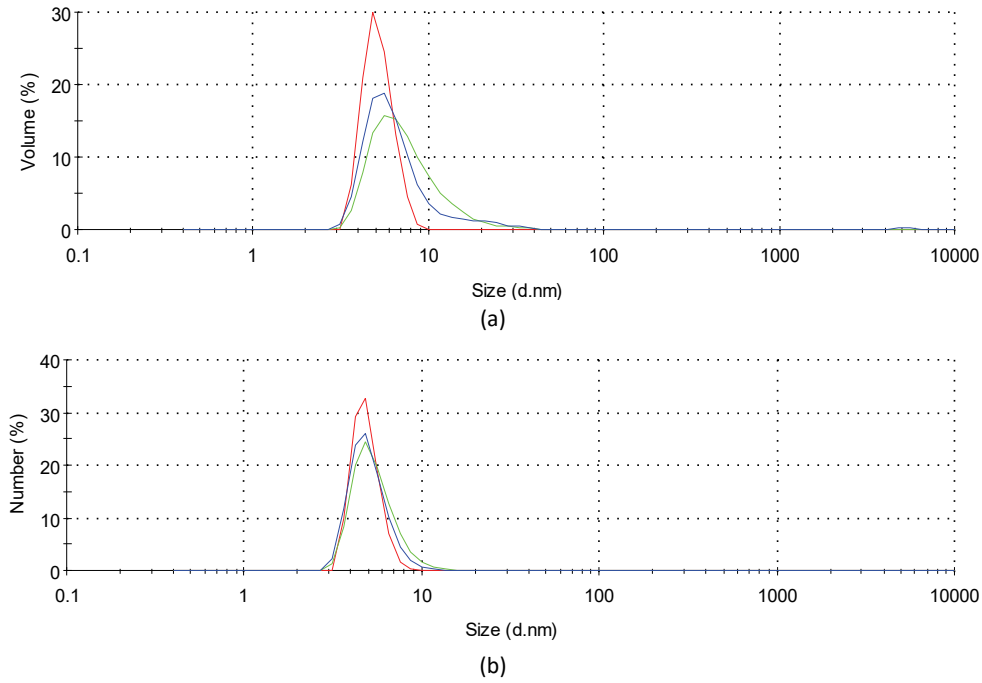

Figure 1. Size distribution of nanoparticles a) by volume and b) by number, in the following samples: cell culture medium RPMI 1640 + 10% FBS (green); aqueous solution of fullerenol (red); and fullerenol in cell culture medium RPMI 1640 + 10% FBS (blue), after incubation for 24 h at 37 °C in the dark.

Table 1 shows the results of measurements for ζ-potential of the following systems: RPMI 1640 + 10% FBS, aqueous solution of FNP pH 6, and aqueous solution of FNP in RPMI + 10% FBS (incubated for 24 h at 37 °C in the dark). ζ-potential of polyanionic fullerenol nanoparticles at pH 6 is –58 mV. After addition of FNP in the cell culture medium RPMI with 10% FBS, ζ-potential of the medium slightly changed from –3.6 to –7.9 mV; ζ-potential of nanoparticles solution changed from –58 to –7.9 mV.

Table 1. ζ-potential of the following systems: RPMI 1640 + 10% FBS, aqueous solution of FNP and aqueous solution of FNP in RPMI + 10% FBS (incubated for 24h at 37 °C in the dark)

Sample	ζ-potential, mV
RPMI 1640 + 10% FBS	–3.6
Aqueous solution of FNP: FNPaq, pH 6	–58
FNPaq + RPMI + 10% FBS	–7.9

It has been confirmed that particles' size has an important role on their adhesion to and interaction with biological cells. It is also known that the size of FNP is an important property in the toxicity analysis, since nanoparticles have a tendency to form agglomerates, which may behave differently from a single nanoparticle. Also, the presence of proteins in the culture medium can change the nanoparticles agglomeration and influence the cellular response. Nanoparticles, which are partially covered by proteins in body fluids, can change reactivity, charge and hydrophobicity [26]. It is also well-known that FNP can pass through the plasma membrane and manifest its biological effects inside the cell [27].

We can conclude that investigated FNP does not have a tendency to form agglomerates, based on the results for distribution of particles by volume and number obtained in our experiment, as well as according to the measurements for ζ-potential after incubation in cell medium. Furthermore, the presence of proteins in the culture medium does not induce significant changes in terms of nanoparticles agglomeration. Results of AFM analysis of FNP in the cell culture medium supplemented with 20% of FBS [25] revealed that FNP (which in water form aggregates of approx. 90 nm) forms a stable and homogenous solution that mostly consists of two dimer particles of 90 nm associated with one smaller nanoparticle of about 40 nm, which was assumed to be a protein from the FBS.

Results obtained in our experiment show that addition of FNP in the cell culture medium with 10% FBS does not influence the size distribution of nanoparticles and does not induce formation of such a large particle, but causes reduction in ζ-potential of nanoparticles (from –58 to –7.9 mV). Monitoring of ζ-potential is particularly important due to possible interactions that can be favored as a result of change in particles' surface charge.

In vitro effects of FNP on the induction of cellular antioxidative capacity, actually on the increased activity of enzymes of the antioxidative system in the cells exposed to oxidative stress, are cell type- and dose-dependent [9]. Results showed that FNP did not induce genotoxic effect, on the contrary antigenotoxic effects of FNP were confirmed in the experiment done on MMC-damaged CHO-K1 cells in concentration of 11.0–221.6 μM [8].

Our present investigation has shown that FNP in both examined concentrations moderates the activities of oxidative enzymes SOD and GR in comparison to the control, which implies that it undoubtedly enters the cells and participates in cell metabolism (Fig. 3). This mild change in enzyme activity does not affect the survival of cells.

Possible mechanisms responsible for the increased activity of SOD in CHO-K1 cells treated with FNP may be explained by the fact that fullerenol acts as NO-scavenger, which prevents superoxide consumption in the reaction of peroxynitrite anion formation, simultaneously increasing O^{2-} concentration and SOD activity as a consequence of superoxide excess [9,28].

Depending on the applied dose, the activity of enzyme GR was both, increased and reduced. The increase in activity of GR indicates the reduced cellular milieu that enables cells to efficiently scavenge free radicals, formed as a result of FNP participating in cellular metabolism, which can clarify the absence of significant influence of FNP on cell survival. Reduced activity of GR in a 3-hour experiment with FNP of higher concentration can be explained by inactivation of this enzyme due to increased level of free radicals, while results of 24-hour experiment suggest the compensatory upregulation of mRNK and reactivation of mentioned enzymes [13].

Fullerenol expressed no influence on GST activity, since it probably did not participate in detoxification of FNP. Furthermore, FNP did not induce formation of oxidative damage products to such extent to activate GST. Study conducted on the freshwater zebrafish exposed to fullerenol ($C_{60}(OH)_{18}$–22(OK4)) analyzed oxidative stress responses on fish brain. They also did not detect any statistically significant changes in GST activity or TBARS level [29].

Application of mitomycin C significantly increases the activity of all three enzymes, which presents the antioxidative response of cells to the applied agent. High activity of SOD in groups pretreated with FNP in comparison with the group treated only with MMC could be explained by the fact that fullerenol nanoparticles already act as NO-scavenger which concomi-

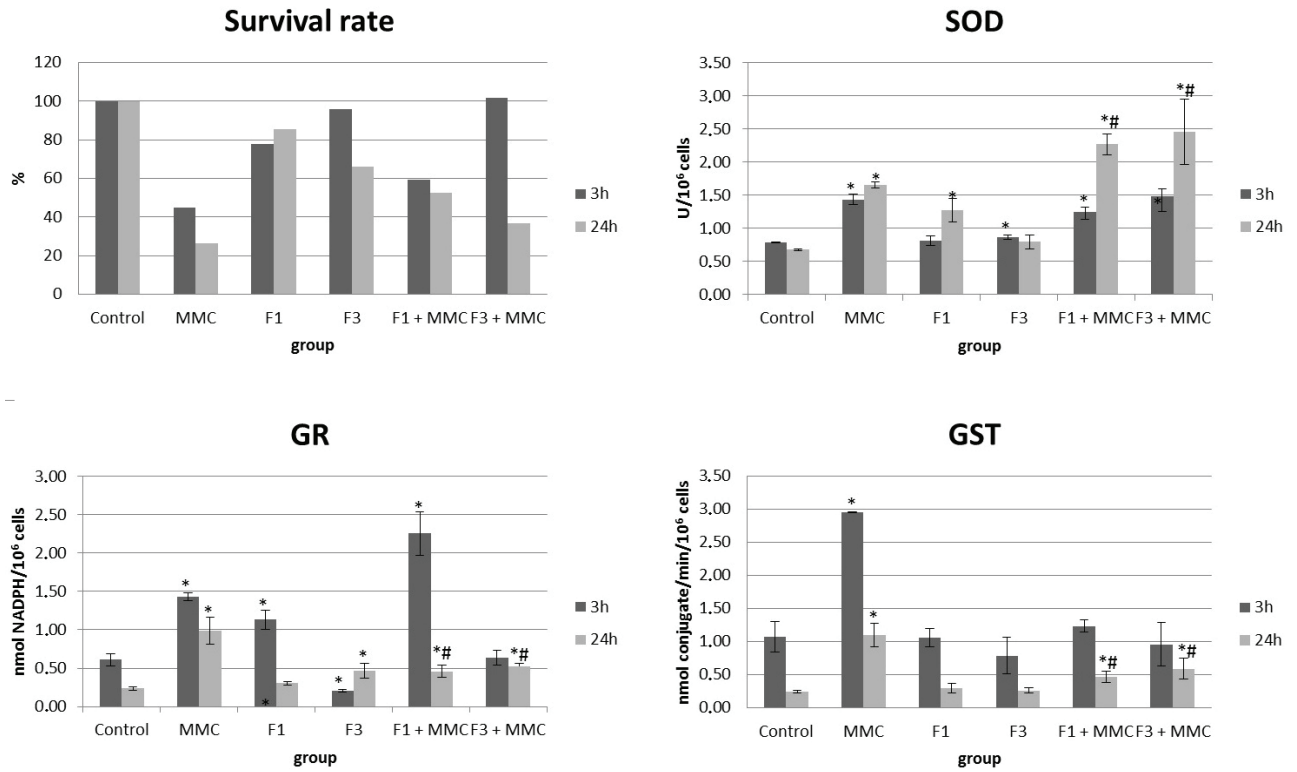

Figure 3. Effect of FNP and MMC on cells survival rate and activity of enzymes SOD, GR, GST in CHO-K1 cell line 3 and 24 h after the treatment. Control – untreated cells; MMC – mitomycin C 0.1 µg/ml; F1 – FNP 0.025 mg/ml; F3 – FNP 0.125 mg/ml; F1 + MMC – FNP 0.025 mg/ml 30 min before mitomycin C 0.1 µg/ml; F3 + MMC – FNP 0.125 mg/ml 30 min before mitomycin C 0.1 µg/ml;
** – $p < 0.05$ vs. control group; # – $p < 0.05$ vs. group treated only with mitomycin C.*

tantly increases the O^{2-} concentration and SOD activity. Addition of MMC leads to more superoxide production and additional influence on the balance between NO and O^{2-} in cells, and consequently high SOD activity.

Pretreatment with the lower concentration of FNP notably increases the activity of GR even in comparison to mitomycin C. This may happen because FNP in such a low concentration does not exhibit potent antioxidative potential, where 24 h after pretreatment the activity of this enzyme was yet to reach the control level, but still was statistically significantly lower than the values in MMC groups. Survival rate of pretreated cells was significantly higher in comparison to those treated only with MMC, which confirms the protective properties of FNP in the range of used concentrations in MMC-damaged CHO-K1 cells [8].

In acute phase, the higher concentration of FNP completely neutralizes the consequences of MMC treatment and normalizes the activity of GR, which was reflected also on the survival percentage of the cells (101.74%). Although the activity of GR after 24 h was increased in comparison to control, the survival rate was significantly higher than survival rate in MMC treated group. The results of GST activity also point out the protective effects of FNP since pretreatment with FNP significantly neutralizes the influence of MMC on the activity of this enzyme. These findings are in accordance with the study conducted A549 cells where pretreatment with $C_{60}(OH)_{24}$ attenuated hydrogen peroxide-induced apoptotic cell death by induction of phase II detoxifying enzymes [30].

As previous works concluded, polyhydroxylated fullerenes, as strong antioxidants, influence the cellular redox state and thus could reduce cell proliferation, which could be exploited for the use of fullerenol as a cytoprotective agent [4,31,32].

CONCLUSION

In summary, the present results demonstrate that polyanion fullerenol nanoparticles reduce mitomycin C--induced oxidative stress in dose- and time-dependent manner, and therefore possess beneficial effects on preventing drug toxicity in CHO-K1 cells. Applied alone, fullerenol nanoparticles influence the cell metabolism moderately and not in such a manner to induce any severe irreversible changes that would consequently lead to the cell death.

Acknowledgment

This work is supported by The Ministry of Education, Science and Technological Development of the Republic of Serbia, project No. III45005 and the Provincial Secretariat for Science and Technological

Development of Vojvodina (grant number 114-451--2056/2011-01).

REFERENCES

[1] S. Wilson, D. Schuster, M. Maggini M. Prato, R. Taylor, in K.M. Kadish, R.S. Ruoff (Eds.), Organic chemistry of fullerenes, Wiley-Interscience, New York, 2000, pp. 91––177.

[2] B. Vileno, P.R. Marcox, M. Lekka, A. Sienkiewicz, T. Fehre, L. Forro, Spectroscopic and physical properties of a highly derivatized C_{60} fullerol, Adv. Funct. Mater. **16** (2006) 120–128.

[3] J.A. Brant, C.O. Robichaund, M. Wiesner, Fullerol cluster formation in aqueous solutions: Implications for environmental release, J. Colloid Interface Sci. **314** (2007) 281–288.

[4] G. Bogdanovic, V. Kojic, A. Djordjevic, J. Canadanovic-Brunet, M. Vojinovic-Miloradov, V.V. Baltic, Modulating activity of fullerenol $C_{60}(OH)_{22}$ on doxorubicin-induced cytotoxicity, Toxicol. *In Vitro* **18** (2004) 629–637.

[5] A. Djordjevic, J. Canadanovic-Brunet, M. Vojinovic-Miloradov, G. Bogdanovic, Antioxidant properties and hypothetical radical mechanism of fullerenol $C_{60}(OH)_{24}$, Oxid. Commun. **27** (2005) 213–218.

[6] J. Grebowski, P. Kazmierska, A. Krokosz, Fullerenols as a New Therapeutic Approach in Nanomedicine, Biomed. Res. Int. (2013), DOI: 10.1155/2013/751913.

[7] J.J. Yin, F. Lao, P.P. Fu, W.G. Wamer, Y. Zhao, P.C. Wang, Y. Qiu, B. Sun, G. Xing, J. Dong, X-J. Liang, C. Chen, The scavenging of reactive oxygen species and the potential for cell protection by functionalized fullerene materials, Biomaterials **30** (2009) 611–621.

[8] J. Mrđanović, S. Šolajić, V. Bogdanović, K. Stankov, G. Bogdanović, A. Djordjevic, Effects of fullerenol $C_{60}(OH)_{24}$ on the frequency of micronuclei and chromosome aberrations in CHO-K1 cells, Mutat. Res: Genet. Toxicol. Environ. Mutagen **680** (2009) 25–30.

[9] V. Bogdanović, K. Stankov, I. Ičević, D. Žikić, A. Nikolić, S. Šolajić, A. Djordjevic, G. Bogdanović, Fullerenol $C_{60}(OH)_{24}$ effects on antioxidative enzymes activity in irradiated human erythroleukemia cell line, J. Radiat. Res. **49** (2008) 321–327.

[10] S. Trajković, S. Dobrić, V. Jačević, V. Dragojević-Simić, Z. Milovanović, A. Djordjevic, Tissue protective effects of fullerenol $C_{60}(OH)_{24}$ and amifostine in irradiated rats, Colloids Surfaces, B **58** (2007) 39–43.

[11] V. Djordjevic-Milic, K. Stankov, R. Injac, A. Djordjevic, B. Srdjenovic, B. Govedarica, N. Radic, V. Dragojevic-Simic, B. Strukelj, Activity of antioxidative enzymes in erythrocytes after a single dose administration of doxorubicin in rats pretreated with fullerenol $C_{60}(OH)_{24}$, Toxicol. Mech. Methods **19** (2009) 24–28.

[12] V. Milic-Torres, B. Srdjenovic, V. Jacevic,V. Dragojevic--Simic, A. Djordjevic, A.L. Simplício, Fullerenol $C_{60}(OH)_{24}$ prevents doxorubicin-induced acute cardiotoxicity in rats, Pharmacol. Rep. **62** (2010) 707–718.

[13] B. Srdjenovic, V. Milic-Torres, N. Grujic, K. Stankov, A. Djordjevic, V. Vasovic, Antioxidant properties of fullerenol $C_{60}(OH)_{24}$ in rat kidneys, testes, and lungs treated with doxorubicin, Toxicol. Mech. Meth. **20** (2010) 298––305.

[14] I. Icevic, S. Vukmirovic, B. Srdjenovic, J. Sudji, A. Djordjevic, R. Injac, V. Vasović, Protective effects of orally applied fullerenol nanoparticles in rats after a single dose of doxorubicin, Hem. Ind. **65** (2011) 329–337.

[15] R. Injac, M. Perse, N. Obermajer, V. Djordjevic-Milic, M. Prijatelj, A. Djordjevic, A. Cerar, B. Strukelj, Potential hepatoprotective effects of fullerenol $C_{60}(OH)_{24}$ in doxorubicin-induced hepatotoxicity in rats with mammary carcinomas, Biomaterials **29** (2008) 3451–3460.

[16] R. Injac, M. Boskovic, M. Perse, E. Koprivec-Furlan, A. Cerar, A. Djordjevic, B. Strukelj, Acute doxorubicin nephrotoxicity in rats with malignant neoplasm can be successfully treated with fullerenol $C_{60}(OH)_{24}$ *via* suppression of oxidative stress, Pharmacol. Rep. **60** (2008) 742–749.

[17] R. Injac, N. Radic, B. Govedarica, M. Perse, A. Cerar, A. Djordjevic, B. Strukelj, Acute doxorubicin pulmotoxicity in rats with malignant neoplasm is effectively treated with fullerenol $C_{60}(OH)_{24}$ trough inhibition of oxidative stress, Pharmacol. Rep. **61** (2009) 335–342.

[18] R. Injac, M. Perse, M. Cerne, N. Potocnik, N. Radic, B. Govedarica, A. Djordjevic, A. Cerar, B. Strukelj, Protective effects of fullerenol $C_{60}(OH)_{24}$ against doxorubicin-induced cardiotoxicity and hepatotoxicity in rats with colorectal cancer, Biomaterials **30** (2009) 1184––1196.

[19] L.Yan, Z. Gu, Y. Zhao, Chemical mechanisms of the toxicological properties of nanomaterials: generation of intracellular reactive oxygen species, Chem. Asian J. **10** (2013) 2342–2353.

[20] D. Siegel, H. Beall, C. Senekowitsch, M. Kasai, H. Arai, N. Gibson, D. Ross, Bioreductive activation of mitomycin C by DT-diaphorase, Biochemistry **31** (1992) 7879–7885.

[21] A. Djordjević, M. Vojinović-Miloradov, N. Petranović, A. Devečerski, D. Lazar, B. Ribar, Catalytic preparation and characterization of $C_{60}Br_{24}$, Fullerene Sci. Technol. **6** (1998) 689–694.

[22] M.C. Black, B. Berenbaum, Factors affecting the dye exclusion test for cell viability, Exp. Cell. Res. **3** (1985) 9––13.

[23] H.P. Mishra, I. Fridovich, The role of superoxide anion in the autoxidation of epinephrine and a simple assay for superoxide dismutase, J. Biol. Chem. **247** (1972) 3170––3175.

[24] E. Beutler, Red Cell Metabolism: A Manual of Biochemical Methods, Grune&Stratton, New York, 1984.

[25] J. Mrđanovic, S. Šolajić, V. Bogdanović, A. Đorđević, G. Bogdanović, R. Injac, Z. Rakočević, Effects of fullerenol nano particles $C_{60}(OH)_{24}$ on micronuclei and chromosomal aberrations' frequency in peripheral blood lymphocytes, Dig. J. Nanomater. Biostruct. **7** (2012) 673––386.

[26] B. Fubini, M. Ghiazza, I. Fenoglio, Physicochemical features of engineered nanoparticles relevant to their toxicity, Nanotoxicology **4** (2010) 347–363.

[27] J.G. Saathoff, A.O. Inman, X.R. Xia, J.E. Riviere, N.A. Monteiro-Riviere, *In vitro* toxicity assessment of three hydroxylated fullerenes in human skin cells, Toxicol. *In Vitro* **25** (2011) 2105–2112.

[28] D. Wink, J. Mitchell, Chemical biology of nitric oxide: Insights into regulatory, cytotoxic and cytoprotective mechanisms of nitric oxide, Free Radic. Biol. Med. **25** (1998) 434–456.

[29] A.M. da Rocha, J.R. Ferreira, D.M. Barros, T.C.B. Pereira, M.R. Bogo, S. Oliveira, V. Geraldo, R.G. Lacerda, A.S. Ferlauto, L.O. Ladeira, M.V.B. Pinheiro, J.M. Monserrat, Gene expression and biochemical responses in brain of zebrafish Danio rerio exposed to organic nanomaterials: Carbon nanotubes (SWCNT) and fullerenol ($C_{60}(OH)_{18}$–22(OK4)), Comp. Biochem. Phys., A **165** (2013) 460–467.

[30] S. Ye, M. Chen, Y. Jiang, M. Chen, T. Zhou, Y. Wang, Z. Hou, L. Ren, Polyhydroxylated fullerene attenuates oxidative stress-induced apoptosis via a fortifying Nrf2-regulated cellular antioxidant defence system. Int. J. Nanomed. **9** (2014) 2073–2087.

[31] R. Injac, N. Radic, B. Govedarica, A. Djordjevic, B. Strukelj, Bioapplication and activity of fullerenol $C_{60}(OH)_{24}$, Afr. J. Biotechnol. **7** (2008) 4050–4940.

[32] V.M. Torres, B. Srdjenovic, in: R.F.Verner, C. Benvegnu (Eds.), Handbook on Fullerene: Synthesis, Properties and Applications, Nova Science Publishers, Inc., Hauppauge, 2012, pp. 197–238.

IZVOD

RASPODELA FULERENOLSKIH NANOČESTICA PO VELIČINI U ĆELIJSKOM MEDIJUMU I NJIHOV UTICAJ NA ANTIOKSIDATIVNE ENZIME U OVARIJALNIM ĆELIJAMA KINESKOG HRČKA

Branislava U. Srdjenovic[1], Marija N. Slavić[2], Karmen M. Stankov[3], Nebojša V. Kladar[1], Danica S. Jović[4], Mariana N. Seke[5], Višnja V. Bogdanović[6]

[1]*Univerzitet u Novom Sadu, Medicinski fakultet, Katedra za farmaciju, Novi Sad, Srbija*
[2]*Institut za biološka istraživanja „Siniša Stanković", Beograd, Srbija*
[3]*Univerzitet u Novom Sadu, Medicinski fakultet, Klinički centar Vojvodine, Novi Sad, Srbija*
[4]*Univerzitet u Novom Sadu, Prirodno-matematički fakultet, Departman za hemiju, biohemiju i zaštitu životne sredine, Novi Sad, Srbija*
[5]*Univerzitet u Beogradu, Institu za nuklearne nauke „Vinča", Beograd, Srbija*
[6]*Institut za onkologiju, Zavod za eksperimentalnu onkologiju, Sremska Kamenica, Srbija*

(Naučni rad)

Zahvaljujući širokoj biološkoj aktivnosti, npr. citoprotektivnom i antiksidativnom svojstvu, fulerenol ima značajnu ulogu u biomedicinskim istraživanjima, na šta ukazuju i rezultati brojnih istraživanja. Cilj ovog istraživanja je bio merenje zeta potencijala i raspodele fulerenol nanočestica u medijumu RPMI 1640 + 10% FBS (Fetal Bovine Serum), kao i ispitivanje uticaja fulerenola na preživljavanje ćelija i aktivnost tri antioksidativna enzima: superoksid-dismutaze, glutation-reduktaze i glutation-S-transferaze, u mitomicinom C tretiranoj ćelijskoj liniji. Istraživanje je obavljeno na ćelijama jajnika kineskog hrčka CHO-K1 (*Chinese Hamster Ovary cells*) koristeći DET test (*Due Exclusion Test*) za brojanje ćelija, kao i set spektrofotometrijskih metoda za određivanje antioksidativne aktivnosti. Ćelije su pre tretmana mitomicinom C tretirane fulerenolom u dve različite koncentracije, a potom inkubirane i analizirane nakon 3 i 24 h. Dodavanje fulerenolskih nanočestica u medijum sa 10% FBS nije izazvalo promene u raspodeli veličina čestica po broju ili zapremini, dok se vrednost zeta potencijala medijuma (ζ) promenila sa –3,6 na –7,9 mV. Fulerenol ispoljava protektivni efekat na ćelije CHO-K1 koje su tretirane mitomicinom C. Mitomicin C povećava aktivnost sva tri ispitana enzima, dok sam fulerenol u veoma maloj meri utiče na aktivnost pomenutih enzima. Pretretman sa fulerenolom smanjuje stres indukovan mitomicinom C po vremenski i dozno zavisnom obrascu. Naše istraživanje potvrđuje da nanočestice fulerenola utiču na redoks stanje i enzimsku aktivnost ispitivane ćelijske linije, što ukazuje na to da mogu sniziti nivo ćelijske proliferacije i naći primenu kao citoprotektivni agens.

Ključne reči: Fulerenol • Mitomicin C • Antioksidativni enzimi • CHO K1 ćelijska linija

Laser influence to biosystems

Sanja D. Jevtić[1], Milesa Ž. Srećković[2], Svetlana S. Pelemiš[3], Ljubica M. Konstantinović[4], Predrag B. Jovanić[5], Lazar D. Petrović[6], Milan M. Dukić[7]

[1]*Railway Technical School, Belgrade, Serbia*
[2]*Faculty of Electrical Engineering, University of Belgrade, Belgrade, Serbia*
[3]*Faculty of Technology, University of East Sarajevo, Zvornik, Bosnia and Herzegovina*
[4]*School of Medicine, University of Belgrade, Belgrade, Serbia*
[5]*Institute for Multidisciplinary Studies, University of Belgrade, Belgrade, Serbia*
[6]*Faculty of Diplomacy and Security, University Union Nikola Tesla, Belgrade, Serbia*
[7]*North Carolina Central University, Durham, USA*

Abstract

In this paper a continuous (cw) lasers in visible region were applied in order to study the influence of quantum generator to certain plants. The aim of such projects is to analyze biostimulation processes of living organisms which are linked to defined laser power density thresholds (exposition doses). The results of irradiation of corn and wheat seeds using He–Ne laser in the cw regime of 632.8 nm, 50 mW are presented and compared to results for other laser types. The dry and wet plant seeds were irradiated in defined time intervals and the germination period plant was monitored by days. Morphological data (stalk thickness, height and cob length) for chosen plants were monitored. From the recorded data, for the whole vegetative period, we performed appropriate statistical data processing. One part of experiments contains the measurements of coefficient of reflection in visible range. Correlation estimations were calculated and discussed for our results. Main conclusion was that there was a significant increment in plant's height and also a cob lenght elongation for corn.

Keywords: laser, biostimulation, biosystems, plants, doses, reflection coefficient, correlation.

Available online at the Journal website: http://www.ache.org.rs/HI/

SCIENTIFIC PAPER

UDC 621.375.826:632/635

Hem. Ind. **69** (4) 433–441 (2015)

doi: 10.2298/HEMIND140415059J

The influence of nuclear particles, electric fields, magnetic fields and electromagnetic (EM) radiation in the whole electromagnetic spectrum, including nuclear and atomic areas, belong to old problems, vastly studied, but not yet completely understood. Earlier investigations covered spontaneous radiation, while up-to--date investigations deal with stimulated radiation e.g. quantum generators (lasers, masers, uvasers, xrasers and gammarasers). There is not enough space for numbering positive or negative influences of electromagnetic radiations, generally speaking in contemporary civilization. In spite of administration and regulative, in dosimetric point of view and technical manuals, accidents are still present [1–8].

Bad influence to human health is in provoked thermal effects as well as electrochemical, mechanical and other effects. The radiation shows some kind of cumulative effects for the whole tissue, but it could be focused to lead to the processes in cells (cell surgery is known today, since first famous data were red blood cell drilled in nine places). Numerous are effects induced by electric and magnetic fields in everyday's life as well as in military and medical applications of RF (radio frequency) devices portion [9–11].

Local irradiation of high intensity RF leads to skin and muscle burns and to ocular damage of various degrees (lens blurring), damage of reproductive organs, changes in central nervous system, blood flow and immune defense mechanisms [12,13].

Well known accidents with radar beams caused by human negligence, deserve further analysis to prove the statement that long irradiation to RF beams of low intensity leads to health damage, cancer disease and lasting consequences to offspring. This could also be considered from the point of view of stimulated radiation in this range, due to maser (quantum generator or amplifier) and its implementation in a number of processes. Sometimes first letter m represents molecular and sometimes microwave, what is common for engineers and physicists.

Industrial growth and power engineering are always focused to power transmission (power lines, high voltage devices, etc.) and human health. Doses regulative are constantly changing in the areas of: influence of electric and magnetic fields, nuclear specified radiation, laser and other quantum generator thresholds and allowed radiation power densities (total cumulative doses). All numbered fields could influence human

Correspondence: S. Pelemiš, Faculty of Technology, University of East Sarajevo, Karakaj 34a, 75400 Zvornik, Bosnia and Herzegovina.
E-mail: alannica@gmail.com
Paper received: 15 April, 2014
Paper accepted: 3 July, 2014

organs (heart, nervous system tissues, reproductive organs and other). Employees on power lines and transformers maintenance, electricians and other personnel in electrical based processes (induction furnace, electrified railways, etc.) are always in danger. Besides that, the influence of laser sources in communication purposes, various monitoring and measurements, laser therapy, mass media applications including open space laser shows present potential threat. Note that laser, maser, iraser, uvaser, xraser and gammaraser, work as quantum generators of stimulated radiation in various portions of the EM spectra, but the last two are not in commercial use.

Biological influences of various fields (electric and magnetic) are usually studied separately for DC and AC regimes, but also in transient regimes, which are very important due to high amplitude values. Some people consider that magnetic field has stronger effect to living creatures.

Usually, AC and DC regimes are vastly studied but transient regimes are very important in real applications of electric power. This is related to power network connections and usage of electrical devices. For dosimetry it is necessary to as precise as possible define this regime with possible overloading.

Electrical and magnetic fields in human body cause induced currents which, with defined density could affect organism, i.e. hearth functioning, nervous system tissues and others. In spite of tremendous work, there are still open issues in this area mainly targeting the fact, that these fields provoke other effects. Considering new methods of LLL therapy (low level laser) the novelties are biphasic dose responses [14–16].

The influence of modern electronic and electric systems is also particular problem of civilization and the questions of allowed doses, besides state regulative, are still opened, depending on various facts (television sets, video terminal, PC monitors, communication devices, GSM mobile devices, etc).

The levels of allowed EM radiation are often expressed by defined zones and allowed surface power densities. Note that both frequency and amplitude of electric field (intensity) have to be taken into account. Due to these facts all of these calculated numbers should be considered just as the quantitative values. Explicitly: the zone of very intensive radiation is with surface power density higher than 10 mW/cm^2 (15 min within 24 h), zone of moderate radiation 0.1–0.9 mW/cm^2 (3 h within 24 h) and zone of weak radiation with less than 0.1 mW/cm^2.

Allowed levels of electromagnetic radiation power density are regulated by national standards. In Sweden, the level of EM power density is 450 μW/cm^2 corresponding to the electric field E = 41 V/m. Serbian standard is more rigid, allowing levels of electromagnetic power densities of 200 μW/cm^2, *i.e.*, E = 27.5 V/m [9,10,17,18].

To compare mentioned values of electromagnetic power densities we remind that radiation of stars is aproximately14 pW/cm^2 and that for human body the value could be approximately 0.5 μW/cm^2.

The laser beam irradiation and allowed levels are new problems in spite of the fact that by frequency range they are parts of electromagnetic spectra. The main difference is that, depending on provoked processes, we could have all the effects as with spontaneous electromagnetic radiation, but many new ones as well.

In area of quantum generators dosimetry is not as detailed as in area of nuclear radiation where exposition and absorption are precisely defined and should be completed with different parameters, corrective factors and different units. Note that when high power lasers interact with the material many nuclear processes appear (X and gamma radiation, neutrons, etc.). Therefore, both dosimetries have to be united. Nuclear dosimetry worldwide still uses SI as well as other units, which is not allowed in our country. In presented paper we chose approach which is the most often implemented in references describing biostimulative (biomodulating) effects. We gave certain parameters for valuating possible maximal input energy levels. Our approach deals with optimal corrections for determining more precise doses and increasing of repeatability. It also deals with nominal laser power and time of exposition. It is interesting that in considering couplings between nuclear and laser radiation to objects from biosphere, laser beam can be used as means of measurement for evaluation of nuclear radiation influence by phosphorescent and other processes. Up to day it seems that only in nuclear dosimetry exist approaches with unit equivalent to biological tissues as rem (Röntgen equivalent man), but not in SI system. Interesting is that in laser influence to plant systems it could be used adequate unit per seed grain. [19–23].

Laser influence in biology and especially medicine usually is studied in four areas: for surgery, biostimulation (modulation, acupuncture), diagnosis and in production of drugs (generally) [16,24–27]. Minimal laser threshold for wound healing (influence to fibroblasts) and overall cell level influence for activation of targeted processes are the objects of numerous investigations [24].

Therefore, in this paper we start with experiments on plants and some objective physical processes which objectivize the point of view. In references, several tenths of cw mW, are used for biostimulation purposes and we wanted to see the influence of selected doses to plants, *i.e.*, plant seeds. The objective was to obtain data which could be correlated and could trace per-

spective for future manipulation of facts. The aim is to give experimental data for determination of minimal levels of irradiation doses for defined purposes and to categorize those levels of influence.

Significant number of references dedicated to interaction of laser beams with materials exist [28–31]. Although mainstream attitudes are formed for several tents of years, a lot of experimental and theoretical work is still needed to obtain reliable data with good repeatability. This is especially true when applied to different plant seeds, related to specific geographical area and to growth of plant during specific year, with defined meteorological situation. Besides this, vegetative periods in plant growth, considering certain plant species influence the level of meteorological influences and other factors (soil type). During previous periods papers often dealt with better wheat crop, corn crop and crop of other plants, than followed more precise research of genetic content, etc. [28–31].

In this paper authors tried to elaborate on performed experiments and to remind of complexity of data which follow experiments. This includes descripttions using coefficient of absorption and reflection, laser beam polarization state, etc. enriched with correlation coefficient.

EXPERIMENTAL

Here presented experiments including wheat (*Tricium aestivum*) and several types of corn (*Zea mays* var. *Amilacae*; var. *Identata*) were conducted in few phases. Wheat and corn seed were irradiated with various types and levels of coherent electromagnetic radiation. Here is presented one of the series of samples and corresponding results.

Certain irradiated seeds were wet, while as control were used dry and wet non-irradiated seed. This principle is applied to all experiments.

The first part of experiment had the following phases:

1. Wet and dry seed were irradiated with He–Ne lasers and different energies. The output power of He–Ne was 50 mW, and wavelength 632.8 nm.
2. Laser beam was expanded by beam expander BET 50 type Laser Collimator Eloma 6, so that obtained beam was of 4.5 cm diameter. The beam was then reflected from the flat mirror to Petry's cup towards samples.
3. The reflected laser beam was monitored by pyroelectric radiometer type Rk3440 with appropriate probe type RkP 345. The density of laser beam was 0.4 mW/cm^2.
4. Irradiation energy doses were 1, 2, 4 and 6 J/cm^2, with exposition times of 250, 500 and 1000 s.

Most of the seeds were planted outdoors, with small part (less than 5%) in laboratory environment. Control groups were planted with treated irradiated seeds in order to have more objective comparison of resulting data.

After germination, growth of the plants as well morphogenetic changes, were monitored and recorded (stalk thickness, height, cob length for the corn and in case of wheat plant height). Obtained changes were registered by days. Depending on plant family, vegetative periods were monitored (germination, blooming and fruit development) and at the end analyzed.

Results were processed and visual interpretation of time dependences of plant height, histograms and 3D relations were given. The correlation dependencies between cob length, height and stalk thickness were studied. All results are given by adequate graphical presentations.

The third part of the experiments was measurement of reflection coefficients of some selected seeds.

RESULTS

In Figure 1 the growth of the non-irradiated wet control group plants is presented in days. Characteristic corn plant sizes were measured for non-irradiated wet control seed and wet seed irradiated with He–Ne 6 J/cm^2 including plant thickness, heights and cob lengths Table 1. They were the subject of statistical analysis. Figure 2 represents histogram of plants sprouted from wet control seeds (height of plants).

In Figure 3 the results of the plant growth after wet seed irradiation using He–Ne laser 6 J/cm^2 are presented. Histogram of wet irradiated seed (He–Ne 6 J/cm^2) is presented in Figure 4.

3D presentation of mutual correspondence between characteristic plant sizes: height, plant thickness and cob length for corn irradiated with He–Ne 6 J/cm^2 is presented in Figure 5.

The results of coefficient of reflection for wheat are presented in Figure 6 [32]. Figure 7 shows data about growth of plants germinated from wet wheat control seed.

DISCUSSION

The wheat (*Tricium aestivum*) was selected as typical long day plant representative. Corn (*Zea mays*) is representative of daily neutral plants, although some varieties belong to long day plants. Depending on growth and the size of the fruits for corn samples (different varieties) it is possible to determine which variety belongs to which type of the plants (long day or daily neutral plants). Concerning wheat as long day plants representative, it is possible to draw certain conclusions about growth of the plants irradiated with different types of laser irradiation (as well as preconditions of those seeds – wet or dry) [33–35].

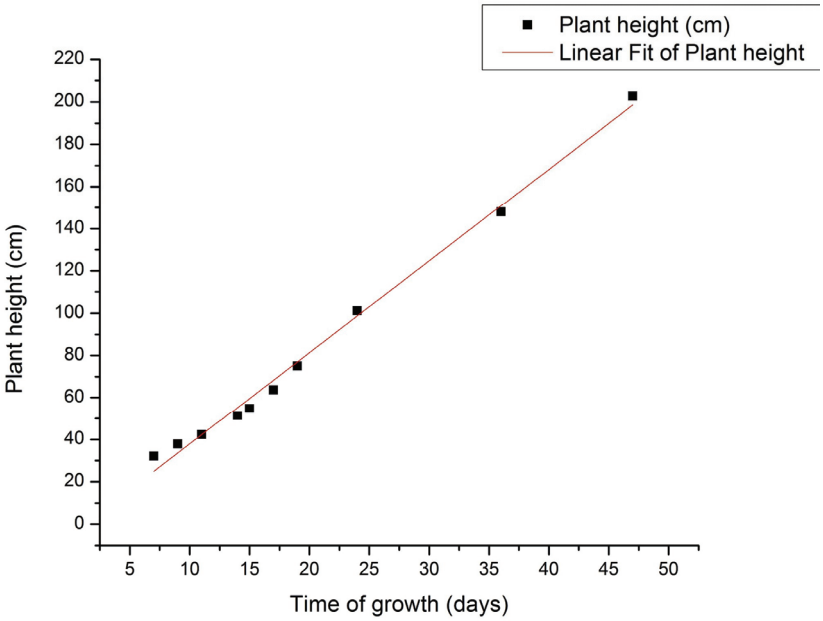

Figure 1. Corn control (non-irradiated) wet seed. Intercept value: –5.52; slope value: 4.34 cm/day.

Table 1. Corn comparison table of plant's characteristic dimensions of plants sprouted from non-irradiated wet control seeds and wet seeds irradiated with He–Ne 6 J/cm^2

Parameter	Stalk thickness, mm	Plant height, cm	Cob length, mm
	Non-irradiated wet seed		
Mean	21.29	234.54	20.08
Std. dev.	2.8	36.02	7.14
Correlation coefficient	Stalk thickness – Plant height	Plant height – Cob length	Stalk thickness – Cob length
	0.764339	0.878498	0.791254
	Wet seed irradiated with He–Ne 6 J/cm^2		
Mean	21.42	256.56	22.23
Std. dev.	2.02	13.51	2.88
Correlation coefficient	Stalk thickness – Plant height	Plant height – Cob length	Stalk thickness – Cob length
	0.607617	0.395461	0.673945

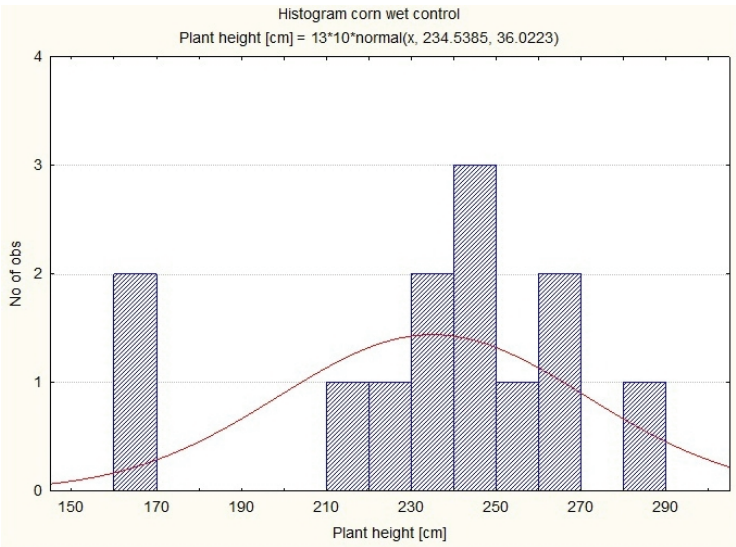

Figure 2. Histogram of wet control (non-irradiated) corn seeds.

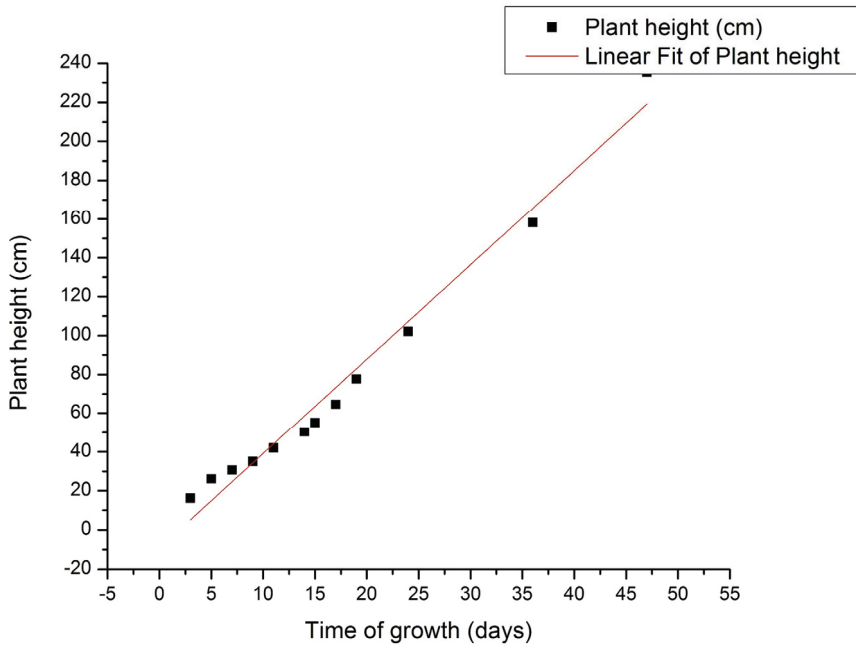

Figure 3. Corn irradiated wet seed (He–Ne laser, 6 J/cm^2). intercept value: –9.43; slope value: 4.86 cm/day.

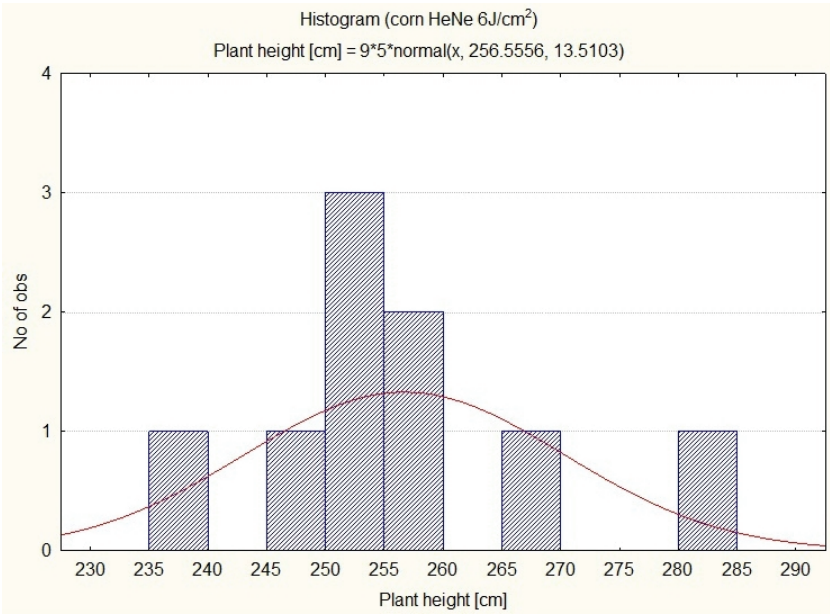

Figure 4. Histogram of wet irradiated corn seed (He–Ne laser, 6 J/cm^2).

In order to *in vivo* trace changes in living organisms, caused by various forms of electromagnetic radiation, mainly irradiated with laser beam, it is necessary to include a whole series of sciences, their methods and explanations. Domain in which results are commented is limited by used statistical methods, and plant characteristic monitoring, expected to be modified by irradiation (height, plant growth rate, fruit characteristics, organoleptic characteristics, genetic characteristics,...).

From the results obtained in this paper, it could be concluded that laser influence is certainly present. The real level of the induced changes could be the object of discussion because the principal question of the quantitative interpretation of results should be confirmed in various plant varieties. On the other hand the data from references in purely biological and biomedical areas do not present enough facts for objectivistic approach, from technical point of view. In spite of obeying the rules in those areas the concrete details were not given, i.e., the coefficient of reflection, absorption for some irradiation of living cells and systems including the situation with plants.

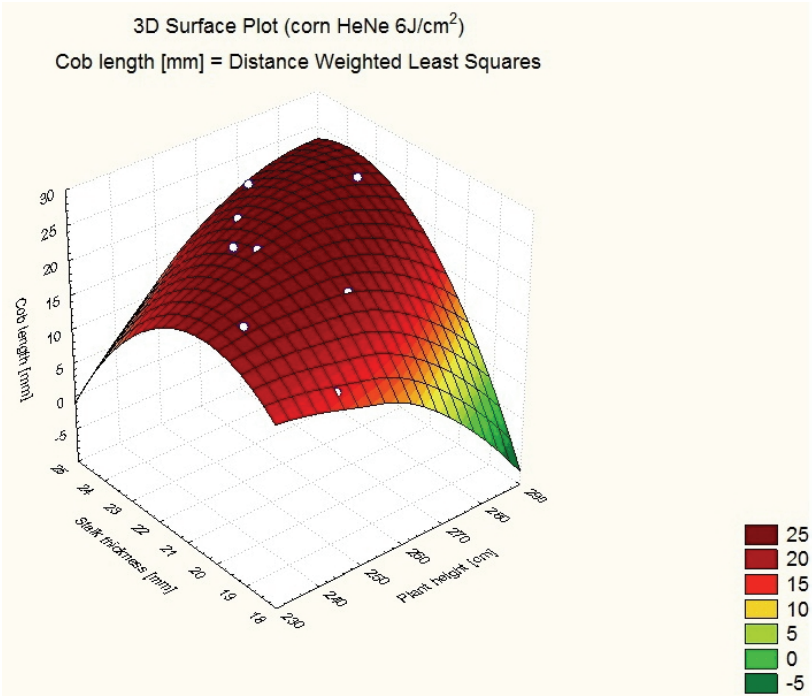

Figure 5. 3D dependence of plant height, stalk thickness and cob length for corn irradiated with He–Ne 6 J/cm^2.

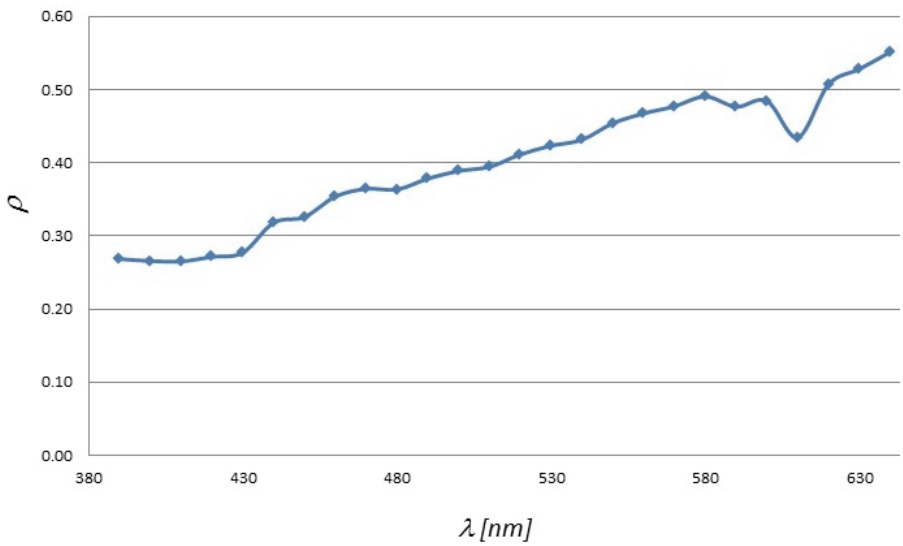

Figure 6. Reflection coefficient of wheat (regular sample).

The deepening of the discussion is related to question should the material whose coefficient of reflection is measured be in powder state (what is demand of the standard equipment) or left as grain.

Considering this paper, the aim of work was to present real parameters with correlation calculation. Some general conclusion could be: correlation dependencies show that from irradiated seed grow plants whose height is comparably greater than those germinated from control seeds. This is expected, concerning the fact that one of the first markers of genetic material change, due to irradiation, is elongation (contribution to height) of plant. Wet corn seed under influence of laser radiation are more susceptible to changes than dry ones. More generally speaking, we could talk about influence of electromagnetic irradiation in laser range of wavelength, power density, etc.

CONCLUSION

It is a general recommendation to avoid unnecessary exposure to magnetic and electric fields and this correspond to the general mainstream in which allowed exposition thresholds (doses) are constantly reducing.

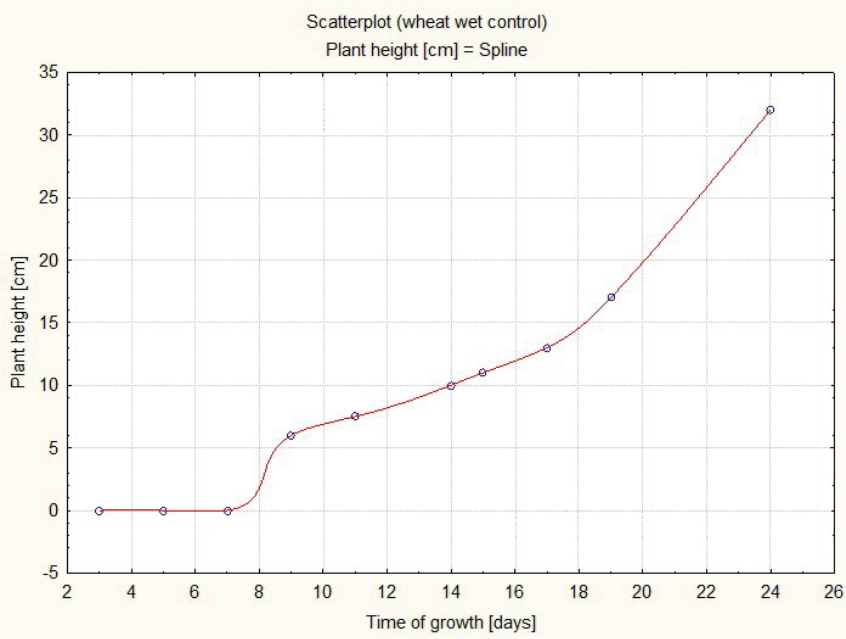

Figure 7. Wheat control (non-irradiated) wet seed.

It is possible to draw parallel between associated magnetic and electric fields of laser with other exposures to electric and magnetic fields (DC and AC). From correlation dependence of plant height and cob length it is possible to conclude that with plant elongation the crop is greater. Corresponding to our other experiments of similar type, here also the use of wet and dry control seed have shown to be a good practice. The results for He-Ne laser gave similar results as those in experiments with GaAs laser for same irradiation parameters, no matter the used wavelengths in visible and in NIR. These issues could be interpreted as quantitative values (real measurable magnitude values) for limited validity for selected exposition ranges – doses and to defined species.

Observing the plots obtained graphically by depicting the growth of plants sprouted from irradiated seeds one could conclude that plant irradiated with smaller irradiation energy (energy density) easily overcame crisis in growth between 30th and 40th day. Concerning plant growth, just by measuring height, it is obvious that irradiated plant needs more light for transition from second vegetative phase to third (germination, springing and flowering). Overall conclusion is that applied levels of energy influenced qualitative shift of plants.

For even further analysis of measured data for all types of plants and their varieties (wheat and corn) it is necessary, based on plant tissues parameters examined, to do appropriate model of seeds (i.e. wheat seed could be modeled using 7 layers with distinct parameters) before irradiation and then to compare real and theoretical cases.

REFERENCES

[1] S. Martelucci, A.N. Chester (Eds.), Lasers in Photobiology and Photo medicine, Plenum Press, New York, 1984.

[2] G.D. Najafpour, Biochemical engineering and biotechnology, Elsevier, Amsterdam, 2007.

[3] D.H. Sliney, M.L. Wohlbarsht, Safety with Lasers and Other Optical Sources, Plenum Press, New York, 1980.

[4] L. Goldman, The Biomedical Laser, Springer, Berlin, 1981.

[5] D. H. Sliney, M. Bitran, W. Murray, Infrared, Visible, and Ultraviolet Radiation, John Wiley & Sons, New York, 2012.

[6] K. Barat (Ed.), Laser safety, Tools and training, Taylor & Francis Group, Abingdon, 2009

[7] M. Srećković, P. Osmokrović, Lj. Konstantinović, V. Arsoski, Izabrane primene lasera u medicini i interakcija lasera sa biomaterijalom, Zavod za fiziku tehničkih fakulteta, Beograd, 2010 (in Serbian).

[8] M. Jeremić, Nejonizujuća zračenja i zaštita, Medicinska knjiga, Beograd, 1995 (In Serbian).

[9] L. Petrović, The Review an Analysis of the Sources of Electromagnetic Interference, 23. Conf. JUKO CIGRE, Herceg Novi, 1997, Section III group 36 - compatibility EEC (In Serbian).

[10] L.D. Petrović, R.V. Radovanović, Electromagnetic Radiation as the cause of environmental pollution, conference, environment and human health, Belgrade, 2005, pp. 10 (In Serbian).

[11] Г.М. Обатуров, Биофизические модели радио-биологических эффектов, Энергоатомиздат, Москва, 1987.

[12] D.V. Palanker, S. Ohad, A. Lewis, N. Laufer, Cold laser technique for cell surgery, Proc. SPIE 1646, Laser-Tissue Interaction III,69, 1992, doi:10.1117/12.137447

[13] Y.Y. Huang, S.K. Sharma, J. Carroll, M.R. Hamblin, Biphasic Dose Response In Low Level Light Therapy – An Update, International Dose Response Society, University of Massachusetts, Dose Response **9** (2011) 602–618.

[14] M.R. Hamblin, R. W. Waynant, J. Anders, Mechanisms for low-light Therapy, SPIE, 2007.

[15] M.H. Niemz, Laser Tissue Interaction. Fundamentals and Applications, Springer-Verlag, Berlin, 2007.

[16] M. Srećković, M. Hrnjak, D. Živković, S. Aranđelović, B. Đuričić, J. Mirčevski, D. Mamula-Tartalja, Laser Interactions and Stimulative Effects in Biomedical Material and The Limits of Stimulatory Effects of Low Power Density He–Ne Laser Radiation on Fibroblast Proliferation in Vitro, Proc. of Lasers 98, Tucson, AR, 1998, W. Corcoran, T. Goldman (Eds.), SoQue, McLain, 1999, pp. 587–593.

[17] M. Elezović, L. Petrović, R. Radovanović, Naponski udari u mreži za napajanje, Energetika 2007, Zlatibor, 2007, pp. 313–318 (in Serbian).

[18] M. Elezović, L. Petrović, Imunost elektronske opreme na promene u mreži za napajanje, Energija – Ekonomija – Ekologija X, 2008, pp. 046–048 (in Serbian).

[19] I. Draganić (Ed.), Radioaktivni izotopi i zračenja I, II, III, Naučna knjiga, Beograd, 1963.

[20] The 2007 Recommendations of the International Commission on Radiological Protection Annals of the ICRP. ICRP publication 103, **37** (2007) 2–4.

[21] 10 CFR 20.1004. US Nuclear Regulatory Commission. 2009.

[22] A.F. Harvey (Ed.), Coherent Light, Wiley-Interscience, New York, 1970, pp. 1144–1151.

[23] B. Gladyszewska, Estimation of a Laser Biostimulation Dose, Int. Agrophys. **25** (2011) 403–405.

[24] О.К. Скобелкин (Ед.), Ласеры в хирургии, Медицина, Москва, 1989.

[25] M. Srećković, S. Aranđelović, D. Nikolić, B. Đuričić, A. Marinović, D. Knežević, V. Branković-Srećković, D. Đapić, Primena terapeutskih i dijagnostičkih laserskih tehnika u biomedicini, veterini i farmaciji, Zbornik XLII Konf. ETRAN, Vrnjačka banja, 1998, pp. 177–180 (In Serbian).

[26] M. Srećković, R. Vasić, M. Dukić, S. Jevtić, P. Jovanić, The Influence of Diode and He-Ne Lasers On Corn and Wheat Seeds, J. Agric. Sci. Technol., B **4** (2014) 165–175.

[27] V. Vujošević-Simić, S. Babić, M. Dukić, A. Mikulić, Optičke osobine uzoraka namirnica i razlika spektralnih karakteristika koeficijenata refleksije za ispravne i infestovane uzorke, Zbornik XLVIII Konf.za ETRAN, Tom III, Čačak, 2004. pp. 253–255 (In Serbian).

[28] T. Karu, Primary and Secondary Mechanisms of Action of Visible to Near-IR Radiation on cells, J. Photochem. Photobiol., B **49** (1999) 1–17.

[29] A.C. Hernandez, P.A. Dominguez, O.A. Cruz, R. Ivanov, C.A. Carballo, B.R. Zapeda, Laser in Agriculture, Int. Agrophys. **24** (2010) 407–422.

[30] A. Dziwulska-Hunek, K. Kornarzynski, A. Matwijczuk, S. Pietruszewski, B. Szor, Effect of Laser and Variable Magnetic Field Simulation on Amaranth Seed Germination, Int. Agrophysics **23** (2009) 229–235.

[31] F.D. Samuilov, R.L. Garifullina, Effects of Laser Irradiation on Microviscosity of Aqueous Medium in Imbibing Maize Seeds as Studied with a Spin Probe Method, Russ. J. Plant Physiol. **54** (2007) 128–131.

[32] S. Babić, Određivanje optičkih karakteristika i obrada nekih neorganskih i organskih materijala pomoću koherentne i nekoherentne svetlosti, Magistarska teza, Elektrotehnički fakultet, Univerzitet u Beogradu, 2005 (in Serbian).

[33] M. Srećković, S. Bojanić, Lj. Konstantinović, M. Dukić, N. Cvetković, J. Mirčevski, D. Nikolić, D. Živković, S. Babić, N. Rakočević, S. Stanković, R. Vasić, J. Ilić, Optical Parameters Measurements And Modeling in Biology And Some Laser Applications In Life, Proceedings of Laser's 2000, Albuquerque, NM, 2000, V.J. Corcoran, T.A. Corcoran (Eds.), SoQue, McLean, 2001,pp. 628–635.

[34] M. Srećković, Lj. Konstantinović, S. Stanković, M. Dukić, R. Vasić, D. Živković, D. Nikolić, S. Babić, R. Sekulić,. Uticaj i primena lasera na biosisteme, organizme i kulture ćelija, XLV Konf. ETRAN, Bukovička Banja, 2001, Zbornik.,Tom III, pp. 211–214 (in Serbian).

[35] S. Pelemiš, M. Srećković, S. Jevtić, F. Živić, Uticaj laserskih snopova u infracrvenom opsegu na bioorganizme i analiza modelovanja za materijale ekvivalentnih parametara, Savremeni materijali (2013) 117.

IZVOD

UTICAJ LASERA NA BIOSISTEME

Sanja D. Jevtić[1], Milesa Ž. Srećković[2], Svetlana S. Pelemiš[3], Ljubica M. Konstantinović[4], Predrag B. Jovanić[5], Lazar D. Petrović[6], Milan M. Dukić[7]

[1]*Železnička tehnička škola, Beograd, Srbija*
[2]*Elektrotehnički fakultet, Univerzitet u Beogradu, Beograd, Srbija*
[3]*Tehnološki fakultet, Univerzitet u istočnom Sarajevu, Zvornik, Bosna i Hercegovina*
[4]*Medicinski fakultet, Univerzitet u Beogradu, Beograd, Srbija*
[5]*Institute za multidisciplinarne studije, Univerzitet u Beogradu, Beograd, Srbija*
[6]*Facultet za diplomatiju i bezbednost, Univerzitet Union Nikola Tesla, Beograd, Srbija*
[7]*North Carolina Central University, Durham, USA*

(Naučni rad)

Uticaj laserskih snopova na žive organizme je već duže vremena predmet proučavanja koji zahteva multidisciplinarni pristup. Kako se podrazumevaju i vidljiva, UV i IC oblast, to se problem može posmatrati i kao proučavanje koje pripada široj problematici uticaja električnih, magnetnih polja i elektromagnetskih polja i talasa na žive organizme. U ovom radu su proučavani eksperimentalno procesi i rezultati delovanja He–Ne lasera na suva i vlažna semena pšenice (*Tricium aestivum*) i kukuruza– *Zea mays*, (var. *Amilacae*; var. *Identata*). Iako je uticaj elektromagnetnog (EM) zračenja na živa bića stari problem, koji je mnogo proučavan, on je još uvek sa mnogo nerešenih pitanja. Ako uz problematiku spontanog EM zračenja postoji veliki broj nerazjašnjenih procesa, utoliko pre to važi za oblast stimulisanih zračenja – kvantnih generatora, koji komercijalno (ili u eksperimentalnom stadijumu) rade od gama do RF (radio frekvencija) oblasti. Laseri su već odavno uključeni u praksu u okviru biomedicine, biologije, a u humanoj medicini odavno su uključeni u oblasti hirurgije, biostimulacije, dijagnostike, farmakologije, akupunkture, itd. Oblast primene lasera se vrlo brzo uključuje u mnogo svakodnevnih primena, a na delovanje zračenja na bioorganizme (biosisteme) se, i pored postojeće regulative, ne obraća dovoljno pažnje. Nove oblasti primene lasera vrlo kratkih impulsa i fenomeni nelinearne optike, otvaraju mnogo novih pitanja. Pragovi za terapeutska dejstva (biostimulaciju) se istražuju i pripadaju zadacima laserske dozimetrije i njenih preciznih stavova, koji se razlikuju od države do države. U radu su opisani izvršeni eksperimenti sa ozračavanjem semena pšenice i kukuruza (suvih i vlažnih). Korišćen je gasni He–Ne laser kontinualnog dejstva (cw, 632,8 nm, 50 mW). Posle klijanja praćen je rast biljaka po danima (debljina i visina stabljike, dužina klipa kukuruza, a za pšenicu visina biljke). Posle praćenja vegetativnih perioda i roda izvršena je analiza dobijenih rezultata sa statističkom obradom podataka. Korišćene su predstave u vidu histograma, 2D predstave i interpretacija u 3D na bazi metode najmanjih kvadrata i neke korelacione analize. U mnogo referenci se uključuje samo talasna dužina lasera i doza, bez osvrtanja na koeficijente refleksije i absorpcije biosistema. Zato je ovde dat koeficijent refleksije, tipičan za pšenicu, kao kvalitativna mera za uračunavanja pravilnije doze, prema tipu lasera. Koeficijenti refleksije biljaka mogu da posluže i za daljinske kontrole (LIDAR) stanja biljnih vrsta na terenu. Eksperimentalni rezultati sa He–Ne laserom su u dobroj saglasnosti (kvalitativnoj) sa rezultatima, dobijenih na bazi poluprovodničkih lasera sa uporedivim dozama. To važi i za uticaj vlažnosti semena, bez obzira da li se radi o He–Ne, gasnim ili poluprovodničkim laserima na opsegu od 800–900 nm.

Ključne reči: Laser • Biostimulacija • Biosistemi • Biljke • Doze • Koeficijent refleksije • Korelacija